

**COMPARATIVE TRANSCRIPTOME ANALYSIS OF
CLINICAL AND ENVIRONMENTAL STRAINS OF
Cryptococcus neoformans AND AN INVESTIGATION ON
ANTI-*Cryptococcus* ACTIVITY OF TRICLOSAN**

ELAHEH MOVAHED

**FACULTY OF MEDICINE
UNIVERSITY OF MALAYA
KUALA LUMPUR**

2017

**COMPARATIVE TRANSCRIPTOME ANALYSIS
OF CLINICAL AND ENVIRONMENTAL STRAINS
OF *Cryptococcus neoformans* AND AN
INVESTIGATION ON ANTI-*Cryptococcus*
ACTIVITY OF TRICLOSAN**

ELAHEH MOVAHED

**THESIS SUBMITTED IN FULFILMENT OF THE
REQUIREMENTS FOR THE DEGREE OF
DOCTOR OF PHILOSOPHY**

**FACULTY OF MEDICINE
UNIVERSITY OF MALAYA
KUALA LUMPUR**

2017

UNIVERSITY OF MALAYA

ORIGINAL LITERARY WORK DECLARATION

Name of Candidate: **ELAHEH MOVAHED**

Registration/Matric No: **MHA 130040**

Name of Degree: **DOCTOR OF PHILOSOPHY**

Title of Project Paper/Research Report/Dissertation/Thesis ("this Work"):
COMPARATIVE TRANSCRIPTOME ANALYSIS OF CLINICAL AND ENVIRONMENTAL STRAINS OF *Cryptococcus neoformans* AND AN INVESTIGATION ON ANTI-*Cryptococcus* ACTIVITY OF TRICLOSAN

Field of Study: **MEDICAL MICROBIOLOGY**

I do solemnly and sincerely declare that:

- (1) I am the sole author/writer of this Work;
- (2) This Work is original;
- (3) Any use of any work in which copyright exists was done by way of fair dealing and for permitted purposes and any excerpt or extract from, or reference to or reproduction of any copyright work has been disclosed expressly and sufficiently and the title of the Work and its authorship have been acknowledged in this Work;
- (4) I do not have any actual knowledge nor do I ought reasonably to know that the making of this work constitutes an infringement of any copyright work;
- (5) I hereby assign all and every rights in the copyright to this Work to the University of Malaya ("UM"), who henceforth shall be owner of the copyright in this Work and that any reproduction or use in any form or by any means whatsoever is prohibited without the written consent of UM having been first had and obtained;
- (6) I am fully aware that if in the course of making this Work I have infringed any copyright whether intentionally or otherwise, I may be subject to legal action or any other action as may be determined by UM.

Candidate's Signature

Date:

Subscribed and solemnly declared before,

Witness's Signature

Date:

Name

Designation: Senior lecturer

ABSTRACT

Cryptococcus neoformans is an opportunistic yeast pathogen which causes meningoencephalitis particularly in HIV-infected patients. The infection can be acquired through the inhalation of desiccated yeast cells and basidiospores originated from the environment, especially from soil contaminated with bird droppings. *C. neoformans* environmental strains display differences in the virulence patterns. Several cellular factors that have been associated with the virulence of *C. neoformans*, include melanin, components of polysaccharide capsule, alpha mating type and phospholipase. At present, the mechanism of gene control in clinical and environmental strains of *C. neoformans* that leads to the virulence of *C. neoformans* is not well understood. This study aims to determine if gene expression differences among clinical and environmental *C. neoformans* strains contributes to different degree of virulence. Additionally, due to the emergence of drug-resistant *C. neoformans* in recent years, this study also aims to investigate the anti-*Cryptococcus* activity of triclosan (2,4,4'-trichloro-2'-hydroxydiphenylether, C₁₂H₁₇Cl₃O₂). A clinical strain (H99) and three environmental strains (H4, S48B and S68B) isolated from soil contaminated with bird droppings were included in this investigation. All the cryptococcal strains were first characterized for their virulence properties using *in vitro* and *in vivo* approaches. India ink staining showed a bigger capsule size in *C. neoformans* H99 strain compared to environmental strains. In the *in vivo* challenge model, an average of $4.73 \pm 1.19 \times 10^5$ colony forming units (cfu)/ml of *C. neoformans* were obtained from the lung homogenates of mice infected intranasally with strain H99. The recovered yeast cells were approximately forty folds higher than those obtained from H4-, S48B-, and S68B-infected mice. To understand the gene transcription underlying the differences in virulence among H99 and environmental strains, RNA was extracted from each strain and a genome-wide microarray study was performed. Microarray analysis revealed a

different transcriptome profile of H99 strain compared to H4, S48B and S68B strains. Out of 7,419 genes (22,257 probes) examined, 41 genes were up-regulated while 24 genes were down-regulated in H99 versus environmental strains. The genes which were up-regulated in H99 strain include Hydroxymethylglutaryl-CoA synthase (*MVA1*), Mitochondrial matrix factor 1 (*MMF1*), Bud-site-selection protein 8 (*BUD8*), High affinity glucose transporter 3 (*SNF3*) and Rho GTPase-activating protein 2 (*RGA2*). Pathway annotation using DAVID bioinformatics resource showed that metal ion binding pathway was highly active in the H99 but not in the environmental strains. Transition metals such as iron, zinc, copper, and manganese are essential elements for the growth and survival of microorganisms including fungi. Siderophore iron transporter genes (*ARN1* and *ARN2*) were up-regulated at 6.7-, 10.2-, and 11.4-folds, and 4.7-, 8.1-, and 5.5-folds, respectively, in H99 strain compared to H4, S48B and S68B strains. Sugar transmembrane transport, another active pathway identified in H99 strain, is essential for the production of capsular polysaccharide antigens in *C. neoformans*. One of the genes in the pathway, *SNF3*, was up-regulated at 15.2-, 8.0- and 5.5-folds in H99 versus H4, S48B and S68B strains. The analyses in this study suggest possible roles of the relevant genes and pathways in fungal pathogenesis.

In the second part of the study, growth inhibition against *C. neoformans* by triclosan was demonstrated. A combination of triclosan with amphotericin B or with fluconazole enhanced the fungicidal effects against *C. neoformans*. Triclosan-treated *C. neoformans* displayed characteristics such as nuclear chromatin condensation, extensive intracellular vacuolation and mitochondrial swelling, which were suggestive of apoptosis-like cell death. In conclusion, this study has linked several genes and pathways in *C. neoformans* with the higher virulence of the H99 strain, as compared to the environmental strains. This study also reports a potential therapeutic value of triclosan as a novel drug or a synergist in the treatment of cryptococcal infection.

ABSTRAK

Cryptococcus neoformans ialah patogen yis oportunistik yang menyebabkan meningoensefalitis khususnya pada pesakit yang dijangkiti HIV. Jangkitan tersebut diperolehi melalui inhalasi sel yis kering dan basidiospora yang berasal dari persekitaran, terutamanya dari najis burung. Strain persekitaran *C. neoformans* menunjukkan perbezaan dalam corak kevirulenan. Beberapa faktor selular yang berkaitan dengan kevirulenan *C. neoformans* adalah melanin, komponen kapsul polisakarida, jenis “mating” alfa dan fosfolipase. Pada masa kini, mekanisme kawalan gen pada strain klinikal dan persekitaran *C. neoformans* yang menyebabkan kevirulenan *C. neoformans* belum lagi difahami sepenuhnya. Kajian ini bertujuan untuk menentukan samada ekspresi gen menyumbang kepada perbezaan darjah kevirulenan di antara strain klinikal dan persekitaran *C. neoformans*. Tambahan lagi, disebabkan kemunculan *C. neoformans* yang rintang kepada ubat kebelakangan ini, kajian ini juga bertujuan untuk menyelidik aktiviti anti-*Cryptococcus* dengan triclosan (2,4,4'-trichloro-2'-hydroxydiphenylether, C₁₂H₁₇Cl₃O₂). Satu strain klinikal (H99) dan tiga strain persekitaran (H4, S48B dan S68B) yang diasingkan dari najis burung telah digunakan dalam kajian ini. Sifat kevirulenan kesemua strain *Cryptococcus* telah dicirikan terlebih dahulu dengan menggunakan pendekatan *in vitro* dan *in vivo*. Pewarnaan dakwat India menunjukkan saiz kapsul strain H99 yang lebih besar berbanding strain persekitaran. Dalam kajian *in vivo* dengan model cabaran, purata $4.73 \pm 1.19 \times 10^5$ unit pembentukan koloni (cfu)/ml telah diperolehi dari homogenat paru-paru tikus yang dijangkiti *C. neoformans* H99 secara intranasal. Jumlah yis yang dipulihkan dari strain H99 dianggarkan empat puluh kali ganda lebih tinggi berbanding dengan yang diperolehi dari tikus-tikus yang dijangkiti strain H4, S48B dan S68B. Untuk memahami transkripsi gen yang mempengaruhi perbezaan kevirulenan strain H99 dengan strain persekitaran, RNA telah diekstrak daripada setiap strain dan kajian “microarray”

keseluruhan genom telah dijalankan. Kajian “microarray” menunjukkan profil transkriptom yang berbeza pada strain H99 berbanding dengan strain H4, S48B dan S68B. Daripada 7,419 gen (22,257 prob) yang dikaji, sejumlah 41 gen dikawalnaik manakala 24 gen dikawalturun secara signifikannya dalam strain H99 berbanding dengan strain persekitaran. Gen-gen yang dikawalnaik pada strain H99 termasuk Hydroxymethylglutaryl-CoA synthase (*MVA1*), Mitochondrial matrix factor 1 (*MMF1*), Bud-site-selection protein 8 (*BUD8*), High affinity glucose transporter3 (*SNF3*) dan Rho GTPase-activating protein 2 (*RGA2*). Anotasi laluan dengan menggunakan sumber bioinformatik DAVID menunjukkan bahawa laluan ikatan logam ion adalah sangat aktif pada strain H99 tetapi tidak pada strain persekitaran. Logam peralihan seperti besi, zink, tembaga dan mangan adalah elemen yang penting untuk perkembangan dan kemandirian mikroorganisma termasuk kulat. Gen siderophore iron transporter (*ARN1* dan *ARN2*) telah dikawalnaik pada 6.7-, 10.2-, dan 11.4-kali ganda, dan 4.7-, 8.1-, dan 5.5-kali ganda pada strain H99 berbanding dengan strain H4, S48B dan S68B. Laluan pengangkut transmembrane gula, satu lagi laluan aktif yang dikenalpasti pada strain H99, adalah penting bagi penghasilan antigen kapsul polisakarida. *SNF3*, salah satu gen pada laluan ini telah dikawalnaik pada 15.2-, 8.0- dan 5.5-kali ganda pada strain H99 berbanding dengan strain H4, S48B dan S68B. Analisis ini mencadangkan peranan penting yang mungkin dimainkan oleh gen dan laluan berkaitan dengan patogenesis kulat. Pada bahagian kedua kajian ini, rintangan pertumbuhan *C. neoformans* oleh triclosan telah dibuktikan. Kombinasi triclosan dengan amphotericin B atau dengan fluconazole meningkatkan kesan fungisid terhadap *C. neoformans*. *C. neoformans* yang dirawat dengan triclosan menunjukkan ciri-ciri seperti kondensasi kromatin nuclear, vakuolasi intrasel yang ekstensif, dan mitokondria yang bengkak, mencadangkan kematian sel secara apoptosis. Kesimpulannya, kajian ini telah mengaitkan beberapa gen dan laluan dalam *C. neoformans* dengan kevirulenan strain

H99 yang lebih tinggi berbanding dengan strain persekitaran. Kajian ini juga membuktikan potensi nilai terapeutik triclosan sebagai ubat baru atau sinergen dalam merawat jangkitan *Cryptococcus*.

University of Malaya

ACKNOWLEDGEMENTS

Though only my name appears on the cover of this thesis, many people have contributed to its production. I owe my gratitude to all those people who have made this possible and because of whom my graduate experience has been one that I will cherish forever.

My deepest gratitude is to my supervisor, Dr. Wong Won Fen. I have been amazingly fortunate to have an advisor who gave me the guidance to recover when my steps faltered. She has been always there to give advice. Her patience and support helped me overcome many crisis situations and finish this journey.

My co-supervisor, Professor Tay Sun Tee, I am deeply grateful to her for the long discussions that helped me sort out the technical details of my work. I am also thankful for her patience for commenting on numerous revisions of this manuscript.

My friends Maryam and Faezeh whose care and supports helped me stay sane through these years. I am also grateful to my lab mates, Grace and Yeow for their assistance.

The love of my life, Aidin, who helped me overcome setbacks and stay strong with his continuous support and care. I greatly value his supports and deeply appreciate his belief in me.

Most importantly, none of this would have been possible without the love and patience of my family. My parents to whom this thesis is dedicated to, has been a constant source of love, concern, support and strength all these years. I would like to express my heart-felt gratitude to my family. They encouraged me throughout this endeavour and provided me the great opportunity of living in beautiful Malaysia.

TABLE OF CONTENTS

ABSTRACT.....	iii
ABSTRAK.....	v
ACKNOWLEDGEMENT.....	x
TABLE OF CONTENTS.....	xi
LIST OF FIGURES.....	xv
LIST OF TABLES.....	xix
LIST OF SYMBOLS AND ABBREVIATIONS.....	xxi
LIST OF APPENDICES.....	xxv
1. CHAPTER 1: INTRODUCTION.....	1
1.1 Introduction.....	1
1.2 Objectives	7
2 CHAPTER 2: LITERATURE REVIEW.....	8
2.1 <i>Cryptococcus</i>	8
2.1.1 <i>C. neoformans</i>	9
2.1.2 Mating type.....	9
2.1.3 Epidemiology	10
2.2 The cryptococcal life cycle	16
2.3 Strain identification and differentiation of Cryptococcal strains	17
2.4 Virulence phenotypes of <i>C. neoformans</i>.....	20
2.4.1 Melanin.....	20
2.4.2 Ability to grow at high temperature	21
2.4.3 Capsule	22
2.4.4 Other possible virulence phenotypes.....	23
2.4.5 Degradative enzymes	24
2.5 Pathogenicity-associated pathways	25
2.6 Clinical versus environmental strains.....	26
2.7 Molecular pathogenesis study of <i>C. neoformans</i>	28
2.8 The host responses to <i>C. neoformans</i> infections.....	29
2.9 Genome of <i>Cryptococcus neoformans</i>	32
2.10 Microarray as gene expression profiling method	33
2.11 Anticryptococcal therapy	35
2.11.1 Cryptococcosis preventive approaches.....	37
2.11.2 Triclosan as a new anti-fungal therapy.....	38

2.11.3	Apoptotic markers	40
3	CHAPTER 3: MATERIALS AND METHODS	41
3.1	Strains and growth conditions	41
3.2	Maintenance of cryptococcal strains.....	41
3.3	Molecular identification <i>C. neoformans</i> strains	41
3.3.1	DNA extraction	41
3.4	Amplification and sequence analysis of the internal transcribed spacer (ITS) region.....	42
3.4.1	Purification of PCR products	43
3.4.2	Sequence determination and analysis.....	43
3.4.3	PCR fingerprinting analysis of <i>C. neoformans</i> strains	43
3.4.4	Agarose gel electrophoresis.....	44
3.4.5	Cluster analysis of four <i>C. neoformans</i> strains.....	44
3.5	Growth curve analysis	45
3.6	<i>In vivo</i> infection study.....	45
3.7	Capsule induction	46
3.8	Phospholipase activity	46
3.9	Laccase activity	46
3.10	Microarray study	47
3.10.1	RNA isolation.....	47
3.10.2	RNA quality and integrity evaluation	48
3.10.3	Microarray	49
3.10.4	Microarray analysis	52
3.10.5	Statistical analysis	53
3.11	Validation of microarray data	53
3.11.1	cDNA synthesis Protocol:	53
3.11.2	Primer design.....	54
3.11.3	Quantitative Real-Time PCR.....	55
3.12	Investigation on anti-<i>Cryptococcus</i> activity	56
3.12.1	Preparation of triclosan	56
3.12.2	Preparation of amphotericin	56
3.12.3	Preparation of fluconazole.....	56
3.13	Disc diffusion assay	56
3.14	Broth microdilution assay	57
3.15	Fungicidal assay	58
3.16	Synergy checkerboard assay	58
3.17	Electron microscopy	59
3.18	Apoptosis assay	60

3.19	Statistical analysis	60
4	CHAPTER 4: RESULTS.....	62
4.1	Amplification and sequence analysis of the internal transcribed spacer (ITS) region of <i>C. neoformans</i> strains.....	62
4.2	Cluster analysis of the clinical H99 and three environmental strains of <i>C. neoformans</i>	64
4.3	<i>In vivo</i> virulence study among clinical and environmental strains of <i>C. neoformans</i>	66
4.3.1	Survival analysis of mice infected with clinical and environmental strains of <i>C. neoformans</i>	66
4.3.2	Morphological changes of mice lung infected with clinical and environmental strains of <i>C. neoformans</i>	67
4.3.3	Determination of the colony forming units of <i>C. neoformans</i> in the organs of mice infected with clinical and environmental strains of <i>C. neoformans</i>	69
4.4	Determination of growth curve in clinical and environmental strains of <i>C. neoformans</i>	72
4.5	Clinical strain H99 shows larger capsule size compared to environmental strains.	73
4.6	Phospholipase activity	75
4.7	Laccase assay	76
4.8	Antimicrobial susceptibility testing using E-test Method	78
4.9	Comparative transcriptome analysis of clinical and environmental strains of <i>C. neoformans</i>	79
4.9.1	RNA extraction.....	79
4.9.2	Gene expression analysis.....	83
4.9.3	Microarray data analysis	83
4.9.3.1	Determination of Pairwise correlation coefficient matrix	84
4.9.3.2	Normalization and filtration.....	86
4.9.3.3	Quality control of samples using principal component analysis ...	88
4.9.4	Fold change analysis	89
4.9.4.1	Heat map analysis	89
4.9.4.2	Scatter plots analysis.....	91
4.9.4.3	Venn diagram analysis.....	93
4.9.5	Identification of significantly up-regulated and down-regulated genes in <i>C. neoformans</i> H99 strain and environmental strains	103
4.9.6	KEGG Pathway analysis	105
4.9.6.1	Pathway annotation of 65 significantly regulated genes.....	113
4.9.7	Gene expression analysis of well-known genes linked to the major virulence phenotypes.....	113
4.10	Antifungal effect of triclosan against <i>C. neoformans</i>	119
4.10.1	Determination of minimum inhibitory concentration (MIC)	120

4.10.2	Evaluation of CFU-based fungicidal assay	121
4.11	Analysis of triclosan synergistic effect with amphotericin B and fluconazole.....	122
4.11.1	Analysis of checkerboard assay	126
4.12	Determination of apoptotic-like cell death (ALCD) mechanism of triclosan on <i>C. neoformans</i>	127
4.12.1	Transmission electron microscopic analysis of triclosan-treated <i>C. neoformans</i>	127
4.12.2	Analysis of inhibitory mechanism of triclosan on <i>C. neoformans</i> using TUNEL apoptosis assay	129
5	CHAPTER 5: DISCUSSION	131
5.1	Comparative analyses of clinical and environmental strains of <i>C. neoformans</i>	131
5.1.1	<i>In vivo</i> virulence analysis of environmental strains of <i>C. neoformans</i> compared to H99 in mice.....	133
5.1.2	Determination of the possible virulence factors of H99 compare to environmental strains.....	134
5.2	Microarray analysis of clinical strain of <i>C. neoformans</i> versus environmental strains	136
5.3	Gene expression analysis of well-known virulence genes of <i>C. neoformans</i>	137
5.4	Pathway analysis	138
5.5	Gene expression analysis of significantly regulated genes	139
5.6	Microarray validation	146
5.7	Antifungal effect of untapped drugs against <i>C. neoformans</i>	147
5.8	Synergism between triclosan and standard drugs.....	150
5.9	Mechanism of action of triclosan.....	151
5.10	Programme cell death mechanism in <i>C. neoformans</i>.....	151
6	CHAPTER 6: CONCLUSION.....	154
6.1	Study limitation.....	155
6.2	Future work.....	155
	REFERENCES	157
	LIST OF PUBLICATIONS AND PRESENTATIONS	189
	APPENDICES	196

LIST OF FIGURES

Figure 2.1. Global burden of HIV-related cryptococcal meningitis	11
Figure 2.2. (a) Percentage of <i>C. neoformans</i> and <i>C. gattii</i> strains from clinical and environmental sources. (b). Geographical distribution of the <i>C. neoformans</i> and <i>C. gattii</i> strains (c). Clinical strains were reported from red-colored countries, whereas both clinical and environmental strains were reported from orange-colored countries	14
Figure 2.3. Environmental sources of cryptococcal meningitis	16
Figure 2.4. Same sex and opposite sex mating system in <i>C. neoformans</i> . During mating of opposite sex, five distinct stages have been described: 1) dikaryon, 2) nuclear fusion, 3) meiotic products, 4) basidiospores, and 5) mitosis, followed by sporulation and release of spores into the environment.....	17
Figure 2.5. Phylogeny of the <i>C. neoformans</i> – <i>C. gattii</i> species complex.....	19
Figure 2.6. India ink stained capsule surrounding <i>C. neoformans</i> cells	23
Figure 2.7. Macrophage and <i>C. neoformans</i> . Yeast cells are phagocytosed (1), enters latency phase (2) in an individual. In the immunocompromised host, the yeast cells can reactivate and multiply intracellularly (3), after lytic burst of the host cells, intracellular yeast cells are released into the extracellular environment and infect more macrophages.	32
Figure 3.1. (A, B and C): Workflow of how the microarray data was generated and processed in Genespring GX.....	51
Figure 3.2. Flow chart of research activities	61
Figure 4.1. Sequence alignment of the ITS gene region of four <i>C. neoformans</i> environmental strains (H4, S48B and S68B strains) with that of H99 strain	63
Figure 4.2 A and B. PCR fingerprinting analyzed by the PyElph software. (A) 5µl of each strain and 100bp ladder was loaded on 2% agarose gel. The PCR fingerprinting patterns generated by using (GTG) ₅ primers was observed. The graph situated below the image is implemented for automatic lane detection base on computing the maximum value of each pixels column. (B) UPGMA algorithm based-dendrogram shows the cluster analysis of four <i>C. neoformans</i> strains. H99 and S48B were grouped in a cluster while S68B and H4 were grouped in another cluster (0.0% difference).	65
Figure 4.3. <i>In vivo</i> virulence study among different <i>C. neoformans</i> strains presented using Kaplan-Meier survival curve.....	67
Figure 4.4. (A, B and C): The gross appearance of lung tissues harvested from infected mice 21 days post-infection. A) Mice infected with environmental strain (S48B), dark	

areas suggesting of multiple hemorrhagic (filled arrowhead) and abscess-like (open arrowhead) surface lesions were seen in S48B- infected mice (shown by arrows). B) Lung infected with clinical strain (H99), severe inflammation can be seen clearly in H99-infected lung tissue (shown by arrow). C) Uninfected mouse lung used as a control.69

Figure 4.5. (A and B): SDA plates inoculated with the lung homogenate of H99 infected mice. Different serial dilutions, A) x1000 and B) x100 in duplicates were prepared from 10µl of each lung homogenate and spread on each plate..... 71

Figure 4.6. Comparison of the results of CFU assay for different strains of *C. neoformans*..... 71

Figure 4.7. The growth curve determination of *C. neoformans* strains (H99, H4, S48B and S68B) cells upon culturing at 37°C with gentle shaking. 72

Figure 4.8. Determination of capsule formation for H4, S48B, S68B and H99 strains of *C. neoformans*.. 74

Figure 4.9. Determination of the phospholipase activity of *C. neoformans* using egg-yolk agar plates. 76

Figure 4.10 Determination of the laccase activity of *C. neoformans* strains using L-Dopa containing medium..... 77

Figure 4.11. Determination of antifungal susceptibility profiles of *C. neoformans* using E-tests..... 78

Figure 4.12. Agarose gel electrophoresis of the RNA extracted from *C. neoformans* strains (H4, S48B, S68B and H99) on a 0.8% agarose gel stained with gel red..... 80

Figure 4.13. Densitometry plot of the total RNA using Bioanalyser analysis. The gel-like image bands showed high quality RNA, that were represented as two distinct bands corresponding to the 18S and 28S ribosomal RNAs..... 81

Figure 4.14. Electropherogram of the total RNA for each sample using Bioanalyser. No contaminating genomic DNA peak was found between the 18S and 28S peaks in all samples as can be seen in the graph. 82

Figure 4.15. Quality control of samples using principal component analysis (PCA) algorithm base on raw signal values* 84

Figure 4.16. Determination of pairwise correlation coefficient matrix (Rep1–2: replicates of samples). 85

Figure 4.17. Box-Whisker Plot on normalized data using the Gene Spring software analysis.....	87
Figure 4.18. Quality control of samples using principal component analysis (PCA) algorithm base on normalized signal values*	88
Figure 4.19. Heat map of Gene expression study (Colour range represents log ₁₀ (FC) of the microarray intensities.).....	90
Figure 4.20. Gene expression analysis of H99 versus environmental strains. Scatter plots show the expressions of total probes in the H99 versus H4, S48B or S68B. X and Y axis show log ₁₀ raw intensity values.....	92
Figure 4.21. Venn diagram shows the distribution and the number of the genes (probes) in each group of comparison.	94
Figure 4.22. qRT-PCR verification. RNAs were extracted from H99, H4, S48B and S68B for qRT-PCR analysis.	104
Figure 4.23. Pathway analysis. Histogram shows a summary of DAVID pathway annotation analysis.	108
Figure 4.24. Heat maps of genes involved in each pathway annotation of 65 significantly regulated genes.....	112
Figure 4.25. qRT-PCR verification. RNAs were extracted from H99, H4, S48B and S68B for qRT-PCR analysis.	118
Figure 4.26 (A and B). Agar disk diffusion assay. (A) Diameters of the inhibition zone after 48 hours of incubation. Data shown is a representative picture of three independent experiments. (B) Graph shows the inhibition diameter (mm) of <i>C. neoformans</i> plate after triclosan treatment.....	120
Figure 4.27. CFU count of the media recovered SDA plates from the wells treated with ≤1 µg/ml of triclosan.	122
Figure 4.28. Synergy effect of triclosan with amphotericin B and fluconazole. (A, B) Agar disk diffusion assay for triclosan (TCS) in combination with (C) amphotericin B (AMB), or (D) fluconazole (FLC) in <i>C. neoformans</i> H99-containing agar plates. Asterisk (*) indicates partial inhibition. Data shown are representative pictures of three independent experiments. (E, F) Graphs show the inhibition diameter (mm) of <i>C. neoformans</i> plate after triclosan treatment in combination with AMB or FLU. X-axis shows Log concentration of triclosan.	124
Figure 4.29. Checkerboard assay. Synergy effect of triclosan with amphotericin B or fluconazole in <i>C. neoformans</i>	127

Figure 4.30. Electron microscopic pictures of *C. neoformans* with or without exposure to triclosan (0.5 µg/ml) for 2 hours. (A, B) Untreated control cells showed intact nucleus and cytoplasm. (C-F) Triclosan-treated *C. neoformans* showed apoptotic morphologies. Note the appearance of apoptotic features such as mitochondrial swelling (arrow) and nuclear chromatin condensation (broken arrow)..... 128

Figure 4.31. Apoptosis of triclosan-treated *C. neoformans* H99 cells was determined by TUNEL assay followed by flow cytometry analysis.. 130

University of Malaya

LIST OF TABLES

Table 2.1. Genes linked to the classical virulence phenotypes (capsule, melanin, temperature and intracellular growth) in <i>C. neoformans</i>	29
Table 2.2. List of studies that have used microarray for identifying virulence genes	35
Table 3.1. Preparation of reagent mixture for RAPD PCR assay for amplification of <i>C. neoformans</i> strains using primer (GTG) ₅	44
Table 3.2. Reagents used for RNA isolation.....	48
Table 3.3. Microarray chip was customized to cover all <i>C. neoformans</i> genes in the Broad Institute database.	52
Table 3.4. cDNA synthesis reagents for Real time PCR	53
Table 3.5. Primer sequences for qRT-PCR analysis. List of the forward and reverse primer sequences (5'-3') of 5 well-known genes linked to the major virulence phenotypes for qRT-PCR analysis.	54
Table 3.6. Primer sequences for qRT-PCR analysis. List of the forward and reverse primer sequences (5'-3') of the up- and down-regulated genes selected for qRT-PCR analysis.....	55
Table 3.7. Preparation of reaction mixture for Real Time PCR.....	56
Table 3.8. Determination of the synergy test using triclosan alone or in combination with amphotericin or fluconazole.....	57
Table 4.1. Numbers of mice died at different days post-infection with <i>C. neoformans</i> H99.....	66
Table 4.2. CFU determination of lung or brain homogenates from <i>C. neoformans</i> -infected mice 20-day post-infection.....	70
Table 4.3. Determination of the phospholipase activity of <i>C. neoformans</i> using egg-yolk agar plates. <i>C. albicans</i> ATCC 90028 used as a positive control.....	75
Table 4.4. Laccase assay of <i>C. neoformans</i> strains.....	77
Table 4.5. Measurements of MIC mean±SD from 2 duplicate plates using MIC strips.	79
Table 4.6. Measurement of RNA concentration and purity of RNA by nanodrop spectrophotometer and Agilent's 2100 Bioanalyser	81
Table 4.7. List of 18 significantly regulated genes overlapped in environmental strains S48B and S68B versus the H99 clinical strain.....	95

Table 4.8. List of 21 significantly regulated genes overlapped in environmental strains H4 and S48B versus the H99 clinical strain.	96
Table 4.9 (continued). List of 77 significantly regulated genes overlapped in environmental strains H4 and S68B versus the H99 clinical strain.	99
Table 4.10. List of 41 genes significantly up-regulated in H99 versus H4, S48B and S68B strains.	100
Table 4.11. List of 24 genes significantly up-regulated in H99 versus H4, S48B and S68B strain.	102
Table 4.12. The 65 significant genes which were differentially regulated in H99 compared to environmental strains were analyzed and top nine regulated pathways are presented.	107
Table 4.13. Pathway annotation by DAVID bioinformatics resource	110
Table 4.14. Comparison of the fold changes of reported well-known virulence genes in H99, H4, S68B and S48B strains.	114
Table 4.15. Measurements of inhibition zones of different concentrations of triclosan (3.125, 6.25, 12.5, 25, 50 and 100 µg) on a <i>C. neoformans</i> H99 SDA agar plate for an incubation period of 48 hours.	119
Table 4.16. MIC-1 (80% inhibition) and MIC-2 (50% inhibition) readings of triclosan in different strains of <i>C. neoformans</i> and <i>C. albicans</i>	121
Table 4.17. Minimum fungicidal concentration (MFC) assay.	122
Table 4.18. Agar disk diffusion assay.	125
Table 4.19. Checkerboard assay. Synergy effect of triclosan with amphotericin B or fluconazole in <i>C. neoformans</i>	126

LIST OF SYMBOLS AND ABBREVIATIONS

Abbreviations	Description
%	Percent
A	Alpha
B	Beta
µg	Microgram
µg/ml	microgram per milliliter
µl	Microliter
°C	degree Celsius
5'-FC	5'-flucytosine
5'-FU	5'-fluorouracil
<i>ADE2</i>	Phosphoribosylaminoimidazole carboxylase
AFLP	amplified fragment length polymorphism
AIDS	acquired immune deficiency syndrome
<i>AIF1</i>	Apoptosis-inducing factor-1
ALCD	apoptosis-like cell death
AmBd	amphotericin B deoxycholate
ANOVA	Analysis of variance
<i>ARN1</i>	Siderophore iron transporter 1
<i>ARN2</i>	Siderophore iron transporter 2
ATCC	America Type Culture Collection
BAC	bacterial artificial chromosome
Bcl2	B-cell lymphoma 2
BLAST	Basic Local Alignment Search tool
Bp	base pair
<i>BUD8</i>	bud-site-selection protein 8
<i>C. albicans</i>	<i>Candida albicans</i>
<i>C. gattii</i>	<i>Cryptococcus gattii</i>
<i>C. neoformans</i>	<i>Cryptococcus neoformans</i>
<i>CAC1</i>	Chloroplastic A acetylcoenzyme carboxylase 1
cAMP	cyclic adenosine monophosphate
<i>CCH1</i>	Calcium channel homolog
<i>CDC48</i>	Cell division cycle
cDNA	complementary deoxyribonucleic acid
CFU	colony forming unit
CFU/mL	colony forming unit/ milliliter
CGH	comparative genome hybridization
<i>CLF1</i>	Crooked neck-like factor
CLSI	Clinical and Laboratory Standards Institute
<i>CNA1</i>	Calcineurin subunit A
<i>CNB1</i>	Calcineurin subunit B

CNS	central nervous system
<i>COR1</i>	Cytochrome c reductase
CSF	cerebrospinal fluid
CTS1	Chitinase
<i>DAK1</i>	DihydroxyAcetone Kinase
DAVID	Database for Annotation, Visualization and Integrated Discovery
DMEM	Dulbecco's Modified Essential Medium
DMSO	demethyl sulfoxide
DNA	deoxyribonucleic acid
dNTP	Deoxynucleotide
dUTP	2'-deoxyuridine 5'-triphosphate
<i>ECM15</i>	Extra cellular mutant
EDTA	Ethylenediaminetetraacetic acid
<i>ENO2</i>	Enolase 2
<i>FAS1</i>	Fatty acid synthase 1
<i>FAS2</i>	Fatty acid synthase 2
FBS	fetal bovine serum
FC	fold change
FcR	Fc receptor
FCS	fetal calf serum
FDR	false discovery rate
FE	fold enrichment
FITC	fluorescein isothiocyanate
FSC	forward scatter
<i>GDA1</i>	Guanosine-diphosphatase
<i>GDH3</i>	Glutamate dehydrogenase
GDP	guanosine diphosphate
<i>GOA1</i>	Guanine nucleotide-binding protein G(o) subunit alpha
<i>GRE2</i>	NADPH-dependent methylglyoxal reductase
GXM	Glucuronoxylomannan
HAART	Highly Active Antiretroviral Therapy
<i>IC11</i>	Isocitrate lyase
IFN- γ	interferon- γ
ITS	internal transcribed spacer
IV	Intravenous
kDa	Kilo Daltons
KEGG	Kyoto Encyclopedia of Genes and Genomes
L-DOPA	L-3, 4-dihydroxyphenylalanine
MALDI-TOF-MS	Matrix-Assisted Laser Desorption/Ionization Time-of-Flight Mass Spectrometry
MAP	mitogen-activated protein
Mb	mega base

Mbp	mega base pairs
<i>MCA1</i>	MetaCaspase1
<i>MCA2</i>	MetaCaspase 2
<i>MDA5</i>	Melanoma Differentiation-Associated protein 5
MHC	major histocompatibility complex
MIF	migration inhibitory factor
ml	Milliliter
mm	Millimeter
mM	Millimolar
<i>MMF1</i>	Mitochondrial matrix factor 1
MMLV	Moloney Murine Leukemia Virus
MOI	multiplicity of infection
MP	Mannoproteins
<i>MPH2</i>	Maltose permease homolog 2
mRNA	messenger RNA
<i>MVA1</i>	Hydroxymethylglutaryl-CoA synthase
Na ₃ VO ₃	sodium orthovanadate
NAD	Nicotinamide adenine dinucleotide
NCBI	National Center for Biotechnology Information
ng	Nanogram
NK cells	natural killer cells
nm	Nanometer
OD	optical density
PBS	phosphate-buffered saline
PCR	polymerase chain reaction
PI	propidium iodide
<i>PKA1</i>	protein kinase A
<i>PLB1</i>	PhosphoLipase B
PMA	phorbol myristate acetate
<i>PUT3</i>	Proline utilization trans-activator
RAPD	random amplified polymorphic DNA
<i>RAS1</i>	Homologous to RAS proto-oncogene
RFLP	Restriction Fragment Length Polymorphism
<i>RGA2</i>	Rho GTPase-activating protein 2
<i>RHO5</i>	Ras Homolog
RIN	RNA integrity number
RIPA	radioimmunoprecipitation assay
RNA	ribonucleic acid
ROS	the reactive oxygen species
Rpm	revolutions per minute
RPMI	Roswell Park Memorial Institute
<i>S. cerevisiae</i>	<i>Saccharomyces cerevisiae</i>

SDA	Sabouraud's dextrose agar
SDB	Sabouraud's dextrose Broth
SDS	sodium dodecyl sulphate
<i>SEC2</i>	Rab guanine nucleotide exchange factor (<i>SEC2</i>)
SFM	serum free medium
<i>SKN7</i>	Suppressor of Kre Null
<i>SNF3</i>	High affinity glucose transporter 3
<i>SPF1</i>	Ion-transporting P-type ATPase
<i>SRE1p</i>	Sterol regulatory element binding protein
<i>STE12</i>	Serine/threonine-protein kinase 12
TEM	transmission electron microscopy
TNF α	tumour necrosis factor alpha
TUNEL	TdT-mediated dUTP nick end labeling
UPGMA	Unweighted Pair Group Method with Arithmetic Mean
<i>URA5</i>	Uracil requiring
<i>URE1</i>	Urease
v/v	volume to volume
VIO	Vancouver Island outbreak
<i>VPH1</i>	vacuolar APT-ase
w/v	weight per volume
YPD	yeast peptone dextrose

LIST OF APPENDICES

Appendix A	Preparation of culture media, reagents and chemicals	196
Appendix B	OD readings of <i>C. neoformans</i> strains	202

University of Malaya

CHAPTER 1: INTRODUCTION

1.1 Introduction

Cryptococcus neoformans has been recognized as an opportunistic yeast pathogen which causes meningoencephalitis especially amongst HIV-infected patients. The infection can be acquired from the inhalation of desiccated yeast cells and basidiospores in the environment, especially from bird droppings. Due to the growing number of susceptible hosts and AIDS patients, the incidents of cryptococcosis have grown significantly in recent years. The emergence of drug resistance and limited antifungal treatment options for cryptococcosis have also resulted in an increase in the morbidity and mortality of the infected individuals (Byrnes *et al.*, 2011). Park *et al.* (2009) reported that approximately 957 900 cases (range, 371, 700-1, 544 000) of cryptococcal meningitis occur globally, with 624 700 deaths (range, 125,000-1, 124,900) recorded by 3 months after the diagnosis of the infection (Park *et al.*, 2009).

C. neoformans enters human hosts through inhalation from the environment. The organism remains harmless unless it expresses virulent factors which promote dissemination into host's circulation (Liu *et al.*, 2012). Virulence factors that have been identified in *C. neoformans* include melanin, polysaccharide capsules such as glucuronoxylomannan (GXM), galactoxylomannan (GalXM), mannoprotein (MP), mating type alpha, phospholipase, superoxide dismutase, cell wall integrity enzymes, protein kinases and urease (Liu *et al.*, 2008). Virulence factors in *C. neoformans*, for example, melanin synthesis render the pathogen protection against host and environmental stresses, while the polysaccharide capsule wall which is comprised of GXM, GalXM and MP, provides protection against phagocytosis. The integrity of these polysaccharides on cell wall enables proper fungal growth, ability to survive environmental stress and to evade host's immune responses. For example, GXM inhibits production of IFN- γ proinflammatory cytokines, suppresses T cell proliferation,

dampens T helper responses and limits major histocompatibility complex (MHC) class II expression on antigen presenting cells (APC) (Monari *et al.*, 2005).

One of the main features that differentiate *C. neoformans* from other fungal pathogens is the polysaccharide capsule surrounding the cell wall (Doering, 2009). Capsule size increases during infection and in different growth conditions such as low iron availability, presence of animal serum, and carbon dioxide concentrations (Vartivarian *et al.*, 1993). Currently our knowledge of capsule regulation is largely based on studies where mutations of certain genes resulted with abnormal capsules. The correlation between capsule size and strain virulence *in vivo* (Clancy *et al.*, 2006), indicates the regulation of capsule formation as a central role in the cryptococcal pathogenesis..

C. neoformans environmental strains display different pathogenicity as observed in their abilities in causing death in the infected mice (Da Silva *et al.*, 2006). It is believed that since the most virulent strains are isolated from the central nervous system in mice, factors that promote neurological infection are most likely to contribute to the increased lethality in mice (Da Silva *et al.*, 2006). In addition, many environmental and clinical strains of serotype A are not able to be differentiated. . However, most environmental strains of *C. neoformans* var. *grubii* (serotype A) are not lethal for mice as opposed to clinical strains (Litvintseva & Mitchell, 2009) and this raised the question on the commonly accepted notion that “fully virulent strains” are readily isolated from the environment (Idnurm *et al.*, 2005). Previous studies have partly revealed the basic mechanism of *C. neoformans* which plays an essential role in the invasion process (Litter *et al.*, 2005) such as capsular component which plays a role in adherence to the host cells prior to the invasion process (Jong *et al.*, 2007). However, there are still unknown genes and pathways which may contribute to the virulence.

Comparison of gene expression profiles of the clinical reference strain H99 and environmental strains can assist in the characterisation of potential virulence genes which are responsible for causing infections in humans. Microarray which facilitate studies on the expression of virulence genes or their RNA products can give an overall picture of gene expression (Tarca *et al.*, 2006). Microarray approach is expected to provide information on the regulation of essential fungal virulence factors in *C. neoformans* (Haynes *et al.*, 2011). For example, a partial-genome microarray can be applied for investigation of gene expression associated with the survival of *C. neoformans* at 37°C, (Kraus *et al.*, 2004). Several genome-wide transcription studies using microarray approach have identified differentially expressed genes among the clinical and environmental strains. Comparison of the gene expression profiles of the clinical and environmental strains have successfully identify various potential genes which are responsible for cryptococcal pathogenicity (Haynes *et al.*, 2011). For example, in a research that compared the transcriptional profiles of *C. neoformans* var. *grubii* strains isolated from the cerebrospinal fluid (CSF) of two AIDS patients, similar expression patterns were noted for the two strains under the same conditions. Virulence genes with stress response functions including *RIM101*, *ENA1*, and *CFO1*, were regulated in the similar fashion as the two clinical strains (Chen *et al.*, 2014).

C. neoformans var. *grubii*, the most common variety of *C. neoformans* (includes strains of serotype A), is responsible for more than 99% of infections in AIDS patients reported worldwide. Another variety of *C. neoformans*, var. *neoformans* (includes serotype D) is also a casusative agent for individuals with immunosuppression (Casadevall & Perfect, 1998). Serotype AD, a hybrid strain between serotypes A and D and the least common serotype, has also been isolated from

clinical specimens and the environment samples (Brandt *et al.*, 1995; Lengeler *et al.*, 2001).

Despite extensive studies in *C. neoformans* var. *grubii*, the population structure, reproduction and the extent of clonality of *C. neoformans* remain unresolved. According to a study that compared clinical and environmental strains of *C. neoformans*; of 800 environmental strains collected from North Carolina, serotypes A and D, as well as serotype AD were identified. Twelve genotypes (A1, A1C-A1, A1-CA2, A2, A3, A4, A5, A6, A6", A7, A8, A8") were characterized among serotype A strain using amplified fragment length polymorphism fingerprinting (AFLP) method. Six of these genotypes (A1, A3, A4, A5, A6, and A7) existed in both clinical and the environmental samples whereas A8 and A8" were found only in clinical samples (Litvintseva *et al.*, 2005).

On the other hand, the widespread use of anti-microbial agents for treatment of fungal infection has caused the emergence of resistant fungal strains globally. Many pathogens including *C. neoformans* demonstrate increasing resistance to antifungal drugs such as amphotericin B and fluconazole (Perfect & Cox, 1999). According to the susceptibility data obtained from 317 clinical strains of *C. neoformans* var. *neoformans*, amphotericin B resistance was noted in 5.3% of the strains, while fluconazole decreased susceptibility was noted in 46.6% of the strains investigated (Perkins *et al.*, 2005). Therefore, it is essential to have studies to discover new drugs or combinations of several anti-microbial drugs for these emerging drug-resistant strains. Some combinations of anti-fungal drugs demonstrated synergistic effect and showed superiority to the currently available therapy (Mukherjee *et al.*, 2005; Munoz *et al.*, 2006). For instance, a combination of fluconazole and amphotericin B provide synergistic effect to the treatment of candidemia (Odds, Frank C, 2003).

Triclosan (2,4,4'-trichloro-2'-hydroxydiphenylether, C₁₂H₁₇Cl₃O₂), is a chlorinated compound used widely for personal healthcare products including soap and tooth paste (Jones *et al.*, 2000). Broad-spectrum anti-microbial properties of triclosan has been demonstrated against bacteria and fungi previously (Schweizer, 2001), with MICs generally ranging from 0.1 to 30 mg/l. Several fungal species including *Candida* species have been reported to be susceptible to triclosan (Regos *et al.*, 1979; Vischer & Regos, 1974). Previous studies reported that triclosan does not affect the host biochemical pathway, but is likely to perturb cell structure resulting in a loss of permeability-barrier functions (Villalaín *et al.*, 2001). Besides, triclosan can exert its activity by inhibiting bacterial and fungal fatty acid synthetic enzyme, enoyl-[acyl-carrier protein] reductase (Zhang *et al.*, 2006). As triclosan activity on *Cryptococcus* has not yet been revealed, this study aims to investigate the anti-fungal activity of triclosan on *Cryptococcus* strains.

The isolation of *C. neoformans* strains from both clinical and environmental samples suggests that fully virulent strains can be found in the environment (Casadevall & Perfect, 1998; Casadevall *et al.*, 2003; Idnurm *et al.*, 2005). Therefore, the virulence of *C. neoformans* is not solely based on the sources of the strains. The virulence of *C. neoformans* in murine model has been investigated for many years whereby environmental strains have been shown to have the ability to cause infections (Emmons, 1951; Kao & Schwahz, 1957). Environmental strains have been reported to cause different severity in mice, with some presenting with signs of cryptococcosis, while others were asymptomatic (Da Silva *et al.*, 2006). In a study to evaluate the virulence of *C. neoformans* strains in mice, the mean lethal dose causing death in 50% of the infected mice has been reported to be significantly higher for environmental strains compared to the clinical strains (Fromtling *et al.*, 1988). Similarly, another study also

reported that the clinical strains were more virulent than the soil strains (Hasenclever & Emmons, 1963).

Since virulence factors help fungi to invade host and cause disease, it is important to identify genes responsible for the production of these virulence factors. Besides, for development of future treatment regimens it is important to search beyond the limited antifungals available today.

This study aimed to identify novel genes which may be associated with the virulence of *C. neoformans*. In the first phase of the study, the infectivity of three environmental *C. neoformans* strains (H4, S48B and S68B) isolated from soil contaminated with bird droppings, and the H99 reference clinical strain, was investigated using C57BL/6 wildtype mice. Genome-wide transcription study using microarray approach was then conducted to identify the differentially expressed genes among the strains. Comparison of the gene expression profiles of the H99 clinical and environmental strains (H4, S48B and S68B) were made using microarray to identify potential genes which are responsible for cryptococcal pathogenicity. In the second part of the study, the anti-fungal effect of triclosan on *C. neoformans* was evaluated and the interactions between triclosan and standard anti-fungal drugs amphotericin B and fluconazole were investigated using microdilution synergy checkerboard assay. Additionally, morphological changes of triclosan-treated *C. neoformans* were examined under transmission electron microscope.

1.2 Objectives

1. To compare the degree of virulence in a clinical reference strain (H99) and four environmental strains of *C. neoformans* isolated from soil contaminated with bird droppings using *in vivo* and *in vitro* methods.
2. To identify specific genes and pathways expressed in the clinical reference strain (H99) which are responsible in the fungal pathogenesis.
3. To evaluate the anti-fungal and fungicidal synergism effects of triclosan in *C. neoformans*.

University of Malaya

CHAPTER 2: LITERATURE REVIEW

2.1 *Cryptococcus*

There are 39 heterobasidiomycetous species in the genus *Cryptococcus*. The *Cryptococcus* genus is characterized as encapsulated budding yeasts. Among all species in the genus, of *Cryptococcus neoformans* and *Cryptococcus gattii* have been recognised as human pathogens which cause cryptococcosis (Casadevall & Perfect, 1998). The divergence of *C. neoformans* and *C. gattii* genomes occurred over 34 million years ago, and this has resulted with two *Cryptococcus* species with distinct differences in the ecological and pathological process (D'souza *et al.*, 2011; Sharpton *et al.*, 2008). *C. neoformans* is now referred to as a species complex consisting of separate species and varieties (Lin & Heitman, 2006) *C. neoformans* var. *grubii* (serotype A), *C. neoformans* var. *neoformans* (serotype D), and *C. gattii* (originally serotypes B and C). *C. neoformans* var. *grubii* and var. *neoformans* (Kwon-Chung *et al.*, 1982a). The combination of different molecular typing techniques have further differentiated *C. neoformans* into five major molecular types, i.e., VNI, VNII and VNB (var. *grubii*), VNIV (var. *neoformans*), VNIII (A × D hybrids). *C. gattii* contains the molecular types VGI, VGII, VGIII, and VGIV for serotypes B and C (Aminnejad *et al.*, 2012). The A and D serotypes are estimated to separate from each other around 18 million years ago as determined by population genetics studies (Xu *et al.*, 2000).

C. neoformans is a pathogen which causes severe disease among immunocompromised individuals worldwide, killing more than 600,000 people per year (Park *et al.*, 2009). It was initially recognised to cause disease in the 1890s when a *Saccharomyces*-like organism was isolated from a young woman with bone infection (Busse, 1894). Francesco Sanfelice later reported the isolation of a similar organism from fermenting peach juice, which he referred as *Saccharomyces neoformans* due to its unique colony morphology (Sanfelice, 1894). Eventually, this organism was renamed in

1901 by Jean-Paul Vuillemin renamed as *Cryptococcus neoformans* since it did not generate ascospores which is a defining feature of *Saccharomyces* (Barnett, 2010).

Other than *C. neoformans* and *C. gattii*, at least 37 other rarely infectious cryptococcal species have also been identified from very diverse geographical locations, including Antarctica and the Himalayas (Casadevall & Perfect, 1998; Kordosis *et al.*, 1998). These organisms resemble *C. neoformans* in the virulence factors, transmission, and host immune response (Ikeda *et al.*, 2000; Mccurdy & Morrow, 2003), but the laccase activity is weaker (Ikeda *et al.*, 2002).

2.1.1 *C. neoformans*

C. neoformans in the clinical sample often present as encapsulated spherical yeasts when viewed under microscope (Mitchell & Perfect, 1995). The size of the capsule varied depending on the cryptococcal strain or the growth environment. Most of the strains appear with a capsule at 4–10 µm in diameter. A heavily encapsulated strains may have a cell diameter of up to 80 µm (Casadevall & Perfect, 1998).

C. neoformans can cause human infections by inhalation of infectious particles (spores or desiccated cells) from soil and avian habitats. Therefore, the lung serves as the portal of entry where the infection begins (Casadevall & Perfect, 1998). In addition to colonization of the host's respiratory tract and stays dormant without causing disease (latency) in healthy people (Garcia-Hermoso *et al.*, 1999), it is also capable of disseminating to other organ of the human body, particularly the central nervous system (CNS) and resulting with meningoencephalitis which can cause fatal if untreated (Casadevall & Perfect, 1998).

2.1.2 Mating type

C. neoformans is found heterothallic and mainly as vegetative haploid form, with each mating type a (MAT_a) or mating type α (MAT_α). Filamentous teleomorph can

form by mating of opposite mating type cells in the event of nutrient limitation (Kwon-Chung, 1975). Most environmental and clinical cryptococcal strains have been found mostly as haploid vegetative yeast (Kwon-Chung, 1976; Lin *et al.*, 2005). *Cryptococcus* can also go through monokaryotic fruiting or same-sex mating; from 2 different α cells to produce α/α diploids and α haploid offspring (Lin *et al.*, 2005). Same-sex mating may provide benefits to survive longer under changing or harsh environments (Lin *et al.*, 2007). The mating type loci have been reported to be responsible for the virulence of *C. neoformans* var. *neoformans* (serotype D) (Kwon-Chung *et al.*, 1992). The involvement of several genes of the mating loci in fungal morphogenesis and virulence have been analysed (Davidson *et al.*, 2003; Lengeler *et al.*, 2000; Wang *et al.*, 2000). For instance, the mating type loci of serotype A does not contribute to the virulence in *C. neoformans* var. *grubii* (Hull & Heitman, 2002; Nielsen *et al.*, 2003).

2.1.3 Epidemiology

While *C. neoformans* is associated with bird droppings (particularly that of pigeons) and causes human infections worldwide, the transmission of *C. gattii* is associated with various tree species (-eucalyptus trees) in the tropical and subtropical regions (Srikanta *et al.*, 2014). However, the emergence of *C. gattii* in Vancouver Island, Canada, a temperate zone has been reported in the 1990s (Marr, 2012). In the pre-AIDS era, the rate of invasive cryptococcosis was reported at 0.8 cases in 1 million individuals annually in USA (Mcneill & Kan, 1995). However, during AIDS epidemic, the rate had ascended to approximately 50 cases in 1 million individuals (Hajjeh *et al.*, 1999). *C. neoformans* infection frequently causes a disadvantage in the HIV-infected patients (Mirza *et al.*, 2003). Upon the usage of fluconazole and the advent of highly active antiretroviral therapy (HAART) since 1990s, the rates of cryptococcal infection decreased to 1 case in every 100,000 persons annually (Van Elden *et al.*, 2000). Countries which are less developed and severely affected by HIV infection, such

as sub-Saharan Africa, showed prevalence rates of 15 to 45% amongst those with advanced HIV infection (Clumeck *et al.*, 1984). Cryptococcal meningitis is a major cause of CNS infections in these endemic regions. The fatality rate of patients without treatment due to cryptococcosis is 100% within the first two weeks of hospitalization (Hakim *et al.*, 2000). Each year, there is an estimation of 1 million cases of cryptococcosis and nearly 625,000 deaths have been reported among HIV/AIDS patients worldwide (Park *et al.*, 2009) (Figure 2.1)

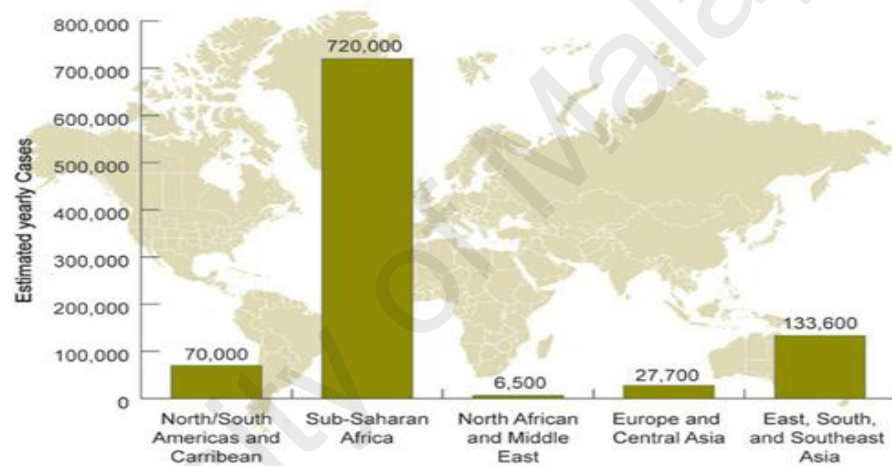
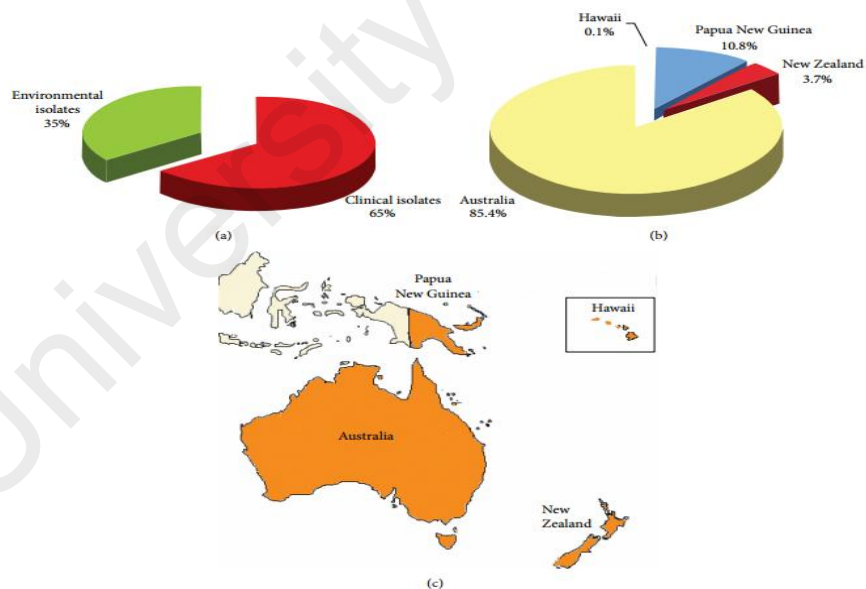


Figure 2.1. Global burden of HIV-related cryptococcal meningitis (Park *et al.*, 2009)

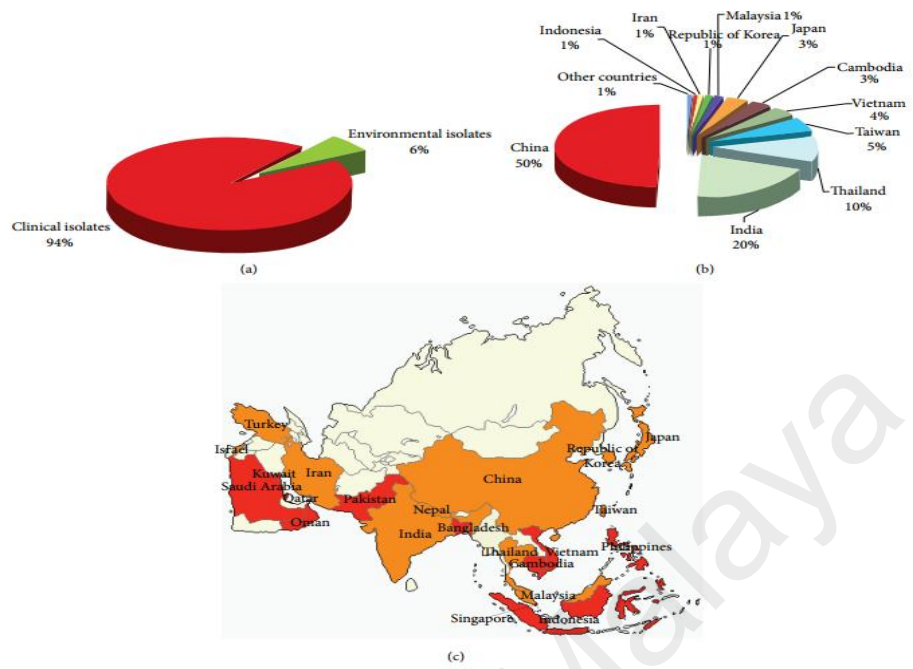
Although cryptococcosis can be caused by other *Cryptococcus* species besides *C. neoformans* (A, D, or AD), serotype A is the most prevalent serotype among in most clinical and veterinary cases reported worldwide (Litvintseva & Mitchell, 2009). However, the virulence of environmental strains of *C. neoformans* has not been thoroughly investigated in murine (Litvintseva & Mitchell, 2009). Cryptococcal infections occur in healthy and immunocompromised human hosts and domestic or wild animals (Marr, 2012), including rabbits, rats, and mice models (Perfect, 2005). The flexibility of these animal models can be applied for investigation of host-fungal

infection studies. Additionally, less complex organisms such as amoebae (Severo *et al.*, 2009), *Dictyostelium* (Desmet *et al.*, 1989), nematodes (Tassie *et al.*, 2003) and *Drosophila* (Tassie *et al.*, 2003) have been studied as potential surrogates for cryptococcal infection models. A nematode model (*Caenorhabditis elegans*) has generated similar virulence results for some mutants compared to the animal models (Liechty *et al.*, 2007). Some *C. gattii* strains not associated with the Vancouver Island–Pacific Northwest outbreak strains have also been reported in different parts of the USA (Marr, 2012). The geographical distribution of *Cryptococcus* strains in each continent has been shown on the maps by Cogliati (2013), as shown in Figure 2.2.

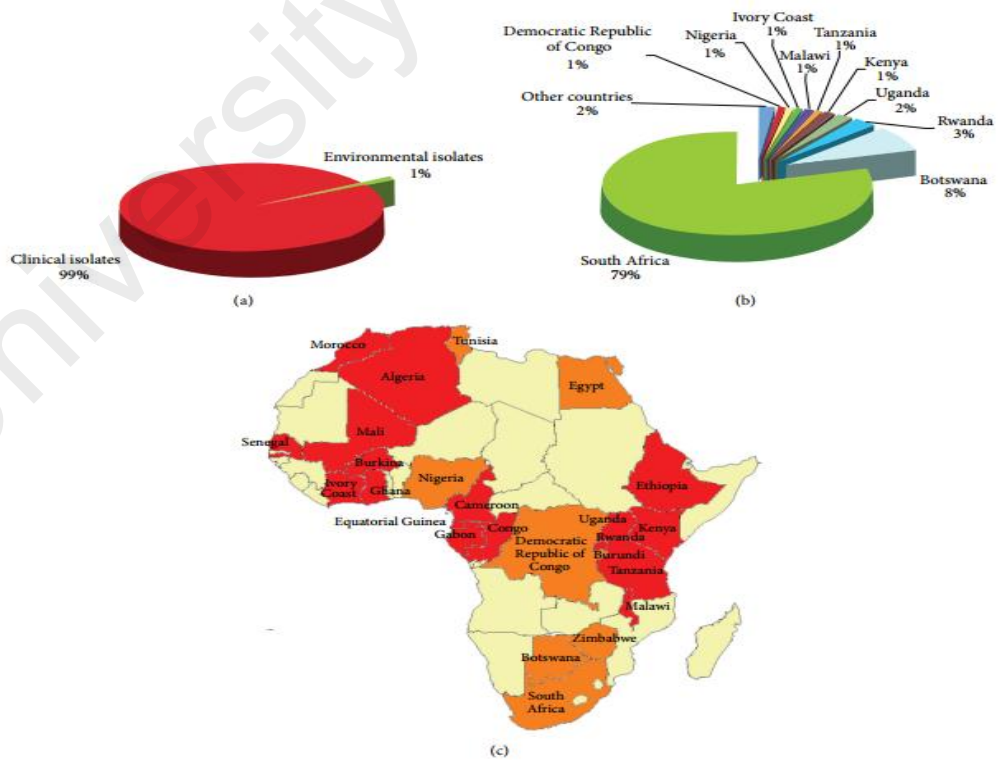
Australia)



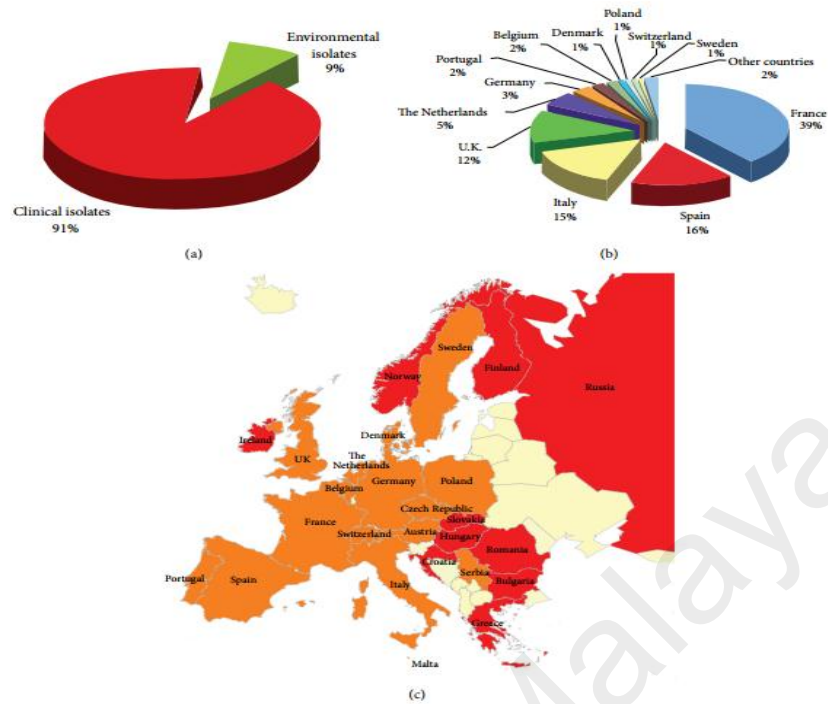
Asia)



Africa)



Europe)



South America)

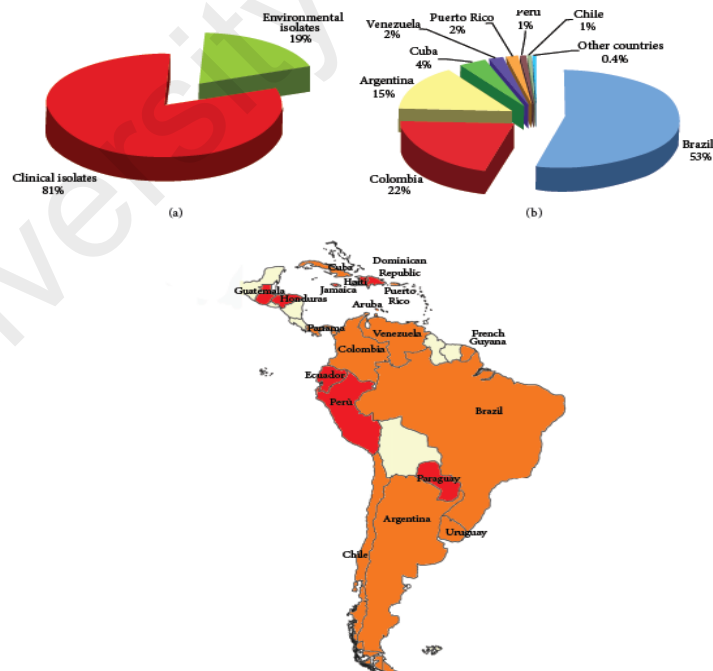


Figure 2.2. (a)Percentage of *C. neoformans* and *C. gattii* strains from clinical and environmental sources. (b). Geographical distribution of the *C. neoformans* and *C. gattii* strains (c). Clinical strains were reported from red-colored countries, whereas both clinical and environmental strains were reported from orange-colored countries (Cogliati, 2013).

The occurrence of cryptococcosis has been reported to be more frequent in adult men with impaired cellular immunity, especially those infected with HIV (Freire *et al.*, 2012; Galanis *et al.*, 2010). Other potential risk factors include immunosuppression by steroid treatment, solid organ transplantation, diabetes, lymphoma, leukaemia, sarcoidosis, cirrhosis, lupus erythematosus and rheumatoid arthritis (Barragan *et al.*, 2014; La Hoz & Pappas, 2013; Pappas, 2013).

The initial *C. neoformans* infection can stay dormant in the infected individuals for long period time. The fungus can be reactivated and cause disease once the host's immune system is compromised or suppressed. Unfortunately, as clinical test to detect latent infection has not been established, the magnitude of infection with the yeast is difficult to be determined. Most people are exposed and acquired antibodies to cryptococcal antigens before the 10 years old (Goldman *et al.*, 2001). These findings imply that asymptomatic cryptococcal infections can be controlled effectively by our immune system (Goldman *et al.*, 2001).

2.2 The cryptococcal life cycle

C. neoformans var. *grubii* and var. *neoformans* have been isolated worldwide from bird excreta and soil (Figure 2.3). Although *Cryptococcus* spp. appears as a budding yeast in most of the conditions, filamentous form can occur during mating and monokaryotic fruiting.

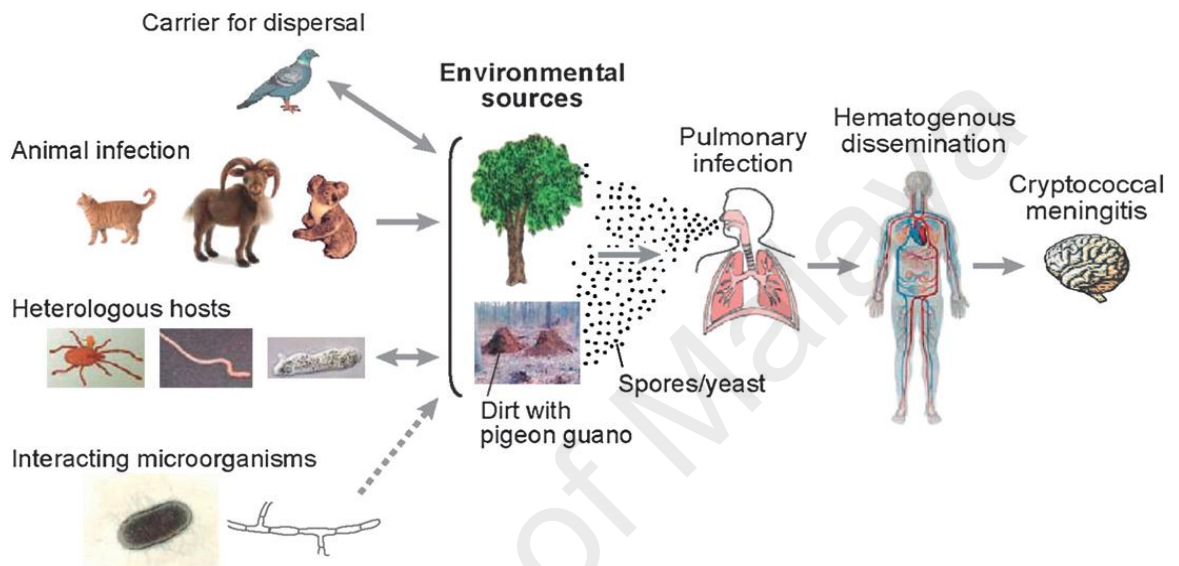


Figure 2.3. Environmental sources of cryptococcal meningitis (Xue, 2012)

The life-cycle of *C. neoformans* includes two distinct forms: asexual and sexual (Hull & Heitman, 2002). The haploid cells of a and α types join and generate dikaryotic filaments during sexual reproduction. This is then followed by fusion of the nuclei between two parental nuclei and the cells undergo meiosis and mitosis. Haploid basidiospores are generated by budding on four characteristic chains. Meiosis occurs during basidium development. Mature basidiospores are spread to the atmosphere and grow into haploid cells (Figure 2.4) (Idnurm *et al.*, 2005; Voelz, 2010). Infection in human can be initiated by exposure to the asexual budding yeast forms. However, a sexual form, the basidiospore, is hypothesized as the infectious propagule.

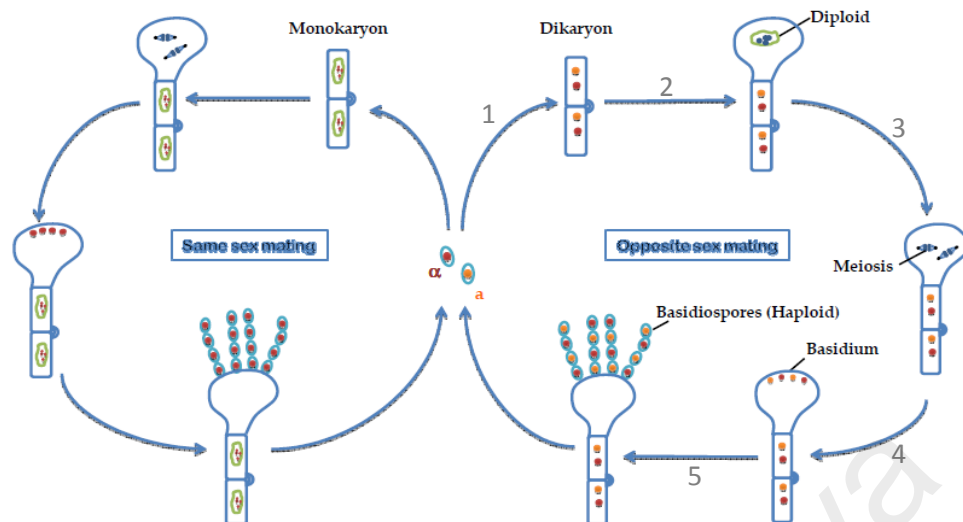


Figure 2.4. Same sex and opposite sex mating system in *C. neoformans*. During mating of opposite sex, five distinct stages have been described: 1) dikaryon, 2) nuclear fusion, 3) meiotic products, 4) basidiospores, and 5) mitosis, followed by sporulation and release of spores into the environment (Idnurm *et al.*, 2005; Voelz, 2010).

2.3 Strain identification and differentiation of Cryptococcal strains

Laboratory diagnosis of *Cryptococcus* infection is based on microscopic observation and culture of the fungal cells. Automatic and semi-automatic methods including Vitek and API 20C AUX are able to provide fast outcomes in less than 3 days. The performance of these tests are limited and require additional tests for final confirmation purpose (Mancini *et al.*, 2013; Massonet *et al.*, 2004).

Matrix-assisted laser desorption/ionisation time-of-flight mass spectrometry (MALDI-TOF-MS) has been used for the detection and identification of yeasts to the subspecies level (Ekström *et al.*, 2000). The technique determines specific protein mass spectra within a few minutes and the spectral profiles are compared with a reference library. Additionally, molecular methods such as PCR and DNA sequence analysis are useful for detection of specific genes in *C. neoformans*/*C. gattii* species complex. (White *et al.*, 1990).

At present, molecular techniques such as nested, multiplex and real-time PCR approaches are able to provide highly precise and specific results for the identification of *C. neoformans/C. gattii* complex DNA in human clinical specimens (Rivera *et al.*, 2015). The PCR results showed that the internal transcribed spacer 1 (ITS-1) and internal transcribed spacer 2 (ITS-2) coding regions of *C. neoformans/C. gattii* nested PCR assay had 100% specificity and 100% sensitivity for detection of upto 2 femtograms of cryptococcal DNA (Rivera *et al.*, 2015). Several target genes including *URA5*, *CAP59*, and ITS (18S, 5.8S, and 28S) have been used for identification of *C. neoformans* complex. The ITS region has been used frequently for identification of cryptococcal strains because of its high degree of sequence variation as compared to other ribosomal DNA regions (Bovers *et al.*, 2007). Development in molecular typing techniques such as pulse field electrophoresis, electrophoretic karyotyping, restriction fragment length polymorphism (RFLP), amplified fragment length polymorphism (AFLP), random amplified polymorphic DNA (RAPD), DNA hybridization studies, multi locus sequence typing (MLST) and polymerase chain reaction fingerprinting have led to further classification of the yeast into nine major genotypes by using a combination of several typing methods: serotype A (VNI, VNII and VNB); D (VNIV); A/D (VNIII) and *C. gattii* (VGI, VGII, VGIII and VGIV) (Cogliati, 2013). The phylogenetic relationship of members within the *C. neoformans–C. gattii* species complex has been presented in Figure 2.5 (Ma, 2009).

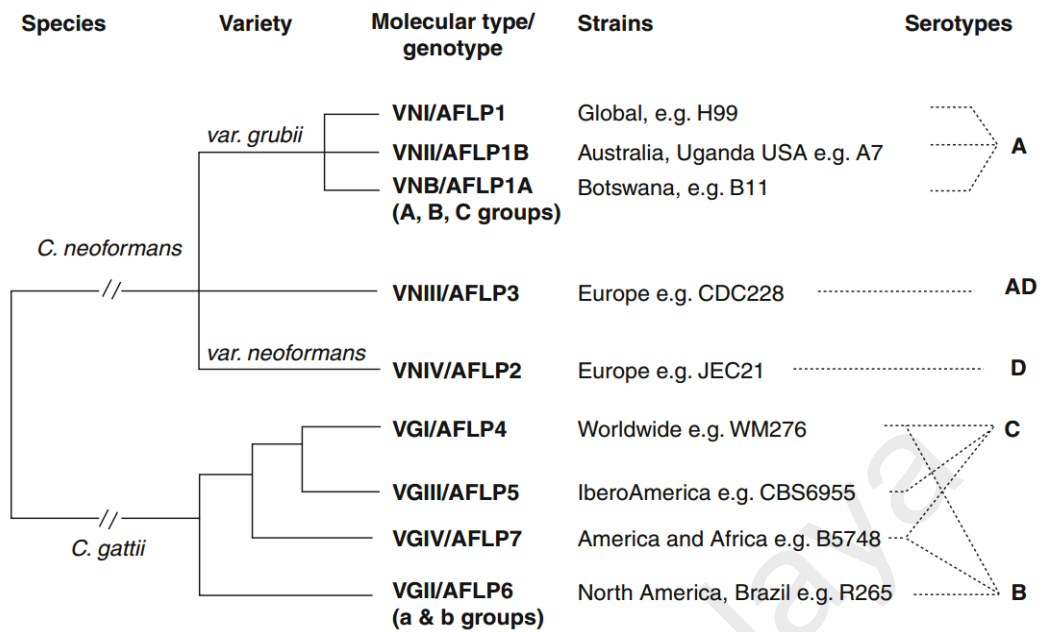


Figure 2.5. Phylogeny of the *C. neoformans*–*C. gattii* species complex by combination of different molecular typing methods including RFLP and MLST . (Ma, 2009).

PCR fingerprinting is a major typing technique used in a global molecular epidemiology study of *C. neoformans* (Meyer *et al.*, 1993). (GTG)₅ primer was used to determine yeast population by comparing the fingerprinting patterns generated from the amplification. The DNA fingerprints of strains isolated from various tissues of infected mice and patients undergoing different drug therapy were stable (Varma & Kwon-Chung, 1992). The advances of molecular techniques have assisted the understanding of taxonomy, identification, diagnosis, phylogeny and evolution of *C. neoformans* (Chen, SC-A *et al.*, 2014). The combination of information provided by different molecular approaches is able to improve diagnostic accuracy. It has been predicted that *C. neoformans var. grubii* (serotype A) and *C. neoformans var. neoformans* (serotype D) are divided genetically for more than 18 million years (Xu *et al.*, 2000) and may have some impact on the pathogenesis of the organism. For example, serine/threonine-protein kinase 12 (*STE12*) gene is crucial in contributing to the virulence of serotype D

(variety *neoformans*) as opposed to serotype A (variety *grubii*) strain (Chang *et al.*, 2001; Yue *et al.*, 1999).

2.4 Virulence phenotypes of *C. neoformans*

Several established virulence phenotypes have been reported in *C. neoformans* to allow its survival within mammalian hosts. These include melanin formation, ability to grow well at higher temperatures (mammalian body, 37°C) and generation of a polysaccharide capsule (Casadevall & Perfect, 1998). Studies on capsule generation, melanin formation, metabolic or other pathways have assisted the scientific community to understand the virulence genes in *C. neoformans* at the molecular level.

2.4.1 Melanin

Staib discovered melanin synthesis of *C. neoformans* in the 1960s (Polacheck, 1991). Melanin synthesis in *C. neoformans* is catalysed by the enzyme laccase, using o-diphenolic substance, including 3,4-dihydroxyphenylalanine (L-DOPA). A gene disruption study reported that wild type *C. neoformans* strain which produces melanin causes a more severe pathogenesis during infection (Casadevall *et al.*, 2000). Melanin is a hydrophobic pigment formed by the oxidative polymerisation which is negatively charged with high molecular weight (Casadevall *et al.*, 2000). *C. neoformans* which is melanised is more resistant to oxidative burst activity (Emery *et al.*, 1994), and phagocytosis (Huffnagle *et al.*, 1991a). thus enable *C. neoformans* to withstand the attack by the innate immunity in the host. Besides, melanised cells is more resistant to commercial drugs such as amphotericin B (Doering, 1999) compared to those without melanin formation. However, some non-*neoformans* cryptococci can also form melanin like *C. podzolicus* even though they are not pathogenic.(Petter *et al.*, 2001).

Melanin has been found to play a protective role for *C. neoformans* both in the host and environment. In the environment, melanin provide protection to *C. neoformans*

against temperature fluctuations (Rosas & Casadevall, 1997), the ionizing radiation of ultra-violet light (Wang & Casadevall, 1994), heavy metal toxicity (Garcia-Rivera & Casadevall, 2001), and hydrolytic enzymes such as those found in bird guano (Rosas & Casadevall, 2001). Non-melanizing mutants of *C. neoformans* show inhibited growth at 37°C (Kwon-Chung *et al.*, 1982b), do not accumulate in brain tissues (Kwon-Chung & Rhodes, 1986), and fail to produce lethal infections in mice (Rhodes *et al.*, 1982). Phenotypes associated with melanin production include resistance to antibody-mediated phagocytosis (Wang *et al.*, 1995) and protection from oxidation (Jacobson & Emery, 1991) as well as the inhibition of tumor necrosis factor alpha (TNF α) production and lymphoproliferation (Huffnagle *et al.*, 1995). Despite its link to virulence, there has been some debates as to whether or not melanin is generated by *C. neoformans* during infection (Liu *et al.*, 1999b; Rosas *et al.*, 2000). Melanin can modulate immune function. Cryptococcal melanin by changing the cytokine levels in the infected patient (Mednick *et al.*, 2005) and activating the complement system (Rosas *et al.*, 2002). Therefore, melanization is linked to virulence in *C. neoformans* whether directly or indirectly.

Disruption of laccase-like genes (*LAC1*) in *C. neoformans* has been shown to generate “albino” mutant with reduced virulence when inoculated into animal models (Salas *et al.*, 1996). There are several genes characterized for melanin formation and expression (Alspaugh *et al.*, 2002; Luberto *et al.*, 2001; Salas *et al.*, 1996; Toffaletti *et al.*, 2004; Yang, Z *et al.*, 2002; Zhu & Williamson, 2003).

2.4.2 Ability to grow at high temperature

The high temperature growth phenotype is one of the characteristic of *Cryptococcus* species. Serotype B and C (variety *gatti*) seem to possess evolutionary drift during growth in high temperature while serotype A

(variety *grubii*) is more resistant to high temperature stress and killing than serotype D (variety *neoformans*) strains (Martinez *et al.*, 2001).

A variety of functions can be related to temperature-related genes including those involved in stress resistancy, signaling pathways, and normal metabolic activities. For example, *VPH1* (vacuolar APT-ase) (Erickson *et al.*, 2001) and *CCN1* (homolog of *CLF1*) (Chung *et al.*, 2003) play important roles in resistance to growth in high temperature (Alspaugh *et al.*, 2000; Odom *et al.*, 1997).

2.4.3 Capsule

The polysaccharide capsule has been recognized as the most unique feature of *C. neoformans*. Capsule contains approximately 90% glucuronoxylomannan (GXM) and 5% galactoxylomannan (GalXM) as major components (Rakesh *et al.*, 2008). The large polymer, GXM has repeating structure of b-D-glucuronosyl, a-1,3-mannose with b-D-xylopyranosyl and 6-O-acetyl branching which defines the serotype of *C. gattii* and *C. neoformans*. GalXM is an α -1,6 galactan consists of β -1,3-galactose-a-1 branches, 4-mannose-a-1,3-mannose (Vaishnav *et al.*, 1998). The mass of GalXM is lesser than GXM: 1.01×10^5 g/mol versus $1.7-7.4 \times 10^6$ g/mol (Mcfadden *et al.*, 2006). Several other mannoproteins (MP) such as MP-98 and MP-99 have been reported (Huang *et al.*, 2002). Genome prediction showed the presence of 53 mannoproteins (Levitz & Specht, 2006) which share some of the structural characterizations at the regions of N-terminal, serine/threonine-rich C-terminal, as well as the glycosylphosphatidylinositol anchor motifs. Importantly, these mannoproteins can be presented by dendritic cells and stimulate T-cell responses (Mansour *et al.*, 2004; Pietrella *et al.*, 2003).

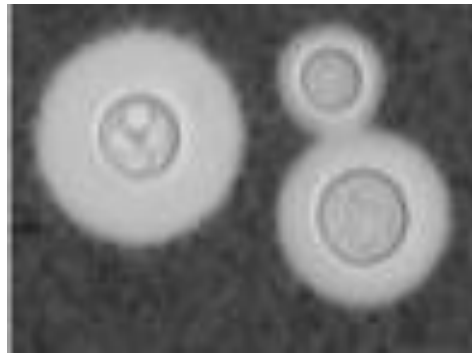


Figure 2.6. India ink stained capsule surrounding *C. neoformans* cells (Van Duin *et al.*, 2004)

The capsular mechanism that protects *C. neoformans* against the host include antiphagocytosis, inhibition of leukocyte migration, complement depletion, antibody unresponsiveness, dysregulation of cytokine secretion and enhancement of HIV infection in the brain (Casadevall & Perfect, 1998) (Figure 2.6). Several capsular synthesis and formation genes in *C. neoformans* have been recognized, through gene mutation studies. All capsule-deficient mutants have been found to be less virulent compared to the wild type strains (Alspaugh *et al.*, 1997; Chang *et al.*, 1997). Genetic manipulation to increase capsule generation can lead to a higher virulence (D'souza *et al.*, 2001; Janbon *et al.*, 2001). Capsular components which comprise more than 90% of the capsular polysaccharide mass are considered key virulence determinants in *C. neoformans*. By increasing the production of these polysaccharides, these molecules can overcome the immune response (Zaragoza *et al.*, 2009).

2.4.4 Other possible virulence phenotypes

There are several other virulence phenotypes in *C. neoformans*, and these include urease production (Cox *et al.*, 2000), phospholipases secretion (Cox *et al.*, 2001), vacuolar acidification (Erickson *et al.*, 2001), mannitol production (Chaturvedi *et al.*, 1996), and oxidative stress reduction (Cox *et al.*, 2003; Missall *et al.*, 2004).

2.4.5 Degradative enzymes

Enzymes play essential roles in the virulence of *C. neoformans*. Lipases, proteases, and DNases that are released during cryptococcal infection process can damage the host tissues, enhance survival of *C. neoformans*, and overcome host immune responses. Urease is expressed by almost all *C. neoformans* strains (Almeida *et al.*, 2015). The cryptococcal urease (URE1) has been reported as an essential virulence attribute as mice infected with URE1-mutated strain were shown to survive for a longer time than the wildtype strain (Cox *et al.*, 2000). URE1 has been reported to enhance CNS invasion of *C. neoformans* by facilitating yeast sequestration within microcapillary beds (Olszewski *et al.*, 2004).

C. neoformans also secretes proteinases which degrade the host proteins during infection process (Casadevall & Perfect, 1998). Protease degrades host collagen, elastin, fibrinogen, as well as immunoglobulins (Chen *et al.*, 1996). The association of proteolytic activity of *C. neoformans* with tissue invasion has been reported (Kwon-Chung & Varma, 2006).

Phospholipases hydrolyse the glycerophospholipids at the ester linkages thus cause destabilisation of membranes and cell lysis (Ghannoum, 2000; Santangelo *et al.*, 1999). *C. neoformans* secretes a type of phospholipase enzyme which is able to hydrolyse and transacylase lysophospholipase. Disruption of *PLB1* gene results in growth inhibition in macrophages and reduced virulence *in vivo* (Cox *et al.*, 2001). Phospholipases can assist in disruption of phagosomal membrane and is associated with virulence in mice in a dose-dependent manner (Chen *et al.*, 1997; Ganendren *et al.*, 2006).

It has been reported that defects in vacuolar acidification results in the loss of virulence phenotypes. The vacuolar (H⁺)-ATPase inhibitor bafilomycin A₁ was found to inhibit virulence expression (Erickson *et al.*, 2001). Mannitol balances the cell

reinforcements produced by both plants and animals and is important as controlling power, coenzymes, and cytoplasmic pH (Meena *et al.*, 2015). In addition, the oxidative defense mechanisms may be impaired and this can result in significant reduction in the pathogenesis (Brown *et al.*, 2007) regardless of the antiphagocytic molecules. It has been reported that *C. neoformans* activates oxidative stress response signalling cascades to detoxify the reactive oxygen species (ROS) or reactive nitrogen species (RNS), and to repair the damages due to oxidative insult when the organism is engulfed by the phagocytes (Upadhyaya *et al.*, 2013).

2.5 Pathogenicity-associated pathways

Several major signalling pathways are responsible for modulating morphological differentiation, virulence and stress responses of *C. neoformans* (Bahn *et al.*, 2005), these include cAMP-PKA and MAPK pathways. The cAMP-PKA pathway, which is functionally conserved in a large group of fungi, is activated by environmental stimuli. The cAMP-PKA pathway regulates some of the critical activities in *C. neoformans*, such as mating process, capsule and melanin generation (Alspaugh *et al.*, 2000). The Mpk1 MAPK pathway on the other hand, regulates growth at high temperature and cell-wall integrity (Gray *et al.*, 1997). The Rho1 GTPase can activate protein kinase C, which subsequently stimulates the Mpk1 MAPK molecule (Kamada *et al.*, 1996). Previous investigations showed that *C. neoformans* mutants lacking Mpk1 caused less pathogenicity during infection in animal (Kraus *et al.*, 2003) and was more susceptible to antifungal drugs (Kraus *et al.*, 2003).

The Ras-Cdc24 pathway and Ca²⁺-calcineurin pathway control *C. neoformans* growth at high temperature independently (Waugh *et al.*, 2002). *C. neoformans* ras1 (homologous to RAS proto-oncogene) mutant fails to polarise at raised temperature and is less virulent when infected in the animal models (Waugh *et al.*, 2002).

2.6 Clinical versus environmental strains

The strains of serotype A have been frequently reported in clinical and veterinary cases. It is also the most predominant serotype among the environmental strains (Litvintseva & Mitchell, 2009). Several epidemiological studies showed that many environmental and clinical strains of serotype A are not able to be differentiated from each other genetically. The virulence of environmental strains of *C. neoformans* in murine has not been thoroughly evaluated (Litvintseva & Mitchell, 2009).

The majority of the clinical and environmental strains in a Brazilian study were identified as *C. neoformans* var. *grubii* serotype A (89.5 and 52.6%, respectively), mating type α (98.1 and 94.7%, respectively) and phospholipase-positive (94.3 and 73.7%, respectively). Based on PCR-fingerprinting results, the majority of the strains were grouped into molecular type VNI (89.5 of the clinical and 52.6% of the environmental strains) (Litvintseva *et al.*, 2005). In Thailand among 365 clinical strains, majority of the strains (around 95% - 99%) were *C. neoformans* molecular type VNI (Kaochaoen *et al.*, 2013). In Korea, *C. neoformans* strains are genetically homogeneous, except few clinical strains were from molecular type VNI (Park *et al.*, 2015). Also, all 120 *C. neoformans* strains in a study were VNI subtype (Chen *et al.*, 2008). At present, nine major molecular types have been identified, i.e., VNI, VNII, VNB, VNIII, and VNIV among *C. neoformans* strains, and VGI, VGII, VGIII, and VGIV among *C. gattii* strains (Cogliati, 2013).

In a study comparing 800 clinical and environmental strains from North Carolina, serotypes A, D, and AD hybrids were the most prevalent serotypes. All environmental and clinical strains of serotype A or D had the *MAT* α mating-type allele (Litvintseva *et al.*, 2005), except the AD hybrids which had *MAT* α allele. The combined molecular data suggested that the environmental strains of *C. neoformans* was predominantly clonal, although recent or past recombination was also possible (Litvintseva *et al.*,

2005). Some studies focus on examining the genotypic diversity among a set of clinical and environmental strains to understand the associations of gene, sources, and clinical symptoms of the infected individual (Cogliati *et al.*, 2016). All of the total 83 *C. neoformans* var. *neoformans* strains collected from 11 countries across Europe, Asia and America, show similar genotype VNIV. The existence of a recombinant rather than a clonal population structure was suspected as comparison with the outgroup *C. neoformans* var. *grubii* strains suggested that the two varieties have different population structures (Cogliati *et al.*, 2016).

On the other hand, Chan & Tay (2010) reported that the enzymatic profiles for clinical and environmental strains of *C. neoformans* were similar, except for the lower proteinase and laccase activities in the environmental strains. A previous study also suggested the presence of primary resistance among *C. neoformans* environmental and clinical strains (Moraes *et al.*, 2003). Thus, surveillance of antifungal susceptibility of *C. neoformans* is crucial to ensure proper management of patients diagnosed with cryptococcosis.

The virulence determinants of environmental strains of *C. neoformans* in murine model have not been thoroughly assessed. Using a murine model, the lethality of clinical and environmental strains of serotype A with identical genotypes was compared in a study (Litvintseva & Mitchell, 2009). Of the 11 environmental strains tested in that study, only one resulted with disease 60 days post-infection, in contrast, 7 of 10 clinical strains killed the mice after 19 to 40 days. Passaging *C. neoformans* environmental strains in mice did not significantly increase their lethality (Litvintseva & Mitchell, 2009).

Since mice are susceptible and affordable, they are particularly useful species to study cryptococcal infection. Several studies reported differences in the susceptibility of

laboratory mice, including BALB/c, C57BL/6J, A/J, CBA/J, and DBA/J, to experimental cryptococcal infection (Corbel & Eades, 1976; Huffnagle *et al.*, 1998). The mice also demonstrated varying degree of susceptibility to cryptococcal infection based on the route of infection (Aguirre *et al.*, 1998). Overall, the factors that influence host's susceptibility to cryptococcal infection are not well described (Zaragoza *et al.*, 2007). As a result, this may pose difficulties for diagnosis and treatment of cryptococcal infection. In addition, different strains can cause different virulence in animal model. For example, different degree of virulence for two well-recognized strains of JEC21 (serotype D) and H99 (serotype A) has been demonstrated in mice (Bahn *et al.*, 2005).

2.7 Molecular pathogenesis study of *C. neoformans*

Several approaches have been applied for molecular pathogenesis studies of *C. neoformans*. These include characterization of evolutionary alterations between the varieties of *C. neoformans* based on their virulence genes, and species and site-specific importance of a virulence gene, and gene expression study correlating the functional roles of phenotype and the impact of a virulence gene on the host immune response (Perfect, 2005). Table 2.1 shows the list of genes which are linked to the classical virulence phenotypes of *C. neoformans* (Perfect, 2005).

Table 2.1. Genes linked to the classical virulence phenotypes (capsule, melanin, temperature and intracellular growth) in *C. neoformans* (Chen, et al., 2014; Perfect, 2005).

Capsule formation	Melanin production	High temperature growth	Intra-cellular growth defect	Stress respons
<i>CAC1</i>	<i>CAC1</i>	<i>CNB1</i>	<i>SOD1</i>	<i>SIT1</i>
<i>PKA1</i>	<i>PKA1</i>	<i>CPA1</i>	<i>SOD2</i>	<i>RIM101</i>
<i>PKR1</i>	<i>PKR1</i>	<i>CCN1</i>	<i>SKN7</i>	<i>ENA1</i>
<i>MAN1</i>	<i>VPH1</i>	<i>TPS1</i>	<i>IPC1</i>	<i>CFO1</i>
<i>CAP59</i>	<i>LAC1</i>	<i>TPS2</i>	<i>AOX1</i>	
<i>STE20</i>	<i>IPC1</i>	<i>MGA2</i>	<i>CTS1</i>	
<i>CAS1</i>	<i>MET3</i>	<i>RAS1</i>	<i>APP1</i>	
<i>CAS2</i>	<i>STE12</i>	<i>SOD2</i>	<i>PIK1</i>	
<i>CAP60</i>	<i>CLC1</i>	<i>TSA1</i>		
<i>CAP10</i>		<i>ILV2</i>		
<i>CAP64</i>		<i>SPE3/LYS9</i>		
<i>VPH1</i>		<i>MPK1</i>		
<i>STE12</i>		<i>SPE3</i>		
		<i>ADE2</i>		
		<i>STE20</i>		

Gene named abbreviations:

GPA1:G Protein Alpha subunit, *CAC1*: chloroplatic A acetylcoenzyme carboxylase 1, *VPH1*:Vacuolar pH, *LAC1*:Longevity-Assurance gene Cognate, *PKR1*: Pichia farinosa Killer toxin Resistance, *CLC1*: Clathrin Light Chain, *SPE3*: Spermidine auxotroph, *TSA1* Thiol-Specific Antioxidant, *ILV2*: IsoLeucine-plus-Valine, *SIT1*:Siderophore Iron Transport, requiring, *RIM101*:Regulator of *IME2*, *CFO1*:Chimeric floral organs1,*ENA1*: Exitus NAtru, *SOD1*: SuperOxide Dismutase, *MET3*: METHionine requiring, *TPS2*:Trehalose-6-Phosphate Synthase 2, *CNA1*: CalciNeurin A, *PLB1*: PhosphoLipase B, *APP1*: Actin Patch Protein, *PIK1*:Phosphatidyl Inositol Kinase, *CPA1*:Carbamyl Phosphate synthetase A, PKA: cAMP-dependent protein kinase catalytic subunit, *CAP*: Catabolite activator protein, *STE12*: Serine/threonine-protein kinase, *SKN7*: Suppressor of Kre Null *MPK*: mitogen-activated protein kinase1, *Ras1*: homologous to RAS proto-oncogene, *TPS1*: Trehalose-6-Phosphate Synthase1, *AOX1*: aldehyde oxidase

2.8 The host responses to *C. neoformans* infections

In contrast to self-limiting infection in normal host, *C. neoformans* invasion is usually not limited to the primary site in immunocompromised individuals, but often spreads to the central nervous system (CNS) (Ma & May, 2009). Therefore, it seems that phagocytes are able to defend *C. neoformans in vivo* or maintain the pathogen during latency (Ma & May, 2009). The cytokines from type 1 helper T cells, such as IFN γ are probably involved in the activation of macrophage and granuloma formation to contain replicating organisms (Ma & May, 2009). The establishment of cryptococcal

infection is prevented with several innate factors including physical barriers. Human serum and saliva contains enzymes with antimicrobial inhibitory effects (Baum & Artis, 1963; Hendry & Bakerspigel, 1969; Igel & Bolande, 1966; Szilagyi *et al.*, 1966). Cellular immune response is responsible to restraint the proliferation of *C. neoformans* by granulomatous inflammation response (Levitz, 1992; Murphy, 1992). Humoral immunity plays a key role to discharge cryptococci from the body (Casadevall, 1995; Levitz *et al.*, 2001). However, *C. neoformans* strains which can convert their morphology can trigger a diverse immune response (Guerrero *et al.*, 2006; Noverr *et al.*, 2003; Noverr *et al.*, 2004; Pietrella *et al.*, 2003).

The importance of phagocytes during a host's immune response to cryptococcal infections has been demonstrated (Rohatgi & Pirofski, 2015). Phagocytosis occurs in some types of the leukocytes (Bulmer & Sans, 1967), including macrophages and neutrophils in mouse (Griffin, 1981; Kozel & Follette, 1981; Mitchell & Friedman, 1972), human (Dong & Murphy, 1997), guinea pig (Bulmer & Tacker, 1975), and swine (Lipovsky *et al.*, 1997). Phagocytosis is initiated by a binding of the yeast by cell surface receptors on the phagocytes and or through complement or antibodies (Mitchell & Perfect, 1995). *C. neoformans* GXM can be recognized by the Toll-like receptor 4 (Shoham *et al.*, 2001) whereas mannoproteins can be recognized by the mannose receptor (Pietrella *et al.*, 2005) and complement receptors (Dong & Murphy, 1997).

Dendritic cells can phagocytose *C. neoformans* (Wozniak *et al.*, 2006), and present antigens to T cells to modulate adaptive immune responses (Crowley *et al.*, 1990). The content of lysosome such as protease enzymes subsequently lyse the phagocytosed *C. neoformans* upon phagolysosome fusion (Wozniak & Levitz, 2008). Dendritic cells are located at the peripheral tissues, this help the cells to pick up and sample any microbial antigens at the proximity, and induce an adaptive immune response towards a harmful pathogen.

Neutrophils is another type of immune cells which contribute to the innate immune response to cryptococcosis. Both macrophages and neutrophils response vigorously to *C. neoformans* infection in the lung (Feldmesser *et al.*, 2000). The number of polymorphonuclear cells increased at the site of infection upon cryptococcal challenge in animal models. However, in contrast to human and other animals, defensin is not found in the neutrophils from the mice model (Eisenhauer & Lehrer, 1992); hence, reseachers should take this into consideration when interpreting the data and comparing with human immune system.

Macrophages, an important phagocyte (Casadevall *et al.*, 1998), is the cell that first encounters inhaled *C. neoformans* (Bolanos & Mitchell, 1989; Feldmesser *et al.*, 1998; Goldman *et al.*, 2000; Levitz, 1993). Capsule is a major anti-phagocytic factor (Kozel & Gotschlich, 1982; Kozel & Mastroianni, 1976) which inhibits phagocytosis by reducing binding of *C. neoformans* to the receptors on macrophages (Kozel & Gotschlich, 1982). Besides, the negative charge surface of capsule results in electrostatic repulsion between fungus and macrophage, hence prevents the likelihood of their contact with each other (Nosanchuk & Casadevall, 1997). It has been reported that phagocytosis may promote the dissemination of *C. neoformans* infection as the pathogen can hide and be transported by macrophages from blood to different organs (Del Poeta, 2004; Luberto *et al.*, 2003) (Figure 2.7).

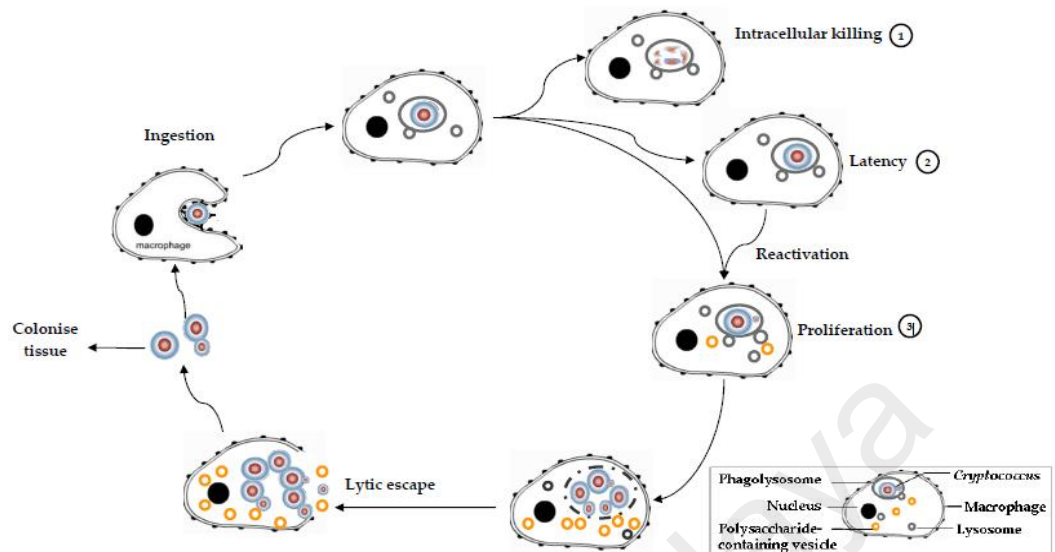


Figure 2.7. Macrophage and *C. neoformans*. Yeast cells are phagocytosed (1), enters latency phase (2) in an individual. In the immunocompromised host, the yeast cells can reactivate and multiply intracellularly (3), after lytic burst of the host cells, intracellular yeast cells are released into the extracellular environment and infect more macrophages (Feldmesser *et al.*, 2001).

2.9 Genome of *Cryptococcus neoformans*

The genome sequences of some *C. neoformans* strains including JEC21 and H99 have been completed (Hu *et al.*, 2008b). *C. neoformans* serotype A H99 reference genome project was first initiated by the Fungal Genome Initiative at the Broad Institute and Fred Dietrich at the Duke Center for Genome Technology. The genome of *C. neoformans* var. *grubii* H99 strain was 18.9 Mb which was assembled into 14 chromosomes (Loftus *et al.*, 2005). The size of JEC21 genome is approximately 20 Mb and contains 6572 genes (Loftus *et al.*, 2005); of which 10% are exclusive genes for *C. neoformans* strains (Idnurm *et al.*, 2005). The genome of *C. neoformans* is rich in transposons, many of which cluster at its centromeric regions (Hu *et al.*, 2008b). The karyotype instability and phenotypic variation may result from these transposons. JEC21 genome is also rich in transposons (~5%) which contributes to gene plasticity

(Loftus *et al.*, 2005). JEC21 and a serotype D strain (B3501A) share high genetic similarity of up to 99.5% (Loftus *et al.*, 2005).

2.10 Microarray as gene expression profiling method

With the availability of genome sequences, comparative analyses of different genotypes of *C. neoformans* and *C. gattii* is now possible. Additionally, the availability of the genome sequences of *C. neoformans* has made the construction of tiling microarrays studies feasible. Microarray is a robust method that allows the simultaneous study of the expression of many genes or RNA products (Tarca *et al.*, 2006). It can be applied for mutation detection, gene mapping and expression studies as well as for differential detection of gene family members (Russo *et al.*, 2003).

The microarray technology is based on hybridization between an array of DNA probes immobilized on a glass slide and labelled free targets in a biological sample (Southern *et al.*, 1999). The targets are generated from reverse transcription followed by labelling of RNA extracts from a biological sample. The hybridization signal produced on each probe reflects the mRNA expression level of the genes in the sample. Hence, the gene expression profile for each biological sample can be revealed based on the signals detected. The signals can be quantified, integrated and normalized using a software (Russo *et al.*, 2003). One of the free online data bases for annotation, visualization and integrated discovery is Database for Annotation, Visualization and Integrated Discovery (DAVID) bioinformatics resource that provides functional annotation for a large list of genes (Huang *et al.*, 2009).

Microarray has been used to provide useful information on the gene expression and function of microorganisms, especially when traditional techniques of genetic analysis failed to provide any clues. The data obtained microarray can serve as a foundation for

further study whenever the complete genome sequences are available (Akhter *et al.*, 2003; Kraus *et al.*, 2004).

Microarray can be applied to determine the expression levels of essential fungal virulence factors in *C. neoformans* (Haynes *et al.*, 2011). Genome-wide transcription study can assist to characterise the differentially expressed genes among the strains. Comparison of the gene expression profiles of the clinical and environmental strains can lead to reveal potential genes which are responsible for cryptococcal virulence. For example, the ability of *C. neoformans* to proliferate at 37°C (an essential virulence factor of *C. neoformans*) has been evaluated using partial-genome microarray. Profile gene expression showed that genes with orthologs involved in stress responses were induced during growth at 37°C, suggesting that a conserved transcriptional program may be used by *C. neoformans* to alter gene expression during stressful conditions.

Additionally, membrane remodeling is an essential component of microbial adaptation to high growth temperatures (Kraus *et al.*, 2004). The basic mechanism by which *C. neoformans* plays an essential role in the invasion process such as capsule formation and melanin production (Litter *et al.*, 2005) has been determined. However, there may be more virulence-associated genes and pathways which remain to be revealed. Comparison of the gene expression profiles of the clinical and environmental strains can contribute to the discovery of genes which are responsible for rendering a higher pathogenicity in the clinical strains.

Table 2.2. List of studies that have used microarray for identifying virulence genes.

Paper title	Reference
A DNA microarray for identification of virulence and antimicrobial resistance genes in <i>Salmonella</i> serovars and <i>Escherichia coli</i>	Chen <i>et al.</i> , 2005
Identification of <i>C. neoformans</i> Temperature-Regulated Genes with a Genomic-DNA Microarray	Kraus <i>et al.</i> , 2004
<i>Cryptococcus gattii</i> Virulence Composite: Candidate Genes Revealed by Microarray Analysis of High and Less Virulent Vancouver Island Outbreak Strains	Ngamskulrungrroj <i>et al.</i> , 2011
Genome-wide expression profiling of the response to short-term exposure to fluconazole in <i>Cryptococcus neoformans</i> serotype A	Florio <i>et al.</i> , 2011
Macrophage Mitochondrial and Stress Response to Ingestion of <i>Cryptococcus neoformans</i>	Coelho <i>et al.</i> , 2015
Sex-induced silencing defends the genome of <i>Cryptococcus neoformans</i> via RNAi	Wang <i>et al.</i> , 2010

2.11 Anticryptococcal therapy

Standard therapy for cryptococcal meningitis includes amphotericin B, flucytosine and fluconazole (World Health Organization, 2011). Fluconazole and amphotericin B disturb the fungal membrane and cause membrane disintegrity. Amphotericin B causes pore generation that increases membrane permeability by disrupting ergosterol, an essential component of the fungal plasma membrane (Brajtburg *et al.*, 1990). Fluconazole inhibits the cytochrome P-450-dependent 14 α -demethylation of lanosterol that is involved in the conversion of lanosterol to 4,4-dimethylcholesta-8(9),14,24-trien-3 β -ol, leading to the depletion of ergosterol and accumulation of sterol precursors, including 14 α -methylated sterols (lanosterol, 4,14-dimethylzymosterol, and 24-

methylenedihydrostanosterol), resulting in the formation of a plasma membrane with altered structure and function (Galgiani, 1990; Ghannoum & Rice, 1999).

Despite several antifungal drugs (amphotericin B, flucytosine, fluconazole) available for the treatment of cryptococcal meningitis, drug resistance frequently occurs (citation needed). In fact, the acute mortality of cryptococcal meningitis despite present therapies still runs between 10% and 25% in the most medically advanced countries (Perfect & Casadevall, 2002). For neurocryptococcosis the mortality rate during the first 3 months of treatment exceeds 20% and in patients who do not receive early treatment it leads to 100% mortality (Perfect *et al.*, 2010). Previous work on this subject established an induction phase for 2 weeks followed by 8 weeks of consolidation and a maintenance phase for not less than a year or as long as patients exhibit CD4+ T cells counts ≤ 200 cells per ml (Perfect *et al.*, 2010). In general the recommended treatment (World Health Organization, 2011) during the induction phase is based on the combination of amphotericin B ($0.7\text{--}1 \text{ mg kg}^{-1} \text{ day}^{-1}$) and 5-flucytosine ($100 \text{ mg kg}^{-1} \text{ day}^{-1}$); in case of unavailability of, or intolerance to any of these drugs, the following regimens have been suggested: (i) amphotericin B ($0.7\text{--}1 \text{ mg kg}^{-1} \text{ day}^{-1}$) and fluconazole (800 mg day^{-1}); (ii) amphotericin B ($0.7\text{--}1 \text{ mg kg}^{-1} \text{ day}^{-1}$) during 5-7 days and fluconazole (1200 mg day^{-1}) to complete 2 weeks of induction; (iii) fluconazole (1200 mg day^{-1}) and flucytosine ($100 \text{ mg kg}^{-1} \text{ day}^{-1}$); or (iv) fluconazole (1200 mg day^{-1}). Liposomal amphotericin B formulations, itraconazole and voriconazole have also been used as alternatives (World Health Organization, 2011). During the consolidation phase fluconazole (400 mg day^{-1}) is suggested and as alternatives itraconazole (400 mg day^{-1}) and amphotericin B ($1 \text{ mg kg}^{-1} \text{ week}^{-1}$) (Organization, 2011). For patients receiving amphotericin B, toxicity monitoring is recommended as preemptive hydration and electrolyte supplementation (World Health Organization, 2011). The antifungal spectrum of this drug seems to be similar to that of voriconazole and posaconazole with potent *in vitro* activity against

many fungal species including *C. neoformans*/*C. gattii* species complex (Guinea *et al.*, 2010; Seifert *et al.*, 2007). Currently, Isavuconazole, -a new broad-spectrum triazole antifungal agent with activity against yeasts, molds, and dimorphic fungi has been approved for the therapy of invasive aspergillosis and mucormycosis (Miceli & Kauffman, 2015).

2.11.1 Cryptococcosis preventive approaches

Currently, besides antifungal resistance and impaired immune system of the host, the presence of other underlying diseases should be considered in cases of therapeutic failures (Cuenca-Estrella, 2010). Among the wide range of options, highly active antiretroviral therapy (HAART) initiation is the most essential and cost-effective preventive approach in reducing incidence and high mortality caused by cryptococcal meningitis in HIV patients. The therapy is initiated at a CD4+ T-cell count of 350 cells per ml, before the cell count declines to less than 200 cells per ml (Cuenca-Estrella, 2010). Patients positive for cryptococcal antigen (CrAg) presenting with symptoms suggestive of cryptococcal meningitis should have a lumbar puncture. India ink or CSF CrAg assay examination is able to exclude active cryptococcal disease before HAART therapy (Brandt & Park, 2013; Mdodo *et al.*, 2011).

A global study of nearly three thousand *C. neoformans* strains shows that >11% of the strains are resistant to fluconazole (Pfaller *et al.*, 2009). Fluconazole-heteroresistant *C. neoformans* has also been detected in a -substantial proportion of clinical strains (Yamazumi *et al.*, 2003). This will cause problems in African countries which the cheaper drug fluconazole is the main therapy applying. To date, cryptococcosis is a continuously increasing medical challenge; due to the high incidence in HIV-infected individuals in developing countries and the emergence of highly virulent strains affecting healthy individuals in developed countries (Yamazumi *et al.*, 2003).

The overexpression and hotspot mutations of genes that encode for efflux ATP-binding cassette (ABC) transporters (Looi *et al.*, 2005) such as CDR1, CDR2 can cause increased drug resistance in fungi (Prasad *et al.*, 1995; Sanglard *et al.*, 1996). Drug permeation ability can be reduced due to changes in fungal phospholipids and membrane sterol composition (Hitchcock *et al.*, 1986). The susceptibility of fungi to a drug can be affected by the alternate usage of enzymes in the same biosynthetic pathway (Howell *et al.*, 1990).

Therefore, the challenge is to elucidate the pathogenesis mechanisms of the pathogens and to prevent infection and disease. Combination of multiple anti-microbial drugs is essential for treatment of microbial infections. In some studies, drug combinations demonstrate synergistic effect and superiority to the currently available therapies (Mukherjee *et al.*, 2005; Munoz *et al.*, 2006). It has been shown that combinational usage of fluconazole plus amphotericin B works better for treatment of candidiasis (Odds, Frank C, 2003). Hence, it is anticipated that further studies to discover new drugs can assist to improve treatment for cryptococcosis.

2.11.2 Triclosan as a new anti-fungal therapy

A chlorinated compound, triclosan (2,4,4'-trichloro-2'-hydroxydiphenylether, $C_{12}H_{17}Cl_3O_2$) is widely used in personal care product such as soap and toothpaste due to its broad-spectrum anti-microbial properties against various species of bacteria and fungi (Schweizer, 2001). The compound also demonstrates safety, efficiency and a long-lasting effect to use for healthcare (Jones *et al.*, 2000). The antifungal effect of triclosan has been reported in several fungal species including *Candida* and *Pseudomonas* species (Regos *et al.*, 1979; Vischer & Regos, 1974). Previous studies reported that triclosan does not affect the host biochemical pathway, but likely to perturb cell structure resulting in a loss of permeability-barrier function (Villalaín *et al.*,

2001). Besides, triclosan can exert its activity by inhibiting bacterial and fungal fatty acid synthetic enzyme, enoyl-[acyl-carrier protein] reductase (Zhang *et al.*, 2006).

The mechanism of action of triclosan is to intercalate and disrupt bacterial cell membrane activities, without causing leakage of intracellular components (Guillén *et al.*, 2004; Villalaín *et al.*, 2001). In addition, triclosan is an inhibitor of the enoyl-reductase of type II fatty acid synthase responsible for the lipid biosynthesis (Heath *et al.*, 2000; Levy *et al.*, 1999; Stewart *et al.*, 1999; Ward *et al.*, 1999). At low doses, triclosan is bacteriostatic and, at higher doses, it becomes bactericidal (Kampf & Kramer, 2004; Yazdankhah *et al.*, 2006). Sub-lethal concentrations of triclosan favor a specific action against type II fatty acid synthase enoyl-reductase (FabI), while at bactericidal concentrations triclosan appears to act against multiple targets, including less specific targets such as the cell membrane (Yazdankhah *et al.*, 2006). Triclosan also has anti-viral (Brading *et al.*, 2004) and anti-malarial activities (Jones *et al.*, 2000; Rao *et al.*, 2003). While triclosan has *in vitro* activity against a broad spectrum of bacteria, it is generally more effective against gram-positive than gram-negative bacteria (Jones *et al.*, 2000). Triclosan is particularly effective against *Staphylococcus aureus* (Jones *et al.*, 2000). However, some clinical strains of *S. aureus* are not as susceptible to triclosan due to the overexpression of FabI (Fan *et al.*, 2002). In addition to its overexpression, the FabI from these strains carries a single amino acid change that prevents the formation of a stable triclosan-NAD⁺-FabI complex (Fan *et al.*, 2002). In gram-negative bacteria, such as *Pseudomonas aeruginosa*, there are several multi-drug efflux pumps that remove a number of drugs, including triclosan, from the cells (Chuanchuen *et al.*, 2001). In addition, some strains of *P. aeruginosa* have been reported to possess a triclosan-resistant enoyl-acyl carrier protein reductase, FabV (Zhu *et al.*, 2010).

Development of standardized antifungal susceptibility testing methods for yeasts (NCCLS M27-A) and molds (M38-P) is important to minimize interlaboratory

reproducibility (Rex *et al.*, 2001). Synergy testing can be performed using Etest, microdilution checkerboard, and time-kill methods (Sopirala *et al.*, 2010). The fractional inhibitory concentration index (FICI) can be calculated for each drug using following formula: $FICI = FIC(\text{triclosan}) + FIC(\text{drug})$, where FIC equals to MIC-2 of the drug in combination divided by the MIC-2 of the drug alone. $FICI \leq 0.5$ indicates synergy, $FICI > 4$ indicates antagonism whereas $0.5 > FICI > 4$ suggests no interaction (additively/indifference) (Odds, F. C., 2003).

2.11.3 Apoptotic markers

Many exogenous and endogenous triggers have been identified to induce yeast apoptosis. Multiple apoptotic regulators are - identified and characterized at the molecular level. Such apoptosis-relevant orthologs include proteases such as the yeast caspase mitochondrial and nuclear proteins that contribute to the execution of apoptosis in a caspase-independent manner. Additionally, - aging and failed mating are among the physiological scenarios which have been discovered to cause apoptosis in yeast (Carmona-Gutierrez *et al.*, 2010). TUNEL test has proven to be a reliable apoptotic marker under multiple cell death-inducing conditions, as demonstrated by correspondence with further apoptotic markers (Büttner *et al.*, 2007; Wissing *et al.*, 2004).

CHAPTER 3: MATERIALS AND METHODS

3.1 Strains and growth conditions

C. neoformans H99 strain (derived from a meningitis patient) was obtained from American Type culture Collection (ATCC) and used as the control strain for most of the experiments in this study. The strain has been identified as *C. neoformans* var. *grubii* (serotype A).

Three environmental strains H4, S48B and S68B were isolated from soil contaminated with bird droppings at different locations in Klang valley, a densely populated city in the central region of Malaysia (Tay *et al.*, 2006). Similar to the H99 strain, all environmental strains were *C. neoformans* serotype A, genotype VNI with an α -mating type (Tay *et al.*, 2006). Yeast strains were maintained at -80°C prior to the study. Cultures were streaked on the Sabouraud's dextrose agar (SDA, Appendix A) and incubated at 37°C for 48 hours. To prepare cell suspension, 2 to 3 single colonies from a freshly prepared agar plate were inoculated into Sabouraud's dextrose broth (SDB) or yeast extract-peptone-dextrose broth (YPD) and incubated at 37°C for 48 hours. All preparation of culture media, reagents and chemicals are listed in detail in Appendix A.

3.2 Maintenance of cryptococcal strains

To store the yeast strains, a volume of 200 μl of each cryptococcal strain culturing in YPD broth for 24 hours at 37°C was added to 1ml of sterilised 50% glycerol in a cryogenic vial, vortexed to homogeneous and stored at -80°C . Upon usage, the yeast will be inoculated onto a YPD agar plate. .

3.3 Molecular identification *C. neoformans* strains

3.3.1 DNA extraction

Genomic DNA was extracted from all the yeast strains using a MasterPure™ Yeast DNA Purification Kit (EpiCenter, Madison, WI). A half loop of yeast colony from a

Potato Dextrose Agar (PDA) plate was suspended in 300 µl yeast cell Lysis solution in a microcentrifuge tube. The cell suspension was mixed thoroughly using a vortex and incubated at 65 °C for 15 minutes. The cell lysate was then placed on ice for 5 minutes and after that 150 µl MPC protein precipitation Reagent (provided in the kit) were added to the mixture. The solution was centrifuged at 15,000 rpm for 10 minutes. The supernatant (400 µl) was then transferred to a clean microcentrifuge tube. Yeast DNA was precipitated using 500 µl isopropanol followed by centrifugation at 15,000 rpm for 10 minutes. The pellet was washed with 0.5 ml 70% ethanol and suspended in 30 µl sterile distilled water. The DNA solution was used as template for PCR assays. The DNA purity and concentration were measured using a nanophotometer (Implen, Germany).

3.4 Amplification and sequence analysis of the internal transcribed spacer (ITS) region

Amplification of the internal transcribed spacer (ITS) region of *C. neoformans*, were performed using forward primer, ITS1 (5'-GTC GTA ACA AGG TTT CCG TAG GTG-3') and reverse primer, ITS4 (5'-TCC TCC GCT TAT TGA TAT GC-3') (White *et al.*, 1990). The PCR reaction mix contained 0.125 µl of 10 mM of each primer, 0.5 µl deoxynucleotides, 1.5 mM MgCl₂ and 2.5 µl 10 x buffer. The suspension was heated at 95°C for 1min in thermocycler. One unit of the Taq Polymerase (Promega) was then added to each tube. PCR conditions were as follows: 36 cycles of denaturing at 94°C for 1 min; annealing at 52°C for 1 min and extension at 72°C for 1 min; and final extension at 72°C for 10 min. PCR products (10 µl) were analysed using gel electrophoresis. The amplicons (approximately 550 bp) were purified and sequenced using ITS1 forward and ITS4 reverse primers.

3.4.1 Purification of PCR products

PCR products were purified using a QIAquick PCR Purification Kit (QIAGEN, Germany). A total of 20 µl amplicon was mixed with 100 µl PB Buffer, transferred into a QIAquick spin column and centrifuged at maximum speed for 30 seconds to remove the flow through. Then, column was washed with 750 µl wash buffer before eluted with 20 µl of elution buffer.

3.4.2 Sequence analysis

Sequencing was performed by Firstbase Laboratory, Shah Alam, Malaysia, using . Big Dye® Terminator Cycle sequencing kits (Applied Biosystems, USA) in an ABI-3730 Genetic Analyzer (Applied Biosystems, USA). The sequences obtained were assembled using Bioedit and analysed with nucleotide-nucleotide BLAST (BLASTN) program (<http://blast.ncbi.nlm.nih.gov/Blast>).

3.4.3 PCR fingerprinting analysis of *C. neoformans* strains

Yeast DNA (25 ng) was amplified in a mixture containing *Taq* polymerase (5 U/µl) (Fermentas, Lithuania), and 100 pmol/µl of each primer (GTG)₅ (5-GTGGTGGTGGTGGTG 3-) (Meyer *et al.*, 1993) in Veriti™ thermal cycler (Applied Biosystems, USA), as stated in Table 3.1. The PCR condition used were: 95°C for 5 minutes, 35 cycles of amplifications (94°C for 20 seconds, 50°C for 1 minute and 72°C for 20 seconds, and a final round at 72°C for 6 minutes (Meyer *et al.*, 1993).

Table 3.1. Preparation of reagent mixture for RAPD PCR assay for amplification of *C. neoformans* strains using primer (GTG)₅

Reagent	Stock Concentration	Volume (μ l)	Final concentration
Primer	100 pmol/ μ l	0.25	25 pmol
dNTPs	10 mM	1	200 μ M
<i>Taq</i> polymerase	5 U/ μ l	0.5	2.5 U
PCR buffer	10 X	5	1 X
MgCl ₂	25 mM	6	50 mM
DNA template		1	25 ng/ μ l
dH ₂ O		36.25	
Total volume		50	

3.4.4 Agarose gel electrophoresis

PCR products and loading dye, 4 μ l and 2 μ l respectively (Fermentas, Lithuania) were loaded onto a 1% agarose gel containing 0.5 μ g/ml gel red (Biotinium, USA), and run at 90 V for 1 hour. Gel was viewed under ultraviolet light using InGenius Gel Documentation System (Syngene, United Kingdom). The formulae for preparation of buffers and the gel prepared are shown in Appendix A3.

3.4.5 Cluster analysis of four *C. neoformans* strains

The PCR fingerprinting pattern generated was then analysed using the unweighted-pair group method with arithmetic mean (UPGMA) of PyElph software (Pavel & Vasile, 2012). The software automatically extracts data from gel images, computes the molecular weights of the analyzed fragments, and compares DNA patterns resulting from PCR fingerprinting analysis. A dendrogram was produced based on cluster analysis performed using the software.

3.5 Growth curve analysis

Three single colonies from each *C. neoformans* strain were inoculated separately into 10 ml of SD broth (Appendix A.1.2). The real-time cell growth of the H99 strain compared to H4, S68B and S48 strains were determined using SDB medium (Appendix B). The yeast cells were cultured at 37°C with agitation at 150 rpm for 108 hours. The optical density (OD) at 600 nm was measured at 6 hours intervals using a Spectronic 20 Genesys spectrophotometer (Thermo Scientific, Milford, MA). The average OD readings (mean \pm SD) for each strain at different time points were calculated.

3.6 *In vivo* infection study

This study was approved by the Faculty of Medicine Ethics Committee for Animal Experimentation at the University of Malaya with ethic reference number: 2013-12-03/MMB/R/E.

A total of 16 C57BL/6 mice were purchased from Jackson Laboratory (Bar Harbor, ME) and maintained in groups of four in separate ventilated cages under specific pathogen free condition. Fresh culture of cryptococcal strains in YPD broth were harvested after 12 hours of incubation at 37°C temperature by centrifugation at 1800 \times g for 10 minutes. The cells were then suspended in phosphate-buffered saline (PBS) and adjusted to 10^7 cells/ml using a hemocytometer. Each mouse was anesthetized and subjected to intraperitoneal injection of a mixture of ketamine (90 mg/kg) and xylazine (10 mg/kg). Intranasal inoculation was performed by pipetting 20 μ l (2×10^5 cells) yeast suspension into the nose of each mice using 200 μ l yellow tips (Corning, USA).

For fungal burden assay, mice (n = 4) were sacrificed at 21-day post-infection. Organs (lung and brain) were excised aseptically and homogenized using two glass slides in 1 ml PBS and then diluted to 10, 100 and 1000 folds. A volume of 20 μ l serially diluted homogenate was plated on SDA plates and cultured at 37°C for 48

hours. Colony forming unit (CFU) per ml was determined by calculating yeast colonies on each plate. For survival study, a total of 6–9 mice were infected. All mice were examined for up to 42 days post infection. Mice which showed severe signs including hunched posture, fur ruffling, weakness, increased respiratory rate and difficulty in breathing will be euthonised.

3.7 Capsule induction

Yeast cells were incubated at 37°C, for 24 hours in 2 ml PBS with or without 10% heat-inactivated fetal bovine serum (FBS) (Life Technologies, Rockville, MD) in six-well plates (SPL Life Sciences, Korea). Inactivation of sera was performed by incubation at 56°C for 30 minutes. To visualize the size of the capsule, a drop of India ink was added to the cell suspension on a glass slide and viewed under light microscope.

3.8 Phospholipase activity

Clinical and environmental *C. neoformans* strains were checked for extracellular phospholipase activity using modified egg-yolk agar plate method (Price *et al.* 1982). Two eggs were sterilised with 95% alcohol for 1 hour. Egg-yolk agar was prepared by adding 10 ml egg yolk to 10 ml distilled water, mixed by inversion and added into a SDA medium containing 1 M sodium chloride and 0.005 M calcium chloride (Appendix A). *C. neoformans* was inoculated onto the plate and incubated at 37 °C for 7 days. Appearance of hazy zone around the colony was recorded. Phospholipase production activity of each strain was calculated as $P_z = a$ (diameter of colony)/ b diameter of the hazy zone (Price *et al.* 1982).

3.9 Laccase activity

Laccase activity was measured by determining the amount of melanised products when cryptococcal strain was exposed to L-3, 4-dihydroxyphenylalanine (L-DOPA) containing medium (Chan & Tay, 2010). The yeast cells which were grown in YPD for

16 hours were inoculated into the medium which contained 10mM MgSO₄ (heptahydrate), KH₂PO₄ 29.4mM, 13mM glycine, 15mM glucose, 0.003 thiamine and 0.001 mM L-Dopa (appendix A6) and incubated at 30°C in a rotary shaker (150rpm) for 4 hours. At the end of the incubation period, yeast cells were pelleted and the optical density (OD₄₉₂) of the supernatant was determined using a spectrophotometer (Biotrak II, Amersham, Germany) (Appendix C).

3.10 Microarray study

3.10.1 RNA isolation

H99 strain and three environmental strains were grown in 10 ml of YPD broth, shaken at 150 rpm at 37°C overnight. The cells were counted using a haemocytometer (10⁹ cells per ml). Yeast cells were harvested by centrifugation at 2000 rpm for 2 minutes. Yeast RNA was isolated using a RNeasy mini kit (Qiagen, Valencia, CA) according to the manufacturer's instruction with minor modifications. Fresh yeast cultures at approximately 10⁹ cells were prepared and washed with cold water and harvested at 1000 ×g 4°C for 5 minutes. The pellet was resuspended in 350 µl of lysis buffer (Appendix A7), and distributed into two 1.5-ml microcentrifuge tubes. The cell wall was lysed by enzymatic disruption. 5µl of 50U lyticase (Sigma-Aldrich, USA) was added to the lysis buffer (Table 3.2). Then, 200 µl of 0.5 mm diameter glass beads (MoBio Laboratories, Carlsbad, CA) were added and the cells were disrupted mechanically with one cycle of agitation at 6800 rpm for 40 seconds using a homogenizer (Precellyse 24 lysis, Berlin technology, France). Samples were incubated on ice for 5 minutes and centrifuged in a microcentrifuge (Hermle, Germany) for 2 minutes at 14,000 rpm. The supernatants were transferred to a new microcentrifuge tube, mixed with 1 volume of 70% ethanol before filtering through a RNeasy spin column provided in the kit. The column was washed and RNA was eluted using 30 µl RNase free water. The quality and quantity of the RNA were analyzed using a

Bioanalyzer 2100 (Agilent Technologies, Palo Alto, CA). Only samples showing RNA integrity number (RIN)>7 were subjected to further analysis. For each sample, two biological replicates (rep1 and rep2) were prepared from two independent yeast cultures for microarray analysis.

Table 3.2. Reagents used for RNA isolation.

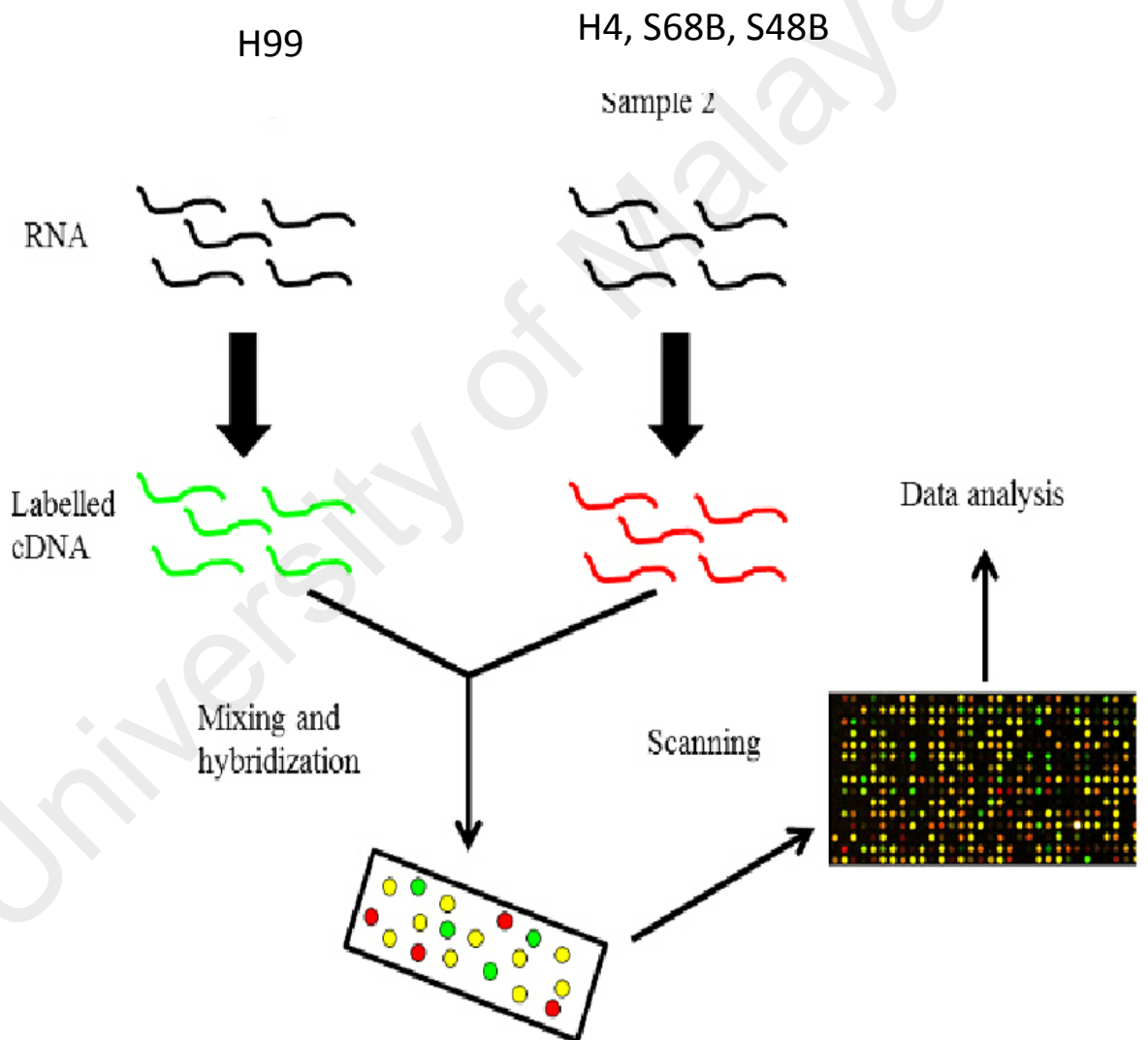
Reagent	volume
50U Lyticize	5 μ l
Lysis buffer	350 μ l
0.5 mm diameter glass beads	200 μ l
RNase free water	30 μ l
70% ethanol	500 μ l

3.10.2 RNA quality and integrity evaluation

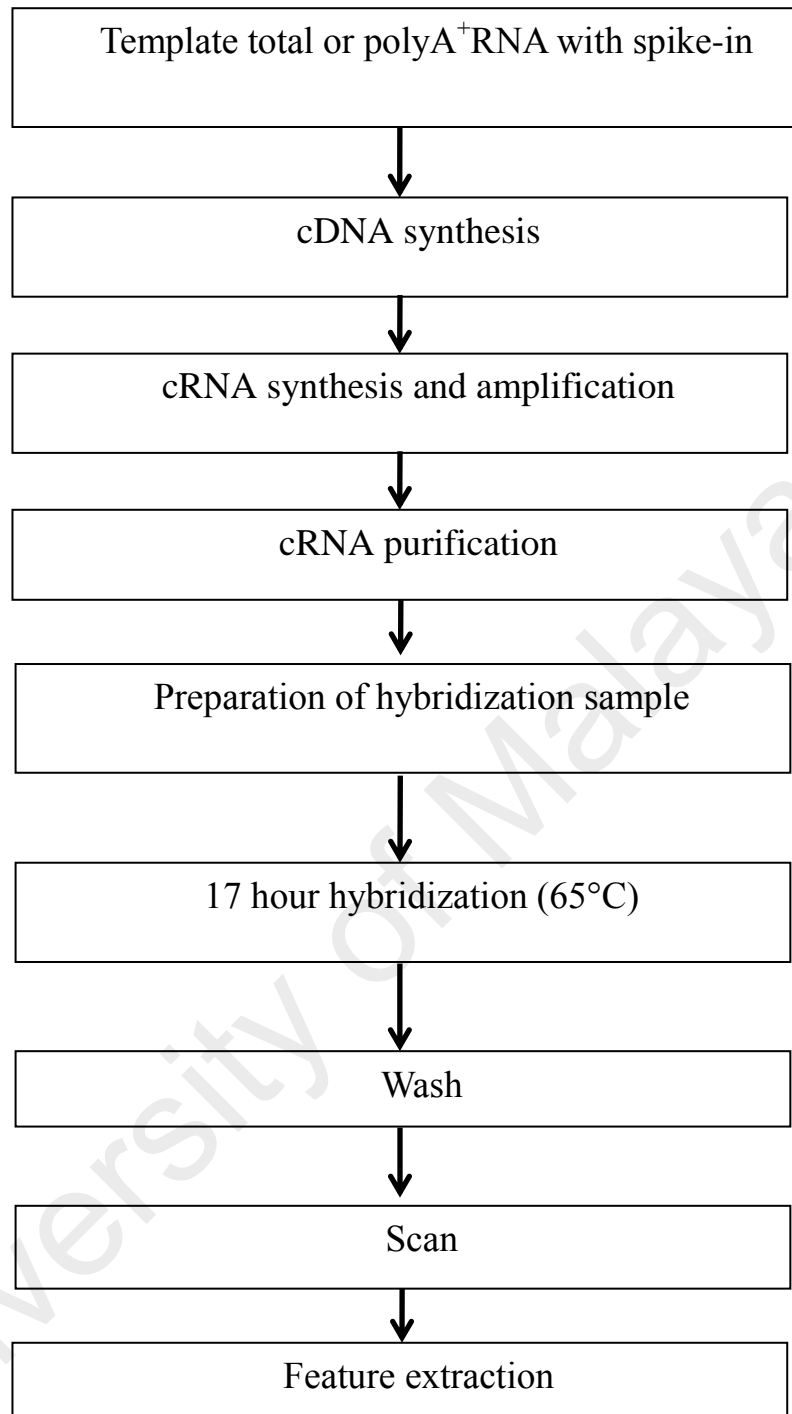
RNA concentration was measured using Nano spectrophotometer (Implen, Germany). Each RNA sample was loaded onto a 2% (w/v) TAE (Tris-acetate-EDTA) agarose gel containing 0.2 μ g/ml gel red (Biotinium, USA). Before loading, 3 μ l each RNA sample was mixed with 5 \times RNA loading dye (Fermentas, Lithuania) and was electrophoresed at 90 V for 40-60 minutes along with 0.2 μ g. RNA fragments (28S:4.8 kilo base pairs and 18S:1.8 kilo base pairs) were viewed under UV light using In Genies bio Imaging gel documentation system (Syngene, United Kingdom).

3.10.3 Microarray

A)



B)



C)

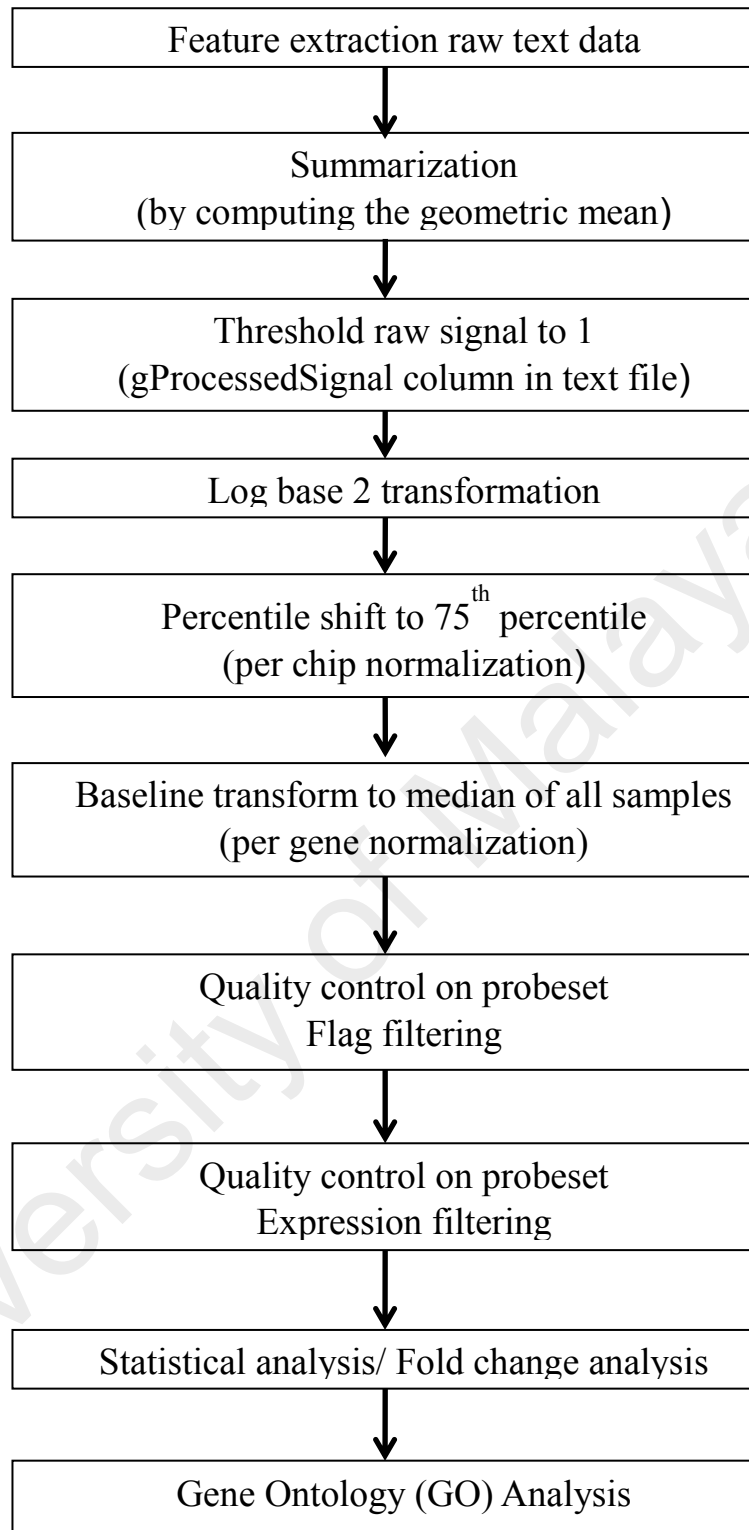


Figure 3.1. (A, B and C): Workflow of how the microarray data was generated and processed in Genespring GX.

3.10.4 Microarray analysis

Customized chips (Design ID: G4102A-066930) were used in this study. Each microarray chip was prepared in an 8-array slide with 22,313 features per array, inclusive of the control probes. The array features were customized based on the transcript sequences available in the online BROAD Institute database (www.broadinstitute.org/annotation/genome/Cryptococcus_neoformans)(Nielsen *et al.*, 2003). A total of 7813 transcript sequences in FASTA format were uploaded into the eArray webtool (Agilent Technologies) to design specific probes against each sequence. Three probes for each transcript were successfully designed for a total number of 7419 transcript sequences (table 3.3). The microarray had a specific Agilent identifier called an AMADID which was used to identify the array which is used. In this experiment the AMADID used was the design ID 66930.

Table 3.3. Microarray chip was customized to cover all *C. neoformans* genes in the Broad Institute database. Three probes were designed for each gene.

All Target	Filter on reading larger than 20 signal intensity and flag detected (to exclude background noise)		Filter on significantly expressed probes (2<fold change<-2) P value<0.05	
22,257 probes	21,069 Probes	7419 Genes (representing 100% percent of H99 genome)	871 Probes	434 Genes

Hierarchical clustering was done (<https://www.blast2go.com>) using “*Saccharomyces*” database. Non-matched genes were annotated using Basic Local Alignment Search Tool (BLAST) to select genes with the highest percentage of similarities. Pathway annotations of significant genes were analyzed using DAVID (<https://david.ncifcrf.gov/>) using “*Saccharomyces*” database.

3.10.5 Statistical analysis

Microarray data was analyzed by a microarray specialized analysis software, Genespring GX (Agilent, USA) using one-way analysis of variance (ANOVA) followed by Bonferroni's post hoc test. Unpaired student's *t*-test was used for comparison between two groups of data. Data were considered statistical significance if $P < 0.05$.

3.11 Validation of microarray data

3.11.1 cDNA synthesis Protocol:

cDNA of RNA samples from clinical and environmental strains was prepared using Moloney Murine Leukemia Virus (MMLV-RT) reverse transcriptase (Invitrogen, USA) according to manufacturer's protocol. Random hexamer and dNTPs, 1 μ l each, were added to 1-5 μ g of each RNA sample and incubated at 65°C for 5 minutes before transferring to ice. A 7 μ l mixture which included 4 μ l buffer, 2 μ l DTT and 1 μ l RNase inhibitor was prepared (Table 3.4) and added to the sample and incubated at 25°C for 10 minutes. 1 μ l Moloney Murine Leukemia Virus Reverse Transcriptase (M-MLV RT) was added to the mixture and incubated at 25°C for 10 minutes. The samples were then incubated at 37°C for 50 minutes. Inactivation of the enzyme was performed at 70°C for 5 minutes. The reaction was diluted with 100 μ l RNase-free H₂O for PCR. The cDNA quality was checked with agarose gel electrophoresis and stored at -20°C.

Table 3.4. cDNA synthesis reagents for Real time PCR

Reagents	Volume
Random hexamer	1 μ l
DTT	2 μ l
RNase-free H ₂ O	100 μ l
M-MLV RT	1 μ l
RNA inhibitor	1 μ l
dNTPs	1 μ l
RNA	5 μ g
Buffer	4 μ l

3.11.2 Primer design

Primers were designed using Primer 3 online software (<http://www.simgene.com/Primer3>). The general parameters of primer design was primer size between 18 to 22 bp, GC% content of 40 to 60%, product size of 200 to 900 bp and melting temperatures in the range of 52 to 58 °C to produce the best results.

Five well-known genes linked to the major virulence phenotypes targeting *SKN7*, *ADE2*, *CAC1*, *PKA1*, *PLB1* genes of *C. neoformans H99* (NC 029745.1) strain was used for designing of the primers. Table 3.5 and 3.6 show the primers used in this study.

Table 3.5. Primers sequences for qRT-PCR analysis. List of the forward and reverse primer sequences (5'-3') of 5 well-known genes linked to the major virulence phenotypes for qRT-PCR analysis. (*GAPDH* was used as endogenous control to normalise the data).

Gene symbol	Gene name	Forward primer (5'->3')	Reverse primer (5'->3')
<i>SKN7</i>	Transcription factor SKN7	GAAGGCACTACGATCC CTCTC	ATGCAACGGGTATAC AGCAAG
<i>ADE2</i>	Phosphoribosylaminoimidazole carboxylase	ACCATACCTGGCAAGT GAGC	TCGTCCTTTGTACGCC GAAA
<i>CAC1</i>	chloroplastic A acetylcoenzyme carboxylase 1	TACCGTGTCGCCTTATT TTTG	CACCAATTTCAACAG CCTCAT
<i>PKA1</i>	cAMP-dependent protein kinase catalytic subunit Pka1	TGGTTTCGCCAAGTAT GTACC	GACCTTCCCGTAGGC ACTAAC
<i>PLB1</i>	Phospholipase B1	ATGAGCATGGTCTTGG TGGG	TACACCACCACGGTG TAAGC
<i>GAPDH</i>	Glyceraldehyde-3-Phosphate Dehydrogenase	AGTACTCCACACATGG TCG	AGACCAACATCAGC

Table 3.6. Primer sequences for qRT-PCR analysis. List of the forward and reverse primer sequences (5'-3') of the up- and down-regulated genes selected for qRT-PCR analysis. (*GAPDH* was used as endogenous control to normalise the data).

Gene symbol	Gene name	Forward primer (5'->3')	Reverse primer (5'->3')
<i>PUT3</i>	Proline utilization trans-activator	CGCGAGTGTTCGCATAC TA	GCGCGAGTTGATACAC TTCA
<i>MVA1</i>	Hydroxymethylglutaryl-CoA synthase	TGTATGGTGAGCATGGCT GT	TGAGGAGTAGCCGAGC AAAT
<i>MMF1</i>	Protein MMF1, mitochondrial	CCCTACCCAACAGTCCTC AA	CCAGCCGATTTGGAGT GTAT
<i>MPH2/3</i>	alpha-glucoside permease	CAACAGGGTAAGTGCGG AAT	GCAGAGGACTCCAAGT CCAG
<i>PLB1</i>	Phospholipase B1	ATGAGCATGGTCTTGGTG GG	GCAGAGGACTCCAAGT CCAG
<i>GAPDH</i>	Glyceraldehyde-3-Phosphate Dehydrogenase	AGTACTCCACACATGGTC G	AGACCAACATCAGC

3.11.3 Quantitative Real-Time PCR

RNA (5 µg) was reverse transcribed as previously described in section 3.11.1. Quantitative Real-Time PCR (qRT-PCR) was performed using SsoAdvanced SYBR Green Supermix (Biorad, Hercules, CA) in a Real-Time PCR 7500 Fast Real-Time PCR System (Applied Biosystems, Foster City, CA), (Table 3.7). Three replicates from each sample was examined using 1 cycle of 2 minutes at 95°C for polymerase activation followed by 40 cycles of 5 seconds at 95°C of denaturation and 20 minutes of 60°C for annealing. The fold change of each gene was calculated using formula ($2^{-\Delta\Delta C_T}$) (Yuan *et al.*, 2006). All samples were run in triplicates and the results were presented as mean \pm SD. The fold change of each gene was calculated using formula ($2^{-\Delta\Delta C_T}$) as follow:

$$2^{-\Delta\Delta C_T} = 2^{-(Ct_{\text{infected}} - Ct_{\text{endogenous}}) - (Ct_{\text{non infected}} - Ct_{\text{endogenous}})}$$

All samples were run in triplicates and the results were presented as mean \pm SD.

Table 3.7. Preparation of reaction mixture for Real Time PCR

Reagent	Stock Concentration	Volume (μl per reaction)	Final concentration
Forward Primer	100 pmol/ μl	0.5	1X
Reverse Primer	100 pmol/ μl	0.5	25 pmol
SYBR® Green Master Mix	5U/ μl	5	2.5 U
cDNA template		0.5	50 ng/ μl
RNase-free H ₂ O		3.5	
Total volume		10	

3.12 Investigation on anti-*Cryptococcus* activity

3.12.1 Preparation of triclosan

Triclosan (Sigma Aldrich, USA) was dissolved in 50% DMSO (Sigma-Aldrich, USA) provide a stock solution of 100 mg/ml and stored at -20°C.

3.12.2 Preparation of amphotericin

Amphotericin (Sigma Aldrich, USA) was dissolved in 50% DMSO to provide a stock solution of of 100 mg/ml and stored at -20°C.

3.12.3 Preparation of fluconazole

Fluconazole (Sigma Aldrich, USA) was dissolved in 50% DMSO to provide a stock solution of 100 mg/ml and stored at -20°C.

3.13 Disc diffusion assay

The disc diffusion assay was performed based on CLSI method. Five single colonies were picked from each culture of *C. neoformans* and inoculated into 10 ml of Sabouraud's dextrose broth (SDB). Cells were grown overnight in a rotary shaker at 200 rpm at 35°C. An aliquot of 100 μl of the yeast suspension at 10^6 CFU/ml was prepared (counted with hemocytometer, Merk, Germany) applied onto the Sabouraud's dextrose

agar plate and spread uniformly using a cotton swab. Then, 6-mm paper discs (Toyo Roshi Co., Japan) impregnated with different concentrations of triclosan (3.125, 6.25, 12.5, 25, 50 and 100 µg) were positioned on a *C. neoformans* agar plate to evaluate the antifungal effect of triclosan.

In the synergy test, 25 µg of a drug alone or in combination were placed onto the agar surface, as shown in Table 3.8. The synergy test was repeated using sub-inhibitory concentrations of 6.25 µg/ml from amphotericin and fluconazole alone and in combination with 6.25 µg/ml, 3.125 µg/ml and 1.56 µg/ml of triclosan. Dimethyl sulfoxide (DMSO) was used as negative control. After incubation at 37°C for 48 h, the diameters of the growth inhibition zone were measured.

Table 3.8. Determination of the synergy test using triclosan alone or in combination with amphotericin or fluconazole

Drug	content
Triclosan	25 µg
Amphotericin	25 µg
Fluconazole	25 µg

3.14 Broth microdilution assay

The drug minimum inhibition concentration (MIC) was determined using the broth microdilution assay as described by Clinical and Laboratory Standards Institute (CLSI) standard (Clsi, 2008), with modification. The inoculum was prepared by picking five colonies (~1 mm diameter) from a fresh culture plate. Colonies were resuspended in 2 ml distilled water and vortexed for 15 seconds. The cell density was adjusted to 75% transmittance at 530 nm wavelength using a spectrophotometer (Thermo Scientific, Milford, MA) (source). A working suspension was made by a 1:50 dilution followed by a 1:10 dilution of the stock suspension with RPMI 1640 medium supplemented with 34.53 mg/ml morpholinepropanesulfonic acid (MOPS) at pH 7.0 to yield a yeast stock suspension of 1.0 to 5.0×10^3 cells/ml. Antifungal drugs, amphotericin B (32 to 0.017

µg/ml), fluconazole (128 to 0.068 µg/ml), and triclosan (128 to 0.068 µg/ml) were serially diluted in 96-well flat-bottomed microtiter plates. The cells suspension (100 µl) were then seeded into the plate and incubated for 48 hours. The growth for *C. albicans* and *C. neoformans* were visually scored after incubation at 37°C for 24 and 48 hours, respectively. Additionally, the microtiter plates were agitated for 5 minutes, and the optical density (OD) at 570 nm wavelength was determined using a spectrophotometer (Thermo Scientific, Milford, MA). All samples were run in duplicate. The MIC-1 was defined as the minimal concentration that resulted in 80% growth inhibition while MIC-2 was defined as the minimal concentration that resulted in 50% of growth inhibition (Yu *et al.*, 2011).

3.15 Fungicidal assay

The Minimum Fungicidal Concentrations (MFCs) of triclosan was determined using a conventional culture-based CFU method from microtitration plate in duplicates (SPL Life Sciences, Korea), as previously described (Meletiadis, *et al.*, 2007). Total amount of 20 and 100 µl from all visually clear wells (with no growth) and the first well with the highest drug concentration showing growth (0.5× MIC) were mixed by pipetting up and down several times, washed and subcultured onto Sabouraud's dextrose agar (SDA) plates in duplicates. The SDA plates were incubated at 37°C for 48 hours, and the CFU were observed for each drug concentration. The MFCs were defined as the lowest drug concentration yielding no growth using 20 µl (CFU20 MFC) and 100 µl (CFU100 MFC). Triclosan was considered fungicidal when the MFC/MIC ratio is ≤ 4 and fungistatic when the MFC/MIC ratio is >4 (Meletiadis, Joseph *et al.*, 2007; Pfaller *et al.*, 2004).

3.16 Synergy checkerboard assay

Antibiotic interactions were evaluated using the checkerboard assay as previously described (Rand *et al.*, 1993). Checkerboards were prepared by using serial dilutions of

amphotericin B (0.004 to 4.0 µg/ml) and fluconazole (0.0156 to 16.0 µg/ml) in the horizontal wells and triclosan (0.25 to 16.0 µg/ml) in the vertical wells. A fungal suspension was prepared as described in broth microdilution assay (approximately 5×10^3 CFU/ml), and 100 µl was inoculated into each well of a 96-well microtiter plate. Plates were read after 48 hours of incubation at 35°C, and the wells without visible signs of growth were identified by placing the plate on a mirrored surface. Each well was resuspended and agitated for 5 minutes, and the OD at 570 nm wavelength was determined with a spectrophotometer. The fractional inhibitory concentration index (FICI) was calculated for each drug using following formula: $FICI = FIC(\text{triclosan}) + FIC(\text{drug})$, where FIC equals to MIC-2 of the drug in combination divided by the MIC-2 of the drug alone. $FICI \leq 0.5$ indicates synergy, $FICI > 4$ indicates antagonism whereas $0.5 > FICI > 4$ suggests no interaction (additivity/indifference) (Odds, F. C., 2003).

3.17 Electron microscopy

Yeast cells of *C. neoformans* H99 strain were pelleted by centrifugation and resuspended in 5 ml of distilled water. The turbidity of the suspension was adjusted with a spectrophotometer to 75% transmittance at 530 nm. The cell suspension was first diluted 1:50 (0.1 ml plus 4.9 ml) with RPMI 1640 medium and treated with 0.5 µg/ml of triclosan at 37°C, for 2 hours. Cells were then collected and fixed with 4% glutaraldehyde fixative for 120 minutes. Cells were washed two times with cacodylate buffer and post fixed with OsO₄:cacodylate buffer (1:1) for 2 hours and kept in cacodylate buffer at 4° C overnight. The samples were washed with distilled water, incubated with uranyl acetate for 10 minutes before another washing step with distilled water. Dehydration was performed using 35%, 50%, 75%, 95% (v/v) ethanol for 10 minutes each, and followed by 100% ethanol, 15 minutes for 3 times. Samples were then incubated with propylene oxide:epon (1:1) for 1 hour, propylene oxide:epon (1:3) for 2 hours and epon for an overnight incubation. This was followed by embedding the

yeast pellet in resin for 5 hours at 37°C followed by 60°C overnight. Images were obtained using *EFTEM LIBRA 120* transmission electron microscope (Carl Zeiss, Oberkochen, Germany). Electron microscopy services were provided by Electron microscopy unit, Faculty of medicine, University of Malaya.

3.18 Apoptosis assay

Cell apoptosis was examined by TdT-mediated dUTP nick end labeling (TUNEL) assay using FLOWTAC kit (Trevigen, Gaithersburg, MD). H99 cells were cultured in SDA for approximately 12 hours to reach the log-phase growth (10^7 cells). The cells were then treated with 2 mM hydrogen peroxide (H_2O_2) or 0.5 μ g/ml triclosan for 4 hours at 37°C. Cells were fixed in 1 ml 3.7% formaldehyde for 10 minutes followed by Cytonin™ permeabilization for 30 minutes. Cells were then washed and resuspended in labeling reaction mix (TdT dNTP mix, TdT enzyme, $1\times Mn^{2+}$, $1\times$ TdT labeling buffer) provided in the kit (Trevigen, Gaithersburg, MD) at 37°C for 1 hour.

The reaction was stopped by adding $1\times$ Stop Buffer followed by staining with 25 μ l Strep-Fluorescein for 10 minutes in dark. Propidium iodide and RNase were added to the cells before analyzed using a FACS Canto cytometer (BD Biosciences, Franklin Lakes, NJ).

3.19 Statistical analysis

Data were analyzed with unpaired two-tailed Student's *t*-test of GraphPad. Samples were considered significant if $P < 0.05$.

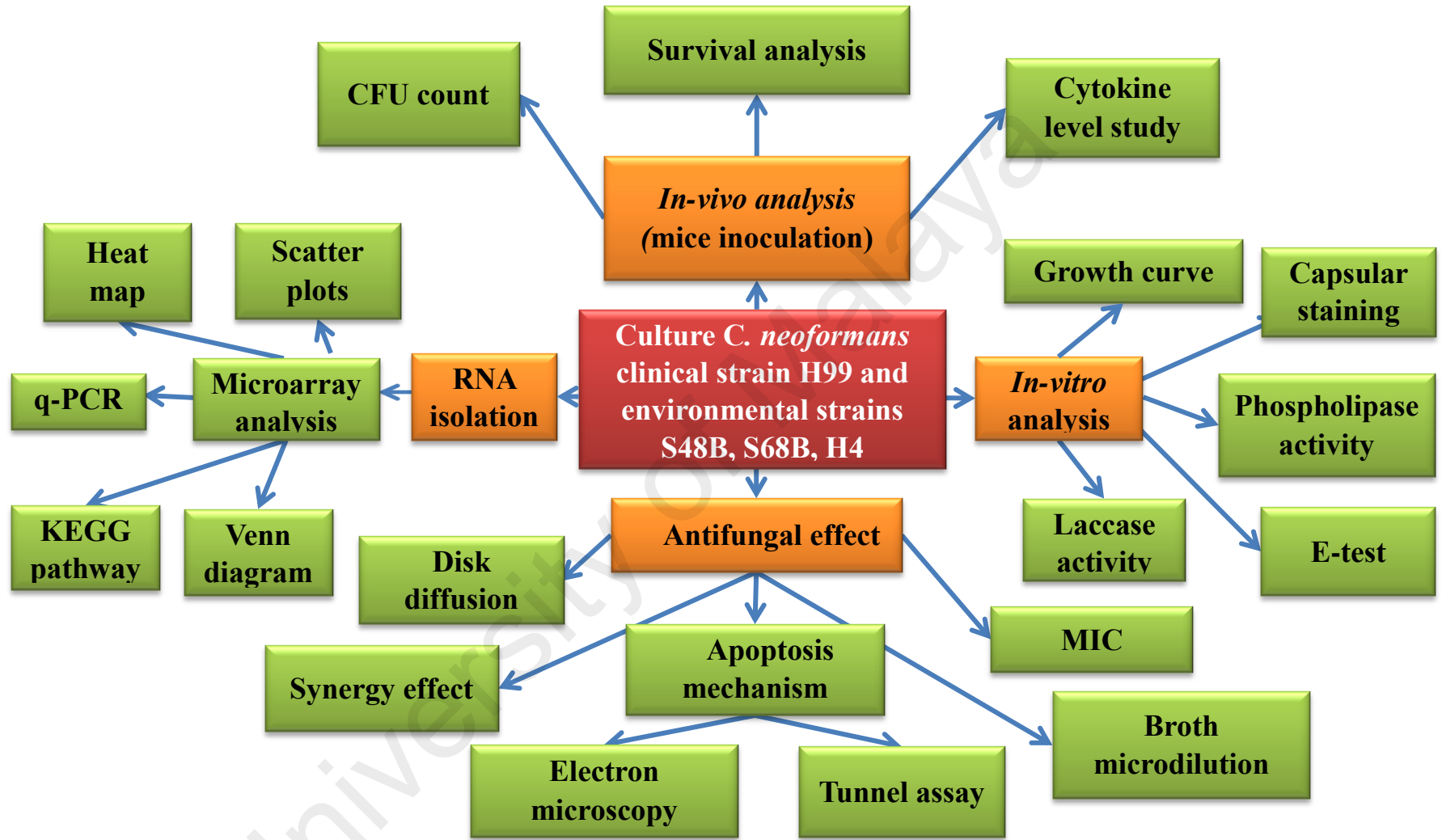


Figure 3.2. Flow chart of research activities

CHAPTER 4: RESULTS

4.1 Amplification and sequence analysis of the internal transcribed spacer (ITS) region of *C. neoformans* strains

C. neoformans var. *grubii* (serotype A) H99, a strain derived from a meningitis patient, was purchased from American Type Culture Collection (ATCC) and used as the control strain for the experiment. Three environmental strains (H4, S48B and S68B) were isolated from soil contaminated with bird droppings at different locations in Klang valley, a densely populated city in the central region of Malaysia (Tay *et al.*, 2005). First, the ITS gene region of each environmental strain was amplified and sequenced to confirm the species of the strains. The sequencing results were aligned with the partial ITS1 and ITS4 region of the H99 strain (GenBank accession no.EF211146.1). The ITS1 and ITS4 sequences are shown in Figure 4.1. The sequence alignment data shows 100% sequence similarities amongst the strains, thus confirming the identity of the environmental strains.

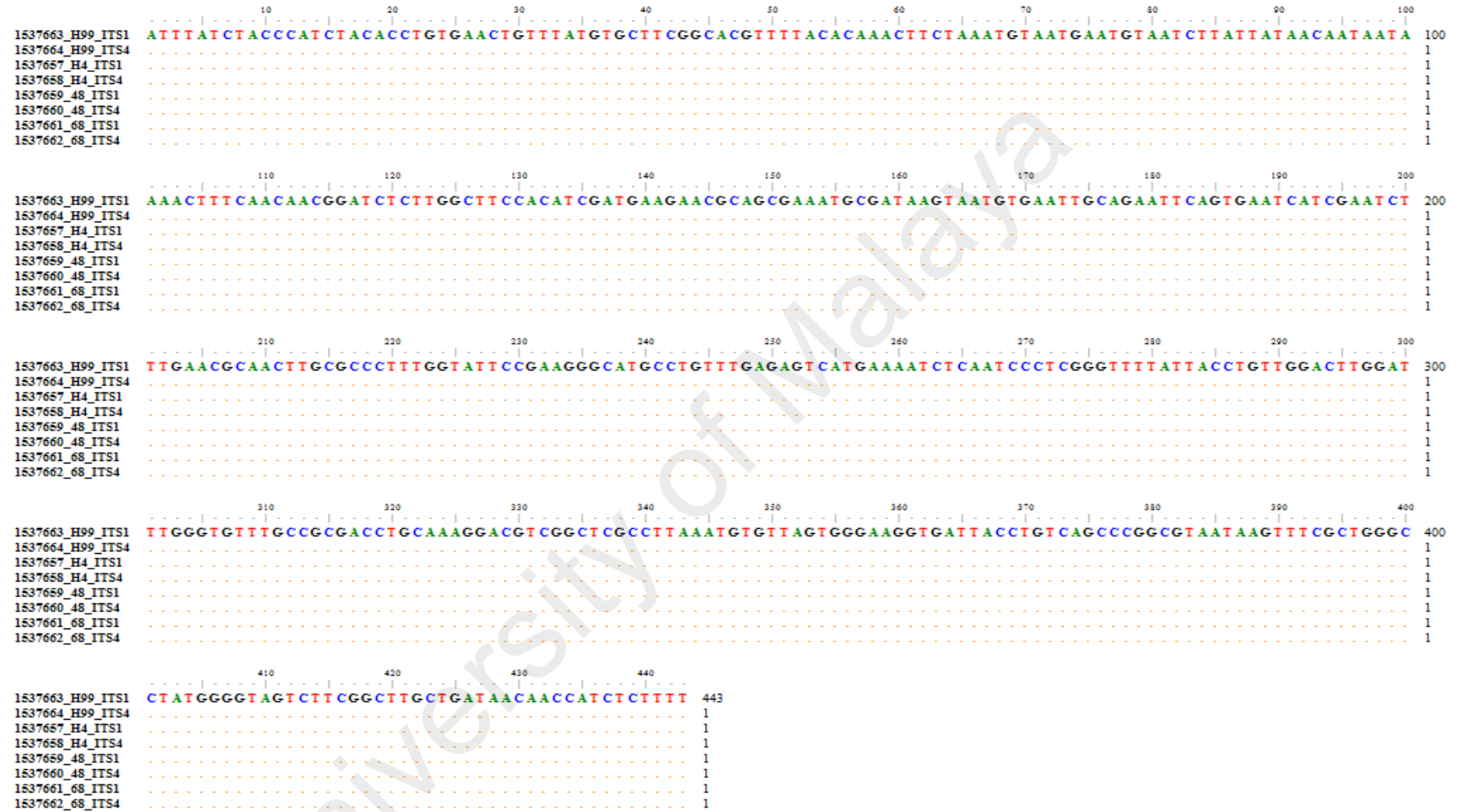


Figure 4.1. Sequence alignment of the ITS gene region of three *C. neoformans* environmental strains (H4, S48B and S68B strains) with that of H99 strain

4.2 Cluster analysis of the clinical H99 and three environmental strains of *C. neoformans*

The PCR products generated from (GTG)₅ primers were loaded on a 2% agarose gel. Figure 4.2 shows the PCR fingerprinting patterns and the cluster analysis of the clinical (H99) and three environmental strains (H4, S48B, and S68B) using PyElph software. A total of 6 DNA fragments (ranging from 400 bp to 1000 bp) were generated for H99 and S48B strains and 7 DNA fragments (ranging from 500 bp to 1500 bp) were observed for S68B and H4 strains (Figure 4.2A). H99 strain was placed in the same cluster with S48B strain while the strains S68B and H4 were clustered together in another group (0.0% difference within the same cluster). The percentages of similarities within these two groups were 92.9% (7.1% difference) (Figure 4.2B).

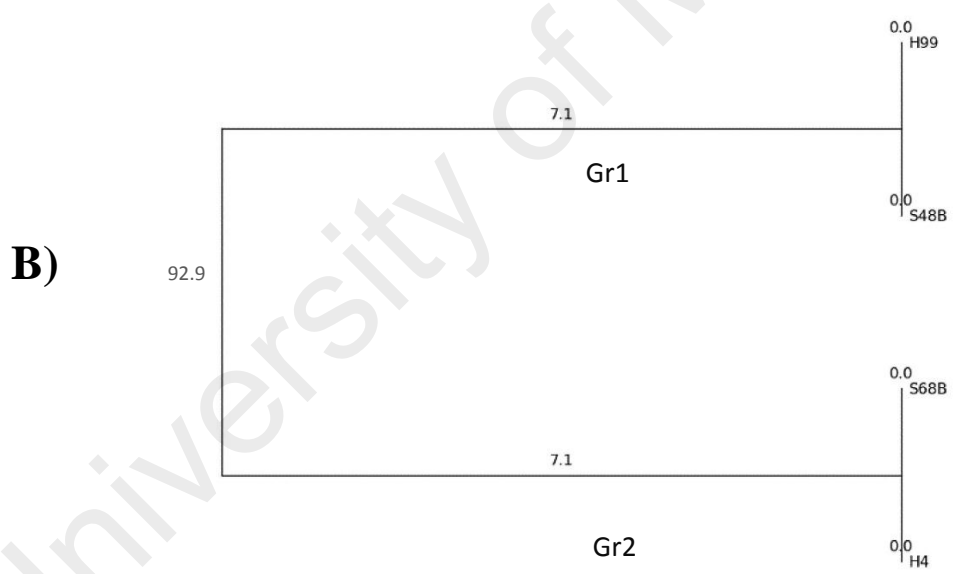
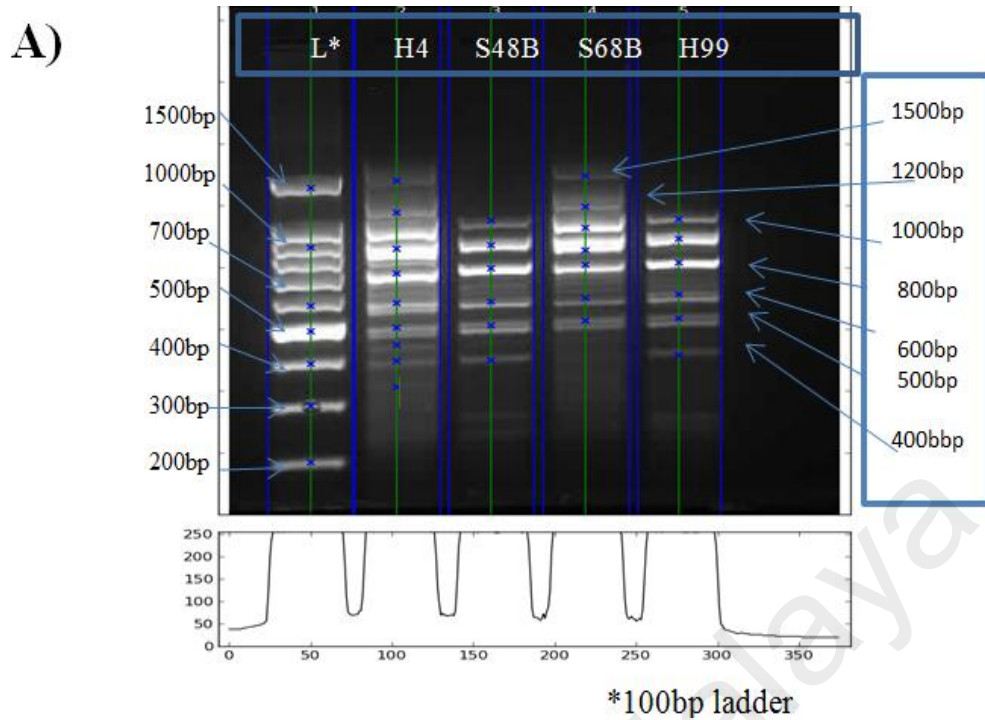


Figure 4.2 A and B. PCR fingerprinting analyzed by the PyElph software. (A) 5 μ l of each strain and 100bp ladder was loaded on 2% agarose gel. The PCR fingerprinting patterns generated by using (GTG)₅ primers was observed. The graph situated below the image was used for automatic lane detection based on the maximum value of each pixel column. (B) UPGMA algorithm based-dendrogram shows the cluster analysis of four *C. neoformans* strains. H99 and S48B were grouped in a cluster while S68B and H4 were grouped in another cluster (0.0% difference). These two groups shared 92.9% similarities.

4.3 *In vivo* virulence study among clinical and environmental strains of *C. neoformans*

4.3.1 Survival analysis of mice infected with clinical and environmental strains of *C. neoformans*

To compare the degree of virulence amongst *C. neoformans* H99 strain and three locally isolated environmental strains, wild type C57BL/6 mice (n=9) at age 8–12 weeks old were intranasally administered with yeast cell suspension. Mice were observed for a period of 42 days as the respiratory tract is the portal of entry. Mice infected with *C. neoformans* H99 strain died starting from day 18, while the remaining of the mice infected with environmental strains survived throughout the 42 days of the observation period (Figure 4.3). Mice infected with H99 strain became inactive after infection and demonstrated laboured breathing. Mice-infected with *C. neoformans* H99 strain died starting from day 18 followed by days 19, 26, 29 and 34. Two H99-infected mice died on day 40 post-infection (Table 4.1). Hence, the mice mortality rate was 77.8% (7 out of 9 mice died). All the mice infected with environmental strains and the control uninfected mice survived throughout the observation period of 42 days (Figure 4.3). Uninfected mice were healthy till the end of the experiment.

Table 4.1. Numbers of mice died at different days post-infection with *C. neoformans* H99.

Days post-infection	No. of mice dying
18	1
19	1
26	1
29	1
34	1
40	2

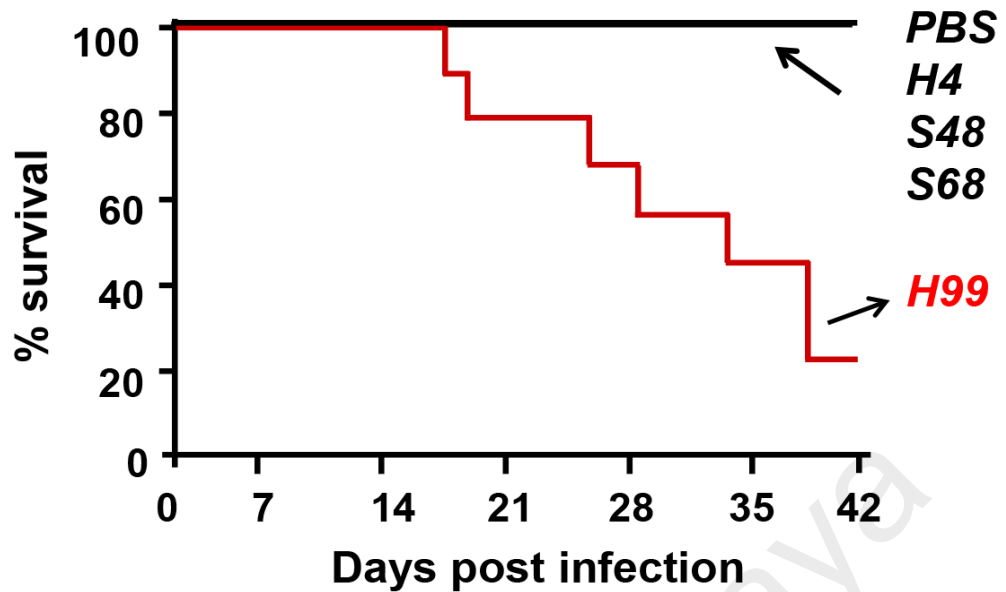


Figure 4.3. *In vivo* virulence study among different *C. neoformans* strains presented using Kaplan-Meier survival curve. Mice were infected with *C. neoformans* clinical strain H99 or environmental strains H4, S48B and S68B, and observed for a period of 42 days.

4.3.2 Morphological changes of mice lung infected with clinical and environmental strains of *C. neoformans*

Lung and brain were excised from mice infected with *C. neoformans* strains at 21 days post infection. H99-infected mice presented with severe damages in lung tissue while there were no morphological changes observed in the brain tissues. Results showed no specific sign of pathological abnormality for mice infected with the environmental strains (H4 and S68B) while necrotic spots were observed in lung infected with S48B environmental strain (Figure 4.4A). Inflammation and nodules formation in the lung tissues of mice infected with H99 strain was observed (Figure 4.4 B).

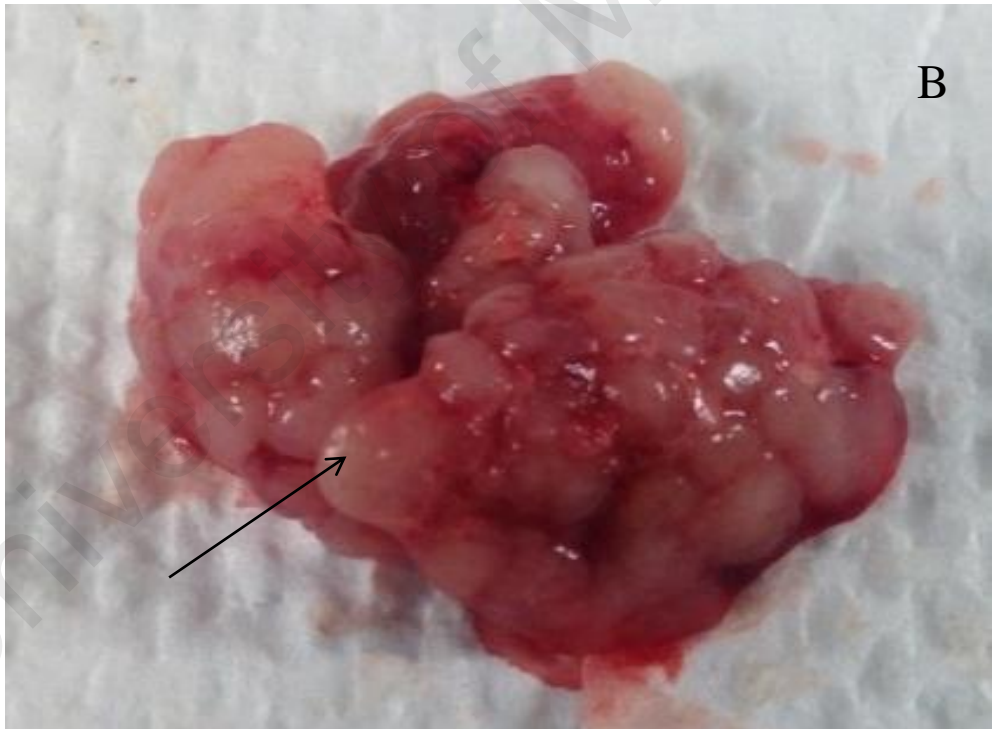
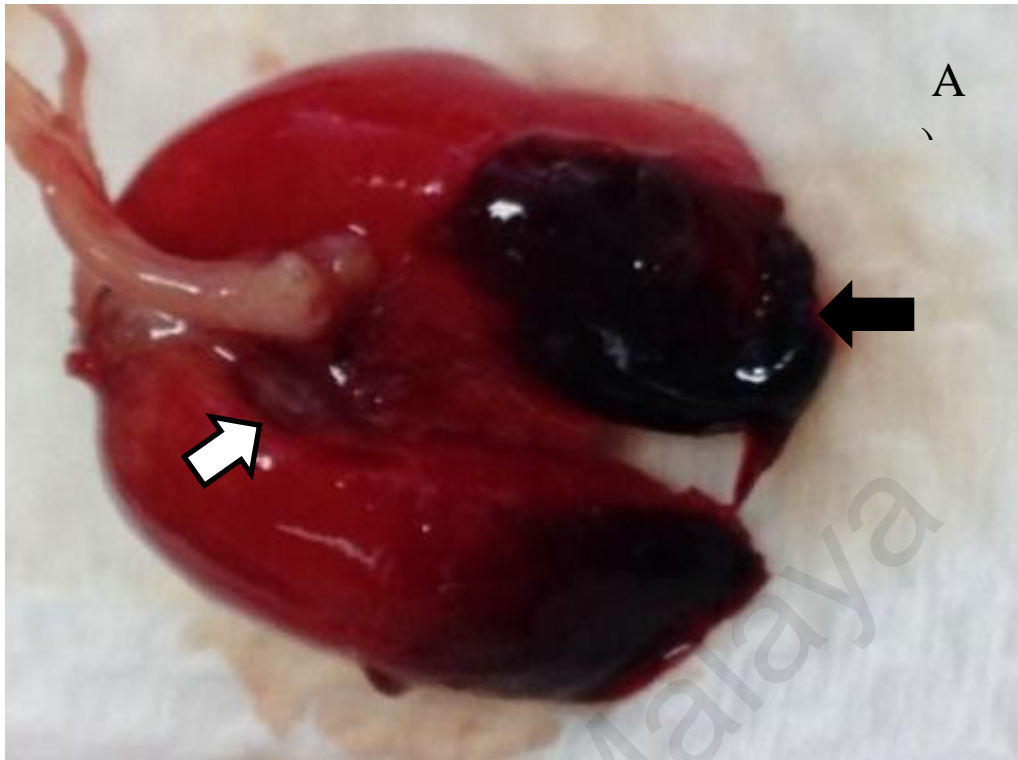




Figure 4.4. (A, B and C): The gross appearance of lung tissues harvested from infected mice 21 days post-infection. A) Mice infected with environmental strain (S48B), dark areas suggesting of multiple hemorrhagic (filled arrowhead) and abscess-like (open arrowhead) surface lesions were seen in S48B-infected mice.. B) Lung infected with clinical strain (H99), severe inflammation can be seen clearly in H99-infected lung tissue (shown by arrow). C) Uninfected mouse lung used as a control.

4.3.3 Determination of the colony forming units of *C. neoformans* in the organs of mice infected with clinical and environmental strains of *C. neoformans*

At 21-day post-infection, the lung (primary infection site) and brain (secondary infection site) of the infected mice were excised, homogenized and plated for CFU counts (Figure 4.5A and B). Homogenates obtained from *C. neoformans*-infected mice (n = 4) were serially diluted and plated onto agar plates in duplicates. The numbers of colonies (CFU/ml) were counted after 48 hours. The fungal load in both lung and brain tissues was higher for mice infected with the H99 strain, comparing to those infected with the environmental strains (Table 4.2 and Figure 4.6). The lung homogenates from the *C. neoformans* H99-infected mice showed an average of $4.73 \pm 1.19 \times 10^5$ CFU/ml, approximately forty folds higher than those obtained from S48B and S68B-infected mice ($0.11 \pm 0.09 \times 10^5$ and $0.11 \pm 0.13 \times 10^5$ CFU/ml, respectively). Consistently, the

brain homogenates from the *C. neoformans* H99-infected mice demonstrated higher CFU counts ($1.33 \pm 0.31 \times 10^5$ CFU/ml) compared to those obtained from S48B and S68B-infected mice ($0.02 \pm 0.03 \times 10^5$ CFU and $0.01 \pm 0.006 \times 10^5$ CFU/ml, respectively). No growth was obtained from homogenates of organs excised from those mice infected with H4 environmental strain, suggesting that H4 strain was probably non-virulent. There was no growth observed in mice inoculated with PBS (as negative control). Hence, based on the findings obtained from the mice virulence study, the degree of virulence for the four strains tested were H99>S48B>S68B>H4.

Table 4.2. CFU determination of lung or brain homogenates from *C. neoformans*-infected mice 21-day post-infection. The CFU counts on the plates were determined and shown as mean \pm SD. Group statistical significance measured was by two-way ANOVA analysis (* $P < 0.05$). PBS was used as negative control.

Sample	Lung CFU/ml (mean+SD)	Brain CFU/ml (mean+SD)
PBS	0	0
H4	0	0
S48B	$0.11 \pm 0.09 \times 10^5$	$0.02 \pm 0.03 \times 10^5$
S68B	$0.11 \pm 0.13 \times 10^5$	$0.01 \pm 0.006 \times 10^5$
H99	$4.73 \pm 1.19 \times 10^5$	$1.33 \pm 0.31 \times 10^5$

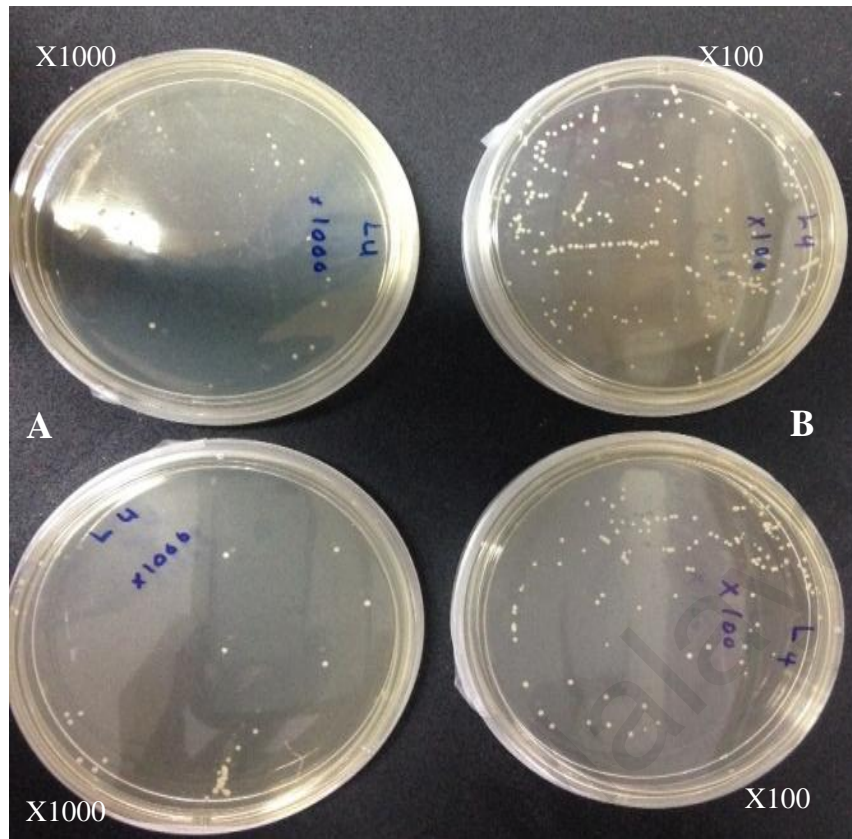


Figure 4.5. (A and B): SDA plates inoculated with the lung homogenate of H99 infected mice. Different serial dilutions, A) x1000 and B) x100 in duplicates were prepared from 10 μ l of each lung homogenate and spread on each plate.

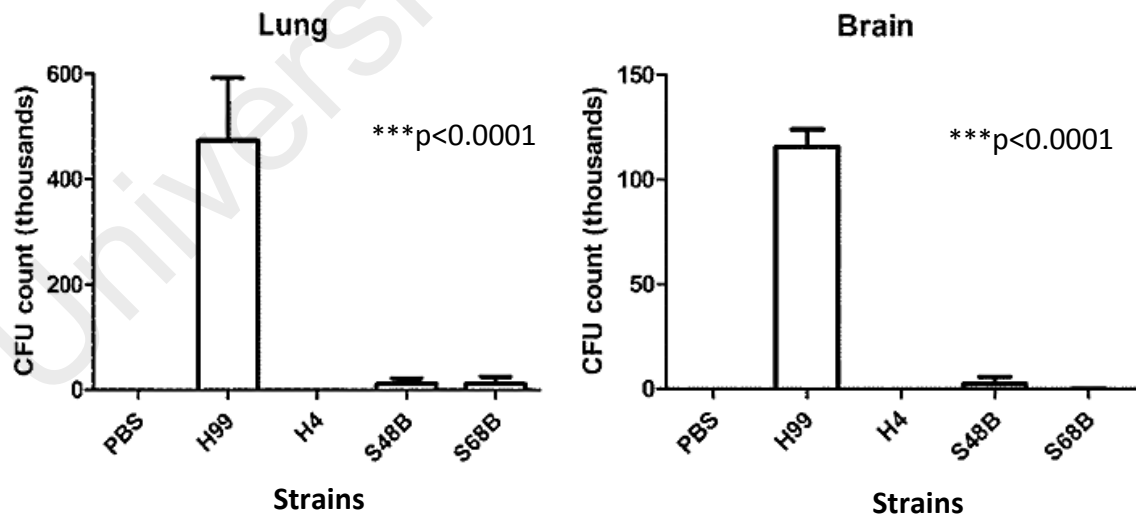


Figure 4.6. Comparison of the results of CFU assay for different strains of *C. neoformans*. Graph was plotted to compare the pathogenicity of *C. neoformans*-infected mice in H99 clinical and environmental strains. CFU formation on the plates was determined and shown as mean \pm SD. Group statistical significance measured was by two-way ANOVA analysis ($*P < 0.05$). PBS was used as negative control.

4.4 Determination of growth curve in clinical and environmental strains of *C. neoformans*

A typical fungal growth curve was performed to assess the growth rate of each cryptococcal strain as the virulence of an organism may be affected by its growth rate. No significant changes were observed in the growth rates of the cryptococcal strains throughout the observation period of 108 hours. However, the least virulent H4 strain demonstrated a relatively higher growth rate compared to the rest of the strains tested, followed by the S48B strain. Meanwhile, S68B and H99 strains showed almost identical growth curve throughout the observation period (Figure 4.7). The result suggests that there is no direct link between *in vitro* growth activity in growth media and the *in vivo* pathogenicity results performed in C57BL/6 mice. It can be proposed that the mice pathogenicity caused by of *C. neoformans* H99 strain infection was not due to extensive cell growth.

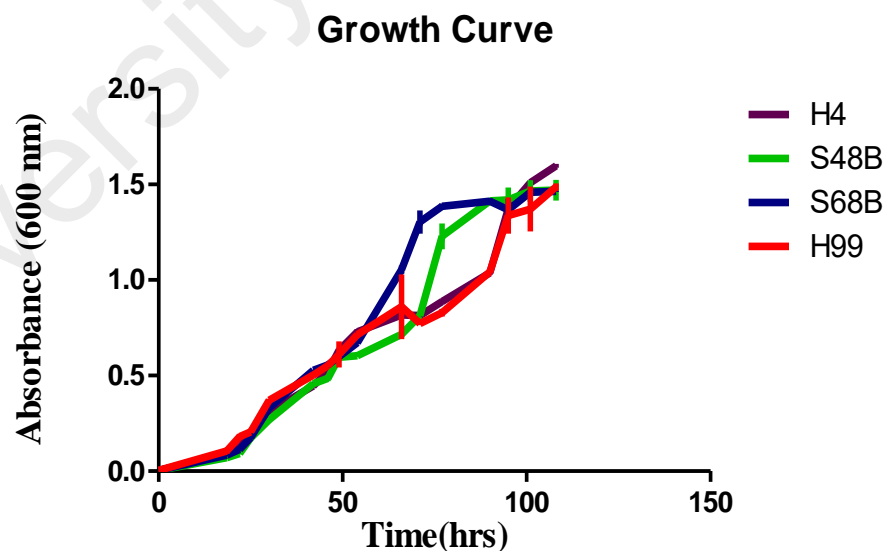


Figure 4.7. The growth curve determination of *C. neoformans* strains (H99, H4, S48B and S68B) cells upon culturing at 37°C with gentle shaking. OD reading for each sample was measured throughout a time course of 108 hours.

4.5 Clinical strain H99 shows larger capsule size compared to environmental strains.

The capsule size of *C. neoformans* is known to increase during *in vivo* infection and is associated with virulence (Zaragoza *et al.*, 2003a). To examine capsule formation ability among all strains, yeast cells were incubated in the presence of 10% FCS at 37°C for 12 hours (Figure 4.8). Interestingly, upon India ink staining, capsules were observed in all environmental strains (Figure 4.8). Among the strains, H99 strain showed the most prominent capsule size which expanded two times more than environmental strains.

University of Malaya

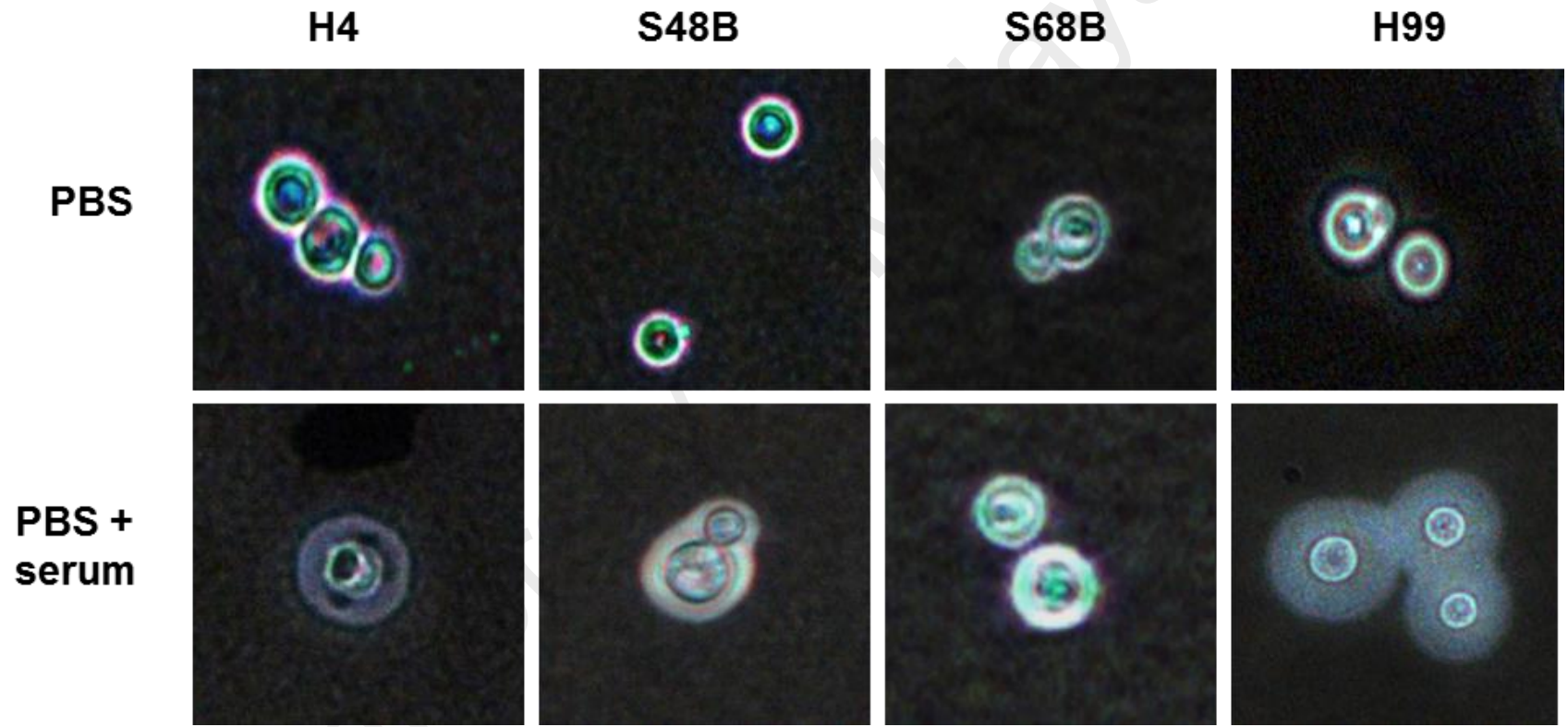


Figure 4.8. Determination of capsule formation for H4, S48B, S68B and H99 strains of *C. neoformans*. Fungal cells were incubated in PBS (with or without the presence of 10% FCS), and incubated for 24 hours at 37°C. Cells were then applied on glass slide for India ink.

4.6 Phospholipase activity

Table 4.3 shows the Pz values calculated based on the measurements of the diameter for colony and haze zone. No significant changes were observed in the phospholipase activity of the cryptococcal strains after an incubation period of 7 days. The environmental S68B strain demonstrated similar phospholipase activity with the H99 clinical strain, relatively slightly higher compared to the rest of the strains tested (Figure 4.9). The result suggests that there is no direct link between phospholipase activity in egg yolk agar plate and the *in vivo* pathogenicity results performed in C57BL/6 mice, suggesting that pathogenicity of *C. neoformans* H99 strain was not due to phospholipase activity.

Table 4.3. Determination of the phospholipase activity of *C. neoformans* using egg-yolk agar plates. *C. albicans* ATCC 90028 was used as a positive control.

Strains	Pz value
<i>C. albicans</i> ATCC 90028	0.57
<i>C. neoformans</i> H4	0.63
<i>C. neoformans</i> S48B	0.72
<i>C. neoformans</i> S68B	0.61
<i>C. neoformans</i> H99	0.61

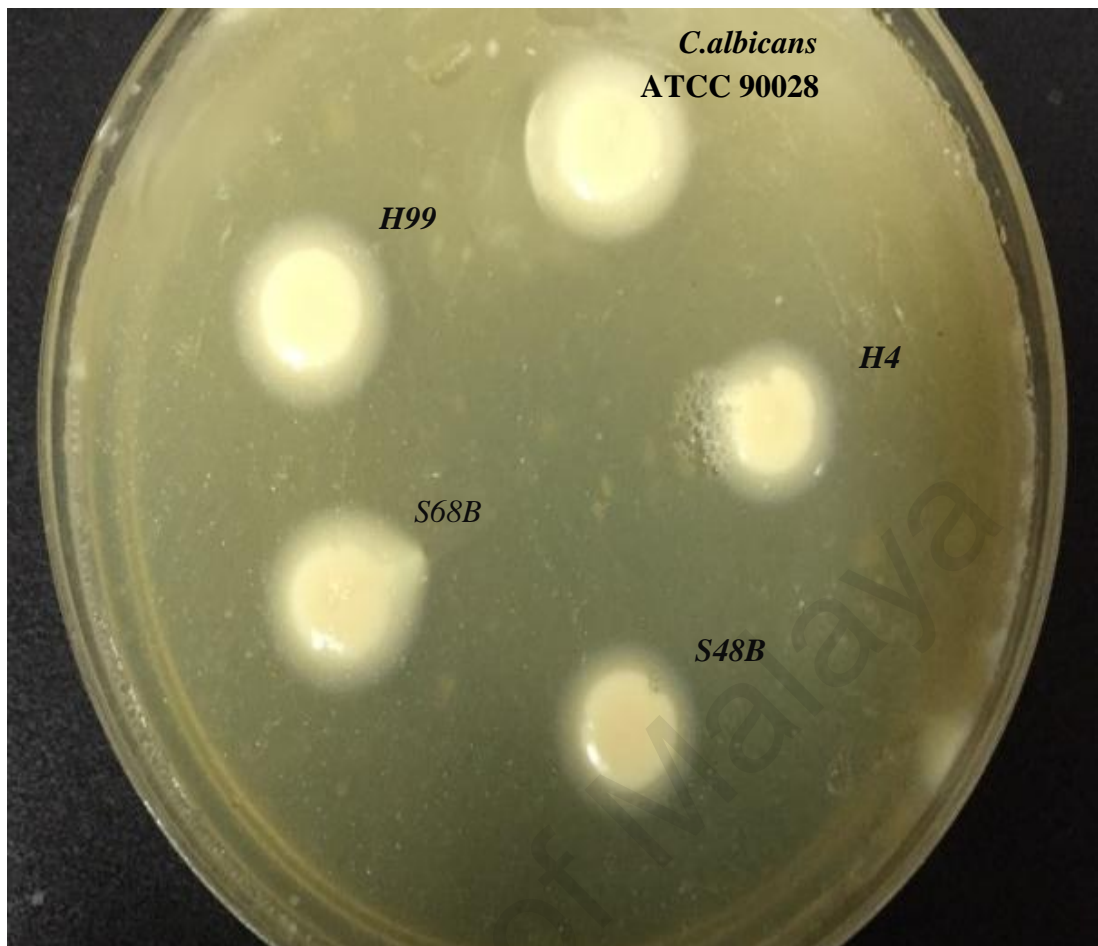


Figure 4.9. Determination of the phospholipase activity of *C. neoformans* using egg-yolk agar plates. An egg-yolk agar plate was inoculated with H99 clinical and three other environmental strains of *C. neoformans* and incubated at 28°C for 7 days. *C. albicans* ATCC 90028 was used as positive control in this assay.

4.7 Laccase assay

The laccase activity was quantitated by measuring the OD₄₉₂ of the melanised products when strains were exposed to L-Dopa containing medium. Table 4.4 shows the readings of the laccase assay. *C. albicans* ATCC 90028 was used as a negative control. *C. neoformans* H99 strain demonstrated higher laccase activity compared to those environmental strains (Figure 4.10).

Table 4.4. Laccase assay of *C. neoformans* strains

Strains	OD ₄₉₂
<i>C. neoformans</i> H4	0.044
<i>C. neoformans</i> S48B	0.041
<i>C. neoformans</i> S68B	0.033
<i>C. neoformans</i> H99	0.066
<i>C. albicans</i> ATCC 90028	0.005

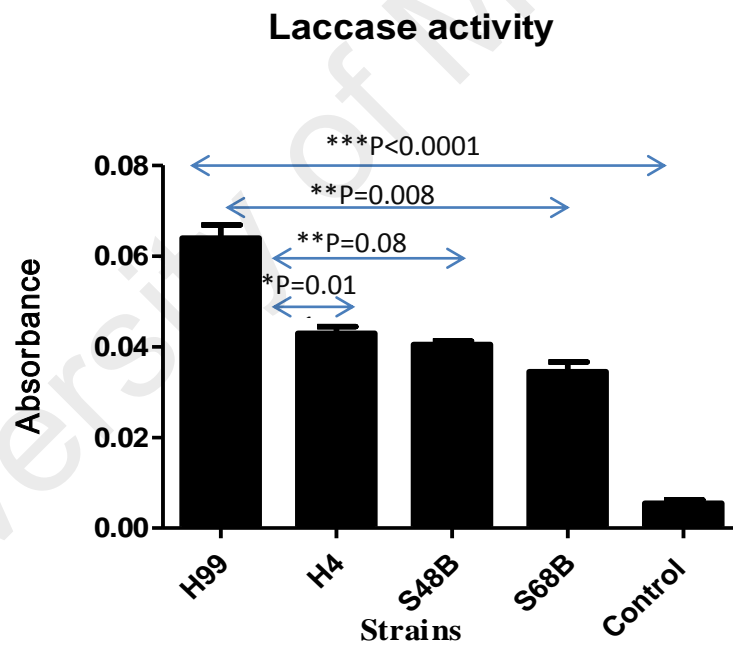


Figure 4.10 Determination of the laccase activity of *C. neoformans* strains using L-Dopa containing medium. L-Dopa containing medium was inoculated with clinical H99 and environmental strains of *C. neoformans* strains and incubated at 30C° for 4 hours. *C. albicans* ATCC 90028 was used as a negative control.

Footnote: P:P value, P \geq 0.01 among H99 clinical strain with each of the environmental strains which shows significant difference in their laccase production.

4.8 Antimicrobial susceptibility testing using E-test Method

All 4 strains showed comparative MIC ($\mu\text{g/ml}$) values, at 1.0 to 1.25 $\mu\text{g/ml}$ for amphotericin B, and 2.0 to 3.0 $\mu\text{g/ml}$ for fluconazole (Figure 4.11 and Table 4.5), indicating strong susceptibility and no significant difference of anti-fungal resistance among H99 and environmental strains.

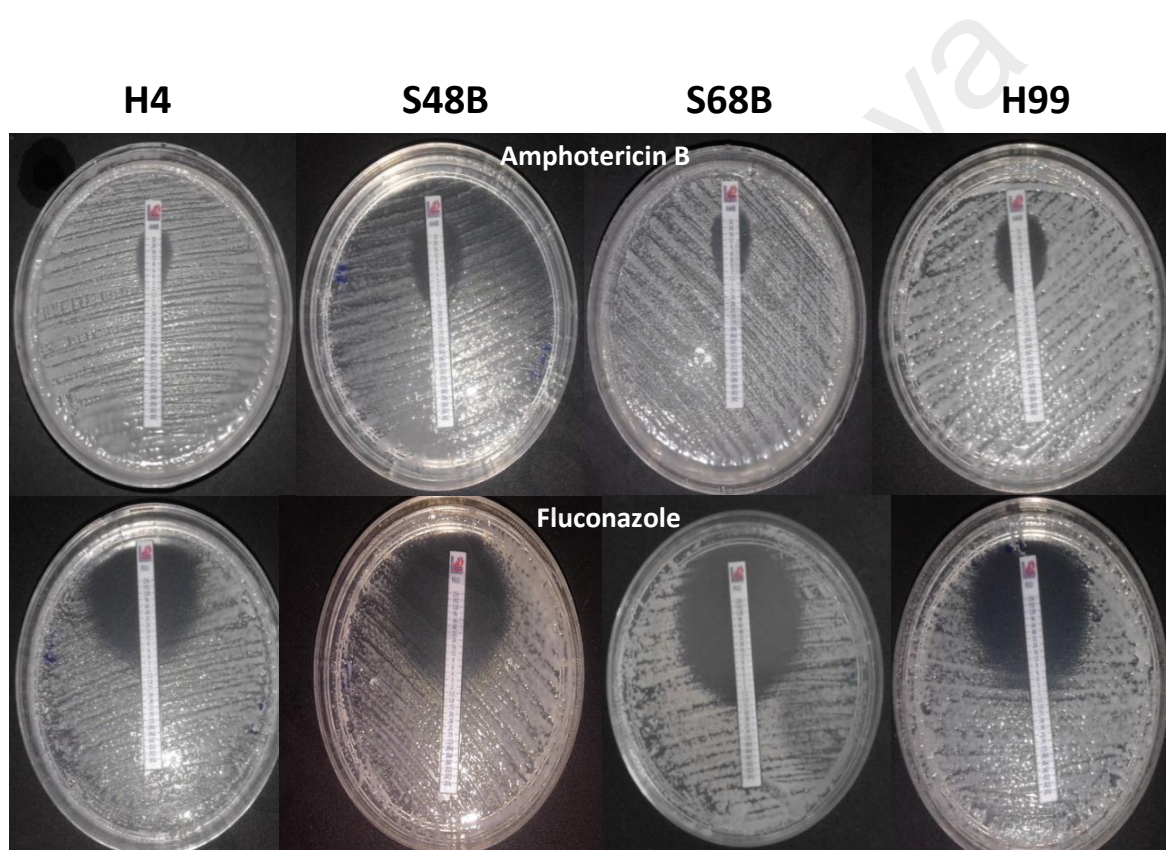


Figure 4.11. Determination of antifungal susceptibility profiles of *C. neoformans* using E-tests. Fungal strains were inoculated evenly onto each SDA plate. An amphotericin B or fluconazole-containing MIC strip was then placed on each plate and incubated at 37°C for 48 hours. Eclipse sizes which intersected with the MIC strips were recorded. Data were representative of two independent experiments.

Table 4.5. Measurements of MIC mean±SD from 2 duplicate plates using MIC strips

Fungal strains	Fluconazole	Amphotricin B
	mean±SD (µg/ml)	mean±SD (µg/ml)
<i>Cryptococcus neoformans H4</i>	2.0±0.0	1.0±0.0
<i>Cryptococcus neoformans S48B</i>	3.0±0.5	1.0±0.0
<i>Cryptococcus neoformans S68B</i>	2.0±0.5	1.25±0.25
<i>Cryptococcus neoformans H99</i>	2.5±0.5	1.0±0.0

4.9 Comparative transcriptome analysis of clinical and environmental strains of *C. neoformans*

4.9.1 RNA extraction

To examine total gene expression in H99 and environmental *C. neoformans* strains, RNA was isolated from the fungal cells cultured at 37°C (mimics the condition during *in vivo* infection) and processed for microarray analysis. Since *C. neoformans* has a strong cell wall and a very thick capsule some step was added to RNeasy mini kit protocol to extract the RNA for microarray. After adding RLT buffer to lyse the spheroplast yeast pellet was mechanically disrupted with one cycle of homogenization at 6800 rpm for 40 seconds using a homogenizer (Precellyse 24 lysis, Berlin technology, France), followed by enzymatic disruption using lyticase (Sigma-Aldrich, USA) to effectively lyse cell wall.

The samples concentrations were between 100 to 300 ng/ml. A ratio of 260/280 of the samples was kept in the range 1.8 ± 0.1 for protein contamination and the ratio of 260/230 for pure samples was between 2.0 and 2.4 to indicate the absence of protein, phenol or other contaminants that absorb strongly at or near 280 nm (Figure 4.12).

Two different methods were performed to assess the quality control and quantification of extracted RNA. The first method measured the quality of RNA

spectrophotometrically using Nanodrop ND-1000 and the second one was the quality assessment of total RNA purity in the sample using Agilent's 2100 Bioanalyser. Using the Nanodrop ND-1000, the RNA concentration determined at OD_{260/280}nm, varied from 254 to 369 ng/μl. The A_{260/280} ratio of ≥ 1.8 and A_{260/230} ratio of ~ 2.0 (Table 4.6).

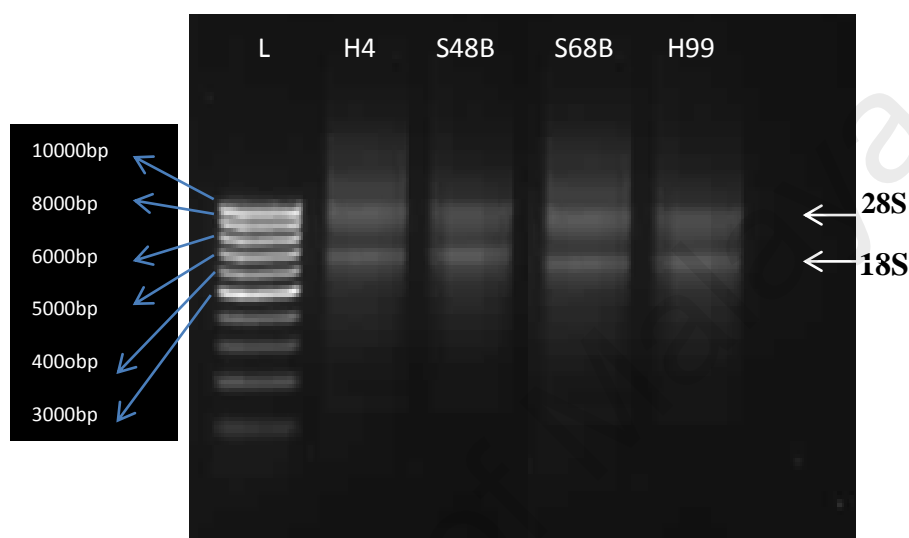


Figure 4.12. Agarose gel electrophoresis of the RNA extracted from *C. neoformans* strains (H4, S48B, S68B and H99) on a 0.8% agarose gel stained with gel red. Lane 1:100 bp ladder, Lanes 2: H4, Lane 3: S48B, Lane 4:S68B and Lane 5: H99

The purity of RNA sample was confirmed using RNA Integrity Number (RIN). Measurements of the RNA quality were generated by the Bioanalyser (Agilent's 2100 Bioanalyser). In the microarray analysis the samples are recommended to have a minimum RIN score of 7.0. All the RNA samples used in this study showed high quality and low degradation, in which the RIN of all samples were found to be ≥ 7 (Table 4.6, and Figure 4.12 to 4.14).

Table 4.6. Measurement of RNA concentration and purity of RNA by nanodrop spectrophotometer and Agilent's 2100 Bioanalyser

Sample ID	Nucleic Acid Conc.	260:280 Ratio	230:260 Ratio	RIN*
H4-1	283.4 ng/μl	2.0	1.7	7.20
H4-2	300.3 ng/μl	1.8	2	7.60
S48B-1	334.9 ng/μl	1.9	1.8	7.50
S48B-2	369.2 ng/μl	1.8	1.8	7
S68B-1	301.6 ng/μl	2.0	1.9	7.70
S68B-2	265.6 ng/μl	1.9	1.9	9
H99-1	361.3 ng/μl	1.8	2	8.10
H99-2	254.7 ng/μl	1.8	1.9	8.30

*RNA Integrity Number

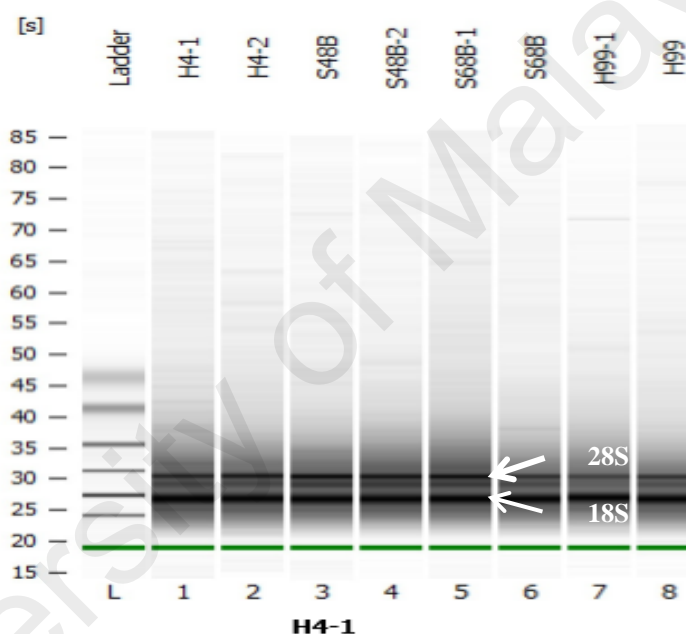


Figure 4.13. Densitometry plot of the total RNA using Bioanalyser analysis. The gel-like image bands showed high quality RNA, that were represented as two distinct bands corresponding to the 18S and 28S ribosomal RNAs.

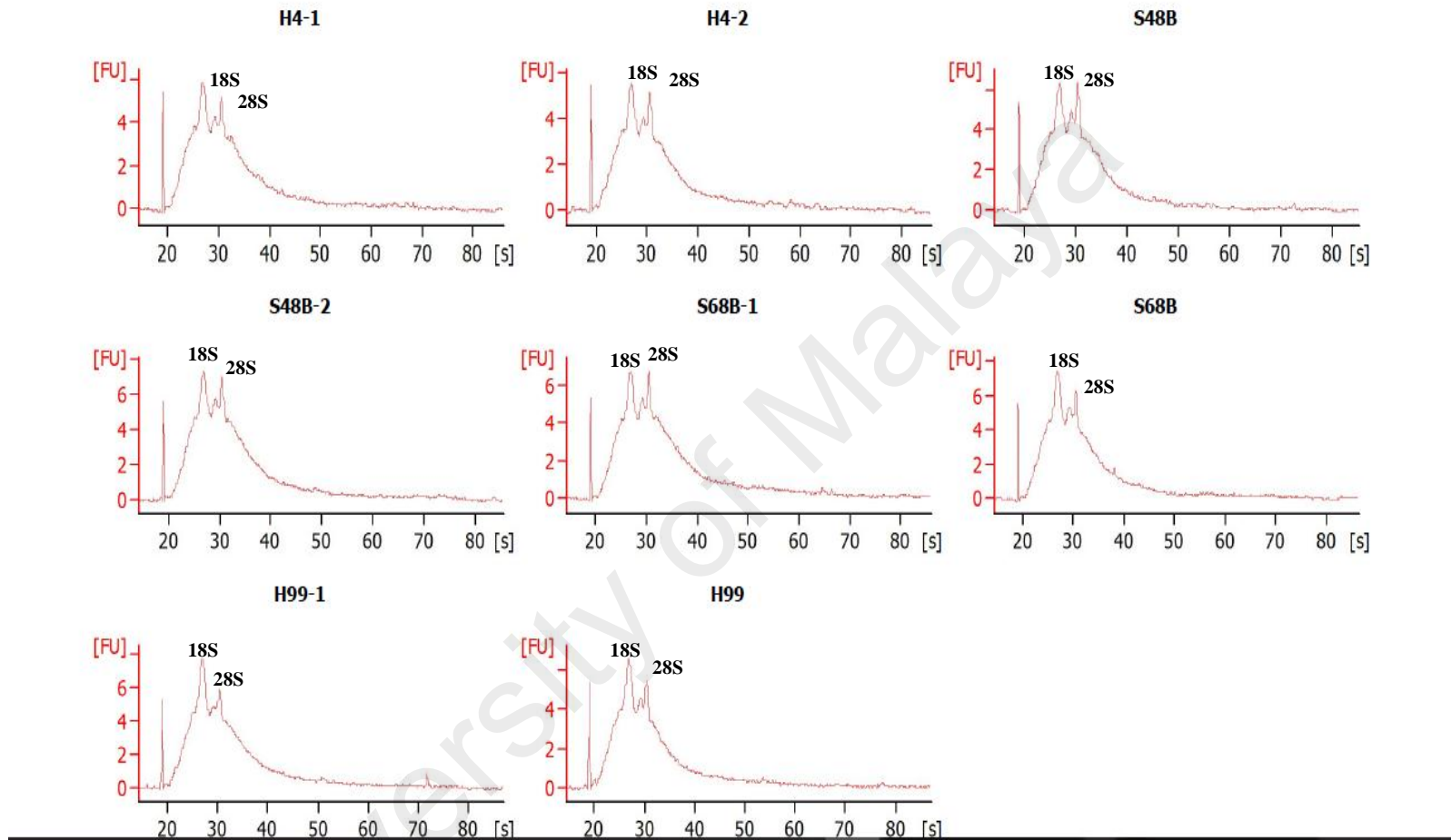


Figure 4.14. Electropherogram of the total RNA for each sample using Bioanalyser. No contaminating genomic DNA peak was found between the 18S and 28S peaks in all samples as can be seen in the graph.

4.9.2 Gene expression analysis

In order to gain deeper insight into the gene expression pattern of clinical and bird dropping strains of *C. neoformans*, microarray analysis was performed. The experimental design in this experiment consists of 4 conditions with duplicate each, namely S48B, S68B, H4 (environmental strains) and H99 (clinical strain). Because the *C. neoformans* microarray chip was not commercially available, microarray slide on an 8-array chip was customized-made. Since *C. neoformans* does not have a catalog product covering it, to customize the product, a database of transcript is needed whereby sequences known to be expressed by the organism has been documented which can be used in the design of the microarray. The transcripts sequence found from BROAD Institute's previous experiment and deposited in the link below.

www.broadinstitute.org/annotation/genome/cryptococcus_neoformans

The sequences are downloaded as a transcript fasta file and uploaded into the Agilent webtool, eArray (<https://earray.chem.agilent.com/>), for the design of specific probes against the transcript sequence. The total numbers of features analyzed on each array were 22,257 probes (7,419 genes) in triplicates.

4.9.3 Microarray data analysis

The quality control filters were used to filter the obtained data in order to determine the quality of hybridisation and the microarray. The outlier samples were also identified and removed. The quality control data obtained showed that not all the arrays on the microarray chip met the expected quality control as it can be seen in the Figure 4.15.

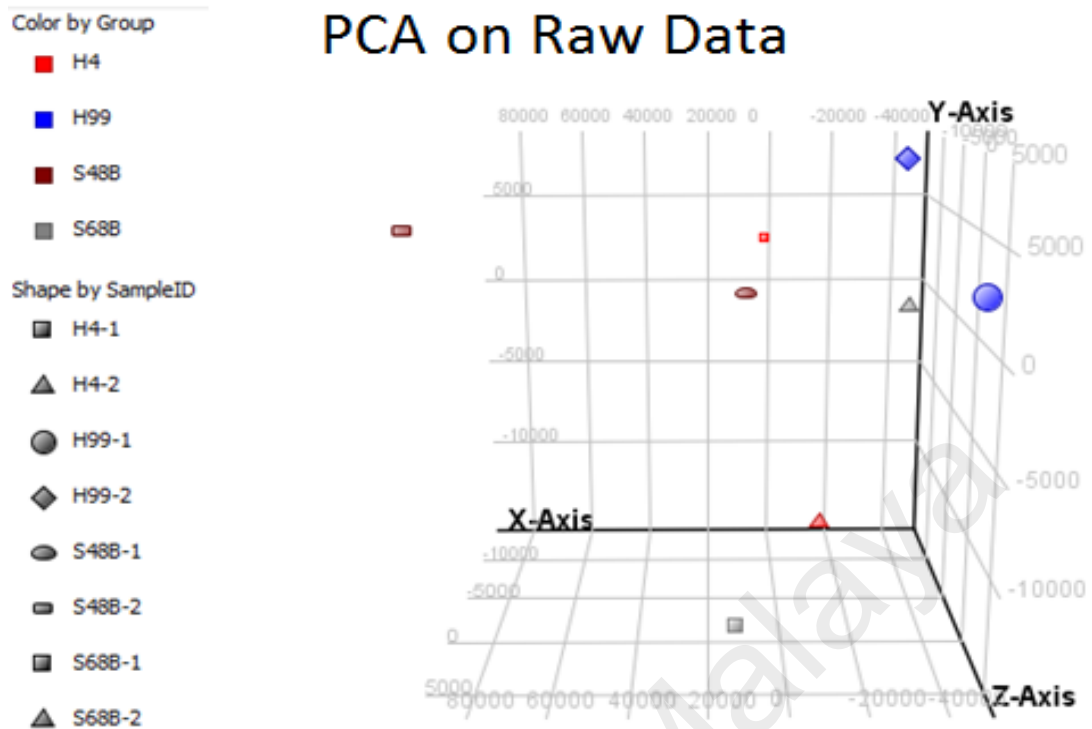


Figure 4.15. Quality control of samples using principal component analysis (PCA) algorithm base on raw signal values*

*Raw Signal Values: The term “raw” signal values refer to the linear data after thresholding and summarization is performed by computing the geometric mean.

4.9.3.1 Determination of Pairwise correlation coefficient matrix

Pairwise correlation coefficient matrixes among all samples tested were as shown in Figure 4.16 Four *C. neoformans* strains (H99, H4, S48B and S68B) were compared. Two independent samples were prepared for each fungal strain. Numbers in the box represents correlation coefficient values among groups. Duplicates of each strain (rep1 and rep2) showed correlation values which ranged from 0.8 to 1.0. The correlation among different strains were at an average of 0.8584 (0.6644 to 0.9682), suggesting that all strains shared a relatively close expression patterns The highest correlation of 1.0 is exists between replicates of one strain and the lowest correlation of 0.664 is observed between S48B and S68B strains (Figure 4.16).

H4 rep1	H4 rep2	S68B rep1	S68B rep2	H99 rep1	H99 rep2	S48B rep1	S48B rep2	
1.0000	0.8612	0.8108	0.7986	0.8364	0.8606	0.7347	0.8359	H4 rep1
0.8612	1.0000	0.8872	0.8584	0.9682	0.9506	0.8335	0.8960	H4 rep2
0.8508	0.8872	1.0000	0.8228	0.8601	0.8987	0.8289	0.8799	S68B rep1
0.7986	0.8534	0.8228	1.0000	0.8933	0.7453	0.6644	0.7196	S68B rep2
0.8364	0.9682	0.8601	0.8933	1.0000	0.8688	0.7761	0.8310	H99 rep1
0.8605	0.9106	0.8987	0.7453	0.8688	1.0000	0.8023	0.9459	H99 rep2
0.7347	0.8335	0.8289	0.6644	0.7261	0.8023	1.0000	0.8397	S48B rep1
0.8359	0.8960	0.8799	0.7196	0.8330	0.9459	0.8337	1.0000	S48B rep2

Figure 4.16. Determination of pairwise correlation coefficient matrix (Rep1–2: replicates of samples). Dark box: high correlation; light box: low correlation

4.9.3.2 Normalization and filtration

The raw numerical data was then transferred to Gene Spring GX software for further analysis. Normalization typically, the first transformation applied to expression data, referred to as normalization, adjusts the individual hybridization intensities to balance them appropriately so that meaningful biological comparisons can be made. There are a number of reasons why data must be normalized, including unequal quantities of starting RNA, differences in labeling or detection efficiencies between the fluorescent dyes used, and systematic biases in the measured expression levels.

Normalization was carried out to minimize the technical variation across the samples and make the distributions across various arrays identical. Expression data were normalized base upon quantities with threshold 1 and baseline to median of all samples. In order to normalize the microarray data, the box-whisker analysis was performed on the distribution of log ratio intensity values of expression of the genes within the samples under the different experimental conditions. Normalization was carried out in order to recognize and identify samples that varied systematically. It was demonstrated that the value of the median for normalization, fell within the inner-quarter range of 75% at the top and the 25th percentile at the bottom for baseline transformation of all samples (Figure 4.17). It provides a very useful and informative summary for continuous variables. It is also useful for comparing the distributions of a continuous variable among mutually exclusive comparison groups.

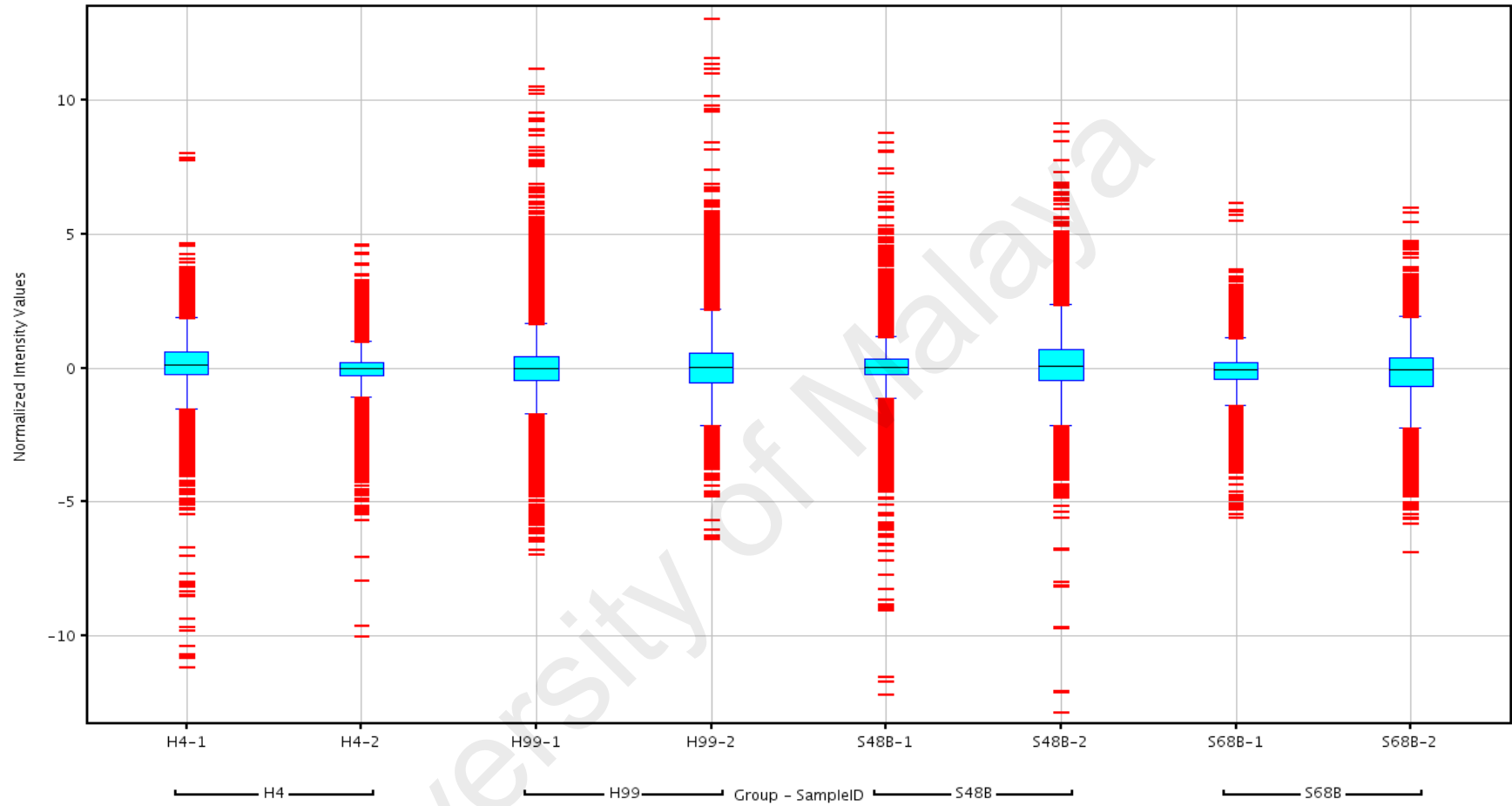


Figure 4.17. Box-Whisker Plot on normalized data using the Gene Spring software analysis

4.9.3.3 Quality control of samples using principal component analysis (PCA)

The normalized data was then filtered by expression base by their signal intensity values. The entity pass the filter if the intensity values between the upper cut-off: 20.0 and the lower cut-off: maximal value. The data were also filtered base on their flag values an undetected spot were removed (Figure 4.18).

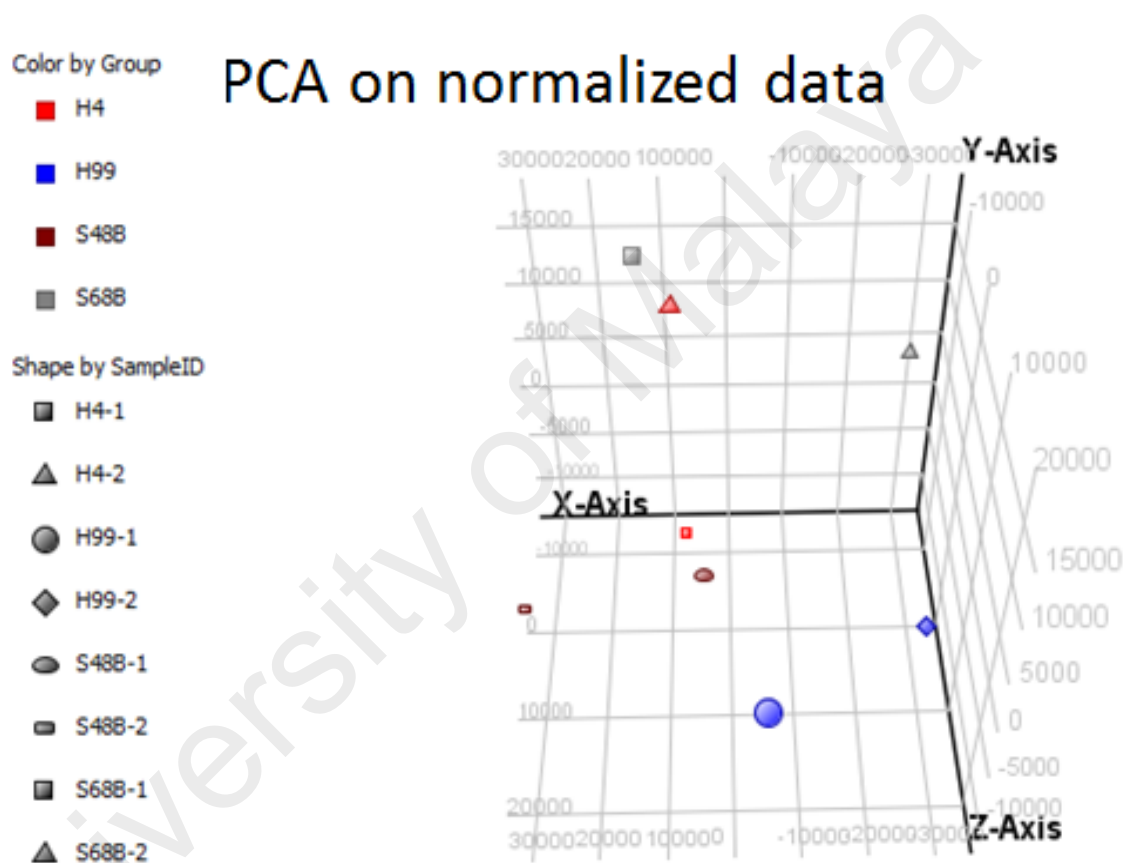


Figure 4.18. Quality control of samples using principal component analysis (PCA) algorithm based on normalized signal values*

*Normalized Signal Values: Normalized" value is the value generated after log transformation and normalization (Percentile Shift, Scale, normalize to control genes or Quantile) and baseline transformatio

4.9.4 Fold change analysis

4.9.4.1 Heat map analysis

To identify differentially expressed genes, fold change (FC) of each probe was calculated by normalizing the expression level in H99 strain to the expression in environmental strains. After microarray result was filtered with $FC < -2$ or $FC > 2$ ($P < 0.05$ by Post-Hoc testing), a total of 871 probes (434 genes) were found to be significantly up- or down-regulated. Note that the number of probes was not exactly three times of the number of genes because some probes were excluded during stringent filtration process. The heat map generated from these 871 significant probes revealed a distinct expression pattern of the H99 strain in comparison to other environmental strains (Figure 4.19). The heat map represents the colour-coded expression levels of the significantly regulated genes. The groups of genes which showed differential expressions in H99 versus other strains are as indicated. Low levels in H99 category indicates the genes with low expression levels in H99 (green) but high expression in the environmental strains (red). In contrast, high levels in H99 category indicates the genes with high expression levels in H99 (red) but show low expression in the environmental strains (green).

Hierarchical clustering based on Euclidean distance metric and Ward's Linkage showed closer distance of H4 to S68B, and H99 to S48B strains, consistent with molecular typing of the strains into Gr1 and Gr2 subtypes, respectively (Tay *et al.*, 2006).

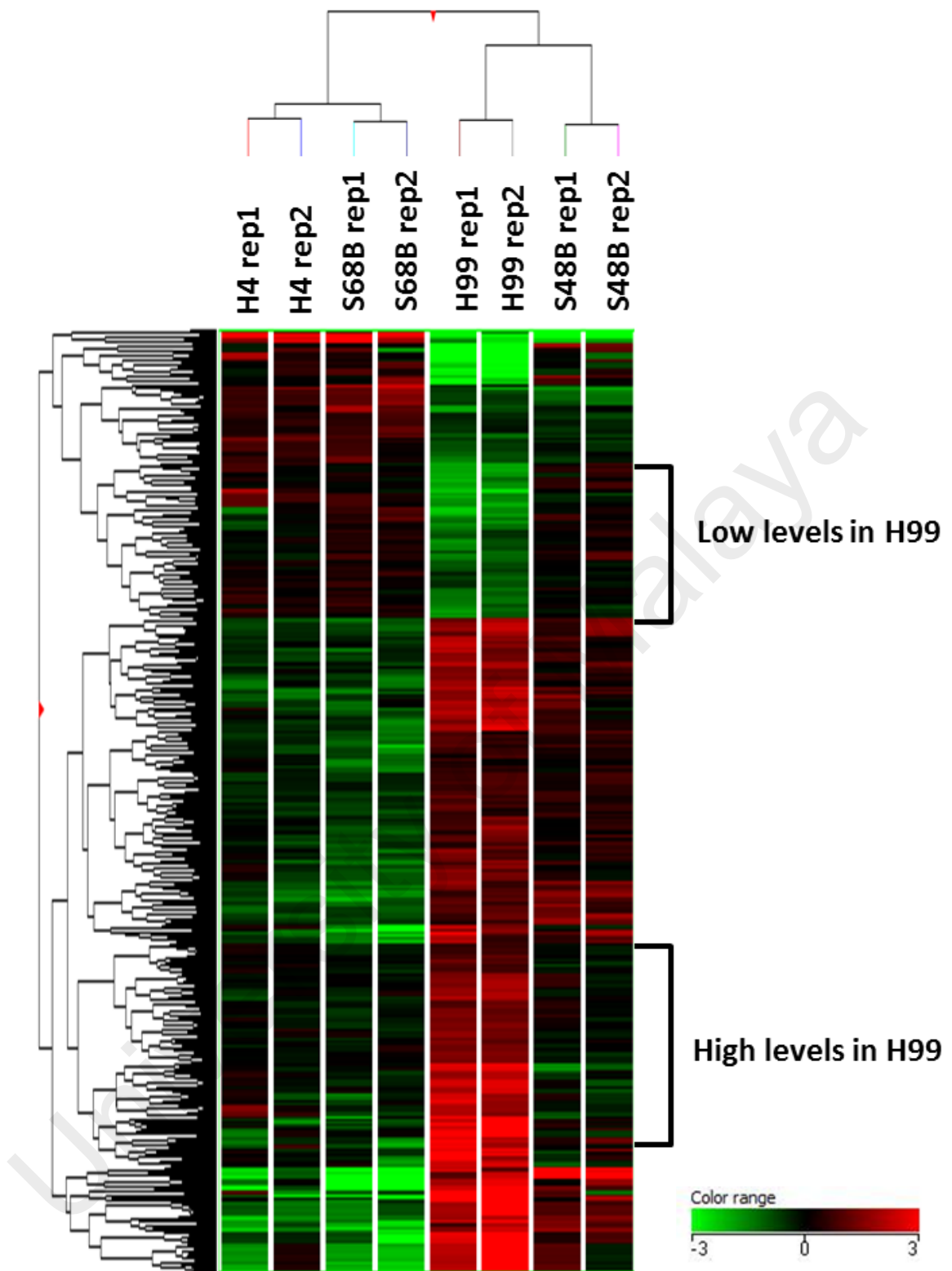


Figure 4.19. Heat map of Gene expression study (Colour range represents \log_{10} (FC) of the microarray intensities).

4.9.4.2 Scatter plots analysis

Scatter plots were used to compare the gene expression of H4, S48B and S68B with H99 strain (Figure 4.20). Majority of the plots were scattered around the medium line, indicating that no differential expressions between two strains. Those plots exceeding upper and lower border lines were determined as up- or down-regulated probes.

University of Malaya

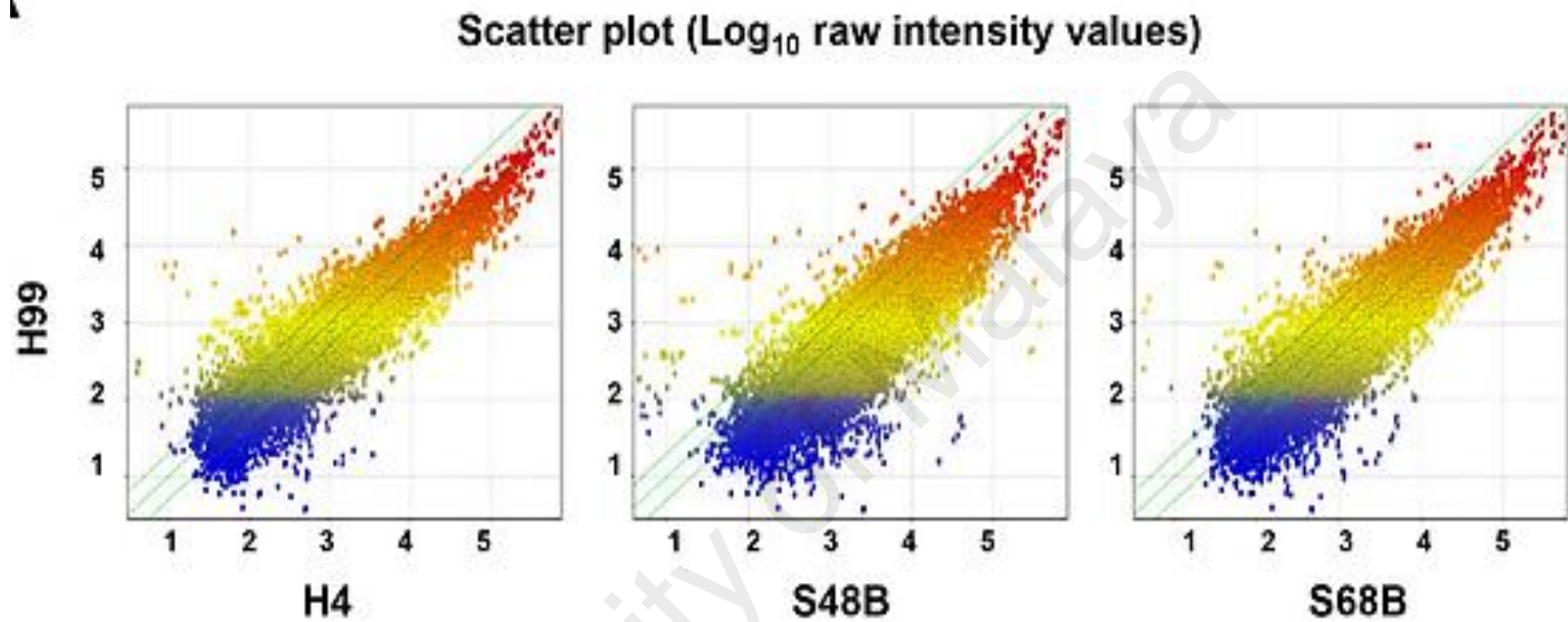


Figure 4.20. Gene expression analysis of H99 versus environmental strains. Scatter plots show the expressions of total probes in the H99 versus H4, S48B or S68B. X and Y axis show log₁₀ raw intensity values.

4.9.4.3 Venn diagram analysis

A Venn diagram was plotted using significantly expressed genes ($FC < -2$ or > 2 , $P < 0.05$) to show the distribution of the differentially regulated probes/genes in each group of comparisons (Figure 4.21). Some overlapping genes were detected between the strains. Remarkably, 133 probes (65 genes) were overlapped among all groups of comparisons, which suggest that these 65 genes were differentially expressed in the H99 clinical strain relative to all H4, S48B and S68B environmental strains. Also, 18 significantly regulated genes overlapped in S48B and S68B versus H99 strain (Table 4.7), 21 significantly regulated genes overlapped in H4 and S48B versus H99 (Table 4.8) and 77 significantly regulated genes overlapped in H4 and S68B versus the H99 strain (Table 4.9) are presented. These genes may have association with the virulence of *Cryptococcus* since H99 strain demonstrated stronger virulence in the intranasal infection of C57BL/6 mice. A list of 65 significant genes was as shown in the table 4.10 to 4.11.

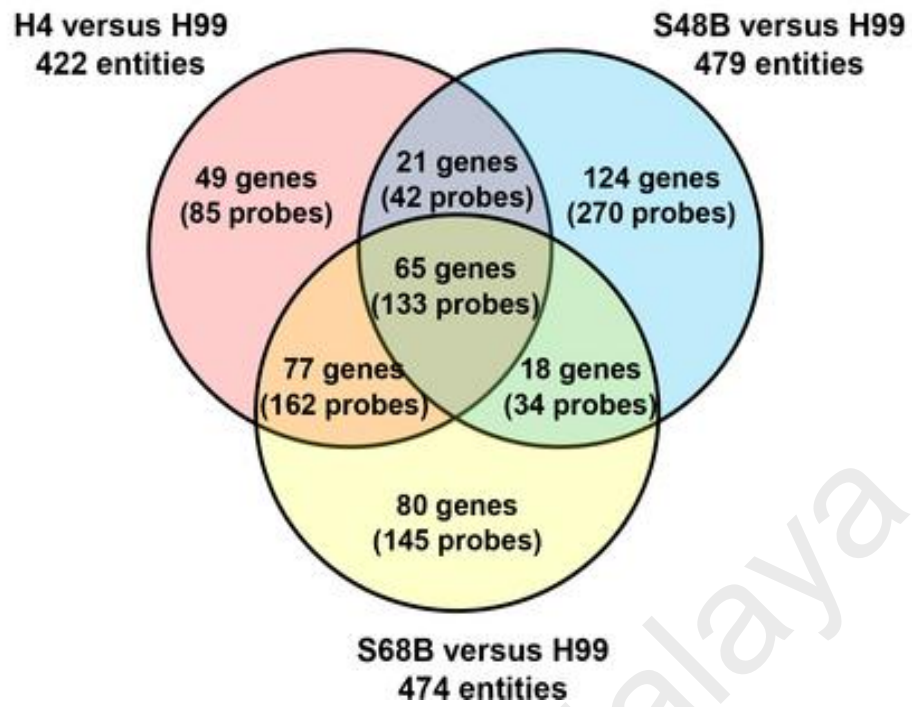


Figure 4.21. Venn diagram shows the distribution and the number of the genes (probes) in each group of comparison.

Table 4.7. List of 18 significantly regulated genes overlapped in environmental strains S48B and S68B versus the H99 clinical strain.

ProbeName	Blast_Hits	Yeast_Gene	Yeast Description	H4 vs H99	S48B vs H99	S68B vs H99
CNAG_01104T0_1176	NP_010368	<i>RRP8</i>	Ribosomal RNA-processing protein 8	-4.7252355	-5.1112723	-5.237372
CNAG_00884T0_2578	NP_013267	<i>SEC10</i>	Exocyst complex component SEC10	1.9174585	3.3260221	2.1916702
CNAG_04984T0_822	NP_014168	<i>PDR16</i>	Phosphatidylinositol transfer protein PDR16	-1.4996136	-2.5975294	-2.0297556
CNAG_05831T0_234	NP_012213	<i>MMF1</i>	Protein MMF1, mitochondrial	-1.9738735	-6.03281	-6.0067697
CNAG_05784T1_1016	NP_012234	<i>SSM4</i>	E3 ubiquitin-protein ligase Doa10	-1.8372158	-2.0021667	-2.017275
CNAG_04163T0_3017	XM_012186240.1	Undefined	H99 hypothetical protein mRNA	2.0962281	3.9628685	3.7869308
CNAG_08026T0_258	XM_012198559.1	Undefined	H99 hypothetical protein mRNA	7.9203568	10.739238	13.644045
CNAG_00915T0_951	XM_012193800.1	Undefined	H99 hypothetical protein, variant mRNA	-15.179825	-21.688839	-30.260221
CNAG_04030T1_174	XM_012192235.1	Undefined	H99 hypothetical protein, variant mRNA	-2.0815067	-4.4501085	-4.7396173
CNAG_03194T1_1194	XM_012195699.1	Undefined	H99 saccharopine dehydrogenase, variant mRNA	-5.4234347	-9.524397	-9.268312
CNAG_04363T0_2424	XM_012196119.1	Undefined	H99 hypothetical protein mRNA	-2.3368309	-2.582688	-3.1163685
CNAG_06411T0_1741	XM_012198089.1	Undefined	H99 hypothetical RNA other	-4.4297647	-6.4282618	-5.8297334
CNAG_04163T0_3019	XM_012196240.1	Undefined	H99 hypothetical protein mRNA	2.0856895	4.0565886	3.8115265
CNAG_05973T0_1088	XM_0121985878.1	Undefined	H99 hypothetical RNA other	5.713868	13.8945465	7.2525487
CNAG_00975T0_1648	XM_0121983830.1	Undefined	H99 hypothetical protein mRNA	-1.8277779	-2.1670954	-2.799351
CNAG_05864T0_1195	XM_0121985197.1	Undefined	H99 hypothetical protein mRNA	2.0441349	3.2885618	3.1624146
CNAG_04737T0_2695	XM_0121986590.1	Undefined	H99 hypothetical protein mRNA	2.422771	3.768463	4.6395855
CNAG_04163T0_3018	XM_0121983747.1	Undefined	H99 exocyst complex component protein mRNA	1.9978547	3.844413	3.6777265

Table 4.8. List of 21 significantly regulated genes overlapped in environmental strains H4 and S48B versus the H99 clinical strain.

ProbeName	Blast_Hits	Yeast_Gene	Yeast Description	H4 vs H99	S48B vs H99	S68B vs H99
CNAG_06485T0_1519	NP_010036	<i>HXT15</i>	Hexose transporter HXT15	5.4714875	7.5484424	3.7739518
CNAG_05290T0_721	XM_012193181.1	<i>SPT3</i>	H99 transcription initiation protein SPT3 mRNA	-4.4245486	-4.5330234	-3.2553318
CNAG_02992T0_1949	NP_010414	<i>SAC6</i>	Fimbrin	5.113758	4.9747524	4.5381193
CNAG_03772T0_1396	NP_010087	<i>SNF3</i>	High-affinity glucose transporter SNF3	-14.77345	-7.7859273	-5.2290144
CNAG_03893T0_2506	NP_012153	<i>SDP1</i>	Dual-specificity protein phosphatase SDP1	4.510563	3.1823912	2.188312
CNAG_02897T0_3690	XM_012192466.1	<i>KCS1</i>	H99 inositol hexaphosphate kinase 1 mRNA	2.2650576	2.0033755	1.8531551
CNAG_02081T0_1432	NP_012665	<i>MNS1</i>	Endoplasmic reticulum mannosyl-oligosaccharide 1,2-alpha-mannosidase	-2.5526907	-3.5166967	-1.9824935
CNAG_06359T0_527	NP_013372	<i>DCS1</i>	Scavenger mRNA-decapping enzyme DcpS	2.5871055	2.4672863	1.8239099
CNAG_02458T0_2508	XM_012194321.1	Undefined	H99 hypothetical protein, mRNA	2.8246646	2.8597243	2.0586314
CNAG_06657T0_337	XM_012194918.1	Undefined	H99 hypothetical protein, mRNA	2.0231686	2.9448981	1.9941508
CNAG_07950T2_292	XM_012191691.1	Undefined	H99 hypothetical protein, mRNA	-6.3171177	-157.97058	-3.0037918
CNAG_04516T0_450	XM_012196461.1	Undefined	H99 WSC domain-containing protein partial mRNA	-21.474234	-41.320652	-4.0286045
CNAG_04978T0_793	XR_001045675.1	Undefined	H99 hypothetical RNA other	3.603485	3.9598951	3.2712266
CNAG_04178T0_1632	XM_012196251.1	Undefined	H99 hypothetical protein partial mRNA	3.9546325	4.591161	2.7555242
CNAG_05411T0_1451	XM_012198363.1	Undefined	H99 endoglucanase mRNA	3.98949	7.2597556	2.2293658
CNAG_04681T1_1101	XM_012196751.1	Undefined	H99 hypothetical protein, variant mRNA	4.8219085	3.7982326	2.4215276
CNAG_07950T1_28	XM_012197488.1	Undefined	H99 hypothetical protein partial mRNA	-17.94614	-92.664795	-5.7165165
CNAG_07613T0_30	XM_012191691.1	Undefined	H99 hypothetical protein partial mRNA	-17.303926	-153.64026	-5.117729
CNAG_01968T0_256	XM_012197127.1	Undefined	H99 hypothetical protein partial mRNA	-19.668829	-160.58186	-5.5283484
CNAG_07447T0_255	XM_012194268.1	Undefined	H99 hypothetical protein partial mRNA	-17.149961	-146.82707	-5.757469
CNAG_07967T0_2323	XM_012193034.1	Undefined	H99 hypothetical protein partial mRNA	2.289409	2.4879375	1.5473541

Table 4.9. List of 77 significantly regulated genes overlapped in environmental strains H4 and S68B versus the H99 clinical strain.

ProbeName	Blast_Hits	Yeast_Gene	Yeast Description	H4 vs H99	S48B vs H99	S68B vs H99
CNAG_01082T0_2892	NP_010550	<i>AKR1</i>	Palmitoyltransferase AKR1	2.8	2.5	3.2
CNAG_07977T0_2326	NP_013199	<i>CHA4</i>	Activatory protein CHA4	-3	1.6	-3.3
CNAG_03960T0_1558	NP_012363	<i>CPS1</i>	Carboxypeptidase S	-2.1	-1.4	-4.2
CNAG_00826T0_1161	NP_013641	<i>DAK1</i>	Dihydroxyacetone kinase 1	-19.8	-2.8	-27
CNAG_06669T0_101	NP_009554	<i>ECM15</i>	UPF0045 protein ECM15	-3.6	-1.2	-3.7
CNAG_03011T0_961	NP_014125	<i>GOR1</i>	Putative 2-hydroxyacid dehydrogenase YNL274C	-6.1	-2.7	-6.2
CNAG_04024T0_1071	NP_012321	<i>HXT8</i>	Hexose transporter HXT8	-2.2	-1.2	-2.3
CNAG_03754T0_697	NP_009717	<i>IFA38</i>	3-ketoacyl-CoA reductase	-17	-1.6	-10.3
CNAG_06540T1_1680	NP_012550	<i>ILV3</i>	Dihydroxy-acid dehydratase, mitochondrial	-2.8	-1.9	-3.8
CNAG_06193T0_3376	NP_012429	<i>IME2</i>	Meiosis induction protein kinase IME2/SME1	2.1	1.7	2
CNAG_06849T0_1075	NP_012300	<i>LYS1</i>	Saccharopine dehydrogenase [NAD ⁺ , L-lysine-forming]	6.5	2	4.5
CNAG_06913T0_1105	NP_009869	<i>MATALPHA1</i>	Mating-type protein ALPHA1	-5.1	-1.3	-6.3
CNAG_07693T1_1606	NP_011569	<i>MUP1</i>	High-affinity methionine permease	-6.2	-2.5	-3.6
CNAG_01964T0_1950	NP_012323	<i>OPT1</i>	Oligopeptide transporter 1	-2.2	-1.4	-2.6
CNAG_00769T0_1432	NP_012407	<i>PBS2</i>	MAP kinase kinase PBS2	4.2	1.5	2.1
CNAG_02810T0_1995	NP_011501	<i>PUF4</i>	Pumilio homology domain family member 4	18.8	-1	26.6
CNAG_02557T0_1834	NP_012886	<i>RGT1</i>	Uncharacterized transcriptional regulatory protein YKL038W	3	-1.4	4.9
CNAG_04171T0_400	NP_013927	<i>ROT1</i>	Protein ROT1	3.1	2.3	2.7
CNAG_00872T0_2329	NP_013915	<i>SGS1</i>	ATP-dependent helicase SGS1	-7.8	-2.2	-10.2
CNAG_01862T0_1344	NP_010825	<i>STL1</i>	Sugar transporter STL1	-4.8	-2.1	-7.4
CNAG_00598T0_1368	NP_011776	<i>TNA1</i>	High-affinity nicotinic acid transporter	-2.7	1.1	-2.4
CNAG_04618T1_1676	NP_010111	<i>UGA3</i>	Transcriptional activator protein UGA3	-3.3	-2.6	-3
CNAG_04820T0_214	NP_014335	<i>YDJI</i>	Mitochondrial protein import protein MAS5	-4.8	1	-6.1
CNAG_00825T0_982	NP_012260	<i>YIA6</i>	Uncharacterized mitochondrial carrier YIL006W	2.3	1.7	2.3
CNAG_04415T0_683	NP_012630	<i>YJR096W</i>	Uncharacterized oxidoreductase YJR096W	-5.8	-3.3	-6.5
CNAG_03973T0_2820	NP_012707	<i>YKL215C</i>	Uncharacterized protein YKL215C	-2	-1.7	-2.9

Table 4.9 (continued). List of 77 significantly regulated genes overlapped in environmental strains H4 and S68B versus the H99 clinical strain.

Probe Name	Blast_Hits	Yeast_Gene	Yeast Description	H4 vs H99	S48B vs H99	S68B vs H99
CNAG_06566T0_1322	NP_013740	<i>YMR027W</i>	UPF0364 protein YMR027W	-2.2	-1.4	-2.3
CNAG_05786T1_1186	NP_015338	<i>YPR013C</i>	Zinc finger protein YPR013C	4.2	2.2	3.5
CNAG_03249T0_375	NP_010669	<i>YRA1</i>	RNA annealing protein YRA1	2	1.9	2.6
CNAG_00001T0_42	XM_012190753.1	Undefined	H99 hypothetical protein	-6.6	-1.2	-13.1
CNAG_00419T0_840	XR_001045344.1	Undefined	H99 hypothetical RNA other	-4.9	-2.4	-5.3
CNAG_00452T0_935	XM_012190927.1	Undefined	H99isovaleryl-CoA dehydrogenase mRNA	-3.4	-1	-4.9
CNAG_00628T0_260	XM_012191458.1	Undefined	H99 hypothetical protein	-5.1	-2.8	-7.6
CNAG_00789T0_10	XM_012193837.1	Undefined	H99 hypothetical protein	-15.6	-3.6	-15.4
CNAG_00838T0_213	XM_012191606.1	Undefined	H99 hypothetical protein	-4.2	-2.7	-4.6
CNAG_00850T0_1291	XM_012191613.1	Undefined	H99 plant-inducible protein mRNA	-8.6	-4.4	-8.4
CNAG_00968T0_122	XM_012193825.1	Undefined	H99 hypothetical protein, variant 2 mRNA	-3.5	-2.1	-3.3
CNAG_01719T0_1081	XM_012197045.1	Undefined	H99 hypothetical protein, variant 2 mRNA	-9	-2.2	-5
CNAG_01929T0_1166	XM_012197463.1	Undefined	H99 hypothetical protein, variant 2 mRNA	-4	-2.4	-3.7
CNAG_01996T1_2788	XM_012197507.1	Undefined	H99 hypothetical protein, variant 2 mRNA	-4	1	-5.5
CNAG_02044T0_146	XM_012194506.1	Undefined	H99 hypothetical protein, variant 2 mRNA	-11.6	-1.7	-14.8
CNAG_02510T1_1342	XM_012194806.1	Undefined	H99 hypothetical protein, variant 2 mRNA	2.8	1.4	2.4
CNAG_02558T0_388	XM_012194288.1	Undefined	H99 cuplin domain-containing protein mRNA	38.7	-3.4	47.7
CNAG_03083T0_301	XM_012192933.1	Undefined	H99 cuplin domain-containing protein mRNA	-4.4	-1.8	-4.1
CNAG_03534T0_494	XM_012195932.1	Undefined	H99 hypothetical protein variant mRNA	-2.4	-1.2	-2.5
CNAG_03664T0_1145	XM_012191983.1	Undefined	High-affinity nickel-transporter mRNA	-2.4	-1.1	-3.1
CNAG_04185T0_665	XM_012196256.1	Undefined	H99 hypothetical protein mRNA	5.7	3.7	5
CNAG_04901T0_649	XM_012196520.1	Undefined	H99 hypothetical protein mRNA	-37.7	-32.5	-56.7
CNAG_05586T0_1375	XM_012198474.1	Undefined	H99 hypothetical protein mRNA	-2.6	-1.3	-4
CNAG_05649T0_777	XM_012198515.1	Undefined	H99 hypothetical protein mRNA	2.2	1.8	2.1
CNAG_05911T0_433	XM_012195906.1	Undefined	H99 hypothetical RNA other	-17.1	-4	-14.4
CNAG_05990T0_1727	XM_012197564.1	Undefined	H99 hypothetical protein mRNA	-3.5	1.6	-3.4
CNAG_06653T0_473	XM_012194876.1	Undefined	H99 hypothetical protein mRNA	-3.2	-2.5	-5.3
CNAG_06653T1_428	XM_012195370.1	Undefined	H99 hypothetical protein mRNA	-3.2	-2.4	-5.2
CNAG_06801T0_415	XM_012191707.1	Undefined	H99 hypothetical protein mRNA	-13	1.9	-101.8

Table 4.9 (continued). List of 77 significantly regulated genes overlapped in environmental strains H4 and S68B versus the H99 clinical strain.

Probe Name	Blast_Hits	Yeast_Gene	Yeast Description	H4 vs H99	S48B vs H99	S68B vs H99
CNAG_06802T0_367	XM_012192350.1	Undefined	H99 hypothetical protein partial mRNA	-13.2	-1.1	-17
CNAG_06912T1_531	XM_012192954.1	Undefined	H99 hypothetical protein variant mRNA	-3.2	1.9	-5.3
CNAG_07304T0_141	XM_012190752.1	Undefined	H99 hypothetical protein mRNA	-11.3	4.5	-40.9
CNAG_07344T1_2441	XM_012191654.1	Undefined	H99 ras guanyl-nucleotide exchange factor	-4.2	-1.5	-4.8
CNAG_07358T0_473	XM_012190897.1	Undefined	H99 hypothetical protein mRNA	-2.4	-1.7	-2.6
CNAG_07389T0_1624	XM_012193763.1	Undefined	H99 flavin –containing monooxygenase partial mRNA	-16.8	-7.9	-39
CNAG_07444T0_1130	XM_012194266.1	Undefined	H99 hypothetical protein mRNA	-15.1	-7.7	-16.9
CNAG_07582T0_282	XM_012193031.1	Undefined	H99 dynein light chain roadblock-type mRNA	2.8	1.8	2.7
CNAG_07956T0_1995	XM_012191699.1	Undefined	H99 WD repeat and SOF domain-containing protein 1 mRNA	3.2	1.6	3.5
CNAG_08020T0_282	XM_012198550.1	Undefined	H99 hypothetical protein mRNA	-10.8	-9.5	-17.2
CNAG_07344T1_2618	XM_012198550.8	Undefined	H99 ras guanyl-nucleotide exchange factor mRNA	-6.7	-2	-8.4
CNAG_06802T0_387	XM_012190832.1	Undefined	H99 hypothetical protein partial mRNA	-15.1	-1.5	-20.7
CNAG_06526T0_608	XM_012194876.1	Undefined	H99 hypothetical protein mRNA	-2.2	-1.3	-2.1
CNAG_05586T1_1223	XM_012198474.1	Undefined	H99 hypothetical protein mRNA	-3.9	-2	-5.1
CNAG_06525T0_578	XM_012194875.1	Undefined	H99 nuclear protein mRNA	2.6	-1.3	4.2
CNAG_02077T0_368	XM_012191442.1	Undefined	H99 nicotinamide mononucleotide permease mRNA	-2.7	-1.1	-3.7
CNAG_02423T0_1380	XM_012194337.1	Undefined	H99 hypothetical protein mRNA	3.2	1	2.4
CNAG_02510T0_1478	XM_012194806.1	Undefined	H99 hypothetical protein, variant 2 mRNA	2.8	1.4	2.3
CNAG_02558T0_418	XM_012194282.1	Undefined	H99 hypothetical protein mRNA	74.2	-3.7	92.2
CNAG_03083T0_310	XM_012192933.1	Undefined	H99 cupin domain-containing protein mRNA	-4.3	-1.9	-4.1
CNAG_03136T0_1290	XM_012195657.1	Undefined	H99 hypothetical protein mRNA	3.1	2.4	2.9
CNAG_07344T0_2678	XM_012191654.9	Undefined	H99 ras guanyl-nucleotide exchange factor mRNA	-6	-1.9	-7.7

Table 4.10. List of 41 genes significantly up-regulated in H99 versus H4, S48B and S68B strains.

Probe Name	Blast_Hits	Yeast_Gene	Yeast Description	H4 vs H99	S48B vsH99	S68Bvs H99
CNAG_03084T0_334	NP_012213	<i>MMF1</i>	Protein MMF1, mitochondrial	-336.6	-133.1	-453.4
CNAG_06956T0_399	NP_192919.1	<i>MVA1</i>	Hydroxymethylglutaryl-CoA synthase	-318.5	-36.1	-1151.7
CNAG_04901T0_584	NP_013457.1	<i>BUD8</i>	Bud-site-selection protein 8	-40.5	-37.5	-62.5
CNAG_03433T0_1016	XM_012195865.1	Undefined	H99 endo alpha-1,4polygalactosaminidase precusure mRNA	-15.3	-15.4	-10.7
CNAG_03772T0_1438	NP_010087	<i>SNF3</i>	High-affinity glucose transporter SNF3	-15.2	-8.0	-5.5
CNAG_03477T0_50	NP_010667.1	<i>RGA2</i>	Rho GTPase-activating protein 2	-13.6	-7.2	-11.9
CNAG_05426T0_545	XM_012198372.1	Undefined	E3 ubiquitin-protein ligase PRP19 [<i>Saccharomyces cerevisiae</i> S288c]	-13.1	-5.2	-10.2
CNAG_01995T0_522	NP_013452.1	<i>DIC1P</i>	Dic1p [<i>Saccharomyces cerevisiae</i> S288c]	-11.6	-12.1	-13.4
CNAG_00826T0_1147	NP_013641	<i>DAK1</i>	Dihydroxyacetone kinase 1	-11.5	-2.6	-10.7
CNAG_06337T0_1243	NP_010872.1	<i>GDA1P</i>	Gda1p [<i>Saccharomyces cerevisiae</i> S288c]	-7.6	-17.5	-6.3
CNAG_07387T0_1849	NP_011816	<i>ARN2</i>	Siderophore iron transporter ARN2	-6.7	-10.2	-11.4
CNAG_04507T0_826	XM_012196454.1	Undefined	H99 hypothetical protein	-6.4	-4.1	-6.6
CNAG_01494T1_640	XM_01217171.1	Undefined	H99 hypothetical protein	-6.0	-5.3	-5.2
CNAG_03400T0_1015	NP_014490	<i>GRE2</i>	NADPH-dependent methylglyoxal reductase GRE2	-5.9	-3.7	-7.9
CNAG_01498T0_1754	NP_013090.1	<i>SOF1P</i>	Sof1p [<i>Saccharomyces cerevisiae</i> S288c]	-5.7	-7.7	-8.1
CNAG_02011T0_1027	NP_010883.3	<i>SPF1</i>	Ion-transporting P-type ATPase SPF1 [<i>Saccharomyces cerevisiae</i> S288c]	-5.4	-2.6	-5.0
CNAG_07428T0_625	NP_015525.1	<i>ARR1P</i>	Arr1p [<i>Saccharomyces cerevisiae</i> S288c]	-4.8	-6.1	-5.9
CNAG_02083T0_1719	NP_011823	<i>ARN1</i>	Siderophore iron transporter ARN1	-4.7	-8.1	-5.5
CNAG_00838T0_310	NP_009353.1	<i>AIM1P</i>	Aim1p [<i>Saccharomyces cerevisiae</i> S288c]	-4.5	-3.1	-4.7
CNAG_04967T0_1021	NP_011608.1	<i>VAS1</i>	Valine--tRNA ligase [<i>Saccharomyces cerevisiae</i> S288c]	-4.5	-4.2	-3.7
CNAG_06653T1_22	NP_014127.1	<i>SEC2P</i>	Sec2p [<i>Saccharomyces cerevisiae</i> S288c]	-4.0	-3.3	-6.6
CNAG_04541T0_1287	NP_011471	<i>RNA15</i>	mRNA 3'-end-processing protein RNA15	-3.9	-3.6	-4.0
CNAG_06411T0_1614	NP_116685.1	<i>PTR3P</i>	Ptr3p [<i>Saccharomyces cerevisiae</i> S288c]	-3.8	-4.9	-4.9
CNAG_04618T1_2110	NP_010111	<i>UGA3</i>	Transcriptional activator protein UGA3	-3.8	-3.0	-3.3

Table 4.10 (Continued). List of 41 genes significantly up-regulated in H99 versus H4, S48B and S68B strains.

Probe Name	Blast_Hits	Yeast_Gene	Yeast Description	H4 vs H99	S48B vs H99	S68B vs H99
CNAG_04618T0_1736	NP_010111	<i>UGA3</i>	Transcriptional activator protein UGA3	-3.4	-3.0	-3.5
CNAG_05644T0_925	NP_012683	<i>YJR149W</i>	Putative 2-nitropropane dioxygenase	-3.1	-2.7	-3.9
CNAG_03393T0_741	NP_012553	<i>TES1</i>	Peroxisomal acyl-coenzyme A thioester hydrolase 1	-3.0	-4.6	-5.3
CNAG_02439T0_493	NP_009974.1	<i>CSG2</i>	mannosylinositol phosphorylceramide synthase regulatory subunit [<i>Saccharomyces cerevisiae</i> S288c	-3.0	-3.2	-2.7
CNAG_02439T1_409	NP_009974.1	<i>RRTL2p</i>	Rrt12p [<i>Saccharomyces cerevisiae</i> S288c]	-3.0	-3.2	-2.6
CNAG_00484T0_1473	XM_012190936.1	Undefined	H99 2-oxoisovalerate dehydrogenase E2 component (dihydrolipoyl transacylase) mRNA	-2.9	-3.0	-2.4
CNAG_04346T0_968	XM_012196355.1	Undefined	H99 dihydrodipicolinate synthase mRNA	-2.9	-3.4	-2.9
CNAG_06540T1_1679	NP_012550	<i>ILV3</i>	Dihydroxy-acid dehydratase, mitochondrial	-2.8	-2.0	-3.9
CNAG_04122T0_1086	NP_013755	<i>ARA2</i>	D-arabinose 1-dehydrogenase	-2.7	-2.7	-2.4
CNAG_02336T0_1615	NP_013031	<i>VBA5</i>	Vacuolar basic amino acid transporter 5	-2.6	-2.6	-4.7
CNAG_07980T0_45	NP_010066.1	<i>GDH2</i>	Glutamate dehydrogenase (NAD(+)) [<i>Saccharomyces cerevisiae</i> S288c]	-2.5	-2.4	-3.2
CNAG_04034T0_839	NP_013086.1	<i>BPT1</i>	ATP-binding cassette bilirubin transporter BPT1 [<i>Saccharomyces cerevisiae</i> S288c]	-2.4	-2.2	-3.1
CNAG_03819T0_544	NP_013706	<i>ERG6</i>	Sterol 24-C-methyltransferase	-2.4	-2.7	-3.2
CNAG_04363T0_2449	NP_011853.1	<i>ETP1P</i>	Etp1p [<i>Saccharomyces cerevisiae</i> S288c]	-2.4	-2.5	-3.0
CNAG_06239T0_1499	NP_013580.1	<i>ERG13</i>	Hydroxymethylglutaryl-CoA synthase [<i>Saccharomyces cerevisiae</i> S288c]	-2.2	-2.7	-2.2
CNAG_06806T0_862	NP_015329	<i>AIM45</i>	Probable electron transfer flavoprotein subunit alpha, mitochondrial	-2.1	-2.7	-2.3
CNAG_05784T1_1057	NP_012234	<i>SSM4</i>	E3 ubiquitin-protein ligase Doa10	-2.1	-2.0	-2.2

Table 4.11. List of 24 genes significantly up-regulated in H99 versus H4, S48B and S68B strain.

Probe Name	Blast-Hit	Gene-Name	Yeast Description	H4 vs H99	S48 vs H99	S68 vs H99
CNAG_05332T0_622	NP_012694	<i>MPH2</i>	Alpha-glucosides permease MPH2/3	57.4	189.8	69.0
CNAG_05333T0_1673	NP_012910	<i>PUT3</i>	Proline utilization trans-activator	51.3	69.7	32.0
CNAG_03087T0_1523	NP_009857	<i>MAL31</i>	Maltose permease MAL31; Maltose permease MAL61	44.8	13.6	23.3
CNAG_01858T0_1311	NP_010021	<i>HMRA1</i>	Mating-type protein A1	21.3	17.6	12.1
CNAG_07313T0_320	XM_012190795.1	Undefined	H99 hypothetical protein mRNA	16.2	151.2	16.3
CNAG_04030T0_242	NP_014029.1	<i>ADE4</i>	amidophosphoribosyltransferase [<i>Saccharomyces cerevisiae</i> S288c]	12.6	5.8	5.0
CNAG_06868T0_730	NP_012044	<i>ENO2</i>	Enolase 2	11.2	9.4	15.3
CNAG_07707T0_1685	NP_015447.1	<i>AXI1P</i>	Ax11p [<i>Saccharomyces cerevisiae</i> S288c]	7.2	4.9	9.4
CNAG_05973T0_1159	NP_013769.1	<i>STB2P</i>	Stb2p [<i>Saccharomyces cerevisiae</i> S288c]	6.2	15.8	8.2
CNAG_05872T0_1058	NP_015171	<i>PEP4</i>	Saccharopepsin	6.1	2.5	4.6
CNAG_04185T0_667	NP_015414.2	<i>YPR089W</i>	Hypothetical protein YPR089W [<i>Saccharomyces cerevisiae</i> S288c]	5.4	3.5	4.8
CNAG_06016T0_1557	NP_012789.2	<i>YKL133C</i>	hypothetical protein YKL133C [<i>Saccharomyces cerevisiae</i> S288c]	5.2	5.9	3.8
CNAG_02992T0_2056	NP_010414	<i>SAC6</i>	Fimbrin	5.0	5.0	4.8
CNAG_05786T1_1058	NP_015338	<i>YPR013C</i>	Zinc finger protein YPR013C	4.6	2.4	3.6
CNAG_02351T0_1732	XM_012194706.1	Undefined	H99 hypothetical protein mRNA	3.8	3.9	4.4
CNAG_04978T0_794	NP_011884.1	<i>YHR020W</i>	proline tRNA ligase [<i>Saccharomyces cerevisiae</i> S288c]	3.7	4.2	3.5
CNAG_06334T0_1554	NP_009405.1	<i>SEN34</i>	Sen34p [<i>Saccharomyces cerevisiae</i> S288c]	3.6	2.6	3.2
CNAG_01533T0_2123	NP_015210	<i>BEM3</i>	GTPase-activating protein BEM3	3.4	5.2	3.4
CNAG_04737T0_2461	NP_013895.1	<i>HOT1P</i>	Hot1p [<i>Saccharomyces cerevisiae</i> S288c]	3.2	5.3	5.5
CNAG_06359T0_714	NP_013372	<i>DCS1</i>	Scavenger mRNA-decapping enzyme DcpS	3.1	3.0	2.3
CNAG_03136T0_1325	XM_012195657.1	Undefined	H99 hypothetical protein mRNA	2.8	2.3	2.8
CNAG_01082T0_3293	NP_010550	<i>AKR1</i>	Palmitoyltransferase AKR1	2.6	2.4	2.9
CNAG_06223T0_1780	NP_014799	<i>NF11</i>	E3 SUMO-protein ligase SIZ2	2.5	2.1	2.2
CNAG_03689T0_1787	NP_013860	<i>SIP5</i>	Protein SIP5	2.5	2.4	2.4
CNAG_07939T0_65	XM_012198165.1	Undefined	H99 hypothetical protein mRNA	2.1	2.6	3.1

4.9.5 Identification of significantly up-regulated and down-regulated genes in *C. neoformans* H99 strain and environmental strains

List of 41 genes significantly up-regulated in H99 versus H4, S48B and S68B strains. Among the genes, five (*MVA1*, *MMF1*, *BUD8*, *SNF3* and *RGA2*) were expressed at an intensely high level in *C. neoformans* H99 relative to environmental strains (Table 4.10). In contrast, genes that showed significant lower expression in H99 strain included *MPH2*, *PUT3*, *MAL31*, *HMRAI* and *ENO2* (Table 4.11). To validate the microarray data, expression of selected top differentially regulated genes including *MVA1*, *MMF1*, *MPH2* and *PUT3* were verified using qRT-PCR (Figure 4.22). Consistent with the microarray data, qRT-PCR showed that expression levels of *MVA1* and *MMF1* were significantly increased in H99 relative to other environmental strains at >142 and >19 folds, respectively. On the other hand, the *MPH2* and *PUT3* were reduced in H99 at >4.2 and >25 folds, respectively.

To examine if the primers used in real-time qRT-PCR can work equally well in all the strains, the sequencing analysis for each strain was performed. Primer hybridization regions for all four genes tested (*MMF1*, *MPH1*, *MVA1* and *PUT3*) showed completely conserved sequences (ranging from 202 to 267 nucleotides) in all *C. neoformans* strains, suggesting equal amplification efficiency.

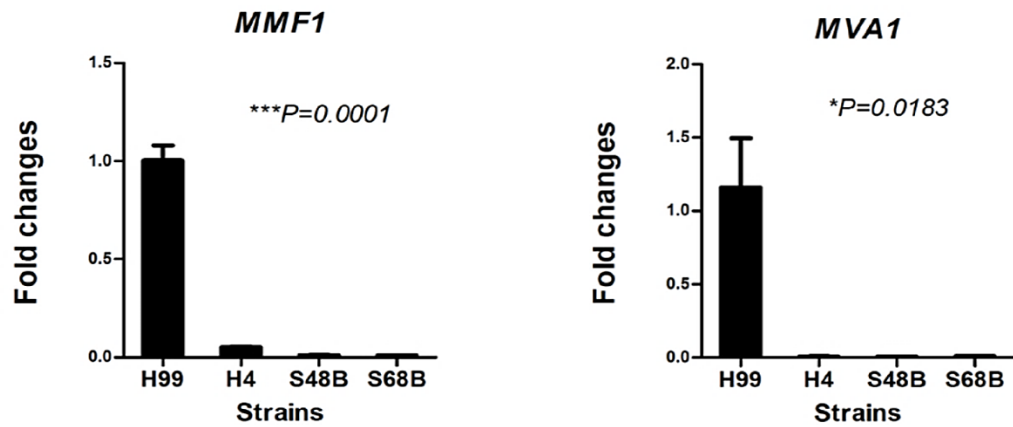
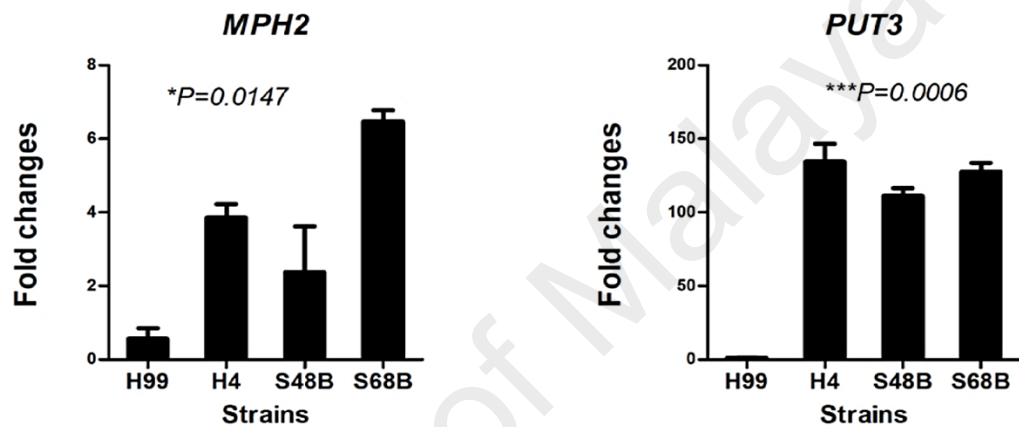
A**B**

Figure 4.22. qRT-PCR verification. RNAs were extracted from H99, H4, S48B strains and S68B for qRT-PCR analysis of 4 top up- and down-regulated genes (*MMF1*, *MPH1*, *MVA1* and *PUT3*). Two independent samples were prepared for each fungal strain. All samples were run in triplicates and data were shown as mean \pm SD. $P < 0.05$ by two-way ANOVA. (*GAPDH* was used as endogenous control to normalise the data).

4.9.6 KEGG Pathway analysis

The over-represented pathway categories of the 65 significantly regulated genes (Table 4.12) were studied for their pathway analysis using The Database for Annotation, Visualization and Integrated Discovery (DAVID) bioinformatics resource based on the Kyoto Encyclopedia of Genes and Genomes (KEGG) databases (Figure 4.23).

Representative annotation of each cluster and gene details of 65 genes are as listed in table 4.10 to 4.11 and figure 4.21. The top 9 pathways involved for 65 genes are presented. Most genes were involved in iron transport with enrichment score of 16.6 to 11 (Table 4.12). Similarly, The top in the list of the over-represented pathways for 65 genes is metal ion binding (GO:0045872) with fold enrichment (FE) at 1.68 (P=0.015). A total of eleven genes (out of the 65 significant genes) are found to be listed in the metal ion binding pathway database, suggesting that considerable numbers of the H99-specific genes were associated with metal ion binding process (Table 4.13). Among these eleven genes 6 genes were down-regulated and 5 genes were up-regulated in environmental strains compare to H99 (Figure 4.23). In addition, three genes which were all up regulated in environmental strain vs H99 were found to be associated with sugar transmembrane transporter activity in fungal cells (GO:0051119) (FE=1.65, P=0.010). Other relevant pathways included, integral to membrane (GO:001602, P=0.42) with 3 up-regulated and 5 down-regulated genes in environmental vs H99, organelle lumen (GO:0043233, P=0.65) with one gene up-regulated in environmental strain among 4 genes, transit peptide: mitochondrion (Up_Seq) with all 4 genes up regulated in H99 compare to environmental strains, transcription factor activity (GO:0003700, P=0.19) and cellular catabolic process (GO:0044257, P=0.12) with just one gene down-regulated in environmental compare to H99. However these five pathways were not statistically significant. The heat map for each pathway was plotted

to show the gene expression level in the group of genes involved in each pathway (Figure 4.24). The genes that were up-regulated in clinical H99 were shown with red color in each pathway, while the genes indicated with green color were up-regulated in environmental strains.

University of Malaya

Table 4.12. The 65 significant genes which were differentially regulated in H99 compared to environmental strains were analyzed and top nine regulated pathways are presented. The representative of each annotation cluster detected was shown. (C) Count represents number of genes which match the pathway database, and % represents the percentage of gene hits among the total genes in the pathway database. Enrichment score (ES) of each group was measured by the geometric mean of the EASE Scores (modified Fisher Exact) associated with the enriched annotation terms that belong to this gene group. Population hit (Pop Hits) represents have the function name in the gene list of interest, and population total (Pop Total) represents - genes in overall population has that function name in the background genome (all genes in the species of interest in DAVID database). False discovery rate (FDR) represents the percentages of test which might be false positive. *P* values were analyzed using Fisher exact score to identify which sub-populations are over- or under-represented in a sample. Data were considered significant if *P*<0.05.

Category	Term	Genes	ES	C	%	Pop Hits	Pop Total	FDR	P
GOTERM_BP_FAT	iron assimilation by chelation and transport	<i>FRE3, ARN1, ARN2</i>	16.6	3	0.51	6	4870	17.5	0.012
GOTERM_BP_FAT	iron chelate transport	<i>FRE3, ARN1, ARN2</i>	16.6	3	0.51	6	4870	17.5	0.012
GOTERM_BP_FAT	siderophore-iron transport	<i>FRE3, ARN1, ARN2</i>	16.6	3	0.51	6	4870	17.5	0.012
GOTERM_MF_FAT	cation symporter activity	<i>DAL4, MAL31, PHO89, ARR3, SMF1, STL1</i>	16.3	6	1.02	11	4190	0.0	0.000
GOTERM_CC_FAT	vacuolar lumen	<i>PEP4, PRC1, ATG15</i>	15.0	3	0.51	8	4595	18.0	0.015
GOTERM_BP_FAT	iron assimilation	<i>FRE3, ARN1, ARN2</i>	12.4	3	0.51	8	4870	29.3	0.022
COG_ONTOLOGY	Amino acid transport and metabolism	<i>SOR1, XYL2, SOR2</i>	11.9	3	0.51	6	975	15.9	0.022
UP_SEQ_FEATURE	metal ion-binding site:Zinc 1	<i>PUT3, GLO2, YDJI, VPS70, GAL4, CPS1, HAP1</i>	11.7	7	1.19	24	6448	0.0	0.000
GOTERM_BP_FAT	siderophore transport	<i>FRE3, ARN1, ARN2</i>	11.0	3	0.51	9	4870	35.5	0.028

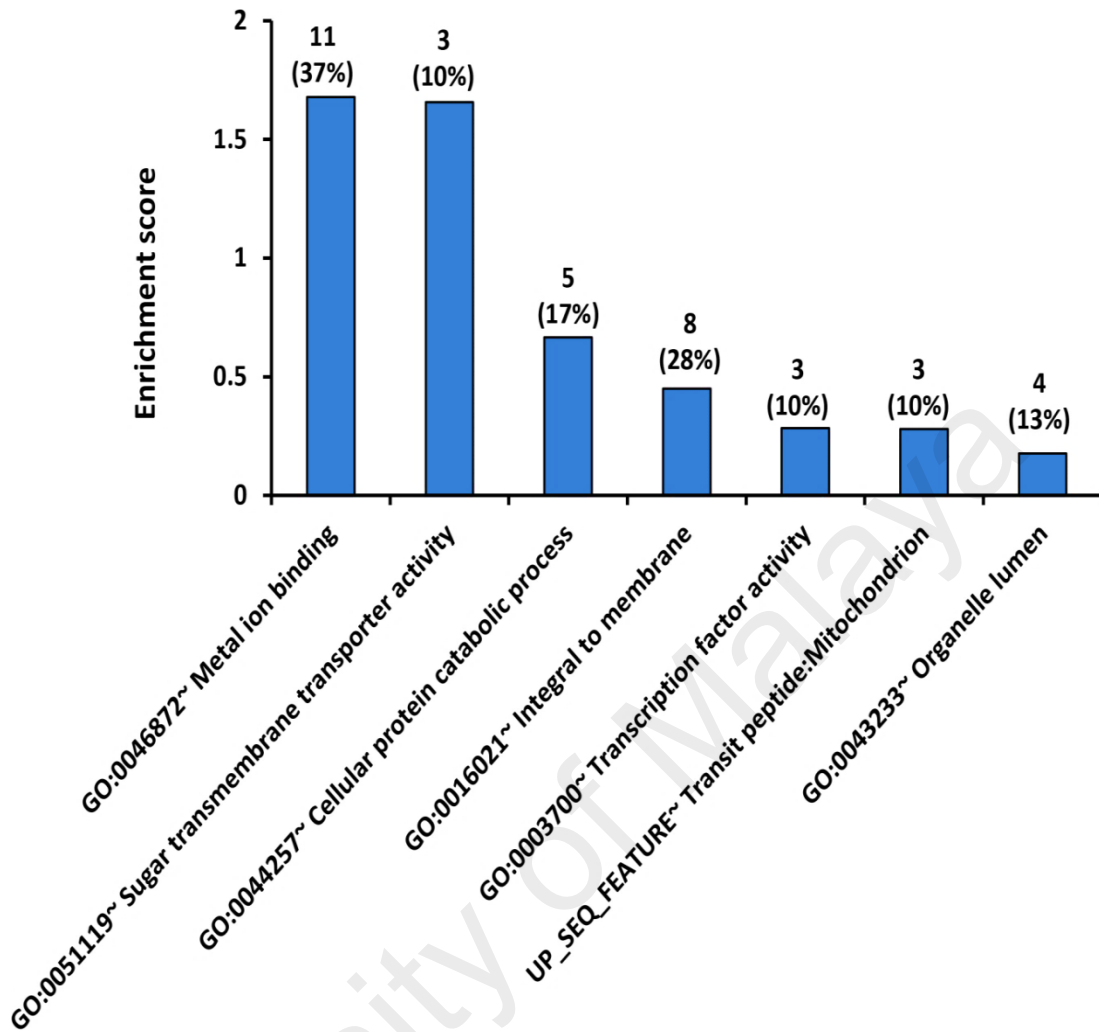


Figure 4.23. Pathway analysis. Histogram shows a summary of DAVID pathway annotation analysis. The 65 genes which were commonly regulated in H99 versus three environmental strains were selected and analyzed. Numbers represents the number of genes and the percentages of genes in the database.

4.9.6.1 Pathway annotation of 65 significantly regulated genes

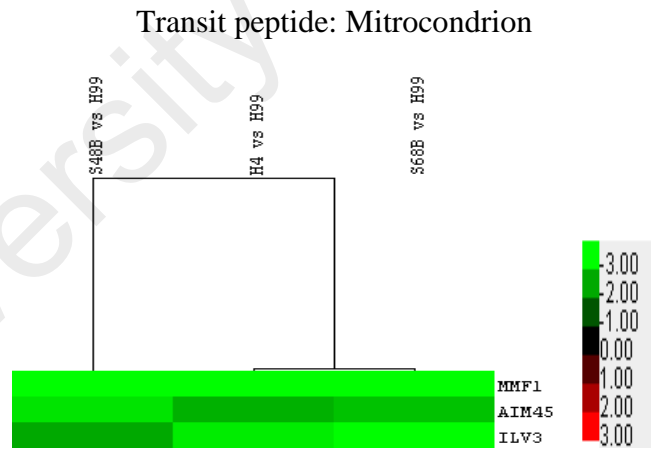
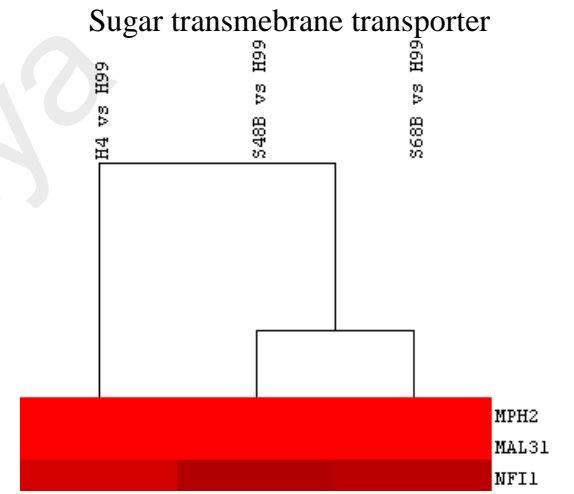
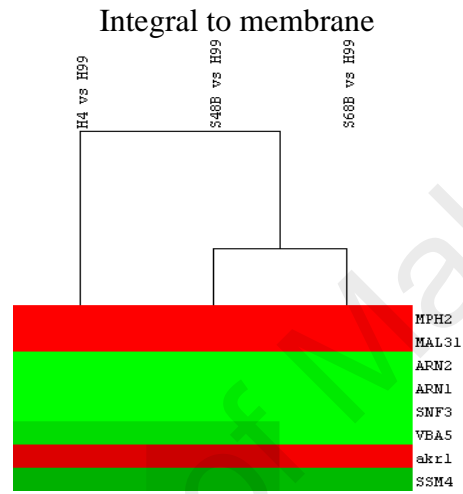
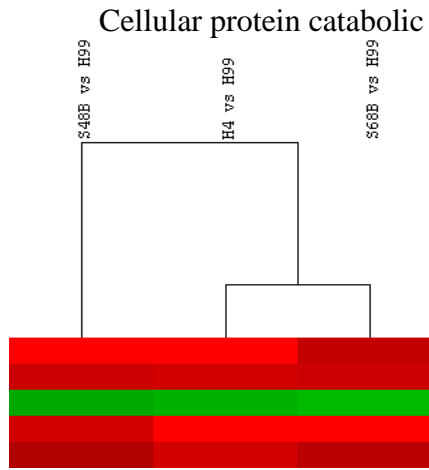
The 65 significant genes (133 overlapped probes) which were differentially regulated in H99 compared to environmental strains were analyzed. The representative of each annotation cluster detected was shown in table 4.12. Count represents number of genes which match the pathway database, and % represents the percentage of gene hits among the total genes in the pathway database. Enrichment score (ES) of each group was measured by the geometric mean of the EASE Scores (modified Fisher Exact)

associated with the enriched annotation terms that belong to this gene group. Population hit (Pop Hits) represents function name in the gene list of interest, and population total (Pop Total) represents genes in overall population has that function name in the background genome (all genes in the species of interest in DAVID database). False discovery rate (FDR) represents the percentages of test which might be false positive. *P* values were analyzed using Fisher exact score to identify which sub-populations are over or under-represented in a sample. Data were considered significant if $*P < 0.05$.

University of Malaya

Table 4.13. Pathway annotation by DAVID bioinformatics resource

Category	Term	Genes	ES	C	%	Pop Hits	Pop Total	FDR	<i>p</i>
GOTERM_MF_FAT	Metal ion binding	<i>UGA3,SSM4,PUT3,YP013C, SAC6, ENO2,AKR2, ARN, ILV3,AKR2,NF11</i>	1.67	11	37.9	830	4190	16.7	0.0159
GOTERM_MF_FAT	Sugar transmembrane transporter activity	<i>MAL31, SNF3,MPH2</i>	1.65	3	10.3	26	4190	10.9	0.0101
GOTERM_BP_FAT	Cellular protein catabolic process	<i>SIP5,PEP4, SSM4,DCS1,NF1</i>	0.66	5	17.2	351	4870	82.9	0.1255
GOTERM_CC_FAT	Integral to membrane	<i>VBA5ARN2MAL31,SNF3,MPH2, AKR1,VBA5, SSM4, ARN1,</i>	0.44	8	27.5	1488	4595	99.7	0.4214
GOTERM_MF_FAT	Transcription factor activity	<i>UGA3, PUT3, HMRA1</i>	0.28	3	10.3	135	4190	91.1	0.1917
UP_SEQ_FEATURE	Transit peptide: Mitrocondrion	<i>AIM45,MMF1,ILV3</i>	0.27	3	10.3	325	6448	99.7	0.415
GOTERM_CC_FAT	Organelle Lumen	<i>PEP4,AIM45,RNA15, MMF1</i>	0.17	4	13.7	783	4595	99.9	0.6522



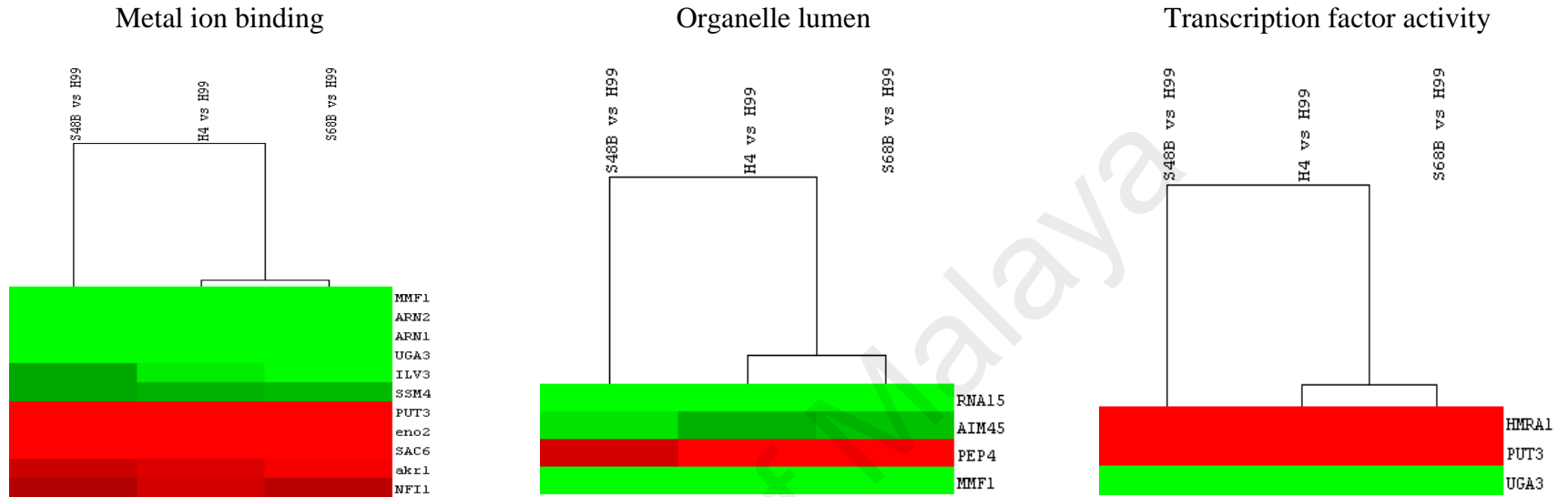


Figure 4.24. Heat maps of genes involved in each pathway annotation of 65 significantly regulated genes. Differential expressions in H99 versus other strains in the groups of genes involved in each pathway are indicated. Low levels in H99 category indicates the genes with low expression levels in H99 (green) but high expression in the environmental strains (red). In contrast, high levels in H99 category indicates the genes with high expression levels in H99 (red) but show low expression in the environmental strains (green).

4.9.7 Gene expression analysis of well-known genes linked to the major virulence phenotypes

Well known virulence genes and their fold changes in H99 compared to H4, S68B and S48B in the microarray results are as presented in Table 4.14. However, none of these genes has been significantly expressed in H99 relative to environmental strains, suggesting a special condition may be needed to induce the expression of these virulence genes. To further confirm the microarray data, RNA was reverse transcribed for gene expression analysis of well-known virulence genes using Real Time PCR assays. Several virulence genes selected in this assay were *ADE2* involved in high temperature growth, *PLB1* and *SKN7* in Intra-cellular growth defect, *CAC1* involved in capsule formation (Perfect, 2005). However, qRT-PCR results showed that expression levels of *ADE*, were >6.4 higher in H99 relative to H4. Also, in *PLB1* and *CAC1* the expression level were higher in H99 relative to S48B at >39 and >56 folds, respectively.

On the other hand, the expression level of *SKN7* was reduced in H99 strain for at least >6 folds, compared to S48B strain respectively. *GAPDH* was used as endogenous control.

Table 4.14. Comparison of the fold changes of reported well-known virulence genes in H99, H4, S68B and S48B strains. No significant difference was observed for all the 28 genes investigated (P>0.05).

Probe Name	Yeast_Gene	Yeast Description	P	FC(H4 vs H99)	FC(S48B vs H99)	FC(S68B vs H99)
CNAG_02294T0_1688	<i>ADE2</i>	Phosphoribosylaminoimidazole carboxylase	0.0877922	-1.4998828	-2.299272	-1.4974705
CNAG_03967T0_1199	<i>CAP1</i>	F-actin-capping protein subunit alpha	0.5461706	3.31529	4.872869	1.9377994
CNAG_02088T0_1291	<i>ATF2</i>	Alcohol O-acetyltransferase 2	0.2686003	-1.8511105	-3.0984976	-1.8507954
CNAG_03967T0_1199	<i>CAP1</i>	F-actin-capping protein subunit alpha	0.5461706	3.31529	4.872869	1.6377994
CNAG_04499T0_717	<i>CLC1</i>	Clathrin light chain	0.7051572	-1.2084926	-1.0032171	-1.6822665
CNAG_00888T0_466	<i>CNBI</i>	Calcineurin subunit B	0.5514112	1.4245626	1.5378755	1.283507
CNAG_00976T0_1005	<i>CPAI</i>	Carbamoyl-phosphate synthase arginine-specific small chain	0.738611	1.272604	-1.5550758	-1.1854311
CNAG_00057T0_991	<i>FBP1</i>	Fructose-1,6-bisphosphatase	0.5204849	2.4410508	2.2990158	3.4004095

Table 4.14 (Continued). Comparison of the fold changes of reported well-known virulence genes in H99, H4, S68B and S48B strains. No significant difference was observed for all the 28 genes investigated (P>0.05).

Probe Name	Yeast_ Gene	Yeast Description	P	FC(H4 vs H99)	FC(S48B vs H99)	FC(S68Bvs H99)
CNAG_06524T1_1165	<i>FRE3</i>	Ferric reductase transmembrane component 3	0.051162	3.7254162	1.830058	3.8880193
CNAG_02090T0_928	<i>Gpa2</i>	Guanine nucleotide-binding protein alpha-2 subunit	0.1595471	-1.8744092	1.5274609	-1.3955437
CNAG_00268T0_2009	<i>ILV2</i>	Acetolactate synthase catalytic subunit, mitochondrial	0.514872	2.9083178	1.1705796	-1.1767081
CNAG_06717T0_1028	<i>LAC1</i>	Sphingosine N-acyltransferase LAC1	0.4256837	-1.5192941	-1.358721	-1.373138
CNAG_07796T0_1971	<i>MET1</i>	Uroporphyrinogen-III C-5-methyltransferase	0.3974671	1.2145467	-3.094961	1.8202717
CNAG_01890T0_2091	<i>MET6</i>	methyltetrahydropteroyltriglutamate homocysteine methyltransferase	0.0814961	1.4246567	-1.3526764	1.2428228

Table 4.14 (Continued). Comparison of the fold changes of reported well-known virulence genes in H99, H4, S68B and S48B strains. No significant difference was observed for all the 28 genes investigated. (P>0.05)

Probe Name	Yeast_Gene	Yeast Description	P	FC(H4 vs H99)	FC(S48B vs H99)	FC(S68B vs H99)
CNAG_06085T0_1515	<i>PLB1</i>	Lysophospholipase 1	0.3998226	-1.2070299	-2.1172945	1.3036641
CNAG_04763T0_2320	<i>PMT2</i>	Dolichyl-phosphate-mannose protein mannosyltransferase 2	0.4390793	1.2132756	1.5278053	-1.4670082
CNAG_04761T0_591	<i>RAS1</i>	Ras-like protein 1	0.2201697	-1.8844544	-1.9418076	-2.365697
CNAG_03409T0_3071	<i>SKN7</i>	Transcription factor SKN7	0.0989085	2.118918	1.5951138	1.4778266
CNAG_01019T0_367	<i>SOD1</i>	Superoxide dismutase [Cu-Zn]	0.8586658	-1.1923045	1.0453014	1.490451
CNAG_04388T0_607	<i>SOD2</i>	Superoxide dismutase [Mn], mitochondrial	0.4010298	-2.3312893	-2.0166457	-1.021935
CNAG_02876T0_1166	<i>SPE1</i>	Ornithine decarboxylase	0.2976911	1.3777045	1.467745	1.4184009
CNAG_01454T0_2349	<i>STE12</i>	Protein STE12	0.2605648	1.0430304	1.8015815	-1.3425711
CNAG_05970T0_2645	<i>STE20</i>	Serine/threonine-protein kinase STE20	0.6307744	1.0951991	-1.2917963	1.3582451

Table 4.14 (Continued). Comparison of the fold changes of reported well-known virulence genes in H99, H4, S68B and S48B strains. No significant difference was observed for all the 28 genes investigated (P>0.05).

Probe Name	Yeast Gene	Yeast Description	P*	FC* (H4 vs H99)	FC(S48B vs H99)	FC(S68B vs H99)
CNAG_05292T0_1888	<i>TPS1</i>	Alpha,alpha-trehalose-phosphate synthase [UDP-forming] 56 kDa subunit	0.2145566	-1.1804496	-1.211615	1.3024496
CNAG_03765T0_2532	<i>TPS2</i>	Trehalose-phosphatase	0.2286499	1.5726377	1.9947807	2.0571895
CNAG_03482T0_578	<i>TSA1</i>	Peroxiredoxin TSA1	0.0749729	1.4780415	-1.6694244	1.1282136
CNAG_03196T0_576	<i>URA5</i>	Orotate phosphoribosyltransferase 1	0.8790087	1.1408387	1.0986692	1.1191927
CNAG_01106T0_66	<i>VPHI</i>	V-type proton ATPase subunit a, vacuolar isoform	0.6868896	1.51768	1.7495183	1.0898443

Footnote: P:P value (P>0.05), significant value is ≥ 2 and ≤ -2 , FC:fold change

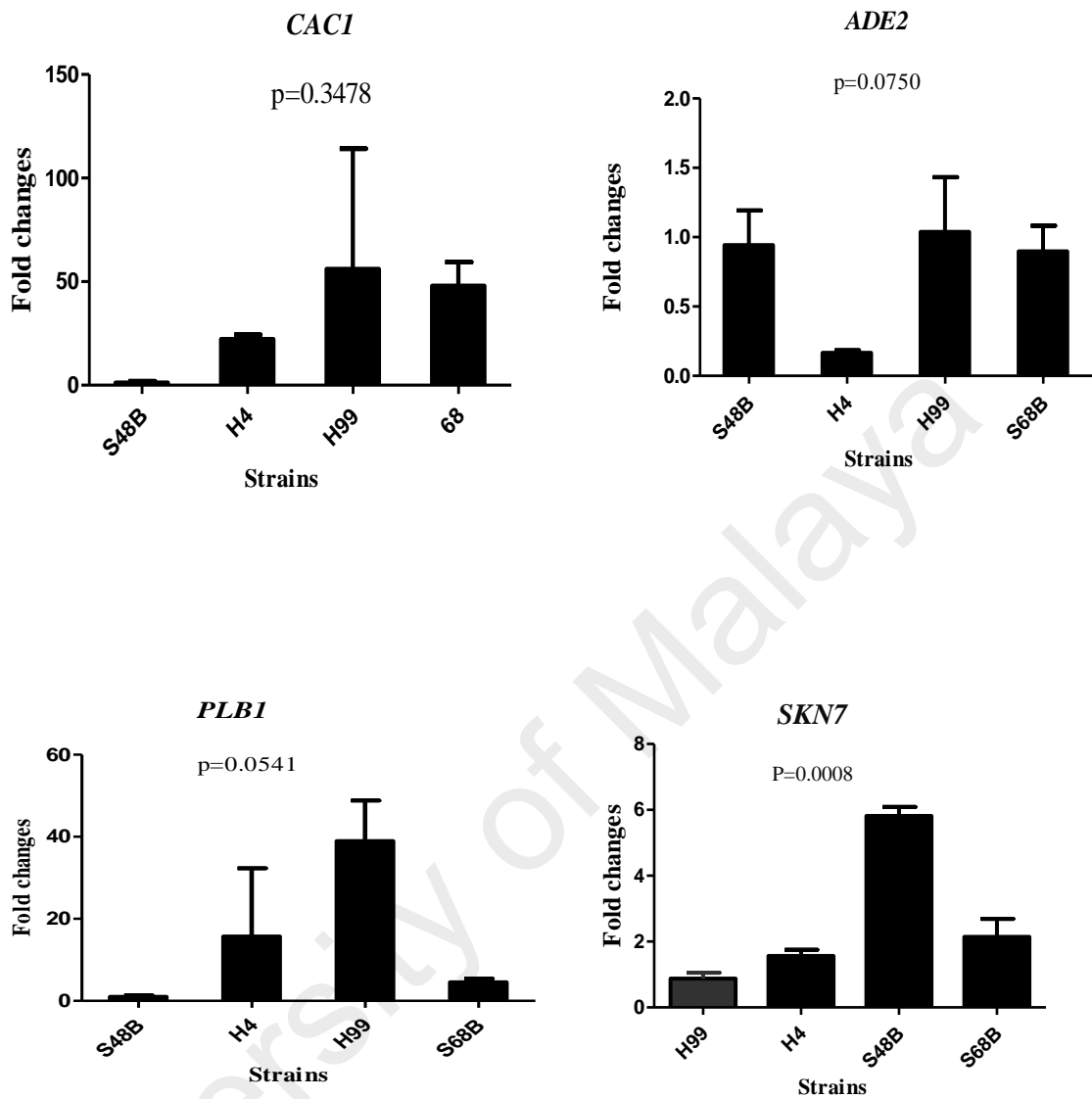


Figure 4.25. qRT-PCR verification. RNAs were extracted from H99, H4, S48B and S68B for qRT-PCR analysis. Two independent samples were prepared for each fungal strain. All samples were run in triplicates and data were shown as mean \pm SD, $P < 0.05$ by two-way ANOVA.

4.10 Antifungal effect of triclosan against *C. neoformans*

Since cryptococcal diseases remains a challenging management issue, with little new drug development or recent definitive researches, this study was furthered to investigate more on anti-*cryptococcal* therapy. To evaluate the antifungal effect of triclosan, 6-mm paper disks impregnated with different contents of triclosan (3.125, 6.25, 12.5, 25, 50 and 100 µg) were positioned on a *C. neoformans* H99 SDA agar plate for an incubation period of 48 hours. Control disk (with DMSO) displayed no inhibitory zone. In contrast, the diameters of the inhibition zones surrounding the triclosan-impregnated disks increased steadily from 7 mm to 17.6 mm in a dose-dependent manner (Table 4.15 and Figure 4.26A). A linear relationship was observed between the inhibition zone size and Log concentration of triclosan (Figure 4.26B).

Table 4.15. Measurements of inhibition zones of different concentrations of triclosan (3.125, 6.25, 12.5, 25, 50 and 100 µg) on a *C. neoformans* H99 SDA agar plate for an incubation period of 48 hours. Control disk (with DMSO) displayed no inhibitory zone.

Triclosan (µg)	Inhibition zone (mm) (mean±SD)
3.125	7±0.33
6.25	9±0.0
12.5	12±0.070
25	15±0.0
50	16±0.70
100	17.6±0.56

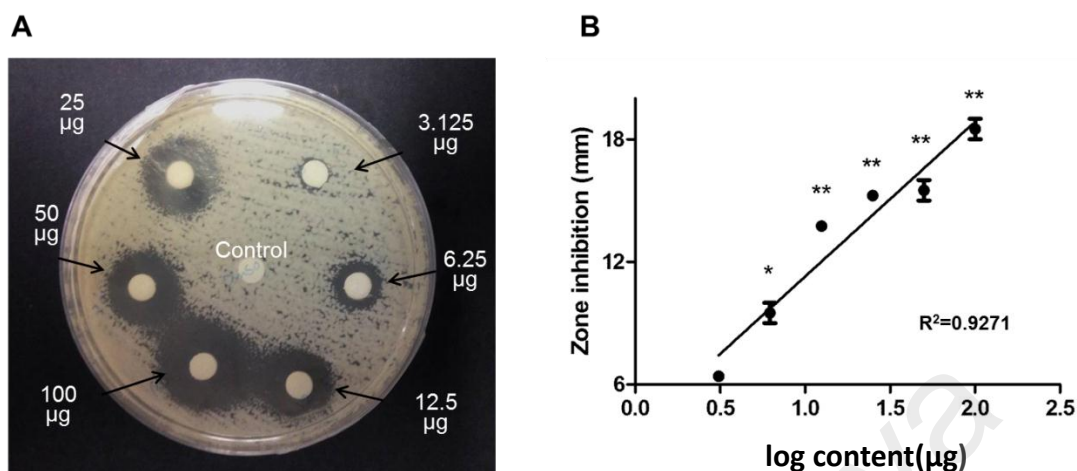


Figure 4.26 (A and B). Agar disk diffusion assay. (A) Diameters of the inhibition zone after 48 hours of incubation. Data shown is a representative picture of three independent experiments. (B) Graph shows the inhibition diameter (mm) of *C. neoformans* plate after triclosan treatment. Data shown are mean \pm SD. * $P < 0.05$, ** $P < 0.01$.

4.10.1 Determination of minimum inhibitory concentration (MIC)

Triclosan MIC-1 and MIC-2 endpoint values, which represent reduction of cell turbidity at 80% and 50%, respectively, were measured by microdilution assay (Table 4.16). Triclosan was fungicidal against *C. neoformans* H99, with MIC-1=3.80 and MIC-2=2.70 µg/ml. Two additional clinical strains have been tested for inhibition to improve the results for characterizing triclosan as a new anti-fungal against *C. neoformans*. Local clinical strains of *C. neoformans* tested (C14 and C17) showed MIC-1 at 5.197 and 4.875 µg/ml, and MIC-2 at 2.130 and 2.280 µg/ml (Table 4.16). Environmental strains *C. neoformans* H4, S48B and S68B strains showed comparable MIC-1 and MIC-2 values ranging from 0.25 to 1.14 µg/ml and 0.08 to 0.54 µg/ml, respectively (Table 4.16). In this study, it has been shown that environmental strains of *C. neoformans* are fairly avirulent compared to most clinical strains. Further, we compared the MIC-1 and MIC-2 of triclosan in *C. neoformans* with two *C. albicans* (90028 and SC5314) strains which were between 16-64 µg/ml, consistent with a previous report (Yu *et al.*, 2011).

The relatively lower MIC values in *C. neoformans* suggest that the triclosan is more potent against *C. neoformans* compared to *C. albicans*.

Table 4.16. MIC-1 (80% inhibition) and MIC-2 (50% inhibition) readings of triclosan in different strains of *C. neoformans* and *C. albicans*. Data are representative of three independent experiments.

Fungal strains	MIC-1 ($\mu\text{g/ml}$)	MIC-2 ($\mu\text{g/ml}$)
<i>Cryptococcus neoformans</i> H99	3.80	2.70
<i>Cryptococcus neoformans</i> C14	5.197	2.130
<i>Cryptococcus neoformans</i> C17	4.875	2.280
<i>Cryptococcus neoformans</i> H4	1.14	0.54
<i>Cryptococcus neoformans</i> S48B	0.37	0.12
<i>Cryptococcus neoformans</i> S68B	0.25	0.08
<i>Candida albicans</i> 90028	59.6	44.0
<i>Candida albicans</i> SC5314	>64	33.8

4.10.2 Evaluation of CFU-based fungicidal assay

A cell culture CFU-based fungicidal assay was then performed to determine if the triclosan was fungicidal or fungistatic (Table 4.17 and figure 4.27). Cells were visualized in the wells with low concentrations ($\leq 0.5 \mu\text{g/ml}$) but no CFU was detected in the media recovered from the wells treated with $\geq 1 \mu\text{g/ml}$, indicating that Minimum fungicidal concentration (MFC) for *C. neoformans* H99 was $1 \mu\text{g/ml}$. The MFC is the lowest drug concentration yielding no growth using $20 \mu\text{l}$ (CFU20 MFC) and $100 \mu\text{l}$ (CFU100 MFC). Thus, the results suggest that triclosan was fungicidal (MFC/MIC-2 ratio = $0.37, \leq 4$).

Table 4.17. Minimum fungicidal concentration (MFC) assay. Total CFU count in the CFU-based fungicidal assay. CFU was detected in the media recovered from the wells treated with $\leq 1 \mu\text{g/ml}$ which indicate $1 \mu\text{g/ml}$ as the lowest drug concentration yielding no growth.

Triclosan ($\mu\text{g/ml}$)	CFU count \pm SD
0.065	>300
0.125	177 \pm 14.14
0.25	163 \pm 4.24
0.5	96 \pm 9.8
1	0
2	0

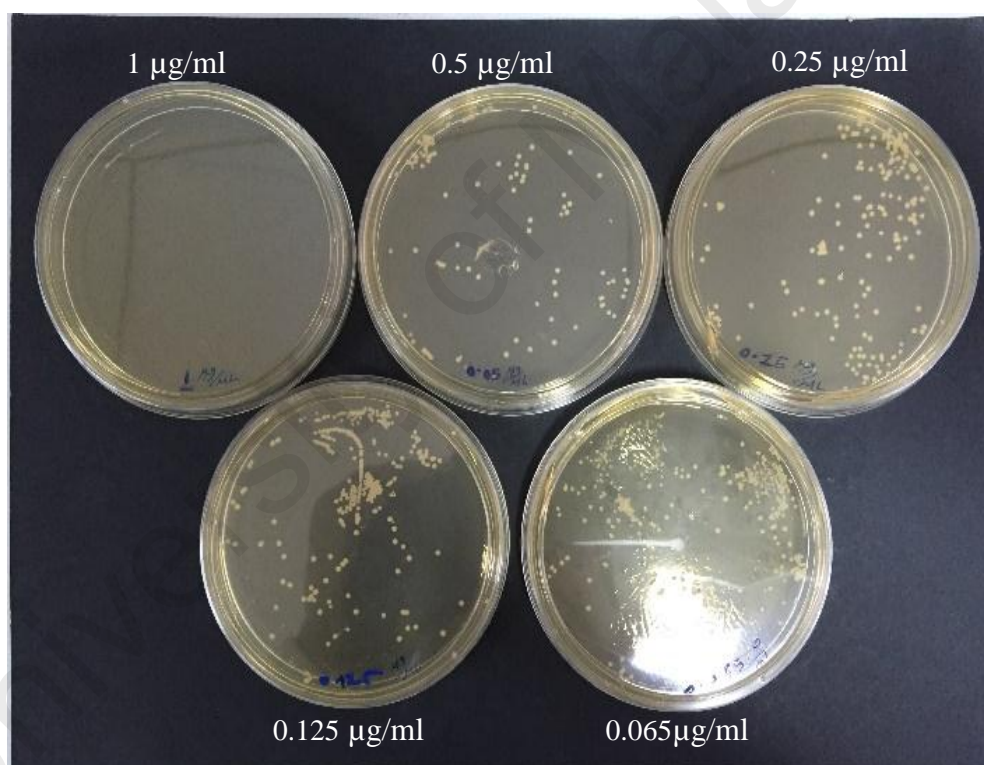


Figure 4.27. CFU count of the media recovered SDA plates from the wells treated with $\leq 1 \mu\text{g/ml}$ of triclosan.

4.11 Analysis of triclosan synergistic effect with amphotericin B and fluconazole

In vitro interactions between triclosan and two standard antifungal agents, amphotericin B and fluconazole were examined using a disk diffusion assay (Figure 4.11). 25 μg of each drug was applied on a disk. (Figure 4.28 and table 4.18) Agar disk diffusion assay for triclosan (1.56, 3.125 and 6.25 $\mu\text{g/ml}$) in combination with at

subinhibitory concentrations (6.25 $\mu\text{g/ml}$) of amphotericin and fluconazole (Figure 4.28C and D). Diameters of the inhibition zone were measured after 48 hours of incubation. Inhibition zone for amphotericin B treatment alone was 10 mm. Noticeably, combinational usage of triclosan plus amphotericin B caused enlargement of the inhibition zone to 17 mm (Figure 4.28C). On the other hand, fluconazole treatment alone showed incomplete inhibition zone of approximately 11 mm, while the combinational usage of triclosan plus fluconazole remarkably augmented the size of inhibition zone to 16 mm (Figure 4.28D). To further confirm the result, the experiment was repeated using sub-inhibitory concentrations of drugs. Increasing concentrations of triclosan at 1.56, 3.125 and 6.25 $\mu\text{g/ml}$ were applied on the paper disks containing 6.25 μg amphotericin B (Figure 4.28C) or fluconazole (Figure 4.28D) and used for disk diffusion assay. No or minimal inhibition zones were observed in the absence of triclosan while addition of triclosan caused enlargement inhibition zone in a dose-dependent manner. Both combinations of triclosan with amphotericin B or fluconazole showed linear inhibition patterns (Figure 4.28E and F).

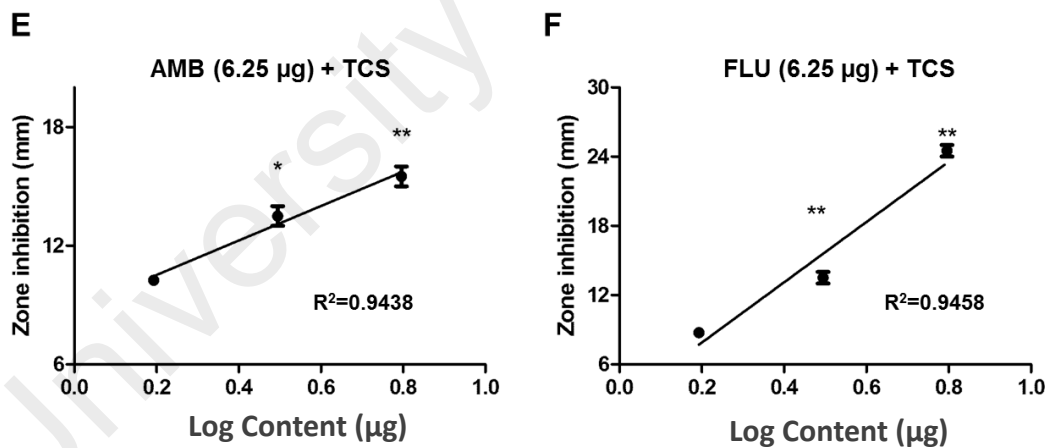
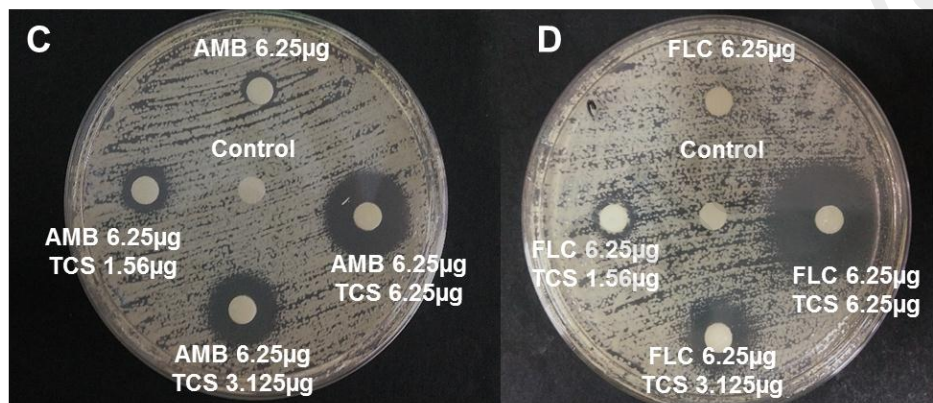
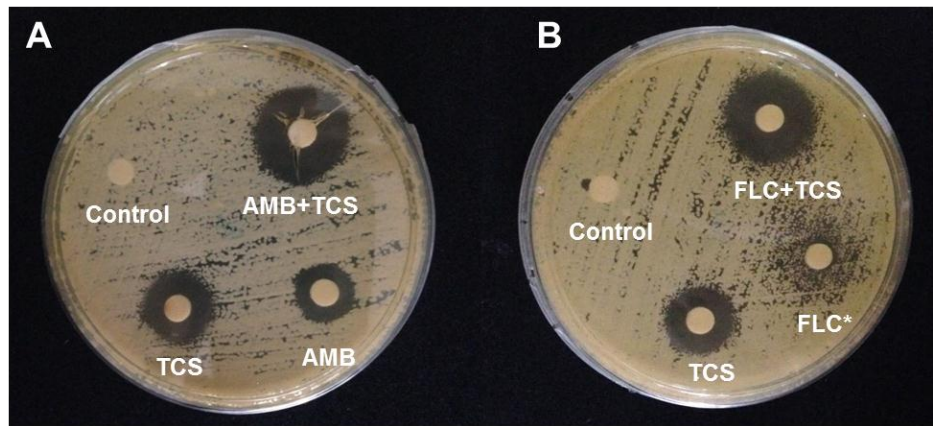


Figure 4.28. Synergy effect of triclosan with amphotericin B and fluconazole. (A, B) Agar disk diffusion assay for triclosan (TCS) in combination with (C) amphotericin B (AMB), or (D) fluconazole (FLC) in *C. neoformans* H99-containing agar plates. Asterisk (*) indicates partial inhibition. Data shown are representative pictures of three independent experiments. (E, F) Graphs show the inhibition diameter (mm) of *C. neoformans* plate after triclosan treatment in combination with AMB or FLU. X-axis shows Log concentration of triclosan. Data shown are mean \pm SD, * $P < 0.05$, ** $P < 0.01$.

Table 4.18. Agar disk diffusion assay. Diameter (mm) of the growth inhibitory zone of *C. neoformans* when treated with drug alone or in combination with triclosan.

Drugs	Inhibition zone (mm)
Amphotericin B	9
Triclosan	12
Amphotericin B + Triclosan	17
Fluconazole	10 (partial)
Triclosan	12
Fluconazole + Triclosan	16

University of Malaya

4.11.1 Analysis of checkerboard assay

The combinational effect of standard drugs and triclosan was further assessed using checkerboard assay to define the median FICI values (Table 4.19). Both combination of drugs i.e. triclosan plus amphotericin B (FICI=0.127), or triclosan plus fluconazole (FICI=0.020) showed FICI value <0.5, indicating the synergistic effects of triclosan with both standard drugs (Figure 4.29).

Table 4.19. Checkerboard assay. Synergy effect of triclosan with amphotericin B or fluconazole in *C. neoformans*. FICI≤0.5 indicates synergistic effect. Data shown are representative of two independent experiments.

	MIC alone (µg/ml)	MIC combined (µg/ml)	FIC (µg/ml)	FICI* (µg/ml)	Remark
Amphotericin B	0.23	0.008	0.035	0.127	Synergy
Triclosan	2.7	0.25	0.092		
Fluconazole	3.2	0.015	0.005	0.020	Synergy
Triclosan	2.7	0.06	0.022		

*The fractional inhibitory concentration index (FICI) was calculated for each drug using following formula: $FICI = \frac{FIC(\text{triclosan})}{MIC(\text{triclosan})} + \frac{FIC(\text{drug})}{MIC(\text{drug})}$, where FIC equals to MIC of the drug in combination divided by the MIC of the drug alone FICI≤0.5 indicates synergy, FICI>4 indicates antagonism whereas 0.5>FICI>4 suggests no interaction.

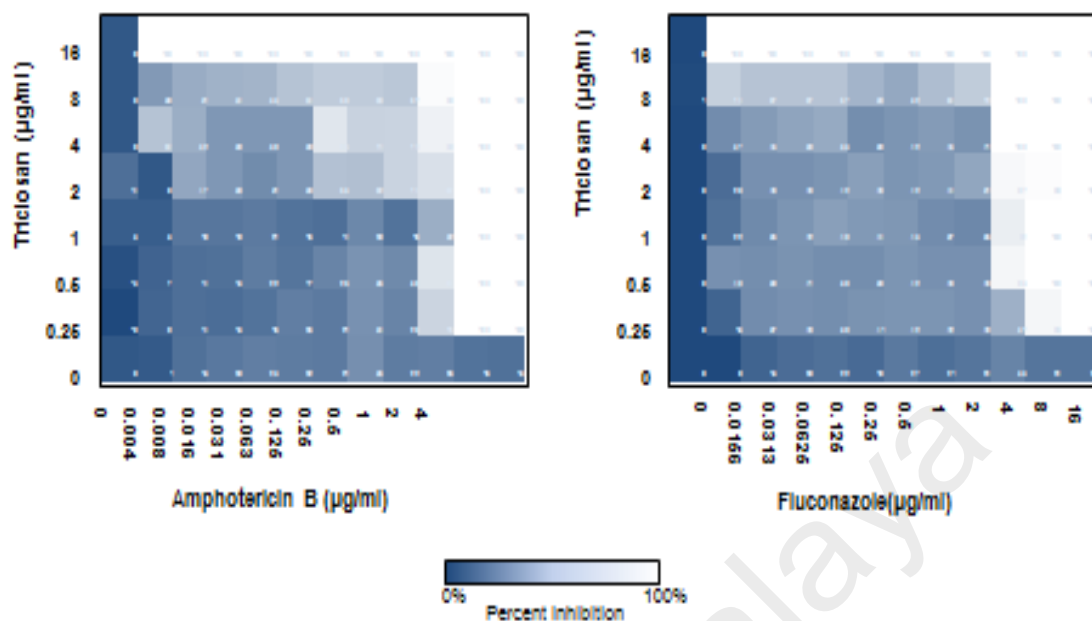


Figure 4.29. Checkerboard assay. Synergy effect of triclosan with amphotericin B or fluconazole in *C. neoformans*

4.12 Determination of apoptotic-like cell death (ALCD) mechanism of triclosan on *C. neoformans*

4.12.1 Transmission electron microscopic analysis of triclosan-treated *C. neoformans*

To examine the inhibitory mechanism of triclosan on *C. neoformans*, control and triclosan-treated (2 hours) cells were processed for visualization under electron microscope. Untreated *C. neoformans* showed an intact cell structure with normal morphologies of nucleus and cytoplasm (Figure 4.30A and B). In contrast, triclosan-treated *C. neoformans* demonstrated disrupted cell morphologies including apparent mitochondrial swelling and extensively enlarged cytoplasmic vacuolations (Figure 4.30C-F). Nuclear chromatin condensation can be also observed. The cell surface fibrillar structure which constitutes polysaccharide component of the cell wall capsule was also disrupted (Mandal *et al.*, 2007). These features collectively suggest that

triclosan-treated *C. neoformans* demonstrated apoptotic-like cell death (ALCD) mechanism.

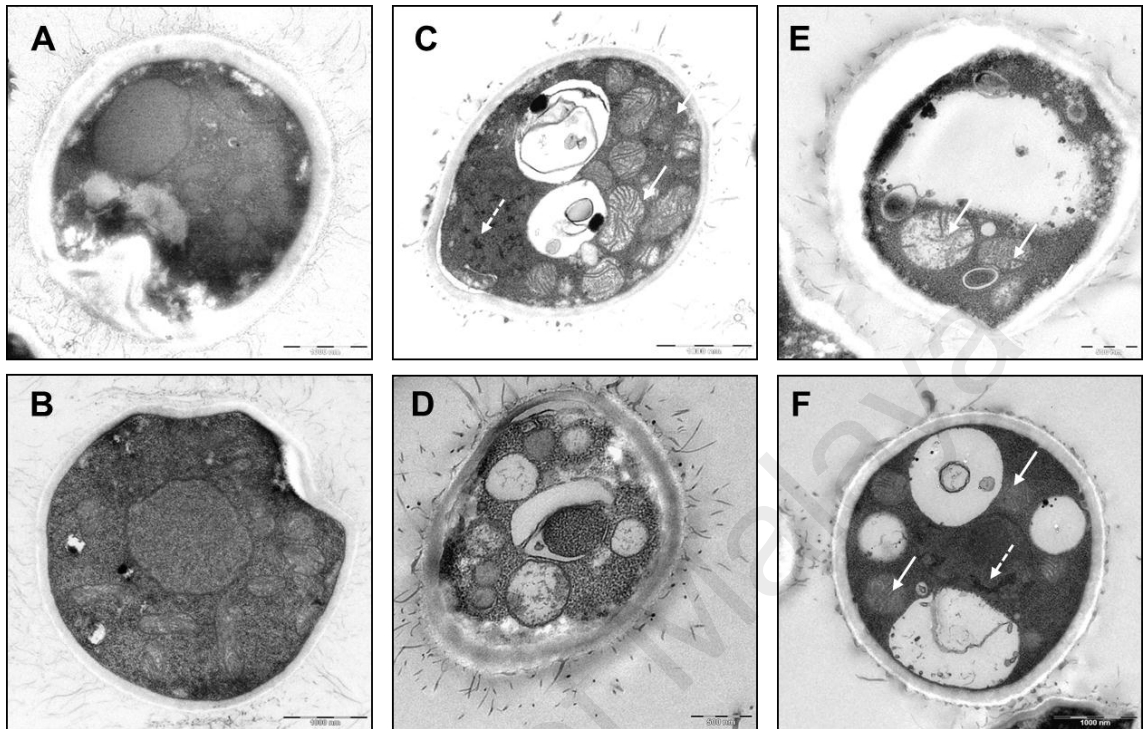


Figure 4.30. Electron microscopic pictures of *C. neoformans* with or without exposure to triclosan (0.5 $\mu\text{g/ml}$) for 2 hours. (A, B) Untreated control cells showed intact nucleus and cytoplasm. (C-F) Triclosan-treated *C. neoformans* showed apoptotic morphologies. Note the appearance of apoptotic features such as mitochondrial swelling (arrow) and nuclear chromatin condensation (broken arrow). Besides, intense cytoplasmic vacuolations were formed in the cells. Cell surface fibrillar structures which form capsule polysaccharide component were also disrupted.

4.12.2 Analysis of inhibitory mechanism of triclosan on *C. neoformans* using TUNEL apoptosis assay

To further confirm if triclosan triggers apoptosis in *C. neoformans* cells, cells were analyzed using TUNEL apoptosis assay followed by flow cytometrical analysis. DNA fragmentation (one of the hallmark of apoptosis) generates free 3'-hydroxyl residues that can be utilized by terminal deoxynucleotidyl transferase to incorporate FITC-tagged dUTP into the blunt ends of double-stranded DNA break. Data showed that 90.7% triclosan-treated *C. neoformans* H99 cells were apoptotic (FITC-positive) compared to only 2.1% in the untreated control. Around 71.4% of apoptotic cells were detected in the positive control (H₂O₂-treated cells). Therefore, triclosan can inhibit *C. neoformans* by inducing ALCD (Figure 4.31).

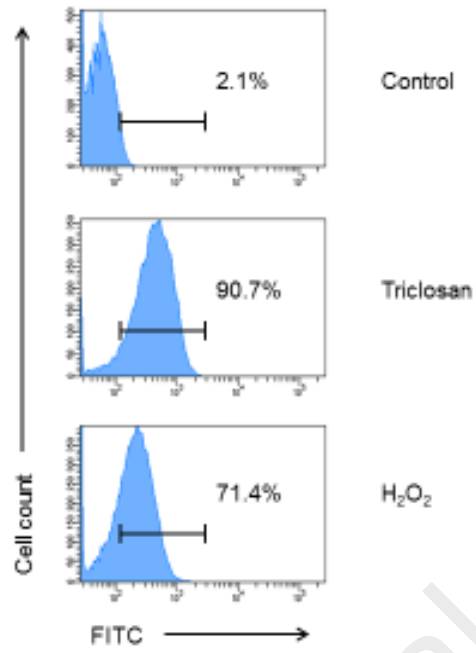


Figure 4.31. Apoptosis of triclosan-treated *C. neoformans* H99 cells was determined by TUNEL assay followed by flow cytometry analysis. *C. neoformans* H99 cells were non-treated (control), treated with triclosan (0.5 $\mu\text{g/ml}$) or H₂O₂ (2 mM) for 4 hours. Percentages of the apoptotic cells are indicated.

CHAPTER 5: DISCUSSION

5.1 Comparative analyses of clinical and environmental strains of *C. neoformans*

The rates of HIV infections are still increasing in many parts of the world, particularly in Africa and Asia (World Health Organization, 2003, 2010). The HIV pandemic has led to a rise in the incidence of opportunistic fungal infections. Among the virulence factors of *C. neoformans* that have been described so far, the polysaccharide capsule and melanin, have been directly associated with the pathogenicity of *C. neoformans*. Cryptococcal strains deficient of these factors have been shown to exhibit reduced virulence (Liu *et al.*, 1999a; Nosanchuk *et al.*, 1999b; Wilder *et al.*, 2002). However, the mechanism of gene control in clinical and environmental *C. neoformans* leading to the virulence of clinical strains is not well understood. This study investigated the phenotypic variation and gene expression profiles of several environmental strains of *C. neoformans* in comparison to a virulent strain obtained from a patient presenting with meningitis (H99 clinical strain).

C. neoformans is common in the environment. The presence of this organism has been associated with weathered pigeon droppings, suggesting that pigeon habitats are a potential source of human infection. Avian droppings, which are abundant in public areas, have been reported as a potential environmental source of *C. neoformans* (Chee & Lee, 2005; Currie *et al.*, 1994; Nosanchuk *et al.*, 1999a; Yamamoto *et al.*, 1995). In fact, the association between *C. neoformans* and pigeons has been reported frequently (Casadevall & Perfect, 1998; Currie *et al.*, 1994; Nishikawa *et al.*, 2003; Nosanchuk *et al.*, 1999a; Yamamoto *et al.*, 1995). - Both pigeons and *C. neoformans* are distributed in many geographical regions (Long, 1981). However, as *C. neoformans* is not able to grow at the pigeon's normal body temperature of 42°C, the pigeons do not acquire cryptococcosis. Nevertheless, *C. neoformans* is able to survive passage through the

intestinal tract of pigeons (Littman & Borok, 1968), and can survive for 2 years in moist or dry pigeon excreta in the dark (Denton & Di Salvo, 1968). *C. neoformans* may compete with certain microorganisms in soil, and can be inhibited by amoeba (Bunting *et al.*, 1979). The close association between serotype A and pigeons is probably due to the conducive ecological niche provided by the pigeon excreta. Little genetic diversity has been reported among clinical and environmental strains, supporting the hypothesis that clonal expansion is essential as a mode of reproduction among clinical and environmental populations of *C. neoformans* (Litvintseva *et al.*, 2005). A few genotypes exist within these two populations. According to a study conducted by Litvintseva *et al.* (2005), six of the seven genotypes originated from the environment were also identified in the clinical isolates, however; the most predominant genotype (A2) was absent from the hospital findings. No relation was found between the genotypes from patients and their underlying disease (Litvintseva *et al.*, 2005).

All the environmental strains (originated from bird droppings) investigated in this study were identified as serotype A (*C. neoformans var. grubii*), and molecular type VNI based on a previous study using URA5-RFLP analysis (Tay *et al.*, 2006). The genetic similarity was 92.9% between the two genotypes, i.e. H4/S68 and H99/S48 strains based on PCR fingerprinting patterns (Figure 4.2A and 4.2B). The strains were also differed in terms of gene expressed through microarray analysis in this study (as shown in Table 4.7 to Table 4.9). Of the three environmental strains, H4 and S68 strains exhibited greater difference than S48 strains in the gene expression profiles, as compared to H99 clinical strains.

5.1.1 *In vivo* virulence analysis of environmental strains of *C. neoformans* compared to H99 in mice

A total of 2×10^5 yeasts cells were used for intranasal inoculation of mice model in this study. Mice provide an excellent model to study cryptococcal infections (Huffnagle *et al.*, 1991b). The finding of a previous study showed that cryptococcal dissemination to the brain occurred in 100% of C57BL/6 mice when infected with approximately 10^4 or 10^5 organisms for intranasal inoculation (Huffnagle *et al.*, 1991b), while infection with lower numbers of organisms was not successful. A previous study on mice infected with yeast suspension inoculated directly into their cerebra suggested that strains isolated from cryptococcal patients were more virulent than the soil strains. Yet, almost half of the soil strains were as pathogenic as strains from human disease (Litvintseva & Mitchell, 2009). Hence, the abilities to cause disease are different among environmental strains; with some mice developed symptoms of cryptococcosis, but others remained asymptomatic.

In another study on mice infected intranasally, most of the environmental strains isolated were non-lethal; only one out of eleven strains tested was virulent, while 7 of 10 clinical strains were lethal for mice within 40 days (Litvintseva & Mitchell, 2009). The authors concluded that the environmental strains were less virulent. In a separate study, most of the environmental strains of *C. neoformans* serotype A were non-lethal to the mice (Allen *et al.*, 2000). Consistent with the above findings, this study found that all three environmental strains were non-lethal to mice. In this study, only two of the three environmental strains (i.e., S48B and S68B) demonstrated disseminated infection, as demonstrated by detectable numbers of CFU in the lung and brain homogenates. Comparatively, H99 clinical strain was highly virulent in mice. A single environmental strain (H4 strain) was considered non-virulent as no cryptococcal organism could be isolated from both lung and brain homogenates (Table 4.2). Based on mice experiment

and the fact that all infected mice survived throughout the experiment (Figure 4.3), this study concluded that the environmental strains were of low infectivity compared to clinical H99 strain.

5.1.2 Determination of the possible virulence factors of H99 compare to environmental strains

Different phenotypic features, such as laccase expression (Salas *et al.*, 1996), the ability to grow at 37°C (Odom *et al.*, 1997), phospholipase activity (Cox *et al.*, 2001) and the presence of a polysaccharide capsule (Bose *et al.*, 2003), have been associated with yeast virulence. Considering the difference in the ability of environmental strains and H99 to disseminate in the mice model, this study has evaluated several phenotypic expression of virulence attributes including capsule induction, and production of laccase and phospholipases.

Although all environmental strains were able to form capsule in the presence of serum (Figure 4.8), H99 strain exhibited the most prominent enlargement in the capsule size. The capsule size of *C. neoformans* is known to increase during *in vivo* infection and the phenomenon is associated with virulence. Several studies reported reduced virulence in cryptococcal strains which were unable to induce capsule growth (Alspaugh *et al.*, 2002; D'souza *et al.*, 2011; Granger *et al.*, 1985; Zaragoza *et al.*, 2003b). The capsule is essential for virulence, since acapsular mutants are avirulent (Fromtling *et al.*, 1982). The bigger capsular size of *C. neoformans* has been associated with resistance to phagocytosis (Kozel & Gotschlich, 1982; Mitchell & Friedman, 1972; Zaragoza *et al.*, 2003b). The presence of capsule is also necessary for survival inside phagocytic cells (Tucker & Casadevall, 2002), as the capsular polysaccharide interferes with a large number of processes involved in the immune response (Chang & Kwon-Chung, 1994; Dong & Murphy, 1995; Fromtling *et al.*, 1982; Macher *et al.*, 1978; Vecchiarelli *et al.*, 1995).

This study found that H99 laccase activity is around 1-2 fold higher than environmental strains (Table 4.4). Previously, it has been reported that clinical strains of *C. neoformans* demonstrated higher laccase activity compared to environmental strains (Chan & Tay, 2010). Melanin generated by laccase has been reported to protect H99 strain against oxidants, antibiotics and microbial proteins (Emery *et al.*, 1994). The black melanin pigments produced by laccase have been shown to alter the cellular charge of fungal cells, making them resistant to phagocytosis (Zhu & Williamson, 2004).

No significant differences were observed in the growth rate (Figure 4.7) and production of phospholipase activity of clinical and environmental strains of *C. neoformans* (Table 4.3). According to a study by Thompson *et al.* (2014) different molecular types of strains from environmental, veterinary, and human sources exhibited different growth rates. At 37°C, VNI strains grew most rapidly, with significant differences seen compared to molecular types VGI, VGIIa, and VGIII. Consistently, the results from this study showed no significant growth rate difference among four VNI (serotype A) strains.

In a study to examine phospholipase activity of *C. neoformans* strains from AIDS patients and bird droppings by using egg-yolk plate method, Vidotto (1998) reported that one of the 21 AIDS strains did not produce phospholipase. In contrast, 34 of the 46 bird dropping strains were negative for phospholipase production. However, all the strains tested in this study were able to produce phospholipase activity, as also reported by Chan and Tay (2000). The difference observed in the phospholipase activity of *C. neoformans* could be due to strain to strain variation or technical variation in assaying the enzyme.

Certain virulence-associated phenotypes are expressed *in vivo*, when *C. neoformans* encounters a wide array of challenges during human infection, including oxidative and nitrosative stresses from immune cells, nutrient limitation and high temperature (Ormerod *et al.*, 2013). As microevolution enables rapid adaptation to selective pressures (Selmecki *et al.*, 2006), it is possible that overexpression of certain virulence phenotypes in clinical strains may occur to permit expansion into new niches in harsh environmental conditions.

5.2 Microarray analysis of clinical strain of *C. neoformans* versus environmental strains

This study hypothesized that the difference in the pathogenicity of clinical and environmental strains could plausibly be a result of their distinct gene transcriptional programs, which render virulent or avirulent characteristics to *C. neoformans*. Therefore, microarray data analysis was conducted to substantiate this hypothesis. Microarray analysis revealed a different transcriptome profile of H99 strain compared to H4, S48B and S68B strains. Out of 7,419 genes (22,257 probes) examined, 41 genes were up-regulated while 24 genes were down-regulated in H99 versus environmental strains. However, it is important to understand that the results of microarray could be affected by the occurrence of genetic changes within the cryptococcal organism itself. Studies have shown that under host stressful conditions such as nutrient limitation, oxidative and nitrosative stresses from immune cells, high frequency adoptive mutations (Dunham *et al.*, 2002) may occur as a result of host selective pressure. This is also supported by the reports on the occurrence of microevolution, genotypic variation and large scale genomic rearrangements in *C. neoformans* (Selmecki *et al.*, 2006). Although the H99 strain is the most clinically prevalent strain with remarkably stable

genome (Morrow *et al.*, 2012), there has been evidence that the genome can become more plastic during infection, with the identification of very different karyotypes (Fries

et al., 1996) amongst patients, and between initial and relapse infections (Morrow *et al.*, 2012).

5.3 Gene expression analysis of well-known virulence genes of *C. neoformans*

The classical virulence phenotypes of *C. neoformans* (capsule, melanin, temperature and intracellular growth) are controlled by many genes (Chen *et al.*, 2014; Perfect, 2005). In this study, the infection caused by environmental strains in mice was not as severe as that of H99 clinical strain. As shown in Figure 4.4, only lung inflammation was observed in two out of three environmental strains and the CFU counts recovered from the brain homogenates were much lower as compared to the H99 clinical strain (Table 4.2). Additionally, based on microarray analysis, no significant difference was observed in the fold change of all 28 well-known virulence genes of H99, H4, S68B and S48B strains genes (Table 4.14). The results are thus suggestive that the environmental strains can be potentially infectious and are capable of causing cryptococcal infections in humans. This finding is in agreement with many previous studies that the clinical strains are originated from an environmental source (Currie *et al.*, 1994; Franzot *et al.*, 1997; Yamamoto *et al.*, 1995). It is believed that many factors (either from the pathogen or the hosts) are involved in triggering a cryptococcal infection in the host. *C. neoformans* is able to establish dormant or latent infections, as healthy individuals are thought to acquire a subclinical infection that remains latent until they become immunosuppressed (Garcia-Hermoso *et al.*, 1999). More extensive study are thus required to understand how environmental strains of *C. neoformans* overcome the host defense while entering, invading and colonizing host tissues, and subsequently causes damage on those tissues.

5.4 Pathway analysis

Pathway annotation analysis using DAVID bioinformatics resource revealed two significant pathways i.e. metal ion intake (ES = 1.67, $P = 0.0159$) and sugar transmembrane transporter activity (ES = 1.65, $P = 0.0101$) that are associated with the virulence of H99 strain. This finding suggests that the ability of metal ion uptake and sugar transmembrane transport might be distinct between the virulent strain H99 and less/non-virulent environmental strains. Transition metals such as iron, zinc, copper, and manganese are essential elements for the growth and survival of microorganisms including fungi. These microorganisms sequester the metal ions from the host cells through expressing high affinity metal ion transporters to import the nutrient ions (Kehl-Fie & Skaar, 2010). Evidences suggest that metal ion intake is involved in microbial pathogenesis. Iron uptake can regulate the transcription and capsule formation in *C. neoformans* (Ding *et al.*, 2013) thus contribute to the fungal cell virulence. In fact, pulmonary infection using *C. neoformans* mutant strains lacking or defective in copper coordination exhibit reduced pulmonary colonization (Zhu *et al.*, 2003). It has been reported that copper was required to restore the activity of defective laccase in a *DVPHI* avirulent mutant of *C. neoformans* (Zhu *et al.*, 2003). Hence, low expression of the environmental strains in metal ion uptake may be a cause for the lower laccase activities of the environmental strains compared to the clinical strains, as noted in a previous study (Chan & Tay, 2010). Besides, mutations in Nickel transporter *NIC1* gene and urease proteins attenuate the invasion of *C. neoformans* into mice central nervous system (Morrow & Fraser, 2013). Up-regulation of siderophore iron transporter *ARN/SIT*-associated genes are discussed below. Another significant pathway identified was sugar transmembrane transport. *C. neoformans* is an encapsulated yeast with sugar-coating, in which the sugar transport regulators are essential for the production of capsular polysaccharide antigens (Jain *et al.*, 2013). In fact, top in the list of the up-

regulated genes in the H99 comprised *SNF3*, a gene which is linked to the sugar transmembrane transport (Bisson *et al.*, 1987; Celenza *et al.*, 1988). It has been shown that *SNF3* was up-regulated at 15.2-, 8.0- and 5.5-fold in H99 versus H4, S48B and S68B strains. Mutations in the yeast *SNF3* gene affect glucose sensing and *SNF3* mutants show defective growth on glucose (Theodoris & Bisson, 2001). In the absence of *SNF3*, yeast cells show reduced lifespan and caloric restriction effectiveness due to impaired mitochondrial activities (Choi *et al.*, 2015).

5.5 Gene expression analysis of significantly regulated genes

Hierarchical clustering based on Euclidean distance metric and Ward's Linkage showed closer distance of H4 to S68B, and H99 to S48B strains (Figures 4.2), consistent with molecular typing of the strains into Gr1 and Gr2 subtypes, respectively. Based on UPGMA algorithm based-dendrogram, H99 and S48B were grouped in a cluster while S68B and H4 were grouped in another cluster and these two groups shared 92.9% similarities. Similarly, microarray data analysis showed that the expression profile of S68B and H4 versus H99 differs from S48B. The list of genes significantly regulated in environmental strains H4 and S68B versus clinical strain H99 showed much closer regulations compared to S48B (Table 4.9). For example, dihydroxy Acetone Kinase (*DAK1*) is one of the genes that was down-regulated at 19.8 in H4, 27 in S68B and 2.8 in S48B compared to H99 (Table 4.10).

According to the study by Molin *et al.*, 2003, *DAK1* is involved in stress adaptation (Molin *et al.*, 2003). *C. neoformans* encounters a multitude of stresses within the human host to which it must adapt in order to survive and proliferate. Upon stressful changes in the external milieu, *C. neoformans* must reprogram its gene expression to properly respond and face stress to maintain homeostasis (Bloom & Panepinto, 2014). It can be hypothesised that the higher expression of *DAK1* in H99 followed by S48B might be related to higher virulence. Another gene with nearly same gene regulation in H4 and

S68B strains is core protein of QH2 cytochrome c reductase (*COR1*). *COR1* is engaged in the mitochondrial inner membrane electron transport chain (Tzagaloff *et al.*, 1986). Mitochondria plays a role in pathogenicity when the cells encounter stress condition (Shingu-Vazquez & Traven, 2011). Perhaps the 2.5 times higher regulation of this gene in H99 and S48B strains might be related to higher virulence in Gr1 group. The other up-regulated gene is *ECM15* with more than 3 times regulation in Gr1 group. It is responsible in dissecting DNA damage response pathways by analysing protein localization and abundance changes during DNA - (Tkach *et al.*, 2012).

A list of 65 genes that were commonly up-or down-regulated in H99 compared to H4, S48B or S68B strains were identified. Referring to the variances of the degree of virulence among H99 and environmental strains (H4, S48B and S68B), it has been hypothesized that the differentially regulated genes in H99 likely play roles in determining the fungal virulence. The main problem encountered in the data analysis was that not all *C. neoformans* genes have been fully characterized and reported. For certain genes, BLAST was carried out to find the closest matched genes from widely studied species i.e. *Saccharomyces cerevisiae*. Functional prediction for many genes was also reviewed based on the previous studies carried out using *S. cerevisiae* or *Candida albicans*. No suitable matches were found for some of the genes reported in (Table 4.7 to 4.11). The highest up-regulated gene in the H99 strain was Mitochondrial matrix factor (*MMF1*), which was up-regulated at 336.6-, 133.1- and 453.4-fold in the *C. neoformans* H99 strain versus other environmental strains. *MMF1* is responsible in the maintenance of intact mitochondria (Kim *et al.*, 2001; Oxelmark *et al.*, 2000).

Mitochondrial is involved in cell response to stress (Apostolova *et al.*, 2011). For example, mitochondrial oxidative respiration is important when there is low oxygen concentrations and nitrosative stress (Apostolova *et al.*, 2011). A low oxidative

respiration and increased susceptibility to reactive oxygen species has been shown in *C. neoformans* mutants with impaired mitochondrial function under hypoxic condition (Ingavale *et al.*, 2008).

Mitochondrial function is essential for metabolic pathways such as the glyoxylate cycle and gluconeogenesis as well as in sustaining cell survival throughout oxidative stress (Price *et al.*, 2011; Rodaki *et al.*, 2009). In addition, the mitochondrial function in membrane lipid homeostasis confers drug tolerance ability in fungus (Price *et al.*, 2011). There has been evidence that mitochondria regulate the of a plant pathogen, - *Heterobasidion annosum* (Olson & Stenlid, 2001). *C. albicans* mutants which lack *GOA1*, a mitochondrial protein or subunits of the mitochondrial pyruvate dehydrogenase complex, show a defect in yeast-to-filamentous switching and impairment in systemic invasion (Kim & Kim, 2010; Vellucci *et al.*, 2007). Besides, the hyper virulence *C. gattii* isolated during the outbreaks in Vancouver Island and North America (Ngamskulrunroj *et al.*, 2011) has been associated with more efficient mitochondrial function (Espinel-Ingroff *et al.*, 2012). The expression level of *Cox1* encoded for a mitochondrial gene, is affected by differences in temperature (Toffaletti *et al.*, 2003). Another contradictory report showed no direct involvement of mitochondria in pathogenicity of *C. neoformans* strains (Toffaletti *et al.*, 2003).

In addition to *MMF1*, four other mitochondrial associated genes were found among the 65 significant genes in H99. These genes were Mitochondrial dicarboxylate transporter (*DICI*), Altered inheritance of Mitochondria protein 1 (*AIM1*), Mitochondrial Dihydroxy-acid dehydratase (*ILV3*), and Mitochondrial probable electron transfer flavoprotein subunit alpha (*AIM45*), which were induced at >2-fold ($P < 0.05$) in the H99 compared to environmental strains, suggesting the active involvement of mitochondrial activity in driving fungal virulence.

Another highly up-regulated gene was a novel gene with unpredicted function, which matches to *S. cerevisiae MVA1* at 53% gene similarity in the NCBI database. *MVA1* was upregulated at 318.5-, 26.1-, and 1151.7-fold in the H99 strain versus H4, S48B and S68B environmental strains. *MVA1* is an acetyl-CoA C-acetyltransferase (also named as hydroxymethylglutaryl-CoA synthase) which changes the acetyl-CoA into hydroxymethylglutaryl-CoA in the cholesterol synthesis pathway. In fungi, acetyl-CoA is important for the synthesis of cell wall chitin and O-acetylation of the capsule (Hu *et al.*, 2008a). Acetylation of capsule polysaccharide enables inhibition of neutrophil migration and suppression of host immune response (Ellerbroek *et al.*, 2004). Importantly, elevated expression of acetyl-CoA production and utilization-associated genes has been detected in *C. neoformans* recovered from the lung of infected mice during pulmonary infection (Hu *et al.*, 2008a).

Another significant up-regulated gene identified in this study, Bud-site-selection protein 8 (*BUD8*), was induced at 40.5-, 37.5- and 62.5-fold. *BUD8* is a transmembrane glycoprotein which participates in the proteins complex to organize and polymerize actin and actin-associated proteins (Taheri *et al.*, 2000; Zahner *et al.*, 1996). The function of *BUD8* is to ensure bipolar budding during cell division and polarized growth (Taheri *et al.*, 2000), important for bud initiation during invasion process (Harkins *et al.*, 2001). Besides, another gene in the top list, *RGA2*, induced at 13.6-, 7.2- and 11.9-fold in H99 compared to environmental strains, was also associated with yeast budding process. *RGA2* is a Rho GTPase-activating protein (*GAP*) of the central polarity regulator *CDC42* that functions to regulate cell morphogenesis and integrity (Villar-Tajadura *et al.*, 2008). In *C. albicans*, hyperphosphorylation of *RGA2* occurs at the bud emergence and governs different forms of polarized morphogenesis (Zheng *et al.*, 2007). The functions of *BUD8* and *RGA2* in *C. neoformans* and their roles in fungal virulence require further investigations.

Other selected genes that were considerably up-regulated and have a reported role in virulence were as discussed below. For instance, two genes in Siderophore iron transporters family, *ARN2* and *ARN1* were up-regulated at 6.7-, 10.2-, and 11.4-fold, and 4.7-, 8.1-, and 5.5-fold, respectively, in H99 when compared to H4, S48B and S68B strains (Table 4.10). Non-reductive uptake of ferric-siderophore complexes is dependent on specific siderophore transporters *ARN1*, *ARN2*, *ARN3* and *ARN4* (Haas, 2003; Lesuisse *et al.*, 2001). Some pathogenic fungi, such as *S. cerevisiae*, have homologues for siderophore transporters that help these fungi to utilize siderophores from competitors (Haas, 2003). *C. albicans ARN1/SIT1* is essential for the fungal epithelial cell invasion (Ardon *et al.*, 2001; Heymann *et al.*, 2002; Kosman, 2003). Whereas in *Aspergillus fumigatus*, loss of ability to synthesize siderophores appears to compromise its virulence (Ding *et al.*, 2013; Hissen *et al.*, 2004; Schrettl *et al.*, 2004). Recently, the transcript for a putative siderophore transporter *ARN1/SIT1* which was increased in *C. neoformans* cells grown in low-iron medium, has been characterized (Lian *et al.*, 2005). Therefore, *ARN1* and *ARN2* may contribute to the fungal cell virulence by controlling the ability of *C. neoformans* to acquire siderophores.

Guanosine-diphosphatase (*GDA1*), a GDPase which functions to hydrolyze GDP to GMP, was induced at 7.6-, 17.5- and 6.3-fold in H99 relative to H4, S48B and S68B (Table 4.10). The adhesive and immunomodulation properties of some fungal pathogens depend on cell wall mannoproteins (Tangen *et al.*, 2007). *GDA1* hydrolyzes the GDP-mannose complexes thus releases mannans to the cell wall. In *GDA1*-mutated *C. albicans*, defect in GDP hydrolysis, O-mannosylation can also result in impaired yeast-hypha transition (Hirschberg *et al.*, 1998). The expression of another up-regulated gene, Ino-transporting P-type ATPase (*SPF1*) was increased at 5.4-, 2.6- and 5.0-fold in H99 versus environmental strains. *SPF1* plays essential role in calcium homeostasis, and its deletion results in calcium influx and increased cellular calcium

contents, leading to expression of the calcium-dependent response elements gene *CCHI* for the cell survival (Hirschberg *et al.*, 1998). Besides, *SPF1* null mutant shows defects in hyphal growth rate and biofilm formation, resulting in severely attenuated virulence in *C. albicans* (Bonilla & Cunningham, 2003).

The expression of NADPH-dependent methylglyoxal reductase (*GRE2*) has increased 5.9-, 3.7- and 7.9-fold in H99 versus H4, S48B and S68B strains (Table 4.10). The cAMP-dependent genes *GRE2* in *C. neoformans* is known to be induced by a variety of environmental stresses, including osmotic and oxidative stresses (Yu *et al.*, 2012). *Cryptococcus* grows well under atmospheric oxygen condition. However, it faces low oxygen concentrations in lungs (approximately 21%) and blood (12%) (Yu *et al.*, 2012). It often affects the brain region with minimal oxygen level (<4 %), suggesting that *Cryptococcus* may possess a mechanism to allow the organism to adapt in such condition. *Cryptococcus* with mutation in the sterol regulatory element binding protein (*SRE1*) gene is unable to proliferation at conditions with low oxygen, and besides causing reduced pathogenicity in animal infection model (Chang *et al.*, 2007; Chun *et al.*, 2007). *SRE1p* is an important component in the cholesterol biosynthesis pathway which helps to sense the oxygen level and generate sterol under low oxygen stress condition (Chang *et al.*, 2007; Lee *et al.*, 2007). In addition, NADPH-dependent methylglyoxal reductase (*GRE2*) involves in metabolism of ergosterol (Maeng *et al.*, 2010), a V-ATPase which functions to repress growth and attenuate fungal virulence in both *S. cerevisiae* and *C.albicans* (Warringer & Blomberg, 2006). On the other hand, NAD(+)-dependent Glutamate dehydrogenase (*GDH2*) was induced at 2.5-, 2.4- and 3.2-fold. *GDH2* degrades the reversible oxidative deamination of glutamate to α -ketoglutarate and ammonia using NAD(H) and NADP(H) as cofactors. It also interacts with *GDH3* and suppresses stress-induced apoptosis in the cells (Zhang *et al.*, 2010).

Therefore, high expression of *GRE2* and *GDH2* in H99 may influence virulence by regulating biochemistry pathways in *C. neoformans*.

Rab guanine nucleotide exchange factor (*SEC2*) was induced at 4.0-, 3.3-, 6.6-fold in H99 compared to H4, S48B and S68B (Table 4.10). *SEC2* functions in polarized directional delivery of post golgi vesicle for exocytosis activity (Elkind *et al.*, 2000; Walch-Solimena *et al.*, 1997). Phosphorylated form of *SEC2* binds preferentially to *SEC15* and a component of exocyst tethering complex which enables fusion of secretory vesicle with plasma membrane (Elkind *et al.*, 2000). The phosphorylation of *SEC2* is necessary to support hyphal in *C. albicans* because during hyphal extension, the distance of hyphal tip and nucleus is far, thus an effective transport machinery through *SEC2* is required (Stalder *et al.*, 2013).

Dihydroxyacetone kinase 1 (*DAK1*) was found to be up-regulated in H99 for 11.5-, 2.6- and 10.7-fold (Table 4.10). *DAK1* functions to catalyze both phosphorylation of dihydroxyacetone (DHA) of glyceraldehyde. In *S. cerevisiae*, detoxification of dihydroxyacetone by *DAK1* is suggested to be a vital part of the physiological response during diverse stress conditions (Caballero-Lima & Sudbery, 2014). For example, by protecting yeast cells from osmotic stress, Glycerol synthesis plays a vital physiological role in the metabolism of yeast (Zhang *et al.*, 2013). Interestingly, *DAK1* has been found to be an interacting protein for *MDA-5*, a pattern recognition receptor on host immune cells. *DAK* interacts with *MDA-5* and blocks its antiviral signaling (Molin *et al.*, 2003). The overexpression of *DAK* inhibits *MDA5*-mediated IFN- β induction and cytoplasmic dsRNA-/virus-induced activation of the IFN- β promoter, whereas these processes can be increased by RNAi knockdown of endogenous *DAK*. It remains to be investigated if the *DAK1* expressed in *C. neoformans* H99 can inhibit *MDA5*-mediated signaling to suppress host immune response.

It has been reported that genomic changes provide selective advantages enabling pathogen to survive and proliferate (Ormerod *et al.*, 2013). It is possible these genomic changes occur as the result of changes in the environmental temperature as well. The clinical strain H99 was taken from a patient with body temperature of 37°C while the environmental strains were isolated from soil with lower environmental temperature and both were grown at 37°C for microarray analysis. It is important to note that genes important for growth at 37°C, contribute to the virulence of *C. neoformans*. Perhaps gene expression is also dependent of this temperature shift from 25°C in environmental strains compare to the steady-state of 37°C growth temperature for H99. It is likely that important genes for stress responses are induced upon a shift from 25°C to 37°C in environmental strains for adaption to alterations in growth environment comparing to long-term adaptation of H99. *MPH2*, *PUT3*, *MAL31*, *HMRA1* and *ENO2* were among the highly induced genes in environmental strains. It is unclear why the genes such as *PUT3* in metal ion binding and *MAL31* and *MPH2* in sugar transmembrane transporter activity which are in the same pathway with highly up regulated genes in H99 are significantly down regulated. However, - regulation of these genes and products at post transcriptional levels in response to environmental changes is possible.

5.6 Microarray validation

Both biological and technical variability can have a great influence on both microarray and qPCR results (Wurmbach *et al.*, 2003) as biological variability cannot be controlled, experimental design is essential to minimize irregularities and ensure adequate replication to eliminate “noise” in the experiment (Morey *et al.*, 2006). However, due to the high cost of microarray analysis, this study was limited to two probe replicates designed for each gene. In addition, the quality of RNA is critical to generate accurate results, as gene expression can be affected by carry-over of contaminating factors. In this study, removal of salts, alcohols, and phenol contaminant

from the RNA extracted is important as these substances can affect reverse transcriptases used in both qPCR and RNA amplification procedures for microarray labelling (Freeman *et al.*, 1999).

Furthermore, different efficiencies of reverse transcriptases and varied priming methods can also affect the results of qPCR and microarray experiments (Freeman *et al.*, 1999). The effects of dye biases (due in part to the physical properties of various dyes that affect efficiencies of incorporation (Yang, YH *et al.*, 2002) and non-specific and/or cross hybridizations of labeled targets to array probes (Chuaqui *et al.*, 2002) are unique to microarray procedures. Likewise, qPCR has its own sources of error including amplification biases (Chuaqui *et al.*, 2002), the exponential amplification of errors (Freeman *et al.*, 1999), mispriming or the formation of primer dimers, and the changing efficiency of qPCR at later cycles (Freeman *et al.*, 1999). In addition, data normalization fundamentally differs between microarray analysis and qPCR. The former requires global normalization, while the latter generally utilizes the expression of one or more reference genes against which all other gene expression is calibrated. Hence, application of normalization criteria play an important role in the correlations between these methods. Perhaps, in this experiment, the above mentioned list of the potential pitfalls in microarray and qPCR methodologies are the sources of error in the real time and microarray gene expression differences although the up or down regulation tally among both methods. In spite of the potential pitfalls in microarray and qPCR methodologies, most sources of error were controlled through robust experimental designs while *in vitro* study closely mimics the *in vivo* condition, good laboratory practices, and rigorous normalization of the data.

5.7 Antifungal effect of untapped drugs against *C. neoformans*

C. neoformans can cause fatal diseases without appropriate treatment. The rise of antimicrobial resistance in recent years has contributed much towards the increased

mortality and morbidity associated with systemic infectious diseases like pneumonia, cryptococcosis, and meningitis (World Health Organization, 2002). Therefore, our urgent need for investigations on more effective antifungal drugs is inevitable. Elucidation and understanding the pathogenesis mechanism underlying infection of *C. neoformans* strains may aid in identification of biomarkers that can be applied in drug targeting and vaccine design against fungal infection.

However, there are only limited studies on the susceptibility of *C. neoformans* (Davey *et al.*, 1998). Hence, it is interesting to have data from different sources, geographical distributions and effect of new antimicrobial agents. However, while the quest for new antimicrobials, including peptides, goes on (Dyatkina *et al.*, 2002; Mitten *et al.*, 2001; Saugar *et al.*, 2002), triclosan has not been explored for anti-*Cryptococcus* activity. During two decades of triclosan application, there have been no reports of triclosan-resistant microbes in the wild (Hay *et al.*, 2001). Considerable efficacy of triclosan in a mouse model of acute systemic infections has been reported in a study conducted by Sharma *et al.* (2003). This study has indicated that, the levels of triclosan in the blood were greater than the MIC of triclosan at the dosage of 40 mg/kg, which explains why triclosan is effective at reducing the bacteremia and increasing the survival time of the mice at this dosage (Sharma *et al.*, 2003). The longer survival time achieved in mice with triclosan clearly pointed out the superiority of triclosan as an antibacterial agent compared to ampicillin and tetracycline for systemic infections (Lacy *et al.*, 1999; Milano *et al.*, 1997; Shapira *et al.*, 1996; Walker *et al.*, 1977; Young *et al.*, 1975). Moreover, all the blood parameters remained within the normal range upon administration of triclosan (Mitruka & Rawnsley, 1977). Results of toxicology studies show that triclosan and its metabolites are well tolerated by a variety of species, including human beings (Bhargava & Leonard, 1996; Desalva *et al.*, 1989; Lyman & Furia, 1969; Tulp *et al.*, 1979). Triclosan is not a carcinogen, mutagen, or teratogen and

has been shown to be safe in reproductive researches (Desalva *et al.*, 1989; Tulp *et al.*, 1979). The excellent safety track record of triclosan in topical use in addition to the finding in this study is suggestive of triclosan as a potent drug to explore in treating systemic fungal infections.

Cryptococcal diseases remain a challenging management issue among AIDS patients. According to Clinical Practice Guidelines for the Management of Cryptococcal Disease 2010 Update by the Infectious Diseases Society of America, polyene and flucytosine, followed by suppressive regimens using fluconazole have been suggested. However, for azole-intolerant individual amphotericin B deoxycholate (AmBd) is prescribed at the moment. The activity of AmBd is weaker than azoles and is associated with intravascular catheter-related infections (Perfect *et al.*, 2010). Besides, the emergence of azole-resistant strains contributed much towards the increased mortality and morbidity in recent years. Moreover, increasing the dose of the azole alone is not beneficial for the patient and combination of another drug is suggested (Perfect *et al.*, 2010).

Perhaps, triclosan can be a good choice in case of azole-intolerant individuals, azole-exposed patients and azole-resistant strains. On the other hand, AmBd carries the risk of nephrotoxicity in transplant recipients as frequent renal failure is reported and thus is not recommended. Therefore, application of a safer drug is essential. Triclosan's safety has been established through acute toxicity, chronic toxicity, mutagenicity, reproduction, and teratology (Mitruka & Rawnsley, 1977).

A large clinical trial compared AmBd with fluconazole for AIDS-associated cryptococcal meningoencephalitis (Reitman & Frankel, 1957), resulted in disappointing outcomes of <50% successful rate, suggesting the requirement to investigate a novel therapeutic drug for the patients with AIDS-associated cryptococcal

meningoencephalitis. Perhaps administration of combination therapy with triclosan could be a good solution.

This study demonstrated the potent antifungal effect of triclosan against *C. neoformans*. In fact, triclosan treatment exerted a stronger growth inhibition in *C. neoformans* compared to *C. albicans*, as evidenced by comparatively lower MIC-1 values (ranged from 0.25 to 3.80 µg/ml) in *C. neoformans* strains tested, compared to MIC-1 values in *C. albicans* (ranged from 59.6 to >64 µg/ml) (Table 4.16).

5.8 Synergism between triclosan and standard drugs

Combined antibiotic therapy can delay the emergence of microbial resistance by producing desirable synergistic effects in the infection treatment (Adwan & Mhanna, 2008). In this study, synergism between triclosan and two standard drugs (amphotericin B and fluconazole) was established. Fluconazole and amphotericin B are commonly used drugs for candidiasis and cryptococcal diseases. Fluconazole is a member of the azole family that targets the Erg11 enzyme (an essential fungal cytochrome P450 lanosterol 14 α -demethylase), thus inhibiting ergosterol (Heilmann *et al.*, 2010; Rodero *et al.*, 2003). Amphotericin B, on the other hand, binds directly to ergosterol and kills yeast cells via ion channel-mediated plasma membrane permeabilization (Gruda & Dussault, 1988). Combinational treatment of triclosan and other drugs has been shown to significantly enhance the drug efficacy against bacteria (Sharma *et al.*, 2003; Tambe *et al.*, 2001). However, two previous reports using *C. albicans* demonstrated opposing results for combinational usage of triclosan plus fluconazole, whereby one showed synergistic effect (Yu *et al.*, 2011) and another showed antagonistic effect (Higgins *et al.*, 2012). In *C. neoformans*, triclosan has observed to act in synergy with fluconazole and amphotericin B (Table 5.1).

5.9 Mechanism of action of triclosan

The mechanism of triclosan-mediated cell disruption has been described in different pathogens. Triclosan triggers changes in bacterial membrane fluidity and functions at a lower concentration, and leads to cell lysis at a higher concentration (Gomez Escalada *et al.*, 2005). It is also known to block lipid synthesis primarily by targeting the carrier protein of the bacterial type II fatty acid synthesis (FASII) pathway (Mcmurry *et al.*, 1998). Contradictory, a recent study shows that *FAS1* and *FAS2* gene overexpression did not alter fungal susceptibility to triclosan and suggests that there may be an alternative target of triclosan in addition to the lipid synthesis pathway (Higgins *et al.*, 2012). Therefore, further investigations are required to elucidate the actual mechanism of action. In mammals, triclosan antagonizes estrogen or androgen receptors, elevates resting cytosolic Ca^{2+} in primary skeletal myotubules (Ahn *et al.*, 2008) and impairs the excitation contraction coupling of cardiac and skeletal function (Cherednichenko *et al.*, 2012).

5.10 Programme cell death mechanism in *C. neoformans*

From electron microscope pictures, it can be hypothesized that triclosan induces ALCD, a programme cell death mechanism in *C. neoformans* because various apoptotic subcellular changes could be visualized as early as 2 hours post treatment. At an early stage of an apoptotic cell, cell shrinkage occurs as a result of organelle condensation and decreased cytoplasm density (Häcker, 2000). During the apoptosis process, free radicals can modify mitochondrial membrane potential thus inducing mitochondrial swelling and fusion of adjacent mitochondria into megamitochondria (Wakabayashi, 1999). Mitochondria release cytochrome c from storage which subsequently activates the caspase cascade leading to nuclear cleavage (Zhang & Ming, 2000) and extensive plasma membrane blebbing (Coleman *et al.*, 2001). Some apoptotic features in triclosan-treated *C. neoformans* cells including condensed nuclear chromatin, DNA

fragmentation and mitochondrial swelling was reported in this study. Perhaps, intensive cytoplasmic vacuolation was due to the decreased cytoplasm density and organelles condensation although the cell structure remained intact as a resultant of rigid fungal cell wall. Several pathogenic fungi have been reported to undergo ALCD (Büttner *et al.*, 2007; Ramsdale, 2008). For instance, mutation of *CDC48* in *S. cerevisiae* shows apoptosis characteristic including chromatin condensation and fragmentation (Madeo *et al.*, 1997). Interestingly, overexpression of mammalian anti-apoptotic Bcl2 rescues fungal cell apoptosis (Longo *et al.*, 1997) while overexpression of pro-apoptotic Bax enhances the cell death effect (Ligr *et al.*, 1998; Manon *et al.*, 1997). ALCD has also been reported in *C. neoformans* when the cells were stimulated with hydrogen peroxide or cultured in the presence of *Staphylococcus aureus* (Ikeda & Sawamura, 2008). The apoptosis pathway in *C. neoformans* is controlled through regulation of apoptosis-inducing factor (*AIF1*) and metacaspases (*MCA1* and *MCA2*) (Semighini *et al.*, 2011).

In addition to electron microscopy, the terminal dUTP nick-end labeling (TUNEL) has been performed to determine DNA fragmentation as another apoptotic marker in the yeast model. Cell death conditions result in positive staining for single-strand breaks and not for double-strand, which are normally associated with apoptosis in mammalian cells. Hydrogen peroxide, which in particular induces ALCD in *C. neoformans* (Semighini *et al.*, 2011), was applied as positive control. A total of 19.3% more apoptotic cells were detected in triclosan-treated *C. neoformans* as compared to those of hydrogen peroxide-treated cells in an experiment conducted by Carmona-Gutierrez *et al.* (2010), involving treatment of *S. cerevisiae* with low doses of hydrogen peroxide (H_2O_2). ROS was proved being key regulators of yeast apoptosis (Carmona-Gutierrez *et al.*, 2010). While low doses of H_2O_2 cause apoptosis, high doses of H_2O_2 induce necrotic phenotypes (Madeo *et al.*, 1999). Several molecular factors are involved in this process, including the Yeast caspase *YCA1* (Madeo *et al.*, 2002), *RHO5*

(Singh *et al.*, 2008) and the *AIF1* (Wissing *et al.*, 2004). Phylogenetic conservation of the core machinery and the core regulators of cell death between yeast and mammals suggested the possibility of using yeast as a research tool to provide new indications in revealing cell death pathways in higher eukaryotes (Carmona-Gutierrez *et al.*, 2010).

In summary, in fulfilling the first objective of this study, comparison has been made on the virulence of clinical (H99 strain) and environmental strains of *C. neoformans* using *in vivo* and *in vitro* methods. Higher virulence of the H99 clinical strain was demonstrated by mice infection experiment, whereby it was the only *C. neoformans* strain which caused death in mice in this study. Additionally, the recovered yeast cells of H99 clinical strain were approximately forty folds higher than those obtained from H4, S48B and S68B-infected mice. The higher virulence of H99 clinical strain was also supported by the finding of a bigger capsule size (by India ink), and laccase activity.

In achieving the second objective, microarray analysis revealed a different transcriptome profile of H99 strain compared to H4, S48B and S68B strains. Additional genes responsible for the virulence of the H99 clinical strain were identified. It is postulated that the environmental strains are also capable of causing cryptococcal infections, as indicated by the expression of major virulence genes reported in previous investigations.

Lastly, the anti-*Cryptococcus* activity of triclosan has been evaluated (third objective of this study). The results demonstrated that a combination of triclosan with amphotericin B or with fluconazole enhanced the fungicidal effects against *C. neoformans*. Additionally, the apoptotic effect of triclosan on *C. neoformans* has been demonstrated using TUNEL assay and TEM observation.

CHAPTER 6: CONCLUSION

This study revealed that out of 7,419 genes (22,257 probes) examined, 41 genes were up-regulated while 24 genes were down regulated in H99 versus environmental H4, S48B and S68B strains. The up-regulated genes in H99 strain include *MVA1*, *MMF1*, *BUD8*, *SNF3* and *RGA2*. Consistent with the microarray data, qRT-PCR showed that expression levels of *MVA1* and *MMF1* were significantly increased in H99 relative to other environmental strains at >142 and >19 folds, respectively. On the other hand, the *MPH2* and *PUT3* were reduced in H99 at >4.2 and >25 folds, respectively. Pathway annotation using DAVID bioinformatics resource showed that metal ion binding was highly active in the clinical but not environmental strains. Transition metals such as iron, zinc, copper, and manganese are essential elements for the growth and survival of microorganisms including fungi. Siderophore iron transporter (*ARN2* and *ARN1*) were up-regulated at 6.7-, 10.2-, and 11.4-fold, and 4.7-, 8.1-, and 5.5-fold, respectively, in H99 compared to H4, S48B and S68B strains. Another active pathway identified in H99 strain was sugar transmembrane transport. *C. neoformans* is an encapsulated yeast with sugar-coating, in which the sugar transport regulators are essential for the production of capsular polysaccharide antigens. *SNF3*, a gene in the sugar transmembrane transport pathway, was up-regulated at 15.2-, 8.0- and 5.5-fold in H99 versus H4, S48B and S68B strains. This study suggests that these genes and pathways may possibly play crucial roles in the fungal pathogenesis.

This study also reveals a strong inhibitory effect of triclosan as well as its synergy with amphotericin B and fluconazole in blocking cell growth of the pathogenic fungus *C. neoformans*. This study reports that triclosan maybe fungicidal by inducing the ALCD mechanism in *C. neoformans*. This study suggests triclosan as a potential

therapeutic drug alone or in combination with standard drugs in the treatment of cryptococcal infection.

6.1 Study limitation

The RNA used for microarray analysis was extracted from clinical and environmental strains grown *in vitro* in a 37°C incubator. This may not completely represent the *in vivo* condition of the *C. neoformans* infection, thus the result needs to be further confirmed using animal model. In addition, microarray assay has yielded a large amount of expression data for all genes, the analysis conducted here was mainly focused on 65 overlapped genes, which were expressed in all environmental strains compared to clinical H99. While there has been enormous volume of raw data available for further analysis, these studies were limited by time and cost.

6.2 Future work

Although comparative gene transcriptome profile can provide us valuable information and prediction of potential virulence genes, further investigations on *C. neoformans* have shown that gene regulation does not always correlate well with their functional activities and that specific null mutants should be evaluated for their role in *C. neoformans* virulence.. This is because the importance of some gene is not fully implicated by their expression profile. For example, *C. neoformans* Isocitrate lyase (*ICll*) gene is highly upregulated during central nervous system infection nonetheless the null mutant for *ICll* does not exhibit an attenuated phenotype *in vivo* (Rude *et al.*, 2002). Therefore, mutagenesis studies of the genes discussed are needed in future study to confirm their functions and roles in fungal pathogenesis. . It is possible that “virulence” genes in *C. neoformans* may be variable or quantitative during infection. This is evidenced based on the observation of Perfect (2005) that some null mutants are completely eliminated from the host and all the host survive, while others

have prolonged survival but the host succumb to infection (Perfect, 2005). Hence, different mammalian models including rabbits and rats should be attempted to distinguish various degrees of virulence potential associated with specific *C. neoformans* genes, as - advocated by Perfect (2005).

University of Malaya

REFERENCES

- Adwan, G., & Mhanna, M. (2008). Synergistic effects of plant extracts and antibiotics on *Staphylococcus aureus* strains isolated from clinical specimens. *Middle-East Journal of Scientific Research*, 3(3), 134-139.
- Aguirre, K. M., Gibson, G. W., & Johnson, L. L. (1998). Decreased resistance to primary intravenous *Cryptococcus neoformans* infection in aged mice despite adequate resistance to intravenous rechallenge. *Infection and Immunity*, 66(9), 4018-4024.
- Ahn, K. C., Zhao, B., Chen, J., Cherednichenko, G., Sanmarti, E., Denison, M. S., Lasley, B., Pessah, I. N., Kultz, D., & Chang, D. (2008). In vitro biologic activities of the antimicrobials triclocarban, its analogs, and triclosan in bioassay screens: receptor-based bioassay screens. *Environment Health Perspect*, 116(9), 1203-1210.
- Akhter, S., McDade, H. C., Gorlach, J. M., Heinrich, G., Cox, G. M., & Perfect, J. R. (2003). Role of alternative oxidase gene in pathogenesis of *Cryptococcus neoformans*. *Infection and Immunity*, 71(10), 5794-5802.
- Allen, L.-A. H., Schlesinger, L. S., & Kang, B. (2000). Virulent strains of *Helicobacter pylori* demonstrate delayed phagocytosis and stimulate homotypic phagosome fusion in macrophages. *The Journal of Experimental Medicine*, 191(1), 115-128.
- Almeida, F., Wolf, J. M., & Casadevall, A. (2015). Virulence-associated enzymes of *Cryptococcus neoformans*. *Eukaryotic Cell*, 14(12), 1173-1185.
- Alspaugh, J. A., Cavallo, L. M., Perfect, J. R., & Heitman, J. (2000). *RAS1* regulates filamentation, mating and growth at high temperature of *Cryptococcus neoformans*. *Molecular Microbiology*, 36(2), 352-365.
- Alspaugh, J. A., Perfect, J. R., & Heitman, J. (1997). *Cryptococcus neoformans* mating and virulence are regulated by the G-protein α subunit *GPA1* and cAMP. *Genes & Development*, 11(23), 3206-3217.
- Alspaugh, J. A., Pukkila-Worley, R., Harashima, T., Cavallo, L. M., Funnell, D., Cox, G. M., Perfect, J. R., Kronstad, J. W., & Heitman, J. (2002). Adenylyl cyclase functions downstream of the $G\alpha$ protein *Gpa1* and controls mating and pathogenicity of *Cryptococcus neoformans*. *Eukaryotic Cell*, 1(1), 75-84.
- Aminnejad, M., Diaz, M., Arabatzis, M., Castañeda, E., Lazera, M., Velegraki, A., Marriott, D., Sorrell, T. C., & Meyer, W. (2012). Identification of novel hybrids between *Cryptococcus neoformans* var. *grubii* VNI and *Cryptococcus gattii* VGII. *Mycopathologia*, 173(5-6), 337-346.
- Apostolova, N., Garcia-Bou, R., Hernandez-Mijares, A., Herance, R., Rocha, M., & Victor, V. M. (2011). Mitochondrial antioxidants alleviate oxidative and nitrosative stress in a cellular model of sepsis. *Pharmaceutical Research*, 28(11), 2910-2919.

- Ardon, O., Bussey, H., Philpott, C., Ward, D. M., Davis-Kaplan, S., Verroneau, S., Jiang, B., & Kaplan, J. (2001). Identification of a *Candida albicans* Ferrichrome Transporter and Its Characterization by Expression in *Saccharomyces cerevisiae*. *Journal of Biological Chemistry*, 276(46), 43049-43055.
- Bahn, Y.-S., Kojima, K., Cox, G. M., & Heitman, J. (2005). Specialization of the HOG pathway and its impact on differentiation and virulence of *Cryptococcus neoformans*. *Molecular Biology of the Cell*, 16(5), 2285-2300.
- Barnett, J. A. (2010). A history of research on yeasts 14: 1 medical yeasts part 2, *Cryptococcus neoformans*. *Yeast*, 27(11), 875-904.
- Barragan, N. C., Sorvillo, F., & Kuo, T. (2014). Cryptococcosis- related deaths and associated medical conditions in the United States, 2000–2010. *Mycoses*, 57(12), 741-746.
- Baum, G. L., & Artis, D. (1963). Characterization of the growth inhibition factor for *Cryptococcus neoformans* (GIFc) in human serum. *The American Journal of the Medical Sciences*, 246(1), 53-57.
- Bhargava, H., & Leonard, P. A. (1996). Triclosan: applications and safety. *American Journal of Infection Control*, 24(3), 209-218.
- Bisson, L., Neigeborn, L., Carlson, M., & Fraenkel, D. (1987). The *SNF3* gene is required for high-affinity glucose transport in *Saccharomyces cerevisiae*. *Journal of Bacteriology*, 169(4), 1656-1662.
- Bloom, A. L., & Panepinto, J. C. (2014). RNA biology and the adaptation of *Cryptococcus neoformans* to host temperature and stress. *Wiley Interdisciplinary Reviews: RNA*, 5(3), 393-406.
- Bolanos, B., & Mitchell, T. (1989). Phagocytosis of *Cryptococcus neoformans* by rat alveolar macrophages. *Medical Mycology*, 27(4), 203-217.
- Bonilla, M., & Cunningham, K. W. (2003). Mitogen-activated protein kinase stimulation of Ca²⁺ signaling is required for survival of endoplasmic reticulum stress in yeast. *Molecular Biology of the Cell*, 14(10), 4296-4305.
- Bose, I., Reese, A. J., Ory, J. J., Janbon, G., & Doering, T. L. (2003). A yeast under cover: the capsule of *Cryptococcus neoformans*. *Eukaryotic Cell*, 2(4), 655-663.
- Bovers, M., Diaz, M., Hagen, F., Spanjaard, L., Duim, B., Visser, C., Hoogveld, H., Scharringa, J., Hoepelman, I., & Fell, J. (2007). Identification of genotypically diverse *Cryptococcus neoformans* and *Cryptococcus gattii* isolates by Luminex xMAP technology. *Journal of Clinical Microbiology*, 45(6), 1874-1883.
- Brading, M., Cromwell, V., Green, A., DeBrabander, S., Beasley, T., & Marsh, P. (2004). The role of Triclosan in dentifrice formulations, with particular reference to a new 0.3% Triclosan calcium carbonate- based system. *International dental journal*, 54(S5), 291-298.
- Brajtburg, J., Powderly, W. G., Kobayashi, G. S., & Medoff, G. (1990). Amphotericin B: current understanding of mechanisms of action. *Antimicrobial Agents and Chemotherapy*, 34(2), 183.

- Brandt, M. E., Hutwagner, L. C., Kuykendall, R. J., & Pinner, R. W. (1995). Comparison of multilocus enzyme electrophoresis and random amplified polymorphic DNA analysis for molecular subtyping of *Cryptococcus neoformans*. The Cryptococcal Disease Active Surveillance Group. *Journal of Clinical Microbiology*, *33*(7), 1890-1895.
- Brandt, M. E., & Park, B. J. (2013). Think fungus—prevention and control of fungal infections. *Emerging Infectious Diseases*, *19*(10), 1688.
- Brown, S. M., Campbell, L. T., & Lodge, J. K. (2007). *Cryptococcus neoformans*, a fungus under stress. *Current Opinion in Microbiology*, *10*(4), 320-325.
- Bulmer, G., & Sans, M. (1967). *Cryptococcus neoformans* II. Phagocytosis by human leukocytes. *Journal of Bacteriology*, *94*(5), 1480-1483.
- Bulmer, G. S., & Tacker, J. R. (1975). Phagocytosis of *Cryptococcus neoformans* by alveolar macrophages. *Infection and Immunity*, *11*(1), 73-79.
- Bunting, L., Neilson, J. B., & Bulmer, G. (1979). *Cryptococcus neoformans*: gastronomic delight of a soil amoeba. *Sabouraudia*, *17*(3), 225-232.
- Busse, O. (1894). Über parasitäre Zelleinschlüsse und ihre Zuchtung. *Zentralbl. Bakteriologie*, *16*, 175-180.
- Büttner, S., Eisenberg, T., Carmona-Gutierrez, D., Ruli, D., Knauer, H., Ruckenstein, C., Sigrist, C., Wissing, S., Kollroser, M., & Fröhlich, K.-U. (2007). Endonuclease G regulates budding yeast life and death. *Molecular Cell*, *25*(2), 233-246.
- Byrnes, E. J., Bartlett, K. H., Perfect, J. R., & Heitman, J. (2011). *Cryptococcus gattii*: an emerging fungal pathogen infecting humans and animals. *Microbes and Infection*, *13*(11), 895-907.
- Caballero-Lima, D., & Sudbery, P. E. (2014). In *Candida albicans*, phosphorylation of Exo84 by Cdk1-Hgc1 is necessary for efficient hyphal extension. *Molecular biology of the cell*, *25*(7), 1097-1110.
- Carmona-Gutierrez, D., Eisenberg, T., Büttner, S., Meisinger, C., Kroemer, G., & Madeo, F. (2010). Apoptosis in yeast: triggers, pathways, subroutines. *Cell Death & Differentiation*, *17*(5), 763-773.
- Casadevall, A. (1995). Antibody immunity and invasive fungal infections. *Infection and Immunity*, *63*(11), 4211.
- Casadevall, A., Cleare, W., Feldmesser, M., Glatman-Freedman, A., Goldman, D. L., Kozel, T. R., Lendvai, N., Mukherjee, J., Pirofski, L.-a., & Rivera, J. (1998). Characterization of a murine monoclonal antibody to *Cryptococcus neoformans* polysaccharide that is a candidate for human therapeutic studies. *Antimicrobial Agents and Chemotherapy*, *42*(6), 1437-1446.
- Casadevall, A., & Perfect, J. R. (1998). *Cryptococcus neoformans* (Vol. 595): Citeseer.
- Casadevall, A., Rosas, A. L., & Nosanchuk, J. D. (2000). Melanin and virulence in *Cryptococcus neoformans*. *Current Opinion in Microbiology*, *3*(4), 354-358.

- Casadevall, A., Steenbergen, J. N., & Nosanchuk, J. D. (2003). 'Ready made' virulence and 'dual use' virulence factors in pathogenic environmental fungi—the *Cryptococcus neoformans* paradigm. *Current Opinion in Microbiology*, 6(4), 332-337.
- Celenza, J. L., Marshall-Carlson, L., & Carlson, M. (1988). The yeast *SNF3* gene encodes a glucose transporter homologous to the mammalian protein. *Proceedings of the National Academy of Sciences*, 85(7), 2130-2134.
- Chan, M., & Tay, S. (2010). Enzymatic characterisation of clinical isolates of *Cryptococcus neoformans*, *Cryptococcus gattii* and other environmental *Cryptococcus spp.* *Mycoses*, 53(1), 26-31.
- Chang, Y., Penoyer, L., & Kwon-Chung, K. (2001). The second *STE12* homologue of *Cryptococcus neoformans* is MATa-specific and plays an important role in virulence. *Proceedings of the National Academy of Sciences*, 98(6), 3258-3263.
- Chang, Y. C., Bien, C. M., Lee, H., Espenshade, P. J., & Kwon-Chung, K. J. (2007). Sre1p, a regulator of oxygen sensing and sterol homeostasis, is required for virulence in *Cryptococcus neoformans*. *Molecular Microbiology*, 64(3), 614-629.
- Chang, Y. C., Cherniak, R., Kozel, T. R., Granger, D. L., Morris, L. C., Weinhold, L. C., & Kwon-Chung, K. (1997). Structure and biological activities of acapsular *Cryptococcus neoformans* 602 complemented with the *CAP64* gene. *Infection and Immunity*, 65(5), 1584-1592.
- Chang, Y. C., & Kwon-Chung, K. (1994). Complementation of a capsule-deficient mutation of *Cryptococcus neoformans* restores its virulence. *Molecular and Cellular Biology*, 14(7), 4912-4919.
- Chaturvedi, V., Flynn, T., Niehaus, W. G., & Wong, B. (1996). Stress tolerance and pathogenic potential of a mannitol mutant of *Cryptococcus neoformans*. *Microbiology*, 142(4), 937-943.
- Chee, H. Y., & Lee, K. B. (2005). Isolation of *Cryptococcus neoformans* var. *grubii* (serotype A) from pigeon droppings in Seoul, Korea. *Journal of microbiology (Seoul, Korea)*, 43(5), 469.
- Chen, J., Varma, A., Diaz, M. R., Litvintseva, A. P., Wollenberg, K. K., & Kwon-Chung, K. J. (2008). *Cryptococcus neoformans* strains and infection in apparently immunocompetent patients, China. *Emerging Infection Disease*, 14(5), 755-762.
- Chen, L.-C., Blank, E. S., & Casadevall, A. (1996). Extracellular proteinase activity of *Cryptococcus neoformans*. *Clinical and Diagnostic Laboratory Immunology*, 3(5), 570-574.
- Chen, S., Zhao, S., McDermott, P. F., Schroeder, C. M., White, D. G., & Meng, J. (2005). A DNA microarray for identification of virulence and antimicrobial resistance genes in *Salmonella* serovars and *Escherichia coli*. *Molecular and Cellular Probes*, 19(3), 195-201.

- Chen, S. C.-A., Meyer, W., & Sorrell, T. C. (2014). *Cryptococcus gattii* infections. *Clinical Microbiology Reviews*, 27(4), 980-1024.
- Chen, S. C., Muller, M., Zhou, J. Z., Wright, L. C., & Sorrell, T. C. (1997). Phospholipase activity in *Cryptococcus neoformans*: a new virulence factor? *Journal of Infectious Diseases*, 175(2), 414-420.
- Chen, Y., Toffaletti, D. L., Tenor, J. L., Litvintseva, A. P., Fang, C., Mitchell, T. G., McDonald, T. R., Nielsen, K., Boulware, D. R., & Bicanic, T. (2014). The *Cryptococcus neoformans* transcriptome at the site of human meningitis. *MBio*, 5(1), e01087-01013.
- Cherednichenko, G., Zhang, R., Bannister, R. A., Timofeyev, V., Li, N., Fritsch, E. B., Feng, W., Barrientos, G. C., Schebb, N. H., & Hammock, B. D. (2012). Triclosan impairs excitation–contraction coupling and Ca²⁺ dynamics in striated muscle. *Proceedings of the National Academy of Sciences*, 109(35), 14158-14163.
- Choi, K.-M., Kwon, Y.-Y., & Lee, C.-K. (2015). Disruption of *Snf3/Rgt2* glucose sensors decreases lifespan and caloric restriction effectiveness through *Mth1/Std1* by adjusting mitochondrial efficiency in yeast. *FEBS Letters*, 589(3), 349-357.
- Chuanchuen, R., Beinlich, K., Hoang, T. T., Becher, A., Karkhoff-Schweizer, R. R., & Schweizer, H. P. (2001). Cross-Resistance between Triclosan and Antibiotics in *Pseudomonas aeruginosa* Is Mediated by Multidrug Efflux Pumps: Exposure of a Susceptible Mutant Strain to Triclosan Selects *nfxB* Mutants Overexpressing *MexCD-OprJ*. *Antimicrobial Agents and Chemotherapy*, 45(2), 428-432.
- Chuaqui, R. F., Bonner, R. F., Best, C. J., Gillespie, J. W., Flaig, M. J., Hewitt, S. M., Phillips, J. L., Krizman, D. B., Tangrea, M. A., & Ahram, M. (2002). Post-analysis follow-up and validation of microarray experiments. *Nature Genetics*, 32, 509-514.
- Chun, C. D., Liu, O. W., & Madhani, H. D. (2007). A link between virulence and homeostatic responses to hypoxia during infection by the human fungal pathogen *Cryptococcus neoformans*. *PLoS Pathogen*, 3(2), e22.
- Chung, S., Mondon, P., Chang, Y. C., & Kwon-Chung, K. J. (2003). *Cryptococcus neoformans* with a mutation in the tetratricopeptide repeat-containing gene, *CCN1*, causes subcutaneous lesions but fails to cause systemic infection. *Infection and Immunity*, 71(4), 1988-1994.
- Clancy, C. J., Nguyen, M. H., Alandoerffer, R., Cheng, S., Iczkowski, K., Richardson, M., & Graybill, J. R. (2006). *Cryptococcus neoformans* var. *grubii* isolates recovered from persons with AIDS demonstrate a wide range of virulence during murine meningoencephalitis that correlates with the expression of certain virulence factors. *Microbiology*, 152(8), 2247-2255.
- CLSI. (2008). M27-A3 Reference method for broth dilution antifungal susceptibility testing of yeast; approved standard- third edition. *Clinical and Laboratory Standards Institute*, 28(14).

- Clumeck, N., Sonnet, J., Taelman, H., Mascart-Lemone, F., De Bruyere, M., Vandepierre, P., Dasnoy, J., Marcelis, L., Lamy, M., & Jonas, C. (1984). Acquired immunodeficiency syndrome in African patients. *New England Journal of Medicine*, 310(8), 492-497.
- Coelho, C., Souza, A. C. O., da Silveira Derengowski, L., de Leon-Rodriguez, C., Wang, B., Leon-Rivera, R., Bocca, A. L., Gonçalves, T., & Casadevall, A. (2015). Macrophage mitochondrial and stress response to ingestion of *Cryptococcus neoformans*. *The Journal of Immunology*, 194(5), 2345-2357.
- Cogliati, M. (2013). Global molecular epidemiology of *Cryptococcus neoformans* and *Cryptococcus gattii*: an atlas of the molecular types. *Scientifica*, 2013.
- Cogliati, M., Zani, A., Rickerts, V., McCormick, I., Desnos-Ollivier, M., Velegraki, A., Escandon, P., Ichikawa, T., Ikeda, R., & Bienvenu, A.-L. (2016). Multilocus sequence typing analysis reveals that *Cryptococcus neoformans* var. *neoformans* is a recombinant population. *Fungal Genetics and Biology*, 87, 22-29.
- Coleman, M. L., Sahai, E. A., Yeo, M., Bosch, M., Dewar, A., & Olson, M. F. (2001). Membrane blebbing during apoptosis results from caspase-mediated activation of *ROCK I*. *Nature Cell Biology*, 3(4), 339-345.
- Corbel, M., & Eades, S. M. (1976). The relative susceptibility of New Zealand black and CBA mice to infection with opportunistic fungal pathogens. *Sabouraudia: Journal of Medical and Veterinary Mycology*, 14(1), 17-32.
- Cox, G. M., Harrison, T. S., McDade, H. C., Taborda, C. P., Heinrich, G., Casadevall, A., & Perfect, J. R. (2003). Superoxide dismutase influences the virulence of *Cryptococcus neoformans* by affecting growth within macrophages. *Infection and Immunity*, 71(1), 173-180.
- Cox, G. M., McDade, H. C., Chen, S. C., Tucker, S. C., Gottfredsson, M., Wright, L. C., Sorrell, T. C., Leidich, S. D., Casadevall, A., & Ghannoum, M. A. (2001). Extracellular phospholipase activity is a virulence factor for *Cryptococcus neoformans*. *Molecular Microbiology*, 39(1), 166-175.
- Cox, G. M., Mukherjee, J., Cole, G. T., Casadevall, A., & Perfect, J. R. (2000). Urease as a virulence factor in experimental cryptococcosis. *Infection and Immunity*, 68(2), 443-448.
- Crowley, M., Inaba, K., & Steinman, R. M. (1990). Dendritic cells are the principal cells in mouse spleen bearing immunogenic fragments of foreign proteins. *The Journal of Experimental Medicine*, 172(1), 383-386.
- Cuenca-Estrella, M. (2010). Antifungicos en el tratamiento de las infecciones sistémicas: importancia del mecanismo de acción, espectro de actividad y resistencias. *Revista Española de Quimioterapia*, 23(4), 169-176.
- Currie, B. P., Freundlich, L. F., & Casadevall, A. (1994). Restriction fragment length polymorphism analysis of *Cryptococcus neoformans* isolates from environmental (pigeon excreta) and clinical sources in New York City. *Journal of Clinical Microbiology*, 32(5), 1188-1192.

- D'Souza, C. A., Alspaugh, J. A., Yue, C., Harashima, T., Cox, G. M., Perfect, J. R., & Heitman, J. (2001). Cyclic AMP-dependent protein kinase controls virulence of the fungal pathogen *Cryptococcus neoformans*. *Molecular and Cellular Biology*, *21*(9), 3179-3191.
- D'Souza, C., Kronstad, J., Taylor, G., Warren, R., Yuen, M., Hu, G., Jung, W., Sham, A., Kidd, S., & Tangen, K. (2011). Genome variation in *Cryptococcus gattii*, an emerging pathogen of immunocompetent hosts. *MBio*, *2*(1), e00342-00310.
- da Silva, E. G., de Assis Baroni, F., Viani, F. C., da Silva Ruiz, L., Gandra, R. F., Auler, M. E., Dias, A. L. T., Gambale, W., & Paula, C. R. (2006). Virulence profile of strains of *Cryptococcus neoformans* var. *grubii* evaluated by experimental infection in BALB/c mice and correlation with exoenzyme activity. *Journal of Medical Microbiology*, *55*(2), 139-142.
- Davey, K., Johnson, E., Holmes, A., Szekely, A., & Warnock, D. (1998). In-vitro susceptibility of *Cryptococcus neoformans* isolates to fluconazole and itraconazole. *Journal of Antimicrobial Chemotherapy*, *42*(2), 217-220.
- Davidson, R. C., Nichols, C. B., Cox, G. M., Perfect, J. R., & Heitman, J. (2003). A MAP kinase cascade composed of cell type specific and non-specific elements controls mating and differentiation of the fungal pathogen *Cryptococcus neoformans*. *Molecular Microbiology*, *49*(2), 469-485.
- Del Poeta, M. (2004). Role of phagocytosis in the virulence of *Cryptococcus neoformans*. *Eukaryotic Cell*, *3*(5), 1067-1075.
- Denton, J., & Di Salvo, A. (1968). The prevalence of *Cryptococcus neoformans* in various natural habitats. *Sabouraudia: Journal of Medical and Veterinary Mycology*, *6*(3), 213-217.
- DeSalva, S., Kong, B., & Lin, Y. (1989). Triclosan: a safety profile. *American Journal of Dentistry*, *2*, 185-196.
- Desmet, P., Kayembe, K. D., & De Vroey, C. (1989). The value of cryptococcal serum antigen screening among HIV-positive/AIDS patients in Kinshasa, Zaire. *AIDS (London, England)*, *3*(2), 77-78.
- Ding, C., Festa, R. A., Chen, Y.-L., Espart, A., Palacios, Ò., Espín, J., Capdevila, M., Atrian, S., Heitman, J., & Thiele, D. J. (2013). *Cryptococcus neoformans* copper detoxification machinery is critical for fungal virulence. *Cell Host & Microbe*, *13*(3), 265-276.
- Doering, T. (2009). How sweet it is! Capsule formation and cell wall biogenesis in *Cryptococcus neoformans*. *Annual of Review Microbiology*, *63*, 223-247.
- Doering, T. L. (1999). A unique α -1, 3 mannosyltransferase of the pathogenic fungus *Cryptococcus neoformans*. *Journal of Bacteriology*, *181*(17), 5482-5488.
- Dong, Z. M., & Murphy, J. W. (1995). Effects of the two varieties of *Cryptococcus neoformans* cells and culture filtrate antigens on neutrophil locomotion. *Infection and Immunity*, *63*(7), 2632-2644.

- Dong, Z. M., & Murphy, J. W. (1997). Cryptococcal polysaccharides bind to CD18 on human neutrophils. *Infection and Immunity*, 65(2), 557-563.
- Dunham, M. J., Badrane, H., Ferea, T., Adams, J., Brown, P. O., Rosenzweig, F., & Botstein, D. (2002). Characteristic genome rearrangements in experimental evolution of *Saccharomyces cerevisiae*. *Proceedings of the National Academy of Sciences*, 99(25), 16144-16149.
- Dyatkina, N. B., Roberts, C. D., Keicher, J. D., Dai, Y., Nadherny, J. P., Zhang, W., Schmitz, U., Kongpachith, A., Fung, K., & Novikov, A. A. (2002). Minor groove DNA binders as antimicrobial agents. 1. Pyrrole tetraamides are potent antibacterials against vancomycin resistant Enterococci and methicillin resistant *Staphylococcus aureus*. *Journal of Medicinal Chemistry*, 45(4), 805-817.
- Eisenhauer, P. B., & Lehrer, R. I. (1992). Mouse neutrophils lack defensins. *Infection and Immunity*, 60(8), 3446-3447.
- Ekström, S., Önnarfjord, P., Nilsson, J., Bengtsson, M., Laurell, T., & Marko-Varga, G. (2000). Integrated microanalytical technology enabling rapid and automated protein identification. *Analytical Chemistry*, 72(2), 286-293.
- Elkind, N. B., Walch-Solimena, C., & Novick, P. J. (2000). The role of the COOH terminus of Sec2p in the transport of post-Golgi vesicles. *The Journal of Cell Biology*, 149(1), 95-110.
- Ellerbroek, P. M., Lefeber, D. J., van Veghel, R., Scharringa, J., Brouwer, E., Gerwig, G. J., Janbon, G., Hoepelman, A. I., & Coenjaerts, F. E. (2004). O-acetylation of cryptococcal capsular glucuronoxylomannan is essential for interference with neutrophil migration. *The Journal of Immunology*, 173(12), 7513-7520.
- Emery, H. S., Shelburne, C. P., Bowman, J. P., Fallon, P. G., Schulz, C. A., & Jacobson, E. S. (1994). Genetic study of oxygen resistance and melanization in *Cryptococcus neoformans*. *Infection and Immunity*, 62(12), 5694-5697.
- Emmons, C. W. (1951). Isolation of *Cryptococcus neoformans* from soil. *Journal of Bacteriology*, 62(6), 685.
- Erickson, T., Liu, L., Gueyikian, A., Zhu, X., Gibbons, J., & Williamson, P. R. (2001). Multiple virulence factors of *Cryptococcus neoformans* are dependent on *VPH1*. *Molecular Microbiology*, 42(4), 1121-1131.
- Espinel-Ingroff, A., Aller, A., Canton, E., Castanon-Olivares, L., Chowdhary, A., Cordoba, S., Cuenca-Estrella, M., Fothergill, A., Fuller, J., & Govender, N. (2012). *Cryptococcus neoformans-Cryptococcus gattii* species complex: an international study of wild-type susceptibility endpoint distributions and epidemiological cutoff values for fluconazole, itraconazole, posaconazole and voriconazole. *Antimicrobial Agents and Chemotherapy*, AAC. 01115-01112.
- Fan, F., Yan, K., Wallis, N. G., Reed, S., Moore, T. D., Rittenhouse, S. F., DeWolf, W. E., Huang, J., McDevitt, D., & Miller, W. H. (2002). Defining and combating the mechanisms of triclosan resistance in clinical isolates of *Staphylococcus aureus*. *Antimicrobial Agents and Chemotherapy*, 46(11), 3343-3347.

- Feldmesser, M., Kress, Y., & Casadevall, A. (1998). Effect of antibody to capsular polysaccharide on eosinophilic pneumonia in murine infection with *Cryptococcus neoformans*. *Journal of Infectious Diseases*, 177(6), 1639-1646.
- Feldmesser, M., Kress, Y., Novikoff, P., & Casadevall, A. (2000). *Cryptococcus neoformans* is a facultative intracellular pathogen in murine pulmonary infection. *Infection and Immunity*, 68(7), 4225-4237.
- Feldmesser, M., Tucker, S., & Casadevall, A. (2001). Intracellular parasitism of macrophages by *Cryptococcus neoformans*. *Trends in Microbiology*, 9(6), 273-278.
- Florio, A. R., Ferrari, S., De Carolis, E., Torelli, R., Fadda, G., Sanguinetti, M., Sanglard, D., & Posteraro, B. (2011). Genome-wide expression profiling of the response to short-term exposure to fluconazole in *Cryptococcus neoformans* serotype A. *BMC Microbiology*, 11(1), 1.
- Franzot, S. P., Hamdan, J. S., Currie, B. P., & Casadevall, A. (1997). Molecular epidemiology of *Cryptococcus neoformans* in Brazil and the United States: evidence for both local genetic differences and a global clonal population structure. *Journal of Clinical Microbiology*, 35(9), 2243-2251.
- Freeman, W. M., Walker, S. J., & Vrana, K. E. (1999). Quantitative RT-PCR: pitfalls and potential. *Biotechniques*, 26, 112-125.
- Freire, A. K. L., dos Santos Bentes, A., de Lima Sampaio, I., Matsuura, A. B. J., Ogusku, M. M., Salem, J. I., Wanke, B., & de Souza, J. V. B. (2012). Molecular characterisation of the causative agents of Cryptococcosis in patients of a tertiary healthcare facility in the state of Amazonas- Brazil. *Mycoses*, 55(3), e145-e150.
- Fries, B. C., Chen, F., Currie, B. P., & Casadevall, A. (1996). Karyotype instability in *Cryptococcus neoformans* infection. *Journal of Clinical Microbiology*, 34(6), 1531-1534.
- Fromtling, R., Shadomy, H., & Jacobson, E. (1982). Decreased virulence in stable, acapsular mutants of *Cryptococcus neoformans*. *Mycopathologia*, 79(1), 23-29.
- Fromtling, R. A., Abruzzo, G. K., & Ruiz, A. (1988). *Cryptococcus neoformans*: A central nervous system isolate from an AIDS patient that is rhinotropic in a normal mouse model. *Mycopathologia*, 102(2), 79-86.
- Galanis, E., MacDougall, L., Kidd, S., & Morshed, M. (2010). Epidemiology of *Cryptococcus gattii*, British Columbia, Canada, 1999–2007. *Emerging Infectious Disease*, 16(2), 251-257.
- Galgiani, J. N. (1990). Fluconazole, a new antifungal agent. *Annals of Internal Medicine*, 113(3), 177-179.
- Ganendren, R., Carter, E., Sorrell, T., Widmer, F., & Wright, L. (2006). Phospholipase B activity enhances adhesion of *Cryptococcus neoformans* to a human lung epithelial cell line. *Microbes and Infection*, 8(4), 1006-1015.

- Garcia-Hermoso, D., Janbon, G., & Dromer, F. (1999). Epidemiological evidence for dormant *Cryptococcus neoformans* infection. *Journal of Clinical Microbiology*, 37(10), 3204-3209.
- Garcia-Rivera, J., & Casadevall, A. (2001). Melanization of *Cryptococcus neoformans* reduces its susceptibility to the antimicrobial effects of silver nitrate. *Medical Mycology*, 39(4), 353-357.
- Ghannoum, M. A. (2000). Potential role of phospholipases in virulence and fungal pathogenesis. *Clinical Microbiology Reviews*, 13(1), 122-143.
- Ghannoum, M. A., & Rice, L. B. (1999). Antifungal agents: mode of action, mechanisms of resistance, and correlation of these mechanisms with bacterial resistance. *Clinical Microbiology Reviews*, 12(4), 501-517.
- Goldman, D. L., Khine, H., Abadi, J., Lindenberg, D. J., Pirofski, L.-a., Niang, R., & Casadevall, A. (2001). Serologic evidence for *Cryptococcus neoformans* infection in early childhood. *Pediatrics*, 107(5), e66-e66.
- Goldman, D. L., Lee, S. C., Mednick, A. J., Montella, L., & Casadevall, A. (2000). Persistent *Cryptococcus neoformans* Pulmonary Infection in the Rat Is Associated with Intracellular Parasitism, Decreased Inducible Nitric Oxide Synthase Expression, and Altered Antibody Responsiveness to Cryptococcal Polysaccharide. *Infection and Immunity*, 68(2), 832-838.
- Gomez Escalada, M., Russell, A., Maillard, J. Y., & Ochs, D. (2005). Triclosan–bacteria interactions: single or multiple target sites? *Letters in applied microbiology*, 41(6), 476-481.
- Granger, D. L., Perfect, J. R., & Durack, D. (1985). Virulence of *Cryptococcus neoformans*. Regulation of capsule synthesis by carbon dioxide. *Journal of Clinical Investigation*, 76(2), 508.
- Gray, J. V., Ogas, J. P., Kamada, Y., Stone, M., Levin, D. E., & Herskowitz, I. (1997). A role for the Pkc1 MAP kinase pathway of *Saccharomyces cerevisiae* in bud emergence and identification of a putative upstream regulator. *The EMBO Journal*, 16(16), 4924-4937.
- Griffin, F. M. (1981). Roles of macrophage Fc and C3b receptors in phagocytosis of immunologically coated *Cryptococcus neoformans*. *Proceedings of the National Academy of Sciences*, 78(6), 3853-3857.
- Gruda, I., & Dussault, N. (1988). Effect of the aggregation state of amphotericin B on its interaction with ergosterol. *Biochemistry and Cell Biology*, 66(3), 177-183.
- Guerrero, A., Jain, N., Goldman, D., & Fries, B. (2006). Phenotypic switching in *Cryptococcus neoformans*. *Microbiology*, 152(1), 3-9.
- Guillén, J., Bernabeu, A., Shapiro, S., & Villalain, J. (2004). Location and orientation of triclosan in phospholipid model membranes. *European Biophysics Journal*, 33(5), 448-453.
- Guinea, J., Hagen, F., Peláez, T., Boekhout, T., Tahoune, H., Torres-Narbona, M., & Bouza, E. (2010). Antifungal susceptibility, serotyping, and genotyping of

clinical *Cryptococcus neoformans* isolates collected during 18 years in a single institution in Madrid, Spain. *Medical Mycology*, 48(7), 942-948.

- Haas, H. (2003). Molecular genetics of fungal siderophore biosynthesis and uptake: the role of siderophores in iron uptake and storage. *Applied Microbiology and Biotechnology*, 62(4), 316-330.
- Häcker, G. (2000). The morphology of apoptosis. *Cell and tissue research*, 301(1), 5-17.
- Hajjeh, R. A., Conn, L. A., Stephens, D. S., Baughman, W., Hamill, R., Graviss, E., Pappas, P. G., Thomas, C., Reingold, A., & Rothrock, G. (1999). Cryptococcosis: population-based multistate active surveillance and risk factors in human immunodeficiency virus—infected persons. *Journal of Infectious Diseases*, 179(2), 449-454.
- Hakim, J. G., Gangaidzo, I. T., Heyderman, R. S., Mielke, J., Mushangi, E., Taziwa, A., Robertson, V. J., Musvaire, P., & Mason, P. R. (2000). Impact of HIV infection on meningitis in Harare, Zimbabwe: a prospective study of 406 predominantly adult patients. *AIDS*, 14(10), 1401-1407.
- Harkins, H. A., Pagé, N., Schenkman, L. R., De Virgilio, C., Shaw, S., Bussey, H., & Pringle, J. R. (2001). *Bud8p* and *Bud9p*, proteins that may mark the sites for bipolar budding in yeast. *Molecular Biology of the Cell*, 12(8), 2497-2518.
- Hasenclever, H. F., & Emmons, C. W. (1963). The prevalence and mouse virulence of *Cryptococcus neoformans* strains isolated from urban areas. *American Journal of Hygiene*, 78(2), 227-231.
- Hay, A. G., Dees, P. M., & Saylor, G. S. (2001). Growth of a bacterial consortium on triclosan. *FEMS Microbiology Ecology*, 36(2-3), 105-112.
- Haynes, B. C., Skowrya, M. L., Spencer, S. J., Gish, S. R., Williams, M., Held, E. P., Brent, M. R., & Doering, T. L. (2011). Toward an integrated model of capsule regulation in *Cryptococcus neoformans*. *PLoS Pathogen*, 7(12), e1002411.
- Heath, R. J., Li, J., Roland, G. E., & Rock, C. O. (2000). Inhibition of the staphylococcus aureus NADPH-dependent enoyl-acyl carrier protein reductase by triclosan and hexachlorophene. *Journal of Biological Chemistry*, 275(7), 4654-4659.
- Heilmann, C. J., Schneider, S., Barker, K. S., Rogers, P. D., & Morschhäuser, J. (2010). An A643T mutation in the transcription factor Upc2p causes constitutive *ERG11* upregulation and increased fluconazole resistance in *Candida albicans*. *Antimicrobial agents and chemotherapy*, 54(1), 353-359.
- Hendry, A. T., & Bakerspiegel, A. (1969). Factors affecting serum inhibited growth of *Candida albicans* and *Cryptococcus neoformans*. *Sabouraudia: Journal of Medical and Veterinary Mycology*, 7(3), 219-229.
- Heymann, P., Gerads, M., Schaller, M., Dromer, F., Winkelmann, G., & Ernst, J. F. (2002). The siderophore iron transporter of *Candida albicans* (*Sit1p/Arn1p*) mediates uptake of ferrichrome-type siderophores and is required for epithelial invasion. *Infection and Immunity*, 70(9), 5246-5255.

- Higgins, J., Pinjon, E., Oltean, H. N., White, T. C., Kelly, S. L., Martel, C. M., Sullivan, D. J., Coleman, D. C., & Moran, G. P. (2012). Triclosan antagonizes fluconazole activity against *Candida albicans*. *Journal of Dental Research*, 91(1), 65-70. doi:10.1177/0022034511425046
- Hirschberg, C. B., Robbins, P. W., & Abeijon, C. (1998). Transporters of nucleotide sugars, ATP, and nucleotide sulfate in the endoplasmic reticulum and Golgi apparatus. *Annual Review of Biochemistry*, 67(1), 49-69.
- Hissen, A., Chow, J., Pinto, L., & Moore, M. (2004). Survival of *Aspergillus fumigatus* in serum involves removal of iron from transferrin: the role of siderophores. *Infection and Immunity*, 72(3), 1402-1408.
- Hitchcock, C. A., Barrett-Bee, K. J., & Russell, N. J. (1986). The lipid composition of azole-sensitive and azole-resistant strains of *Candida albicans*. *Microbiology*, 132(9), 2421-2431.
- Howell, S., Mallet, A., & Noble, W. (1990). A comparison of the sterol content of multiple isolates of the *Candida albicans* Darlington strain with other clinically azole-sensitive and-resistant strains. *Journal of Applied Bacteriology*, 69(5), 692-696.
- Hu, G., Cheng, P. Y., Sham, A., Perfect, J. R., & Kronstad, J. W. (2008a). Metabolic adaptation in *Cryptococcus neoformans* during early murine pulmonary infection. *Molecular Microbiology*, 69(6), 1456-1475.
- Hu, G., Liu, I., Sham, A., Stajich, J. E., Dietrich, F. S., & Kronstad, J. W. (2008b). Comparative hybridization reveals extensive genome variation in the AIDS-associated pathogen *Cryptococcus neoformans*. *Genome Biology*, 9(2), R41.
- Huang, C., Nong, S.-h., Mansour, M. K., Specht, C. A., & Levitz, S. M. (2002). Purification and characterization of a second immunoreactive mannoprotein from *Cryptococcus neoformans* that stimulates T-cell responses. *Infection and Immunity*, 70(10), 5485-5493.
- Huang, D. W., Sherman, B. T., & Lempicki, R. A. (2009). Systematic and integrative analysis of large gene lists using DAVID bioinformatics resources. *Nature Protocols*, 4(1), 44-57.
- Huffnagle, G. B., Boyd, M. B., Street, N. E., & Lipscomb, M. F. (1998). IL-5 is required for eosinophil recruitment, crystal deposition, and mononuclear cell recruitment during a pulmonary *Cryptococcus neoformans* infection in genetically susceptible mice (C57BL/6). *The Journal of Immunology*, 160(5), 2393-2400.
- Huffnagle, G. B., Chen, G.-H., Curtis, J. L., McDonald, R. A., Strieter, R. M., & Toews, G. B. (1995). Down-regulation of the afferent phase of T cell-mediated pulmonary inflammation and immunity by a high melanin-producing strain of *Cryptococcus neoformans*. *The Journal of Immunology*, 155(7), 3507-3516.
- Huffnagle, G. B., Yates, J., & Lipscomb, M. F. (1991a). Immunity to a pulmonary *Cryptococcus neoformans* infection requires both CD4+ and CD8+ T cells. *The Journal of Experimental Medicine*, 173(4), 793-800.

- Huffnagle, G. B., Yates, J. L., & Lipscomb, M. (1991b). T cell-mediated immunity in the lung: a *Cryptococcus neoformans* pulmonary infection model using SCID and athymic nude mice. *Infection and Immunity*, 59(4), 1423-1433.
- Hull, C. M., & Heitman, J. (2002). Genetics of *Cryptococcus neoformans*. *Annual Review of Genetics*, 36(1), 557-615.
- Idnurm, A., Bahn, Y.-S., Nielsen, K., Lin, X., Fraser, J. A., & Heitman, J. (2005). Deciphering the model pathogenic fungus *Cryptococcus neoformans*. *Nature Reviews Microbiology*, 3(10), 753-764.
- Igel, H. J., & Bolande, R. P. (1966). Humoral defense mechanisms in cryptococcosis: substances in normal human serum, saliva, and cerebrospinal fluid affecting the growth of *Cryptococcus neoformans*. *The Journal of Infectious Diseases*, 75-83.
- Ikeda, R., & Sawamura, K. (2008). Bacterial and H₂O₂ stress-induced apoptosis-like events in *Cryptococcus neoformans*. *Research in Microbiology*, 159(9), 628-634.
- Ikeda, R., Sugita, T., Jacobson, E. S., & Shinoda, T. (2002). Laccase and melanization in clinically important *Cryptococcus* species other than *Cryptococcus neoformans*. *Journal of Clinical Microbiology*, 40(4), 1214-1218.
- Ikeda, R., Sugita, T., & Shinoda, T. (2000). Serological Relationships of *Cryptococcus* spp.: Distribution of Antigenic Factors in *Cryptococcus* and Intraspecies Diversity. *Journal of Clinical Microbiology*, 38(11), 4021-4025.
- Ingavale, S. S., Chang, Y. C., Lee, H., McClelland, C. M., Leong, M. L., & Kwon-Chung, K. J. (2008). Importance of mitochondria in survival of *Cryptococcus neoformans* under low oxygen conditions and tolerance to cobalt chloride. *PLoS Pathogen*, 4(9), e1000155.
- Jacobson, E. S., & Emery, H. S. (1991). Catecholamine uptake, melanization, and oxygen toxicity in *Cryptococcus neoformans*. *Journal of Bacteriology*, 173(1), 401-403.
- Jain, N., Cordero, R. J., Casadevall, A., & Fries, B. C. (2013). Allergen1 regulates polysaccharide structure in *Cryptococcus neoformans*. *Molecular Microbiology*, 88(4), 713-727.
- Janbon, G., Himmelreich, U., Moyrand, F., Improvisi, L., & Dromer, F. (2001). Cas1p is a membrane protein necessary for the O- acetylation of the *Cryptococcus neoformans* capsular polysaccharide. *Molecular Microbiology*, 42(2), 453-467.
- Janbon, G., Ormerod, K. L., Paulet, D., Byrnes III, E. J., Yadav, V., Chatterjee, G., Mullapudi, N., Hon, C.-C., Billmyre, R. B., & Brunel, F. (2014). Analysis of the genome and transcriptome of *Cryptococcus neoformans* var. *grubii* reveals complex RNA expression and microevolution leading to virulence attenuation. *PLoS Genetic*, 10(4), e1004261.
- Jones, Jampani, H. B., Newman, J. L., & Lee, A. S. (2000). Triclosan: a review of effectiveness and safety in health care settings. *American Journal of Infection Control*, 28(2), 184-196.

- Jong, A., Wu, C.-H., Chen, H.-M., Luo, F., Kwon-Chung, K. J., Chang, Y. C., LaMunyon, C. W., Plaas, A., & Huang, S.-H. (2007). Identification and characterization of *CPSI* as a hyaluronic acid synthase contributing to the pathogenesis of *Cryptococcus neoformans* infection. *Eukaryotic Cell*, 6(8), 1486-1496.
- Kamada, Y., Qadota, H., Python, C. P., Anraku, Y., Ohya, Y., & Levin, D. E. (1996). Activation of yeast protein kinase C by *Rho1* GTPase. *Journal of Biological Chemistry*, 271(16), 9193-9196.
- Kampf, G., & Kramer, A. (2004). Epidemiologic background of hand hygiene and evaluation of the most important agents for scrubs and rubs. *Clinical Microbiology Reviews*, 17(4), 863-893.
- Kao, C., & Schwahz, J. (1957). The Isolation of *Cryptococcus neoformans* from Pigeon Nests. With Remarks on the Identification of Virulent Cryptococci. *American Journal of Clinical Pathology*, 27(6), 652-663.
- Kaocharoen, S., Ngamskulrungraj, P., Firacative, C., Trilles, L., Piyabongkarn, D., Banlunara, W., Poonwan, N., Chaiprasert, A., Meyer, W., & Chindamporn, A. (2013). Molecular epidemiology reveals genetic diversity amongst isolates of the *Cryptococcus neoformans/C. gattii* species complex in Thailand. *PLoS Neglected Tropical Disease*, 7(7), e2297.
- Kehl-Fie, T. E., & Skaar, E. P. (2010). Nutritional immunity beyond iron: a role for manganese and zinc. *Current Opinion in Chemical Biology*, 14(2), 218-224.
- Kim, J. M., Yoshikawa, H., & Shirahige, K. (2001). A member of the YER057c/yjgf/Uk114 family links isoleucine biosynthesis and intact mitochondria maintenance in *Saccharomyces cerevisiae*. *Genes to Cells*, 6(6), 507-517.
- Kim, S.-Y., & Kim, J. (2010). Roles of dihydrolipoamide dehydrogenase *Lpd1* in *Candida albicans* filamentation. *Fungal Genetics and Biology*, 47(9), 782-788.
- Kordossis, T., Avlami, A., Velegraki, A., Stefanou, I., Georgakopoulos, G., Papalambrou, C., & Legakis, N. (1998). First report of *Cryptococcus laurentii* meningitis and a fatal case of *Cryptococcus albidus* cryptococcaemia in AIDS patients. *Medical Mycology*, 36(5), 335-339.
- Kosman, D. J. (2003). Molecular mechanisms of iron uptake in fungi. *Molecular Microbiology*, 47(5), 1185-1197.
- Kozel, T., & Gotschlich, E. (1982). The capsule of *Cryptococcus neoformans* passively inhibits phagocytosis of the yeast by macrophages. *The Journal of Immunology*, 129(4), 1675-1680.
- Kozel, T. R., & Follette, J. L. (1981). Opsonization of encapsulated *Cryptococcus neoformans* by specific anticapsular antibody. *Infection and Immunity*, 31(3), 978-984.
- Kozel, T. R., & Mastroianni, R. P. (1976). Inhibition of phagocytosis by cryptococcal polysaccharide: dissociation of the attachment and ingestion phases of phagocytosis. *Infection and Immunity*, 14(1), 62-67.

- Kraus, P. R., Boily, M.-J., Giles, S. S., Stajich, J. E., Allen, A., Cox, G. M., Dietrich, F. S., Perfect, J. R., & Heitman, J. (2004). Identification of *Cryptococcus neoformans* temperature-regulated genes with a genomic-DNA microarray. *Eukaryotic Cell*, 3(5), 1249-1260.
- Kraus, P. R., Fox, D. S., Cox, G. M., & Heitman, J. (2003). The *Cryptococcus neoformans* MAP kinase *Mpk1* regulates cell integrity in response to antifungal drugs and loss of calcineurin function. *Molecular Microbiology*, 48(5), 1377-1387.
- Kwon-Chung, K. (1975). A new genus, *Filobasidiella*, the perfect state of *Cryptococcus neoformans*. *Mycologia*, 1197-1200.
- Kwon-Chung, K. (1976). Morphogenesis of *Filobasidiella neoformans*, the sexual state of *Cryptococcus neoformans*. *Mycologia*, 821-833.
- Kwon-Chung, K., Bennett, J., & Rhodes, J. (1982a). Taxonomic studies on *Filobasidiella* species and their anamorphs. *Antonie Van Leeuwenhoek*, 48(1), 25-38.
- Kwon-Chung, K., Polacheck, I., & Popkin, T. (1982b). Melanin-lacking mutants of *Cryptococcus neoformans* and their virulence for mice. *Journal of Bacteriology*, 150(3), 1414-1421.
- Kwon-Chung, K., & Rhodes, J. (1986). Encapsulation and melanin formation as indicators of virulence in *Cryptococcus neoformans*. *Infection and Immunity*, 51(1), 218-223.
- Kwon-Chung, K. J., Edman, J. C., & Wickes, B. L. (1992). Genetic association of mating types and virulence in *Cryptococcus neoformans*. *Infection and Immunity*, 60(2), 602-605.
- Kwon-Chung, K. J., & Varma, A. (2006). Do major species concepts support one, two or more species within *Cryptococcus neoformans*? *FEMS Yeast Research*, 6(4), 574-587.
- La Hoz, R. M., & Pappas, P. G. (2013). Cryptococcal infections: changing epidemiology and implications for therapy. *Drugs*, 73(6), 495-504.
- Lacy, M. K., Nicolau, D. P., Banevicius, M. A., Nightingale, C. H., & Quintiliani, R. (1999). Protective effect of trovafloxacin, ciprofloxacin and ampicillin against *Streptococcus pneumoniae* in a murine sepsis model. *Journal of Antimicrobial Chemotherapy*, 44(4), 477-481.
- Lee, H., Bien, C. M., Hughes, A. L., Espenshade, P. J., Kwon-Chung, K. J., & Chang, Y. C. (2007). Cobalt chloride, a hypoxia-mimicking agent, targets sterol synthesis in the pathogenic fungus *Cryptococcus neoformans*. *Molecular Microbiology*, 65(4), 1018-1033.
- Lengeler, K. B., Cox, G. M., & Heitman, J. (2001). Serotype AD strains of *Cryptococcus neoformans* are diploid or aneuploid and are heterozygous at the mating-type locus. *Infection and Immunity*, 69(1), 115-122.

- Lengeler, K. B., Wang, P., Cox, G. M., Perfect, J. R., & Heitman, J. (2000). Identification of the MATa mating-type locus of *Cryptococcus neoformans* reveals a serotype A MATa strain thought to have been extinct. *Proceedings of the National Academy of Sciences*, 97(26), 14455-14460.
- Lesuisse, E., Blaiseau, P.-L., Dancis, A., & Camadro, J.-M. (2001). Siderophore uptake and use by the yeast *Saccharomyces cerevisiae*. *Microbiology*, 147(2), 289-298.
- Levitz, S. (1993). Macrophage-*Cryptococcus* interactions. *Immunology Series*, 60, 533-543.
- Levitz, S. M. (1992). Overview of host defenses in fungal infections. *Clinical Infectious Diseases*, 14(Supplement 1), S37-S42.
- Levitz, S. M., Nong, S.-h., Mansour, M. K., Huang, C., & Specht, C. A. (2001). Molecular characterization of a mannoprotein with homology to chitin deacetylases that stimulates T cell responses to *Cryptococcus neoformans*. *Proceedings of the National Academy of Sciences*, 98(18), 10422-10427.
- Levitz, S. M., & Specht, C. A. (2006). The molecular basis for the immunogenicity of *Cryptococcus neoformans* mannoproteins. *FEMS Yeast Research*, 6(4), 513-524.
- Levy, C. W., Roujeinikova, A., Sedelnikova, S., Baker, P. J., Stuitje, A. R., Slabas, A. R., Rice, D. W., & Rafferty, J. B. (1999). Molecular basis of triclosan activity. *Nature*, 398(6726), 383-384.
- Lian, T., Simmer, M. I., D'Souza, C. A., Steen, B. R., Zuyderduyn, S. D., Jones, S. J., Marra, M. A., & Kronstad, J. W. (2005). Iron-regulated transcription and capsule formation in the fungal pathogen *Cryptococcus neoformans*. *Molecular Microbiology*, 55(5), 1452-1472.
- Liechty, C. A., Solberg, P., Were, W., Ekwaru, J. P., Ransom, R. L., Weidle, P. J., Downing, R., Coutinho, A., & Mermin, J. (2007). Asymptomatic serum cryptococcal antigenemia and early mortality during antiretroviral therapy in rural Uganda. *Tropical Medicine & International Health*, 12(8), 929-935.
- Ligr, M., Madeo, F., Fröhlich, E., Hilt, W., Fröhlich, K.-U., & Wolf, D. H. (1998). Mammalian Bax triggers apoptotic changes in yeast. *FEBS Letters*, 438(1-2), 61-65.
- Lin, X., & Heitman, J. (2006). The biology of the *Cryptococcus neoformans* species complex. *Annual Review of Microbiology*, 60, 69-105.
- Lin, X., Hull, C. M., & Heitman, J. (2005). Sexual reproduction between partners of the same mating type in *Cryptococcus neoformans*. *Nature*, 434(7036), 1017-1021.
- Lin, X., Litvintseva, A. P., Nielsen, K., Patel, S., Floyd, A., Mitchell, T. G., & Heitman, J. (2007). alpha AD alpha hybrids of *Cryptococcus neoformans*: evidence of same-sex mating in nature and hybrid fitness. *PLoS Genetic*, 3(10), 1975-1990.
- Lipovsky, M. M., Gekker, G., Anderson, W. R., Molitor, T. W., Peterson, P. K., & Hoepelman, A. I. (1997). Phagocytosis of Nonopsonized *Cryptococcus neoformans* by Swine Microglia Involves CD14 Receptors. *Clinical Immunology and Immunopathology*, 84(2), 208-211.

- Litter, J., Keszthelyi, A., Hamari, Z., Pfeiffer, I., & Kucsera, J. (2005). Differences in mitochondrial genome organization of *Cryptococcus neoformans* strains. *Antonie Van Leeuwenhoek*, 88(3-4), 249-255.
- Littman, M. L., & Borok, R. (1968). Relation of the pigeon to cryptococcosis: natural carrier state, heat resistance and survival of *Cryptococcus neoformans*. *Mycopathologia*, 35(3), 329-345.
- Litvintseva, A. P., Kestenbaum, L., Vilgalys, R., & Mitchell, T. G. (2005). Comparative analysis of environmental and clinical populations of *Cryptococcus neoformans*. *Journal of Clinical Microbiology*, 43(2), 556-564.
- Litvintseva, A. P., & Mitchell, T. G. (2009). Most environmental isolates of *Cryptococcus neoformans* var. *grubii* (serotype A) are not lethal for mice. *Infection and Immunity*, 77(8), 3188-3195.
- Liu, L., Tewari, R. P., & Williamson, P. R. (1999a). Laccase protects *Cryptococcus neoformans* from antifungal activity of alveolar macrophages. *Infection and Immunity*, 67(11), 6034-6039.
- Liu, L., Wakamatsu, K., Ito, S., & Williamson, P. R. (1999b). Catecholamine oxidative products, but not melanin, are produced by *Cryptococcus neoformans* during neuropathogenesis in mice. *Infection and Immunity*, 67(1), 108-112.
- Liu, O. W., Chun, C. D., Chow, E. D., Chen, C., Madhani, H. D., & Noble, S. M. (2008). Systematic genetic analysis of virulence in the human fungal pathogen *Cryptococcus neoformans*. *Cell*, 135(1), 174-188.
- Liu, T.-B., Perlin, D. S., & Xue, C. (2012). Molecular mechanisms of cryptococcal meningitis. *Virulence*, 3(2), 173-181.
- Loftus, B. J., Fung, E., Roncaglia, P., Rowley, D., Amedeo, P., Bruno, D., Vamathevan, J., Miranda, M., Anderson, I. J., & Fraser, J. A. (2005). The genome of the basidiomycetous yeast and human pathogen *Cryptococcus neoformans*. *Science*, 307(5713), 1321-1324.
- Long, J. L. (1981). Introduced birds of the world: The worldwide history, distribution and influence of birds introduced to new environments.
- Longo, V. D., Ellerby, L. M., Bredesen, D. E., Valentine, J. S., & Gralla, E. B. (1997). Human *Bcl-2* reverses survival defects in yeast lacking superoxide dismutase and delays death of wild-type yeast. *The Journal of Cell Biology*, 137(7), 1581-1588.
- Looi, C. Y., D'Silva, E. C., Seow, H. F., Rosli, R., Ng, K. P., & Chong, P. P. (2005). Increased expression and hotspot mutations of the multidrug efflux transporter, *CDR1* in azole-resistant *Candida albicans* isolates from vaginitis patients. *FEMS Microbiology Letters*, 249(2), 283-289.
- Luberto, C., Martinez-Mariño, B., Taraskiewicz, D., Bolaños, B., Chitano, P., Toffaletti, D. L., Cox, G. M., Perfect, J. R., Hannun, Y. A., & Balish, E. (2003). Identification of *App1* as a regulator of phagocytosis and virulence of *Cryptococcus neoformans*. *Journal of Clinical Investigation*, 112(7), 1080.

- Luberto, C., Toffaletti, D. L., Wills, E. A., Tucker, S. C., Casadevall, A., Perfect, J. R., Hannun, Y. A., & Del Poeta, M. (2001). Roles for *inositol-phosphoryl ceramide synthase 1 (IPC1)* in pathogenesis of *C. neoformans*. *Genes & Development*, *15*(2), 201-212.
- Lyman, F., & Furia, T. (1969). Toxicology of 2, 4, 4'-trichloro-2'-hydroxy-diphenyl ether. *IMS, Industrial Medicine and Surgery*, *38*(2), 64.
- Ma, H. (2009). *Intracellular parasitism of macrophages by Cryptococcus*. University of Birmingham.
- Ma, H., & May, R. C. (2009). Virulence in *Cryptococcus* species. *Advances in Applied Microbiology*, *67*, 131-190.
- Macher, A. M., Bennett, J. E., Gadek, J. E., & Frank, M. M. (1978). Complement depletion in cryptococcal sepsis. *The Journal of Immunology*, *120*(5), 1686-1690.
- Madeo, F., Fröhlich, E., & Fröhlich, K.-U. (1997). A yeast mutant showing diagnostic markers of early and late apoptosis. *The Journal of Cell Biology*, *139*(3), 729-734.
- Madeo, F., Fröhlich, E., Ligr, M., Grey, M., Sigrist, S. J., Wolf, D. H., & Fröhlich, K.-U. (1999). Oxygen stress: a regulator of apoptosis in yeast. *The Journal of Cell Biology*, *145*(4), 757-767.
- Madeo, F., Herker, E., Maldener, C., Wissing, S., Lächelt, S., Herlan, M., Fehr, M., Lauber, K., Sigrist, S. J., & Wesselborg, S. (2002). A caspase-related protease regulates apoptosis in yeast. *Molecular Cell*, *9*(4), 911-917.
- Maeng, S., Ko, Y.-J., Kim, G.-B., Jung, K.-W., Floyd, A., Heitman, J., & Bahn, Y.-S. (2010). Comparative transcriptome analysis reveals novel roles of the *Ras* and cyclic AMP signaling pathways in environmental stress response and antifungal drug sensitivity in *Cryptococcus neoformans*. *Eukaryotic Cell*, *9*(3), 360-378.
- Mancini, N., De Carolis, E., Infurnari, L., Vella, A., Clementi, N., Vaccaro, L., Ruggeri, A., Posteraro, B., Burioni, R., & Clementi, M. (2013). Comparative evaluation of the Bruker Biotyper and Vitek MS matrix-assisted laser desorption ionization-time of flight (MALDI-TOF) mass spectrometry systems for identification of yeasts of medical importance. *Journal of Clinical Microbiology*, JCM. 00841-00813.
- Mandal, P., Roy, T. S., Das, T. K., Banerjee, U., Xess, I., & Nosanchuk, J. D. (2007). Differences in the cell wall architecture of melanin lacking and melanin producing *Cryptococcus neoformans* clinical isolates from India: an electron microscopic study. *Brazilian Journal of Microbiology*, *38*(4), 662-666.
- Manon, S., Chaudhuri, B., & Guérin, M. (1997). Release of cytochrome c and decrease of cytochrome c oxidase in Bax-expressing yeast cells, and prevention of these effects by coexpression of Bcl-x L. *FEBS Letters*, *415*(1), 29-32.
- Mansour, M. K., Yauch, L. E., Rottman, J. B., & Levitz, S. M. (2004). Protective efficacy of antigenic fractions in mouse models of cryptococcosis. *Infection and Immunity*, *72*(3), 1746-1754.

- Marr, K. A. (2012). *Cryptococcus gattii* as an important fungal pathogen of western North America. *Expert Review of Anti-infective Therapy*, 10(6), 637-643.
- Martinez, L. R., Garcia-Rivera, J., & Casadevall, A. (2001). *Cryptococcus neoformans* var. *neoformans* (serotype D) strains are more susceptible to heat than *C. neoformans* var. *grubii* (serotype A) strains. *Journal of Clinical Microbiology*, 39(9), 3365-3367.
- Massonet, C., Van Eldere, J., Vanechoutte, M., De Baere, T., Verhaegen, J., & Lagrou, K. (2004). Comparison of VITEK 2 with ITS2-fragment length polymorphism analysis for identification of yeast species. *Journal of Clinical Microbiology*, 42(5), 2209-2211.
- Mccurdy, L. H., & Morrow, J. D. (2003). Infections due to *non-neoformans* cryptococcal species. *Comprehensive Therapy*, 29(2-3), 95-101.
- McFadden, D. C., De Jesus, M., & Casadevall, A. (2006). The physical properties of the capsular polysaccharides from *Cryptococcus neoformans* suggest features for capsule construction. *Journal of Biological Chemistry*, 281(4), 1868-1875.
- McMurry, L. M., Oethinger, M., & Levy, S. B. (1998). Triclosan targets lipid synthesis. *Nature*, 394(6693), 531-532. doi:10.1038/28970
- McNeill, J., & Kan, V. (1995). Decline in the incidence of cryptococcosis among HIV-related patients. *Journal of Acquired Immune Deficiency Syndromes and Human Retrovirology*, 206(207), 207.
- Mdodo, R., Moser, S. A., Jaoko, W., Baddley, J., Pappas, P., Kempf, M. C., Aban, I., Odera, S., & Jolly, P. (2011). Antifungal susceptibilities of *Cryptococcus neoformans* cerebrospinal fluid isolates from AIDS patients in Kenya. *Mycoses*, 54(5), e438-e442.
- Mednick, A. J., Nosanchuk, J. D., & Casadevall, A. (2005). Melanization of *Cryptococcus neoformans* affects lung inflammatory responses during cryptococcal infection. *Infection and Immunity*, 73(4), 2012-2019.
- Meena, M., Prasad, V., Zehra, A., Gupta, V. K., & Upadhyay, R. S. (2015). Mannitol metabolism during pathogenic fungal-host interactions under stressed conditions. *Frontiers in Microbiology*, 6.
- Meletiadis, J., Antachopoulos, C., Stergiopoulou, T., Pournaras, S., Roilides, E., & Walsh, T. J. (2007). Differential fungicidal activities of amphotericin B and voriconazole against *Aspergillus* species determined by microbroth methodology. *Antimicrobial Agents and Chemotherapy*, 51(9), 3329-3337.
- Meletiadis, J., Antachopoulos, C., Stergiopoulou, T., Pournaras, S., Roilides, E., & Walsh, T. J. (2007). Differential fungicidal activities of amphotericin B and voriconazole against *Aspergillus* species determined by microbroth methodology. *Antimicrob Agents Chemother*, 51(9), 3329-3337. doi:10.1128/AAC.00345-07
- Meyer, W., Mitchell, T. G., Freedman, E., & Vilgalys, R. (1993). Hybridization probes for conventional DNA fingerprinting used as single primers in the polymerase

chain reaction to distinguish strains of *Cryptococcus neoformans*. *Journal of Clinical Microbiology*, 31(9), 2274-2280.

- Miceli, M. H., & Kauffman, C. A. (2015). Isavuconazole: a new broad-spectrum triazole antifungal agent. *Clinical Infectious Diseases*, 61(10), 1558-1565.
- Milano, S., Arcoleo, F., D'Agostino, P., & Cillari, E. (1997). Intraperitoneal injection of tetracyclines protects mice from lethal endotoxemia downregulating inducible nitric oxide synthase in various organs and cytokine and nitrate secretion in blood. *Antimicrobial Agents and Chemotherapy*, 41(1), 117-121.
- Mirza, S. A., Phelan, M., Rimland, D., Graviss, E., Hamill, R., Brandt, M. E., Gardner, T., Sattah, M., de Leon, G. P., & Baughman, W. (2003). The changing epidemiology of cryptococcosis: an update from population-based active surveillance in 2 large metropolitan areas, 1992–2000. *Clinical Infectious Diseases*, 36(6), 789-794.
- Missall, T. A., Pusateri, M. E., & Lodge, J. K. (2004). Thiol peroxidase is critical for virulence and resistance to nitric oxide and peroxide in the fungal pathogen, *Cryptococcus neoformans*. *Molecular Microbiology*, 51(5), 1447-1458.
- Mitchell, T. G., & Friedman, L. (1972). In vitro phagocytosis and intracellular fate of variously encapsulated strains of *Cryptococcus neoformans*. *Infection and Immunity*, 5(4), 491-498.
- Mitchell, T. G., & Perfect, J. R. (1995). Cryptococcosis in the era of AIDS--100 years after the discovery of *Cryptococcus neoformans*. *Clinical Microbiology Reviews*, 8(4), 515-548.
- Mitruka, B. M., & Rawnsley, H. M. (1977). Clinical biochemical and hematological reference values in normal experimental animals. *Clinical biochemical and hematological reference values in normal experimental animals*.
- Mitten, M., Meulbroek, J., Nukkala, M., Paige, L., Jarvis, K., Oleksijew, A., Tovcimak, A., Hernandez, L., Alder, J., & Ewing, P. (2001). Efficacies of ABT-773, a new ketolide, against experimental bacterial infections. *Antimicrobial Agents and Chemotherapy*, 45(9), 2585-2593.
- Molin, M., Norbeck, J., & Blomberg, A. (2003). Dihydroxyacetone Kinases in *Saccharomyces cerevisiae* Are Involved in Detoxification of Dihydroxyacetone. *Journal of Biological Chemistry*, 278(3), 1415-1423.
- Monari, C., Pericolini, E., Bistoni, G., Casadevall, A., Kozel, T. R., & Vecchiarelli, A. (2005). *Cryptococcus neoformans* capsular glucuronoxylomannan induces expression of fas ligand in macrophages. *The Journal of Immunology*, 174(6), 3461-3468.
- Mondon, P., Petter, R., Amalfitano, G., Luzzati, R., Concia, E., Polacheck, I., & Kwon-Chung, K. (1999). Heteroresistance to Fluconazole and Voriconazole in *Cryptococcus neoformans*. *Antimicrobial Agents and Chemotherapy*, 43(8), 1856-1861.

- Moraes, E., Primola, N., & Hamdan, J. S. (2003). Antifungal susceptibility of clinical and environmental isolates of *Cryptococcus neoformans* to four antifungal drugs determined by two techniques. *Mycoses*, 46(5- 6), 164-168.
- Morey, J. S., Ryan, J. C., & Van Dolah, F. M. (2006). Microarray validation: factors influencing correlation between oligonucleotide microarrays and real-time PCR. *Biological Procedure Online*, 8(1), 175-193.
- Morrow, C. A., & Fraser, J. A. (2013). Is the Nickel-Dependent Urease Complex of *Cryptococcus* the Pathogen's Achilles' Heel? *MBio*, 4(4), e00408-00413.
- Morrow, C. A., Lee, I. R., Chow, E. W., Ormerod, K. L., Goldinger, A., Byrnes, E. J., Nielsen, K., Heitman, J., Schirra, H. J., & Fraser, J. A. (2012). A unique chromosomal rearrangement in the *Cryptococcus neoformans* var. *grubii* type strain enhances key phenotypes associated with virulence. *MBio*, 3(2), e00310-00311.
- Mukherjee, P. K., Sheehan, D. J., Hitchcock, C. A., & Ghannoum, M. A. (2005). Combination treatment of invasive fungal infections. *Clinical Microbiology Reviews*, 18(1), 163-194.
- Munoz, P., Singh, N., & Bouza, E. (2006). Treatment of solid organ transplant patients with invasive fungal infections: should a combination of antifungal drugs be used? *Current Opinion in Infectious Diseases*, 19(4), 365-370.
- Murphy, J. W. (1992). Cryptococcal immunity and immunostimulation *Microbial Infections* (pp. 225-230): Springer.
- Ngamskulrungrroj, P., Price, J., Sorrell, T., Perfect, J. R., & Meyer, W. (2011). *Cryptococcus gattii* virulence composite: candidate genes revealed by microarray analysis of high and less virulent Vancouver island outbreak strains. *PLoS One*, 6(1), e16076.
- Nielsen, K., Cox, G. M., Wang, P., Toffaletti, D. L., Perfect, J. R., & Heitman, J. (2003). Sexual cycle of *Cryptococcus neoformans* var. *grubii* and virulence of congenic a and α isolates. *Infection and Immunity*, 71(9), 4831-4841.
- Nishikawa, M. M., Lazera, M. S., Barbosa, G. G., Trilles, L., Balassiano, B. R., Macedo, R. C., Bezerra, C. C., Pérez, M. A., Cardarelli, P., & Wanke, B. (2003). Serotyping of 467 *Cryptococcus neoformans* isolates from clinical and environmental sources in Brazil: analysis of host and regional patterns. *Journal of Clinical Microbiology*, 41(1), 73-77.
- Nosanchuk, J. D., & Casadevall, A. (1997). Cellular charge of *Cryptococcus neoformans*: contributions from the capsular polysaccharide, melanin, and monoclonal antibody binding. *Infection and Immunity*, 65(5), 1836-1841.
- Nosanchuk, J. D., Rudolph, J., Rosas, A. L., & Casadevall, A. (1999a). Evidence that *Cryptococcus neoformans* is melanized in pigeon excreta: implications for pathogenesis. *Infection and Immunity*, 67(10), 5477-5479.
- Nosanchuk, J. D., Valadon, P., Feldmesser, M., & Casadevall, A. (1999b). Melanization of *Cryptococcus neoformans* in murine infection. *Molecular and Cellular Biology*, 19(1), 745-750.

- Noverr, M. C., Cox, G. M., Perfect, J. R., & Huffnagle, G. B. (2003). Role of *PLB1* in pulmonary inflammation and cryptococcal eicosanoid production. *Infection and Immunity*, *71*(3), 1538-1547.
- Noverr, M. C., Williamson, P. R., Fajardo, R. S., & Huffnagle, G. B. (2004). *CNLAC1* is required for extrapulmonary dissemination of *Cryptococcus neoformans* but not pulmonary persistence. *Infection and Immunity*, *72*(3), 1693-1699.
- Odds, F. C. (2003). Fluconazole plus amphotericin B combinations are not contraindicated and may add benefit for the treatment of candidemia. *Clinical Infectious Diseases*, *36*(10), 1229-1231.
- Odds, F. C. (2003). Synergy, antagonism, and what the checkerboard puts between them. *J Antimicrob Chemother*, *52*(1), 1. doi:10.1093/jac/dkg301
- Odom, A., Muir, S., Lim, E., Toffaletti, D. L., Perfect, J., & Heitman, J. (1997). Calcineurin is required for virulence of *Cryptococcus neoformans*. *The EMBO Journal*, *16*(10), 2576-2589.
- Olson, Å., & Stenlid, J. (2001). Plant pathogens: mitochondrial control of fungal hybrid virulence. *Nature*, *411*(6836), 438-438.
- Olszewski, M. A., Noverr, M. C., Chen, G.-H., Toews, G. B., Cox, G. M., Perfect, J. R., & Huffnagle, G. B. (2004). Urease expression by *Cryptococcus neoformans* promotes microvascular sequestration, thereby enhancing central nervous system invasion. *The American Journal of Pathology*, *164*(5), 1761-1771.
- World Health Organization. (2002). *The world health report 2002: reducing risks, promoting healthy life*: World Health Organization.
- World Health Organization. (2003). *HIV/AIDS epidemiological surveillance update for the WHO African Region 2002*: World Health Organization, Regional Office for Africa.
- World Health Organization. (2010). *World health statistics 2010*: World Health Organization.
- World Health Organization. (2011). Rapid advice: diagnosis, prevention and management of cryptococcal disease in HIV-infected adults, adolescents and children: December 2011.
- Ormerod, K. L., Morrow, C. A., Chow, E. W., Lee, I. R., Arras, S. D., Schirra, H. J., Cox, G. M., Fries, B. C., & Fraser, J. A. (2013). Comparative genomics of serial isolates of *Cryptococcus neoformans* reveals gene associated with carbon utilization and virulence. *G3: Genes/ Genomes/ Genetics*, *3*(4), 675-686.
- Oxelmark, E., Marchini, A., Malanchi, I., Magherini, F., Jaquet, L., Hajibagheri, M. N., Blight, K. J., Jauniaux, J.-C., & Tommasino, M. (2000). Mmf1p, a novel yeast mitochondrial protein conserved throughout evolution and involved in maintenance of the mitochondrial genome. *Molecular and Cellular Biology*, *20*(20), 7784-7797.
- Pappas, P. G. (2013). Cryptococcal infections in non-HIV-infected patients. *Transactions of the American Clinical and Climatological Association*, *124*, 61.

- Park, B. J., Wannemuehler, K. A., Marston, B. J., Govender, N., Pappas, P. G., & Chiller, T. M. (2009). Estimation of the current global burden of cryptococcal meningitis among persons living with HIV/AIDS. *AIDS*, 23(4), 525-530.
- Park, S. H., Choi, S. C., Lee, K. W., Kim, M.-N., & Hwang, S. M. (2015). Genotypes of Clinical and Environmental Isolates of *Cryptococcus neoformans* and *Cryptococcus gattii* in Korea. *Mycobiology*, 43(3), 360-365.
- Pavel, A. B., & Vasile, C. I. (2012). PyElph-a software tool for gel images analysis and phylogenetics. *BMC Bioinformatics*, 13(1), 1.
- Perfect, J. R. (2005). *Cryptococcus neoformans*: a sugar-coated killer with designer genes. *FEMS Immunology & Medical Microbiology*, 45(3), 395-404.
- Perfect, J. R., & Casadevall, A. (2002). Cryptococcosis. *Infectious Disease Clinics of North America*, 16(4), 837-874.
- Perfect, J. R., & Cox, G. M. (1999). Drug resistance in *Cryptococcus neoformans*. *Drug Resistance Updates*, 2(4), 259-269.
- Perfect, J. R., Dismukes, W. E., Dromer, F., Goldman, D. L., Graybill, J. R., Hamill, R. J., Harrison, T. S., Larsen, R. A., Lortholary, O., & Nguyen, M.-H. (2010). Clinical practice guidelines for the management of cryptococcal disease: 2010 update by the Infectious Diseases Society of America. *Clinical Infectious Diseases*, 50(3), 291-322.
- Perkins, A., Gomez-Lopez, A., Mellado, E., Rodriguez-Tudela, J. L., & Cuenca-Estrella, M. (2005). Rates of antifungal resistance among Spanish clinical isolates of *Cryptococcus neoformans* var. *neoformans*. *Journal of Antimicrobial Chemotherapy*, 56(6), 1144-1147.
- Petter, R., Kang, B., Boekhout, T., Davis, B., & Kwon-Chung, K. (2001). A survey of heterobasidiomycetous yeasts for the presence of the genes homologous to virulence factors of *Filobasidiella neoformans*, *CNLAC1* and *CAP59*. *Microbiology*, 147(8), 2029-2036.
- Pfaller, M., Diekema, D., Gibbs, D., Newell, V., Bijie, H., Dzierzanowska, D., Klimko, N., Letscher-Bru, V., Lisalova, M., & Muehlethaler, K. (2009). Results from the ARTEMIS DISK Global Antifungal Surveillance Study, 1997 to 2007: 10.5-year analysis of susceptibilities of noncandidal yeast species to fluconazole and voriconazole determined by CLSI standardized disk diffusion testing. *Journal of Clinical Microbiology*, 47(1), 117-123.
- Pfaller, M., Sheehan, D., & Rex, J. (2004). Determination of fungicidal activities against yeasts and molds: lessons learned from bactericidal testing and the need for standardization. *Clinical Microbiology Reviews*, 17(2), 268-280.
- Pietrella, D., Corbucci, C., Perito, S., Bistoni, G., & Vecchiarelli, A. (2005). Mannoproteins from *Cryptococcus neoformans* promote dendritic cell maturation and activation. *Infection and Immunity*, 73(2), 820-827.
- Pietrella, D., Fries, B., Lupo, P., Bistoni, F., Casadevall, A., & Vecchiarelli, A. (2003). Phenotypic switching of *Cryptococcus neoformans* can influence the outcome of the human immune response. *Cellular Microbiology*, 5(8), 513-522.

- Polacheck, I. (1991). The discovery of melanin production in *Cryptococcus neoformans* and its impact on diagnosis and the study of virulence. *Zentralblatt für Bakteriologie*, 276(1), 120-123.
- Prasad, R., De Wergifosse, P., Goffeau, A., & Balzi, E. (1995). Molecular cloning and characterization of a novel gene of *Candida albicans*, *CDR1*, conferring multiple resistance to drugs and antifungals. *Current Genetics*, 27(4), 320-329.
- Price, M. F., Wilkinson, I. D., & Gentry, L. O. (1982). Plate method for detection of phospholipase activity in *Candida albicans*. *Sabouraudia*, 20(1), 7-14.
- Price, M. S., Betancourt-Quiroz, M., Price, J. L., Toffaletti, D. L., Vora, H., Hu, G., Kronstad, J. W., & Perfect, J. R. (2011). *Cryptococcus neoformans* requires a functional glycolytic pathway for disease but not persistence in the host. *MBio*, 2(3), e00103-00111.
- Rakesh, V., Schweitzer, A. D., Zaragoza, O., Bryan, R., Wong, K., Datta, A., Casadevall, A., & Dadachova, E. (2008). Finite-element model of interaction between fungal polysaccharide and monoclonal antibody in the capsule of *Cryptococcus neoformans*. *The Journal of Physical Chemistry B*, 112(29), 8514-8522.
- Ramsdale, M. (2008). Programmed cell death in pathogenic fungi. *Biochimica et Biophysica Acta (BBA)-Molecular Cell Research*, 1783(7), 1369-1380.
- Rand, K. H., Houck, H. J., Brown, P., & Bennett, D. (1993). Reproducibility of the microdilution checkerboard method for antibiotic synergy. *Antimicrob Agents Chemother*, 37(3), 613-615.
- Rao, S. P. R., Surolia, A., & Surolia, N. (2003). Triclosan: a shot in the arm for antimalarial chemotherapy. *Molecular and Cellular Biochemistry*, 253(1-2), 55-63.
- Regos, J., Zak, O., Solf, R., Vischer, W. A., & Weirich, E. G. (1979). Antimicrobial spectrum of triclosan, a broad-spectrum antimicrobial agent for topical application. II. Comparison with some other antimicrobial agents. *Dermatologica*, 158(1), 72-79.
- Reitman, S., & Frankel, S. (1957). A colorimetric method for the determination of serum glutamic oxalacetic and glutamic pyruvic transaminases.
- Rex, J. H., Pfaller, M. A., Walsh, T. J., Chaturvedi, V., Espinel-Ingroff, A., Ghannoum, M. A., Gosey, L. L., Odds, F. C., Rinaldi, M. G., & Sheehan, D. J. (2001). Antifungal susceptibility testing: practical aspects and current challenges. *Clinical Microbiology Reviews*, 14(4), 643-658.
- Rhodes, J. C., Polacheck, I., & Kwon-Chung, K. (1982). Phenoloxidase activity and virulence in isogenic strains of *Cryptococcus neoformans*. *Infection and Immunity*, 36(3), 1175-1184.
- Rivera, V., Gaviria, M., Muñoz-Cadavid, C., Cano, L., & Naranjo, T. (2015). Validation and clinical application of a molecular method for the identification of *Cryptococcus neoformans/Cryptococcus gattii* complex DNA in human clinical specimens. *Brazilian Journal of Infectious Diseases*, 19(6), 563-570.

- Rodaki, A., Bohovych, I. M., Enjalbert, B., Young, T., Odds, F. C., Gow, N. A., & Brown, A. J. (2009). Glucose promotes stress resistance in the fungal pathogen *Candida albicans*. *Molecular biology of the cell*, 20(22), 4845-4855.
- Rodero, L., Mellado, E., Rodriguez, A. C., Salve, A., Guelfand, L., Cahn, P., Cuenca-Estrella, M., Davel, G., & Rodriguez-Tudela, J. L. (2003). G484S amino acid substitution in *lanosterol 14- α demethylase (ERG11)* is related to fluconazole resistance in a recurrent *Cryptococcus neoformans* clinical isolate. *Antimicrobial agents and chemotherapy*, 47(11), 3653-3656.
- Rohatgi, S., & Pirofski, L.-a. (2015). Host immunity to *Cryptococcus neoformans*. *Future Microbiology*, 10(4), 565-581.
- Rosas, A., MacGill, R., Nosanchuk, J. D., Kozel, T., & Casadevall, A. (2002). Activation of the alternative complement pathway by fungal melanins. *Clinical and Diagnostic Laboratory Immunology*, 9(1), 144-148.
- Rosas, A. L., & Casadevall, A. (2001). Melanization decreases the susceptibility of *Cryptococcus neoformans* to enzymatic degradation. *Mycopathologia*, 151(2), 53-56.
- Rosas, Á. L., & Casadevall, A. (1997). Melanization affects susceptibility of *Cryptococcus neoformans* to heat and cold. *FEMS microbiology letters*, 153(2), 265-272.
- Rosas, Á. L., Nosanchuk, J. D., Feldmesser, M., Cox, G. M., McDade, H. C., & Casadevall, A. (2000). Synthesis of polymerized melanin by *Cryptococcus neoformans* in infected rodents. *Infection and Immunity*, 68(5), 2845-2853.
- Rude, T. H., Toffaletti, D. L., Cox, G. M., & Perfect, J. R. (2002). Relationship of the glyoxylate pathway to the pathogenesis of *Cryptococcus neoformans*. *Infection and immunity*, 70(10), 5684-5694.
- Russo, G., Zegar, C., & Giordano, A. (2003). Advantages and limitations of microarray technology in human cancer. *Oncogene*, 22(42), 6497-6507.
- Salas, S., Bennett, J., Kwon-Chung, K., Perfect, J., & Williamson, P. (1996). Effect of the laccase gene *CNLAC1*, on virulence of *Cryptococcus neoformans*. *The Journal of Experimental Medicine*, 184(2), 377-386.
- Sanfelice, F. (1894). Contributo alla morfologia e biologia dei blastomiceti che si sviluppano nei succhi di alcuni frutti. *Ann Igien*, 4, 463-495.
- Sanglard, D., Ischer, F., Monod, M., & Bille, J. (1996). Susceptibilities of *Candida albicans* multidrug transporter mutants to various antifungal agents and other metabolic inhibitors. *Antimicrobial Agents and Chemotherapy*, 40(10), 2300-2305.
- Santangelo, R. T., Nouri-Sorkhabi, M. H., Sorrell, T. C., Cagney, M., Chen, S. C., Kuchel, P. W., & Wright, L. C. (1999). Biochemical and functional characterisation of secreted phospholipase activities from *Cryptococcus neoformans* in their naturally occurring state. *Journal of Medical Microbiology*, 48(8), 731-740.

- Saugar, J. M., Alarcón, T., López-Hernández, S., López-Brea, M., Andreu, D., & Rivas, L. (2002). Activities of polymyxin B and cecropin A-melittin peptide CA (1-8) M (1-18) against a multiresistant strain of *Acinetobacter baumannii*. *Antimicrobial Agents and Chemotherapy*, 46(3), 875-878.
- Schrettl, M., Bignell, E., Kragl, C., Joechl, C., Rogers, T., Arst, H. N., Haynes, K., & Haas, H. (2004). Siderophore biosynthesis but not reductive iron assimilation is essential for *Aspergillus fumigatus* virulence. *The Journal of Experimental Medicine*, 200(9), 1213-1219.
- Schweizer, H. P. (2001). Triclosan: a widely used biocide and its link to antibiotics. *FEMS Microbiology Letters*, 202(1), 1-7.
- Seifert, H., Aurbach, U., Stefanik, D., & Cornely, O. (2007). In vitro activities of isavuconazole and other antifungal agents against *Candida* bloodstream isolates. *Antimicrobial Agents and Chemotherapy*, 51(5), 1818-1821.
- Selmecki, A., Forche, A., & Berman, J. (2006). Aneuploidy and isochromosome formation in drug-resistant *Candida albicans*. *Science*, 313(5785), 367-370.
- Semighini, C. P., Averette, A. F., Perfect, J. R., & Heitman, J. (2011). Deletion of *Cryptococcus neoformans* AIF ortholog promotes chromosome aneuploidy and fluconazole-resistance in a metacaspase-independent manner. *PLoS Pathogen*, 7(11), e1002364-e1002364.
- Severo, C. B., Xavier, M. O., Gazzoni, A. F., & Severo, L. C. (2009). Cryptococcosis in children. *Paediatric Respiratory Reviews*, 10(4), 166-171.
- Shapira, L., Soskolne, W. A., Houry, Y., Barak, V., Halabi, A., & Stabholz, A. (1996). Protection against endotoxic shock and lipopolysaccharide-induced local inflammation by tetracycline: correlation with inhibition of cytokine secretion. *Infection and Immunity*, 64(3), 825-828.
- Sharma, S., Ramya, T., Surolia, A., & Surolia, N. (2003). Triclosan as a systemic antibacterial agent in a mouse model of acute bacterial challenge. *Antimicrobial Agents and Chemotherapy*, 47(12), 3859-3866.
- Sharpton, T. J., Neafsey, D. E., Galagan, J. E., & Taylor, J. W. (2008). Mechanisms of intron gain and loss in *Cryptococcus*. *Genome Biology*, 9(1), 1.
- Shingu-Vazquez, M., & Traven, A. (2011). Mitochondria and fungal pathogenesis: drug tolerance, virulence, and potential for antifungal therapy. *Eukaryotic Cell*, 10(11), 1376-1383.
- Shoham, S., Huang, C., Chen, J.-M., Golenbock, D. T., & Levitz, S. M. (2001). Toll-like receptor 4 mediates intracellular signaling without TNF- α release in response to *Cryptococcus neoformans* polysaccharide capsule. *The Journal of Immunology*, 166(7), 4620-4626.
- Singh, K., Kang, P. J., & Park, H.-O. (2008). The Rho5 GTPase is necessary for oxidant-induced cell death in budding yeast. *Proceedings of the National Academy of Sciences*, 105(5), 1522-1527.

- Sopirala, M. M., Mangino, J. E., Gebreyes, W. A., Biller, B., Bannerman, T., Balada-Llasat, J.-M., & Pancholi, P. (2010). Synergy testing by Etest, microdilution checkerboard, and time-kill methods for pan-drug-resistant *Acinetobacter baumannii*. *Antimicrobial Agents and Chemotherapy*, *54*(11), 4678-4683.
- Southern, E., Mir, K., & Shchepinov, M. (1999). Molecular interactions on microarrays. *Nature Genetics*, *21*, 5-9.
- Srikanta, D., Santiago-Tirado, F. H., & Doering, T. L. (2014). *Cryptococcus neoformans*: historical curiosity to modern pathogen. *Yeast*, *31*(2), 47-60.
- Stalder, D., Mizuno-Yamasaki, E., Ghassemian, M., & Novick, P. J. (2013). Phosphorylation of the Rab exchange factor Sec2p directs a switch in regulatory binding partners. *Proceedings of the National Academy of Sciences*, *110*(50), 19995-20002.
- Stewart, M. J., Parikh, S., Xiao, G., Tonge, P. J., & Kisker, C. (1999). Structural basis and mechanism of enoyl reductase inhibition by triclosan. *Journal of Molecular Biology*, *290*(4), 859-865.
- Sun, S., & Xu, J. (2009). Chromosomal rearrangements between serotype A and D strains in *Cryptococcus neoformans*. *PLoS One*, *4*(5), e5524.
- Szilagyi, G., Reiss, F., & Smith, J. C. P. (1966). The anticryptococcal factor of blood serum. *Journal of Investigative Dermatology*, *46*, 306-308.
- Taheri, N., Köhler, T., Braus, G. H., & Mösch, H. U. (2000). Asymmetrically localized *Bud8p* and *Bud9p* proteins control yeast cell polarity and development. *The EMBO Journal*, *19*(24), 6686-6696.
- Tambe, S., Sampath, L., & Modak, S. (2001). In vitro evaluation of the risk of developing bacterial resistance to antiseptics and antibiotics used in medical devices. *Journal of Antimicrobial Chemotherapy*, *47*(5), 589-598.
- Tangen, K. L., Jung, W. H., Sham, A. P., Lian, T., & Kronstad, J. W. (2007). The iron- and cAMP-regulated gene *SIT1* influences ferrioxamine B utilization, melanization and cell wall structure in *Cryptococcus neoformans*. *Microbiology*, *153*(1), 29-41.
- Tarca, A. L., Romero, R., & Draghici, S. (2006). Analysis of microarray experiments of gene expression profiling. *American Journal of Obstetrics and Gynecology*, *195*(2), 373-388.
- Tassie, J.-M., Pepper, L., Fogg, C., Biraro, S., Mayanja, B., Andia, I., Paugam, A., Priotto, G., & Legros, D. (2003). Systematic screening of cryptococcal antigenemia in HIV-positive adults in Uganda. *JAIDS Journal of Acquired Immune Deficiency Syndromes*, *33*(3), 411-412.
- Tay, S., Chai, H., Na, S., Hamimal, H., Rohani, M., & Soo-Hoo, T. (2005). The isolation, characterization and antifungal susceptibilities of *Cryptococcus neoformans* from bird excreta in Klang Valley, Malaysia. *Mycopathologia*, *159*(4), 509-513.

- Tay, S., Lim, H., Tajuddin, T., Rohani, M., Hamimah, H., & Thong, K. (2006). Determination of molecular types and genetic heterogeneity of *Cryptococcus neoformans* and *C. gattii* in Malaysia. *Medical Mycology*, 44(7), 617-622.
- Theodoris, G., & Bisson, L. F. (2001). DDSE: downstream targets of the *SNF3* signal transduction pathway. *FEMS Microbiology Letters*, 197(1), 73-77.
- Thompson, G. R., Albert, N., Hodge, G., Wilson, M. D., Sykes, J. E., Bays, D. J., Firacative, C., Meyer, W., & Kontoyiannis, D. P. (2014). Phenotypic differences of *Cryptococcus molecular* types and their implications for virulence in a *Drosophila* model of infection. *Infection and Immunity*, 82(7), 3058-3065.
- Tkach, J. M., Yimit, A., Lee, A. Y., Riffle, M., Costanzo, M., Jaschob, D., Hendry, J. A., Ou, J., Moffat, J., & Boone, C. (2012). Dissecting DNA damage response pathways by analysing protein localization and abundance changes during DNA replication stress. *Nature Cell Biology*, 14(9), 966-976.
- Toffaletti, D. L., Del Poeta, M., Rude, T. H., Dietrich, F., & Perfect, J. R. (2003). Regulation of *cytochrome c oxidase subunit 1 (COX1)* expression in *Cryptococcus neoformans* by temperature and host environment. *Microbiology*, 149(4), 1041-1049.
- Toffaletti, D. L., Nielsen, K., Dietrich, F., Heitman, J., & Perfect, J. R. (2004). *Cryptococcus neoformans* mitochondrial genomes from serotype A and D strains do not influence virulence. *Current Genetics*, 46(4), 193-204.
- Tucker, S. C., & Casadevall, A. (2002). Replication of *Cryptococcus neoformans* in macrophages is accompanied by phagosomal permeabilization and accumulation of vesicles containing polysaccharide in the cytoplasm. *Proceedings of the National Academy of Sciences*, 99(5), 3165-3170.
- Tulp, M. T. M., Sundström, G., Martron, L., & Hutzinger, O. (1979). Metabolism of chlorodiphenyl ethers and Irgasan® DP 300. *Xenobiotica*, 9(2), 65-77.
- Tzagaloff, A., Wu, M., & Crivellone, M. (1986). Characterization of *COR1*, the structural gene for the 44-kilodalton core protein of yeast coenzyme QH 2-cytochrome c reductase. *Journal of Biological Chemistry*, 261, 17163-17169.
- Upadhyaya, R., Kim, H., Jung, K. W., Park, G., Lam, W., Lodge, J. K., & Bahn, Y. S. (2013). Sulphiredoxin plays peroxiredoxin- dependent and- independent roles via the HOG signalling pathway in *Cryptococcus neoformans* and contributes to fungal virulence. *Molecular Microbiology*, 90(3), 630-648.
- Vaishnav, V. V., Bacon, B. E., O'Neill, M., & Cherniak, R. (1998). Structural characterization of the galactoxylomannan of *Cryptococcus neoformans Cap67*. *Carbohydrate Research*, 306(1), 315-330.
- van Elden, L. J., Walenkamp, A. M., Lipovsky, M. M., Reiss, P., Meis, J. F., de Marie, S., Dankert, J., & Hoepelman, A. I. (2000). Declining number of patients with cryptococcosis in the Netherlands in the era of highly active antiretroviral therapy. *AIDS*, 14(17), 2787-2788.
- Varma, A., & Kwon-Chung, K. (1992). DNA probe for strain typing of *Cryptococcus neoformans*. *Journal of Clinical Microbiology*, 30(11), 2960-2967.

- Vartivarian, S. E., Anaissie, E. J., Cowart, R. E., Sprigg, H. A., Tingler, M. J., & Jacobson, E. S. (1993). Regulation of cryptococcal capsular polysaccharide by iron. *Journal of Infectious Diseases*, *167*(1), 186-190.
- Vecchiarelli, A., Retini, C., Pietrella, D., Monari, C., Tascini, C., Beccari, T., & Kozel, T. R. (1995). Downregulation by cryptococcal polysaccharide of tumor necrosis factor alpha and interleukin-1 beta secretion from human monocytes. *Infection and Immunity*, *63*(8), 2919-2923.
- Vellucci, V. F., Gygax, S. E., & Hostetter, M. K. (2007). Involvement of *Candida albicans* pyruvate dehydrogenase complex protein X (Pdx1) in filamentation. *Fungal Genetics and Biology*, *44*(10), 979-990.
- Villalaín, J., Mateo, C. R., Aranda, F. J., Shapiro, S., & Micol, V. (2001). Membranotropic effects of the antibacterial agent triclosan. *Archives of Biochemistry and Biophysics*, *390*(1), 128-136.
- Villar- Tajadura, M. A., Coll, P. M., Madrid, M., Cansado, J., Santos, B., & Pérez, P. (2008). *Rga2* is a Rho2 GAP that regulates morphogenesis and cell integrity in *S. pombe*. *Molecular Microbiology*, *70*(4), 867-881.
- Vischer, W. A., & Regos, J. (1974). Antimicrobial spectrum of Triclosan, a broad-spectrum antimicrobial agent for topical application. *Zentralbl Bakteriolog Orig A*, *226*(3), 376-389.
- Voelz, K. (2010). *Macrophage-cryptococcus interactions during cryptococcosis*. University of Birmingham.
- Wakabayashi, T. (1999). Structural changes of mitochondria related to apoptosis: swelling and megamitochondria formation. *Acta Biochimica Polonica*, *46*(2), 223-237.
- Walch-Solimena, C., Collins, R. N., & Novick, P. J. (1997). Sec2p mediates nucleotide exchange on Sec4p and is involved in polarized delivery of post-Golgi vesicles. *The Journal of Cell Biology*, *137*(7), 1495-1509.
- Walker, C. B., Nitzan, D., & Wilkins, T. D. (1977). Chemotherapy of an experimental *Bacteroides fragilis* infection in mice. *Antimicrobial Agents and Chemotherapy*, *11*(3), 435-440.
- Wang, P., Perfect, J. R., & Heitman, J. (2000). The G-protein β subunit *GPB1* is required for mating and haploid fruiting in *Cryptococcus neoformans*. *Molecular and Cellular Biology*, *20*(1), 352-362.
- Wang, X., Hsueh, Y.-P., Li, W., Floyd, A., Skalsky, R., & Heitman, J. (2010). Sex-induced silencing defends the genome of *Cryptococcus neoformans* via RNAi. *Genes & Development*, *24*(22), 2566-2582.
- Wang, Y., Aisen, P., & Casadevall, A. (1995). *Cryptococcus neoformans* melanin and virulence: mechanism of action. *Infection and Immunity*, *63*(8), 3131-3136.
- Wang, Y., & Casadevall, A. (1994). Decreased susceptibility of melanized *Cryptococcus neoformans* to UV light. *Applied and Environmental Microbiology*, *60*(10), 3864-3866.

- Ward, W. H., Holdgate, G. A., Rowsell, S., McLean, E. G., Pauptit, R. A., Clayton, E., Nichols, W. W., Colls, J. G., Minshull, C. A., & Jude, D. A. (1999). Kinetic and structural characteristics of the inhibition of enoyl (acyl carrier protein) reductase by triclosan. *Biochemistry*, 38(38), 12514-12525.
- Warringer, J., & Blomberg, A. (2006). Involvement of yeast *YOL151W/GRE2* in ergosterol metabolism. *Yeast*, 23(5), 389-398.
- Waugh, M. S., Nichols, C. B., DeCesare, C. M., Cox, G. M., Heitman, J., & Alspaugh, J. A. (2002). *Ras1* and *Ras2* contribute shared and unique roles in physiology and virulence of *Cryptococcus neoformans*. *Microbiology*, 148(1), 191-201.
- White, T. J., Bruns, T., Lee, S., & Taylor, J. (1990). Amplification and direct sequencing of fungal ribosomal RNA genes for phylogenetics. *PCR Protocols: A Guide to Methods and Applications*, 18(1), 315-322.
- Wilder, J. A., Olson, G. K., Chang, Y. C., Kwon-Chung, K. J., & Lipscomb, M. F. (2002). Complementation of a capsule deficient *Cryptococcus neoformans* with *CAP64* restores virulence in a murine lung infection. *American Journal of Respiratory Cell and Molecular Biology*, 26(3), 306-314.
- Wissing, S., Ludovico, P., Herker, E., Büttner, S., Engelhardt, S. M., Decker, T., Link, A., Proksch, A., Rodrigues, F., & Corte-Real, M. (2004). An AIF orthologue regulates apoptosis in yeast. *The Journal of Cell Biology*, 166(7), 969-974.
- Witt, M. D., Lewis, R. J., Larsen, R. A., Milefchik, E. N., Leal, M. A. E., Haubrich, R. H., Richie, J. A., Edwards, J. E., & Ghannoum, M. A. (1996). Identification of patients with acute AIDS-associated cryptococcal meningitis who can be effectively treated with fluconazole: the role of antifungal susceptibility testing. *Clinical Infectious Diseases*, 22(2), 322-328.
- Wozniak, K. L., & Levitz, S. M. (2008). *Cryptococcus neoformans* enters the endolysosomal pathway of dendritic cells and is killed by lysosomal components. *Infection and Immunity*, 76(10), 4764-4771.
- Wozniak, K. L., Vyas, J. M., & Levitz, S. M. (2006). *In vivo* role of dendritic cells in a murine model of pulmonary cryptococcosis. *Infection and Immunity*, 74(7), 3817-3824.
- Wurmbach, E., Yuen, T., & Sealfon, S. C. (2003). Focused microarray analysis. *Methods*, 31(4), 306-316.
- Xu, J., Vilgalys, R., & Mitchell, T. G. (2000). Multiple gene genealogies reveal recent dispersion and hybridization in the human pathogenic fungus *Cryptococcus neoformans*. *Molecular Ecology*, 9(10), 1471-1481.
- Yamamoto, Y., Kohno, S., Koga, H., Kakeya, H., Tomono, K., Kaku, M., Yamazaki, T., Arisawa, M., & Hara, K. (1995). Random amplified polymorphic DNA analysis of clinically and environmentally isolated *Cryptococcus neoformans* in Nagasaki. *Journal of Clinical Microbiology*, 33(12), 3328-3332.
- Yamazumi, T., Pfaller, M., Messer, S., Houston, A., Boyken, L., Hollis, R., Furuta, I., & Jones, R. (2003). Characterization of heteroresistance to fluconazole among

- clinical isolates of *Cryptococcus neoformans*. *Journal of Clinical Microbiology*, 41(1), 267-272.
- Yang, Y. H., Dudoit, S., Luu, P., Lin, D. M., Peng, V., Ngai, J., & Speed, T. P. (2002). Normalization for cDNA microarray data: a robust composite method addressing single and multiple slide systematic variation. *Nucleic Acids Research*, 30(4), e15-e15.
- Yang, Z., Pascon, R. C., Alspaugh, A., Cox, G. M., & McCusker, J. H. (2002). Molecular and genetic analysis of the *Cryptococcus neoformans* *MET3* gene and a met3 mutant. *Microbiology*, 148(8), 2617-2625.
- Yazdankhah, S. P., Scheie, A. A., Høiby, E. A., Lunestad, B.-T., Heir, E., Fotland, T. Ø., Naterstad, K., & Kruse, H. (2006). Triclosan and antimicrobial resistance in bacteria: an overview. *Microbial Drug Resistance*, 12(2), 83-90.
- Young, D. S., Pestaner, L., & Gibberman, V. (1975). Effects of drugs on clinical laboratory tests. *Clinical Chemistry*, 21(5), 1D-432D.
- Yu, L., Ling, G., Deng, X., Jin, J., Jin, Q., & Guo, N. (2011). In vitro interaction between fluconazole and triclosan against clinical isolates of fluconazole-resistant *Candida albicans* determined by different methods. *Antimicrobial Agents and Chemotherapy*, 55(7), 3609-3612.
- Yu, Q., Wang, H., Xu, N., Cheng, X., Wang, Y., Zhang, B., Xing, L., & Li, M. (2012). *Spf1* strongly influences calcium homeostasis, hyphal development, biofilm formation and virulence in *Candida albicans*. *Microbiology*, 158(Pt 9), 2272-2282.
- Yuan, J. S., Reed, A., Chen, F., & Stewart, C. N. (2006). Statistical analysis of real-time PCR data. *BMC Bioinformatics*, 7(1), 1.
- Yue, C., Cavallo, L. M., Alspaugh, J. A., Wang, P., Cox, G. M., Perfect, J. R., & Heitman, J. (1999). The *STE12α* homolog is required for haploid filamentation but largely dispensable for mating and virulence in *Cryptococcus neoformans*. *Genetics*, 153(4), 1601-1615.
- Zahner, J. E., Harkins, H. A., & Pringle, J. R. (1996). Genetic analysis of the bipolar pattern of bud site selection in the yeast *Saccharomyces cerevisiae*. *Molecular and Cellular Biology*, 16(4), 1857-1870.
- Zaragoza, O., Alvarez, M., Telzak, A., Rivera, J., & Casadevall, A. (2007). The relative susceptibility of mouse strains to pulmonary *Cryptococcus neoformans* infection is associated with pleiotropic differences in the immune response. *Infection and Immunity*, 75(6), 2729-2739.
- Zaragoza, O., Fries, B. C., & Casadevall, A. (2003a). Induction of capsule growth in *Cryptococcus neoformans* by mammalian serum and CO₂. *Infection and Immunity*, 71(11), 6155-6164.
- Zaragoza, O., Rodrigues, M. L., De Jesus, M., Frases, S., Dadachova, E., & Casadevall, A. (2009). The capsule of the fungal pathogen *Cryptococcus neoformans*. *Advances in Applied Microbiology*, 68, 133-216.

- Zaragoza, O., Taborda, C. P., & Casadevall, A. (2003b). The efficacy of complement-mediated phagocytosis of *Cryptococcus neoformans* is dependent on the location of C3 in the polysaccharide capsule and involves both direct and indirect C3-mediated interactions. *European Journal of Immunology*, *33*(7), 1957-1967.
- Zhang, J. H., & Ming, X. (2000). DNA fragmentation in apoptosis. *Cell Research*, *10*(3), 205-211.
- Zhang, L., Tang, Y., Guo, Z., & Shi, G. (2013). Engineering of the glycerol decomposition pathway and cofactor regulation in an industrial yeast improves ethanol production. *Journal of Industrial Microbiology & Biotechnology*, *40*(10), 1153-1160.
- Zhang, Y.-M., White, S. W., & Rock, C. O. (2006). Inhibiting bacterial fatty acid synthesis. *Journal of Biological Chemistry*, *281*(26), 17541-17544.
- Zhang, Y.-Q., Gamarra, S., Garcia-Effron, G., Park, S., Perlin, D. S., & Rao, R. (2010). Requirement for ergosterol in V-ATPase function underlies antifungal activity of azole drugs. *PLoS Pathogen*, *6*(6), e1000939.
- Zheng, X. D., Lee, R. T. H., Wang, Y. M., Lin, Q. S., & Wang, Y. (2007). Phosphorylation of Rga2, a Cdc42 GAP, by CDK/Hgc1 is crucial for *Candida albicans* hyphal growth. *The EMBO Journal*, *26*(16), 3760-3769.
- Zhu, L., Lin, J., Ma, J., Cronan, J. E., & Wang, H. (2010). Triclosan resistance of *Pseudomonas aeruginosa* PAO1 is due to FabV, a triclosan-resistant enoyl-acyl carrier protein reductase. *Antimicrobial Agents and Chemotherapy*, *54*(2), 689-698.
- Zhu, X., Gibbons, J., Zhang, S., & Williamson, P. R. (2003). Copper-mediated reversal of defective laccase in a *Δvph1* avirulent mutant of *Cryptococcus neoformans*. *Molecular Microbiology*, *47*(4), 1007-1014.
- Zhu, X., & Williamson, P. R. (2003). A CLC-type chloride channel gene is required for laccase activity and virulence in *Cryptococcus neoformans*. *Molecular Microbiology*, *50*(4), 1271-1281.
- Zhu, X., & Williamson, P. R. (2004). Role of laccase in the biology and virulence of *Cryptococcus neoformans*. *FEMS Yeast Research*, *5*(1), 1-10.

LIST OF PUBLICATIONS AND PRESENTATIONS

Publication

1. Movahed, E., Munusamy, K., Tan, G. M. Y., Looi, C. Y., Tay, S. T., & Wong, W. F. (2015). Genome-Wide Transcription Study of *Cryptococcus neoformans* H99 Clinical Strain versus Environmental Strains. *PLoS One*, *10*(9), e0137457.
2. Movahed, E., Tan, G. M. Y., Munusamy, K., Yeow, T. C., Tay, S. T., Wong, W. F., & Looi, C. Y. (2016). Triclosan Demonstrates Synergic Effect with Amphotericin B and Fluconazole and Induces Apoptosis-Like Cell Death in *Cryptococcus neoformans*. *Frontiers in microbiology*, *7*.

Poster presentation

1. Elaheh Movahed, Komathy Munusamy, Tee Cian Yeow, Grace Min Yi Tan, Chung Yeng Looi, Won Fen Wong, Sun Tee Tay. Synergistic Effect of Triclosan with Amphotericin B and Fluconazole against *Cryptococcus neoformans*. Presented at Golden Helix Symposia 2015. University Malaya, Malaysia.
2. Elaheh Movahed, Komathy Munusamy, Grace Min Yi Tan, Chung Yeng Looi, Won Fen Wong, Sun Tee Tay. Genome-wide transcription study of *Cryptococcus neoformans* H99 clinical strain versus environmental strains. Presented at International Congress of Malaysian Society of Microbiology (ICMSM) 2015, 7-10 December 2015, Batu Feringhi, Penang, Malaysia.

Workshops/ Courses

1. Basic Immunology Course. 23rd to 27th July 2013. University Malaya. Malaysia.
2. Animal Experimental Unit (AEU) induction course. 2nd April 2014. University Malaya.
3. BD FACS Canto II Flow Cytometer Basic Operator Training. 10th to 12th December 2014. University Malaya. Malaysia.